Modelling the dispersal and behaviour of fish early life-stages

William E. Butler

Dissertation submitted in partial fulfillment of a
Philosophiae Doctor degree in Biology

PhD Committee
Professor Guðrún Marteinsdóttir
Professor Steven C. Campana
Professor Øyvind Fiksen

Opponents
Dr. Alejandro Gallego
Dr. Pierre Pepin

Faculty of Life and Environmental Sciences
School of Engineering and Natural Sciences
University of Iceland
Reykjavík, December 2020

Modelling the dispersal and behaviour of fish early life-stages
Modelling the ecology of pelagic early life-stages
Dissertation submitted in partial fulfillment of a *Philosophiae Doctor* degree in Biology

Faculty of Life and Environmental Sciences
School of Engineering and Natural Sciences
University of Iceland
Sturlugata 7
101 Reykjavik
Iceland

Telephone: (+354) 525 4000

Bibliographic information:
William E. Butler, 2020, *Modelling the dispersal and behaviour of fish early life-stages*, PhD dissertation, Faculty of Life and Environmental Sciences, University of Iceland, 229 pp.

Author ORCID: 0000-0002-3286-0748

Printing: Háskólaprent, Fálkagata 2, Reykjavík
Reykjavík, Iceland, December 2020

Abstract

The population dynamics of marine fish are driven by many top-down and bottom-up processes operating across multiple life-history stages. The majority of teleosts produce large quantities of offspring which experience high mortality rates early in life. Changes in mortality during this period can therefore have large impacts on first year-class strength. As early-life stage mortality is generally driven by density-independent processes associated with the environment, a stock's ability to produce large quantities of viable eggs influences the number of larvae that successfully settle. This causal relationship—from spawner to offspring—forms the backbone of this thesis. To examine the early-life stages, physical egg properties were measured, and a suite of models employed to understand the vertical positioning, dispersal patterns, and behavioural activities of fish eggs and larvae. The empirical results provided new species-specific information regarding the egg traits of two gadoids. The models highlighted the importance of including the following components into drift models: (1) intraspecific variation in egg density, (2) larval vertical migrations, and (3) a high temporal resolution. Furthermore, the location of spawning grounds is shown to greatly influence connectivity between spawning and nursery grounds. A simple method to capture adaptive vertical migrations in drift models is provided and a new approach to evaluating whether stocks are in a collapsed state is proposed. Taken together, the thesis provides novel data and insights into the early-life stages of commercially important Icelandic gadoids, and a series of recommendations and proposed methodologies for quantitatively evaluating aspects of marine population dynamics.

Útdráttur

Stofnsveiflur sjávarfiska er knúnar áfram af mörgum þáttum sem hafa áhrif á afkomu fiska á öllum lífsstigum. Flestir beinfiskar gefa af sér mikinn fjölda afkvæma sem verða fyrir hárri dánartíðni snemma á lífsleiðinni. Breytingar á dánartíðni á þessu lífsskeiði geta því haft mikil áhrif á styrk tiltekinna árganga. Dánartíðni snemma á æviskeiðinu er almennt óháð þéttleika og því hafa umhverfisþættir meiri áhrif á yfirlifun en stærð árganganna. Við breytilegar umhverfisaðstæður eru meiri líkur á að einhver afkvæmi komist af ef upphafsfjöldi þeirra er hár. Þetta orsakasamband frá foreldri til afkvæma er megin viðfangsefni þessarar ritgerðar. Rannsóknin hófst með sýnatökum og mælingum á stærð og eðlisþyngd eggja og lirfa þorskfiska og þær notaðar til að byggja líkön sem voru keyrð til að skoða lóðrétta og lárétta dreifingu og atferli afkvæmanna. Niðurstöður mælingana leiddu í ljós mun á eiginleikum hrogna hjá tveimur tegundum þorskfiska. Við gerð slíkra líkana er mikilvægt að: 1) taka tillit til breytileika í eðlisþyngd eggja á milli tegunda; 2) líkja eftir lóðréttu fari fisklirfa og 3) keyra líkönin í hárri upplausn hvað varðar tíma. Einnig kom í ljós að staðsetning hrygningarsvæða getur haft mikil áhrif á far afkvæma og sagt til um inn á hvað uppeldissvæði þau rata. Í þessu verkefni eru lagðar fram nýjar niðurstöður um þætti sem hafa áhrif á árgangastyrk þorskfiska. Þessar niðurstöður munu nýtast við fiskveiðistjórnun og rannsóknir á fiskstofnum ekki bara við Ísland heldur um heim allan.

This thesis is dedicated to my Dad, Robert Butler,
and
to the memory of my Mum, Janet Butler (1951-2002).

Table of Contents

List of Figures

List of Tables

List of Papers

This thesis consists of four original papers. These will be referred to in the text based on their respective numbers:

Paper 1: Butler, W.E., Guðmundsdóttir, L.Ó., Logemann, K., Langbehn, T.J., Marteinsdóttir, G., 2020. *Egg size and density estimates for three gadoids in Icelandic waters and their implications for the vertical distribution of eggs along a stratified water column*. J. Mar. Syst. 204. https://doi.org/10.1016/j.jmarsys.2019.103290

Paper II: Butler, W.E., Logemann, K., Marteinsdóttir, G. *Dispersal trajectories and connectivity matrices for larval cod spawned in southern Icelandic waters*. Manuscript.

Paper III: Butler, W.E., Jørgensen, C., Opdal, A.F., Fouzai, N., Fiksen, Ø. *Can proximate cue-based rules produce optimal behavioural responses in a complex environment?* Manuscript.

Paper IV: Yletyinen, J*. and Butler, W.E.*, Ottersen, G., Andersen, K.H., Bonanomi, S., Diekert, F.K., Folke, C., Lindegren, M., Nordström, M.C., Richter, A., Rogers, L., Romagnoni, G., Weigel, B., Whittington, J., Blenckner, T., Stenseth, N.C. *When is a fish stock collapsed*? Manuscript.

*Contributed equally

Additional papers I have worked on but not included in the thesis:

Boonstra, W.J., Ottosen, K.M., Ferreira, A.S.A., Richter, A., Rogers, L.A., Pedersen, M.W., Kokkalis, A., Bardarson, H., Bonanomi, S., Butler, W., Diekert, F.K., Fouzai, N., Holma, M., Holt, R.E., Kvile, K., Malanski, E., Macdonald, J.I., Nieminen, E., Romagnoni, G., Snickars, M., Weigel, B., Woods, P., Yletyinen, J., Whittington, J.D., 2015. *What are the major global threats and impacts in marine environments?* Investigating the contours of a shared perception among marine scientists from the bottom-up. Mar. Policy 60, 197–201. https://doi.org/10.1016/j.marpol.2015.06.007

Holt, R.E., Woods, P.J., Ferreira, A.S.A., Bardarson, H., Bonanomi, S., Boonstra, W.J., Butler, W.E., Diekert, F.K., Fouzai, N., Holma, M., Kokkalis, A., Kvile, K., Macdonald, J.I., Malanski, E., Nieminen, E., Ottosen, K.M., Pedersen, M.W., Richter, A., Rogers, L., Romagnoni, G., Snickars, M., Törnroos, A., Weigel, B., Whittington, J.D., Yletyinen, J., 2017. *Avoiding pitfalls in interdisciplinary education*. Clim. Res. 74, 121–129. https://doi.org/10.3354/cr01491

Pedersen, M.W., Kokkalis, A., Bardarson, H., Bonanomi, S., Boonstra, W.J., Butler, W.E., Diekert, F.K., Fouzai, N., Holma, M., Holt, R.E., Kvile, K., Nieminen, E., Ottosen, K.M., Richter, A., Rogers, L.A., Romagnoni, G., Snickars, M., Törnroos, A., Weigel,

B., Whittington, J.D., Woods, P., Yletyinen, J., Ferreira, A.S.A., 2016. *Trends in marine climate change research in the Nordic region since the first IPCC report*. Clim. Change 134, 147–161. https://doi.org/10.1007/s10584-015-1536-6

Acknowledgements

First and foremost, I would like to thank my supervisor, Guðrún Marteinsdóttir, for taking me onto this project, welcoming me to Iceland, and sharing your knowledge and curiosity about the Icelandic ecosystem. I am particularly grateful for the encouragement to pursue my own interests and avenues, and the incisive comments when I have gone too far afield. I thank Steve Campana for his insightful and thorough comments on my thesis, the writing tips and encouragement, and the post-work workouts on the squash court.

During 2013, I spent four months at the University of Bergen. I would like to thank all members of the Theoretical Ecology Group for their hospitality during this period. The group's passion for adaptive behaviour has left an indelible impression upon me that has undoubtedly shaped the contours of this thesis (beyond our collaborative work). I would like to thank the "Optimal versus Rule" group for the fruitful discussions. In particular, I thank Øyvind Fiksen for his supervision, hands-on guidance and help with individual-based modelling, and for encouraging me to embrace a picture that is bigger than a larval fish.

To my distinguished opponents, Pierre Pepin and Alejandro Gallego, thank you for taking the time to review this thesis.

The project was funded by Nordforsk via the Nordic Centre for Research on Marine Ecosystems and Resources under Climate Change (NorMER). I thank Nils Christian Stenseth who spearheaded NorMER, Jason Wittingham who coordinated the programme, and all the fellow NorMER-ians who made the annual meetings such a source of great fun, both scientifically and socially. Special thanks to Johanna Yletyinen who seeded the idea for the fish stock collapse paper and has been a wonderful collaborator ever since.

Studying in MARICE, I have worked alongside a wonderful set of people. For the chat, collaborations, and fun times, I thank everyone who has passed through MARICE's doors since I started. Specifically, I thank Kai Logemann for developing the tools that facilitated much of the work in this thesis, for sharing his knowledge, feedback, sailing boat space, and patience when responding to all my questions and requests. And to Jed Macdonald, thanks mate, from the first beverage to the last, it has been a pleasure. I will refrain from calling this thesis my magnum opus, purely because Macdonald and Butler 20XX looms (slowly and from a distance) on the horizon!

Despite spending the majority of my PhD engulfed in R and Fortran, I did manage to venture out into the field and laboratory in the first year. This experience was made all the more enjoyable (and efficient) by working alongside Tom Langbehn. For all the hard work and boundless enthusiasm, thanks, Tom. I also thank the captain and crew of the "Friðrik Sigurðsson ÁR", "Kristbjörg ÍS 177", "Kristbjörg VE-71" and "Örn KE 14" for their hospitality and help whilst sampling in the field, as well as the the staff at the Marine Research Institute's Mariculture Laboratory at Staður for their technical assistance and hospitality whilst conducting laboratory experiments.

Having now dwelled in Iceland for a number of years, I have had the privilege of making many friends who have enriched my time here and contributed (in a good way) either directly or indirectly to this project. Rather than leading off this thesis with an inaccuracy by omitting someone, I simply extend my thanks to each and every one of my friends.

Finally, to my partner, Xindan Xu, thank you for all the support, the games, the chat, the cooking, the trips, and everything else over the last five years. And to Dad, Jackie, Jodie, and Lottie, thank you for encouraging me to take on the project and for supporting me throughout its duration, I promise to explain it all one day!

1 Introduction

1.1 Thesis overview

1.1.1 Marine population dynamics

"It is better to be a big fish in a small pond than a small fish in a mighty ocean" – Anon.

This proverb highlights that the importance of an individual declines as their sphere of influence decreases. However, taken literally, it also contains a simple ecological truth: it is better to be a big fish in a small pond than a small fish in the ocean because mortality rates are (in most cases) substantially lower for larger fish. Most marine fish produce large numbers of offspring of which only a small number survive to settlement. This relationship reflects the exceptionally high mortality rates that marine early life-stages experience, a natural corollary of which is that small changes in early life-stage mortality can have large impacts on year-class strength (Houde 1987).

The high mortality of marine fish early life-stages has generated an extensive body of research trying to establish links between early life-stage survival and recruitment variability. Johann Hjort laid the groundwork for these studies with two hypotheses: (1) the critical-period hypothesis, and (2) the aberrant drift hypothesis (Hjort 1914, 1926). The critical period hypothesis suggests that bad year-classes result from the failure of first-feeding larvae to find suitable feeding conditions. The second hypothesis states that variation in recruitment is a result of advection to unfavourable habitats (i.e. habitats from which juveniles cannot return to recruit). These hypotheses have been refined and expanded upon in several subsequent paradigms (see reviews by Houde 2008 and Hare 2014). Biophysical interactions lie at the heart of (most of) these hypotheses because the environment shapes the potential for the early life-stages to feed, grow and die – processes that define the success of an individual and thus the collective year-class strength.

There are three sources of mortality for the early life-stages: starvation, predation, and advective losses. Starvation lies at the heart of the critical-period hypothesis but has been hard to prove empirically (Leggett and DuBlois 1994). This is mostly due to difficulties in establishing (1) accurate prey fields and (2) relationships between larvae in low condition and those that actually die from starvation (Peck and Hufnagl 2012). Whether or not an individual larva will starve depends on its ability to encounter, capture, and ingest food. This is not solely a function of prey abundance; it depends on a larva's initial state (e.g. Garrido et al. 2015), its physical abilities – which greatly improve through ontogeny – and the ambient environment which can mediate trophodynamic interactions in complex ways. For instance, depleted energy reserves (the first stage of starvation) can lead indirectly to increased mortality via decreased growth (Takasuka et al. 2003), hindered anti-predatory responses, or altered foraging behaviours (Vollset et al. 2013; Jørgensen et al. 2013). Furthermore, encounter rates of first-feeding larvae are strongly dependent on turbulence because the larvae have limited motile abilities (MacKenzie et al. 1994; Sundby 1997), even under high prey concentrations, feeding can be limited when viscous forces dominate over inertial ones (China and Holtzman 2014).

Predation is considered to be the most important source of mortality for the early life-stages (Houde 2008; Peck and Hufnagl 2012) and typically displays a decline through ontogeny as larvae grow and develop improved sensory and locomotive abilities (Peterson and Wroblewski 1984; McGurk 1986). This trend of size-selective mortality has generated a number of paradigms that highlight the benefits of growing fast or minimising the stage-duration (Bailey and Houde 1989; Houde 1997; Takasuka et al. 2003). These paradigms were expanded upon by Fiksen and Jørgensen (2011) and Jørgensen et al. (2013) who used an evolutionary perspective to highlight that survival is reduced at low prey concentrations, but through increased predation rather than reduced growth. In low prey concentrations, individuals will maintain high growth rates by taking "riskier" foraging decisions which leads to greater mortality at the population level through predation rather than starvation. Such approaches highlight that individuals are equipped with a diverse set of behaviours to cope with a range of environmental conditions and that vital rates such as growth and mortality should emerge from behavioural interactions rather than taking presumed forms (e.g. low prey = low growth).

Advective losses are incurred through the dispersal of early life-stages to unfavourable habitats (Sinclair 1988). Considerable variation can exist in the amplitude and direction of currents throughout the water column. This means that fish eggs and larvae separated by small vertical distances can take vastly different drift trajectories which can lead to variation in the quality of habitat experienced during the first feeding "critical period" and in the transport success of early life-stages to suitable nursery grounds (Parada et al. 2003; Fiksen et al. 2007; Kuroda et al. 2014). This is a purely physical process for fish eggs, yet several examples exist of how the physical properties of eggs are adapted to environments in a way that facilitates retention or favourable vertical positions through biophysical interactions (e.g. Sundby et al. 2001). For larvae (and young juveniles), biophysical interactions are complicated by an individual's capacity to move between habitats. Larvae may "knowingly" follow cues to suitable nursery habitats (e.g. Paris et al. 2013) or retention may be facilitated indirectly through foraging behaviours (e.g. Ospina-Alvarez et al. 2012). To understand these processes, complex spatially explicit models are required that can both simulate hydrodynamic processes at a high resolution and incorporate the movements (horizontal and/or vertical) of individual organisms.

The contemporary notion of recruitment variability integrates a complex mixture of processes operating across multiple life-stages (Houde 2008; Hare 2014; Somarakis et al. 2019). Whilst the survival of the early life-stages is undoubtedly of great importance, processes operating at each subsequent life-stage can also contribute to recruitment variation (e.g. Ottersen et al. 2014). For instance, the number and quality (traits that promote survival) of eggs produced depends upon the abundance of spawning adults, the size/age-structure of the spawning population, its sex composition, and its underlying distribution(s) of maternal traits. This links the survival of early-life stages to the spawning population because increases in the production of viable eggs improves the chances that a larger number of larvae will survive and potentially recruit.

Relationships between spawning stock biomass (SSB) and recruitment have proven difficult to ascertain with confidence, often the fits of stock-recruitment models can be improved by incorporating additional information (e.g. size structure) or using an alternative proxy of reproductive potential such as total egg production (e.g. Marteinsdottir and Thorarinsson 1998; Trippel 1999; Marshall et al. 2006; Takasuka et al. 2019). However, many of the world's fish stocks are managed via biomass-specific thresholds,

some depleted stocks have responded well to management strategies based on these thresholds (e.g. Fernandes and Cook 2013) and some have shown little recovery despite reductions in fishing effort (Hutchings 2015). The absence of recovery is indicative of a "collapsed" state – the endpoint of a depletion – which can have substantial impacts on ecosystem structure, functioning, and services. For this reason, detecting and distinguishing between depleted and collapsed states is of considerable importance for rebuilding fish stocks to sustainable levels.

1.1.2 Objectives

This thesis is based on the concepts outlined above. The overall objective is to utilise bottom-up and top-down quantitative approaches to understand the population dynamics of marine fish. Specifically, the thesis aims to provide novel data and insights regarding the early life-stages of commercially important Icelandic gadoids, as well as to provide a series of recommendations and proposed methodologies for quantitatively evaluating aspects of marine population dynamics. **Papers I**, **II** and **III** focus on the biophysical interactions that shape the survival of marine fish early life-stages. **Paper IV** focuses on the relationship between a fish stock's reproductive potential (SSB) and production. A brief overview of each paper is as follows:

In **Paper I**, the egg size and density of three Icelandic gadoids was measured and utilised in a 1-dimensional model to examine how vertical egg distributions vary between species at inshore and offshore spawning locations. In **Paper II**, a 3-dimensional Lagrangian particle tracking model was developed to examine how both the magnitude and direction of egg and larval dispersal vary between inshore and offshore spawning locations. In **Paper III**, a 1-dimensional model that simulated the foraging behaviour of a larval fish was developed. The model was used to test and develop a method for incorporating adaptive vertical movements into drift models. In **Paper IV**, a top-down approach was adopted to assess the relationship between reproductive potential (SSB) and production. Specifically, how to identify when a decline in SSB has led to impaired production.

1.2 Icelandic marine ecosystem

1.2.1 Atlantic cod (Gadus morhua)

The Atlantic cod is an iconic species which is of considerable historical, social, and cultural importance (Kurlansky 1997). Distributed throughout the North Atlantic, cod inhabit a broad range of habitats from shallow to deep (down to ~600 m) waters and from marine to brackish environments. Cod can live up to 25 years old and show considerable variation in life-history traits between stocks (Salvanes et al. 2004; ICES 2005). For instance, the age at which 50% of the stock is mature ranges from 2 – 7 years (ICES 2005). Feeding primarily on crustaceans when small and teleosts when large, cod are (or "were" in some cases) an important component of ecosystem functioning (Frank 2005). The ontogenetic shift in diet is commonly seen throughout North Atlantic cod stocks, although specific prey preferences are system specific (Link et al. 2009). In Iceland, declines in cod condition have been linked to declines in capelin abundance (Astthorsson et al. 2007). Another consistent feature of North Atlantic cod stocks is the existence of multiple migratory types, with some components displaying sedentary/resident localised behaviours, others undertaking seasonal migrations with a homing component, and others undertaking large migrations without showing signs of site fidelity (see Robichaud and Rose 2004).

Icelandic cod fishery

The fisheries of Atlantic cod have provided food and sustained livelihoods for centuries, and when the populations have collapsed, substantial socio-economic and ecological impacts have resulted (Hutchings and Myers 1994; Hammerschlag et al. 2019). In Iceland, cod have provided a valuable source of sustenance to the population since the first settlement (Jónsson 1994). Over the past centuries, the cod population has undergone several large fluctuations, including a possible collapse in the 17th century, that have been linked to large scale temperature fluctuations (Jónsson 1994; Ólafsdóttir et al. 2014). In the second half of the 20th century, sustained increases in fishing effort led to a greater influence of harvest rates on population abundance (Schopka 1994). The SSB underwent a gradual decline from the 50s to the 80s. Underlying this decline were contrasting trends of increasing effort and decreasing yield (Jakobsson and Stefánsson 1998) – an indication of overexploitation. In particular, the removal of larger, older individuals led to a truncated age-distribution that reduced the stocks reproductive potential (Marteinsdottir and Thorarinsson 1998) making the stock more susceptible to the unfavourable environmental conditions that have occurred intermittently since 1965 (Schopka 1994; Jakobsson and Stefánsson 1998; Astthorsson et al. 2007). The persistence of low stock levels triggered (in part) the implementation of the "individual transferable quota system" in 1984 and the subsequent harvest control rule in 1996 (Chambers and Carothers 2017; Elvarsson et al. 2020). From the late 90s, SSB has gradually increased and is currently (as of 2018) at its highest level since 1960 (ICES 2019).

Spawning biology of Icelandic cod

Cod are an iteroparous broadcast spawning species. Individual females can produce millions of eggs that are released in batches throughout the spawning season (Murua and Saborido-Rey 2003). The quantity and quality of the eggs produced are tightly linked to the traits (size and condition) of individual spawners (Marteinsdóttir and Steinarsson 1998; Marteinsdottir and Begg 2002), whilst the activity patterns of individual spawners (where and when to spawn) are often tightly linked to environmental features (e.g. Grabowski et al. 2012). Such relationships – that link spawner traits to larval viability via the environment – can have significant implications for a stock's structure and thus its spawning potential (Marteinsdóttir and Pardoe 2008).

The Icelandic cod stock is managed as a single unit (or state variable). However, as with many other Atlantic cod stocks, the population consists of multiple components. Take, for instance, the generalisation that Icelandic cod spawn from mid-March to mid-May in spawning grounds southwest and west of Iceland. This statement captures the essence of spawning activity patterns but not the variation. Firstly, smaller spawning grounds in the west, north, and east of Iceland also contribute (at least intermittently) to the surviving pelagic larval population (Begg and Marteinsdottir 2000, 2002; Brickman et al. 2007), potentially buffering the resilience of the stock to environmental fluctuations (Marteinsdottir et al. 2000). Secondly, females spawn progressively later in the season from the west to the north to the east of Iceland (Begg and Marteinsdottir 2000).

Variations in spawner traits and spatiotemporal spawning patterns also exist at a finer scale within the main spawning grounds SW of Iceland. Larger fish spawn closer to shore, produce more eggs of a larger size, and have a longer duration of spawning (Marteinsdottir et al. 2000; Marteinsdottir and Begg 2002). Inshore and offshore spawning components

have been discriminated via genetic discontinuities and otolith characteristics (Jónsdóttir et al. 2006a, b; Petursdottir et al., 2006; Pampoulie et al. 2006) and reflect the existence of two ecotypes that vary in habitat use and foraging behaviour (e.g. Bardarson et al. 2017). Despite a degree of spatial overlap at spawning, these ecotypes may be reproductively isolated due to fine-scale habitat preferences (Grabowski et al. 2011).

The existence of offshore and inshore intraspecific spawning components is a common feature globally. The differences in distance-to-shore between these components naturally engenders variation in the environmental gradients experienced by the respective early life-stages. Inshore spawning grounds are typically situated in proximity to freshwater runoff, and in the path of nearshore circulation patterns that may differ substantially from offshore counterparts. Brickman et al. (2007) found little variation between SW spawning sub-components in drift trajectories; however, their offshore spawning sub-component comprised multiple potential spawning sub-components (Marteinsdottir et al., 2000b; Petursdottir et al., 2006). One of the aims of this thesis is to examine how the vertical and horizontal transport of cod eggs and larvae varies between the inshore and offshore spawning grounds due to their respective hydrodynamic regimes.

The Iceland-Greenland connection

A degree of mixing exists between the Icelandic and Greenlandic cod stocks (e.g. Bonanomi et al. 2015, 2016). Pelagic 0-group fish surveys have highlighted that a fraction of the early life-stages spawned in Icelandic waters drift towards Greenland (Begg and Marteinsdottir 2000; Wieland and Hovgård 2002), whilst tagging studies have shown that some mature individuals migrate from Greenland to Iceland (Jónsson 1994). This is considered to be a one-way system with adult cod rarely migrating out of Icelandic waters (Jónsson 1994). Both the drift of larvae to Greenland and the natal homing of adults to Iceland have occurred intermittently in time (i.e. not every year) and, at various points in the 20th century, been beneficial to both stocks. For example, very strong recruitment events in the Iceland stock prior to 1950 were partly driven by high levels of immigration of adult cod from Greenland (Schopka 1994; Astthorsson and Vilhjalmsson 2002), and the successful transport of early life-stages to Greenlandic waters has to a degree aided the replenishment of the offshore Greenlandic stock (Stein and Borovkov 2004; Therkildsen et al. 2013). Both the transport of larvae/juveniles to Greenland and the immigration of adults from Greenland were reduced from the 70s, potentially as a result of the reduced stock sizes (Schopka 1994) or because of temperature-induced changes in the regional currents (Dickson and Brander 1993).

1.2.2 Icelandic haddock and saithe

Haddock (*Melanogrammus aeglefinus*) and saithe (*Pollachius virens*) share similar reproductive strategies with cod (Murua and Saborido-Rey 2003). In Iceland, they are important components of the Icelandic ecosystem and of considerable economic importance, though to a lesser extent than cod (Astthorsson et al. 2007). The main spawning grounds for both species are also SW of Iceland. However, despite spatial and temporal overlap in spawning activity, there are distinct differences between the three species. The most notable of these differences is the sequential nature of spawning activity in time, with saithe spawning from late January to mid-March, cod from mid-March to mid-May, and haddock from early April to late May (Jónsson and Pálsson 2013). Interspecific differences also exist in spawning site location, with the main spawning grounds for saithe located further offshore than for cod and haddock (Marteinsdottir et al. 2000; Armannsson et al. 2007). These interspecific differences in spawning activity will

generate environmental exposures for eggs and larvae that vary between the three species. In particular, distance-to-shore may have a large influence on early life stage survival due to the influence of freshwater runoff (described below).

1.2.3 Hydrography

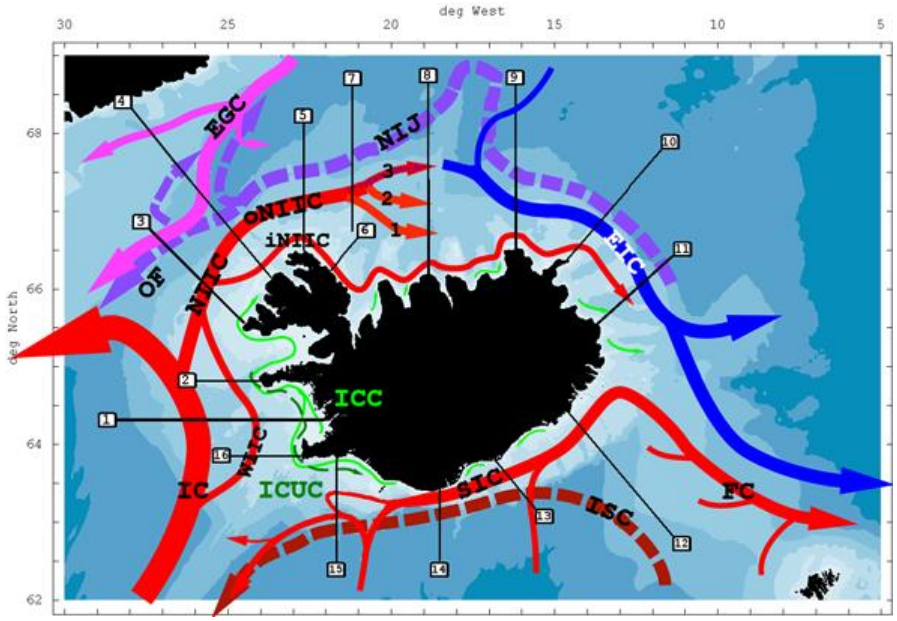

Figure 1*: Proposed three-dimensional circulation scheme of Icelandic waters based on the 3-d hydrodynamic model CODE (Logemann et al. 2013). The boxed numbers show the 16 sections used to analyse the model output. Dashed arrows denote deep currents. The abbreviations are: EGC – East Greenland Current, EIC – East Icelandic Current, FC – Faroe Current, IC – Irminger Current, ICC – Icelandic Coastal Current, ICUC – Icelandic Coastal Undercurrent, iNIIC – inner NIIC, ISC – Icelandic Slope Current, NIJ – North Icelandic Jet, NIIC – North Icelandic Irminger Current, OF – Overflow, oNIIC – outer NIIC, SIC – South Icelandic Current, WIIC – West Icelandic Irminger Current. Image and caption taken from Logemann et al. 2013.*

Iceland is located at the intersection of the Mid-Atlantic ridge and the Greenland-Scotland ridge, and at the confluence of Atlantic and Arctic water masses. The system of submarine ridges constrains the mixing and circulation of these water masses and has a great influence on Iceland's regional hydrography and marine ecosystem (Valdimarsson and Malmberg 1999; Jonsson and Valdimarsson 2005; Astthorsson et al. 2007; Valdimarsson et al. 2012; Logemann et al. 2013).

The Atlantic water originates from the Gulf Stream; it is warm, saline, rich in nutrients, and enters the Icelandic system through various offshoots of the North Atlantic Drift. The Polar water is cold, fresh (relative to the Atlantic water) and low in nutrients. It originates in the surface layer of the Arctic Ocean and enters the Icelandic system via the East Icelandic Current and small parts of the East Greenland Current (Fig. 1). Due to their contrasting properties, the relative amount of each water mass has important implications for the marine ecosystem (Astthorsson and Vilhjálmsson 2002; Astthorsson et al. 2007; Jónsson and Valdimarsson 2012; Valdimarsson et al. 2012). For instance, primary production is generally greater in southern waters owing to the stable presence of the

warm, nutrient rich Atlantic water. Whilst on the northern shelf, both primary and secondary productivity are strongly influenced by the ratio of Atlantic to Polar water masses which varies considerably in an interannual basis (Thórdardóttir 1984; Astthorsson and Gislason, 1998; Zhai et al. 2012; Valdimarsson et al. 2012).

For species that spawn SW and W of Iceland, the transportation of eggs and larvae to the nursey grounds in the north is facilitated by the Irminger Current and the Icelandic Coastal Current. The former current enters the Icelandic system along the western flank of Reykjanes ridge (a component of the mid-Atlantic ridge). It flows westwards and northwards before bifurcating prior to Denmark Strait. Large volumes of water are transported across to Greenland and a smaller portion flows over Denmark Strait continuing the clockwise flow around Iceland as the North Icelandic Irminger Current (Fig. 1). The Icelandic Coastal Current is driven by pressure gradients resulting from a freshwater induced density front (Logemann et al. 2013). The current originates south of Iceland, flows clockwise alongshore until finally mixing with the North Icelandic Irminger Current. As many species spawn close to shore in this current's path, it is a crucial mechanism for the transportation of the early life-stages to the north (Olafsson 1985; Begg and Marteinsdottir 2002; Brickman et al. 2007; Jonasson et al. 2009).

Freshwater runoff also has considerable influence on coastal ecosystem dynamics SW and W of Iceland where the main spawning grounds are located. In general, the thermocline develops mid-late May in southern Icelandic waters. Therefore, stratification throughout the spawning periods for cod and saithe (and to a lesser extent, haddock) is predominantly determined by the interaction between freshwater runoff and wind stress (Thórdardóttir 1986). This varies considerably on an interannual basis but when wind stress is low, the presence of coastal water stabilizes the water column, providing the conditions (including nutrients) to initiate the early phytoplankton bloom (Thórdardóttir 1986; McGinty et al. 2016). This has important implications for secondary production which includes key prey species for gadoid larvae (Thórdardóttir 1986; Gislason et al. 1994; Gislason et al. 2016).

1.3 Individual-based models

1.3.1 Overview

Individual- or agent-based models (hereafter referred to as IBMs) are bottom-up simulation models that are commonly used to examine population and community dynamics (DeAngelis and Grimm 2014). The central concept underpinning IBMs is that populations consist of distinct, autonomous individuals, and through the interactions of these individuals with each other and the environment, population properties emerge (Grimm and Railsback 2005). Traditional analytical models generally treat populations as homogeneous units characterised by mean values. However, considerable intraspecific variation in traits can exist within these units, and this variation can have impacts on higher levels of biological organisation (Bolnick et al. 2011; Violle et al. 2012). IBMs address this by focusing on the individual, the level of organisation at which interactions occur (Huston 1988). A brief description of how intraspecific variation is incorporated into IBMs is outlined below.

Each individual possesses a unique set of attributes, this set is typically referred to as an attribute vector (Chambers 1993). This describes the state of the individual and can consist of any number of diverse variables, for instance, an individual's spatial location, gut fullness, or size. The attribute vector can also include a strategy vector that determines

how the individual behaves at each timestep. This may parameterise rules that link an individual's behaviour to its state and/or ambient environment at each timestep. The initial population is therefore characterised by a distribution(s) of attributes that (1) can be tracked in time to follow an individual's state, and (2) can govern how each individual interacts with biotic and/or abiotic features. Demographic features (e.g. vital rates or spatial distributions) thus emerge from the behaviours of multiple, distinct individuals.

The behaviours of individuals are assumed to be honed by natural selection and thus operate in a way that maximises (directly or indirectly) fitness (Grimm and Railsback 2005). The approach of individual fitness-maximisation more closely reflects reality than top-down approaches and provides the basic mechanisms to explore how populations respond to existing and potentially novel environmental gradients in adaptive (or maladaptive) ways (Stillman et al. 2015).

1.3.2 Adaptive behaviour

"Individual behaviour that results from adaptive traits instead of being directly specified. Adaptive behaviour therefore is an outcome of both the trait and the conditions at the time the trait is executed" – Grimm and Railsback (2005).

To explain adaptive behaviours, they are often broken down to ultimate and proximate causes (Mayr 1961). Ultimate causes explain **why** behavioural actions are taken, often from an evolutionary perspective (i.e. fitness-maximisation). Examples include predator avoidance and energetic gain. Proximate causes explain **how** behaviours work, they have an immediate, mechanical influence on a trait (Laland et al. 2011) and can arise from both internal and external sources. The prevalence of foraging schedules that are in some way synchronised with the light-dark cycle makes optical gradients a common proximate cause of foraging behaviours. Another common proximate cause is hunger, or to be more specific, the biochemical signals of hunger/satiation.

Behaviours will often be driven by multiple ultimate goals (Nathan et al. 2008). For example, energetic gain and predator avoidance are rarely mutually exclusive. Hiding in a secure refuge for eternity would be the optimal predator avoidance strategy were it not for the risk of starvation and physiological impairment. The need for energy and safety creates a trade-off that has shaped foraging behaviours such as activity levels and habitat choice (Lima and Dill 1990; Houston et al. 1993; Werner and Anholt 1993). Similarly, multiple proximate causes may underly observed behaviours. The presence of a single cue may elicit an adaptive response, but the presence of two cues may produce a better one (e.g. Amo et al. 2004). Organisms receive multiple data-streams simultaneously and may possess sophisticated methods to integrate this information (Munoz and Blumstein 2012). To gain insights into potential behavioural responses to future (and potentially novel) environments, understanding how this wealth of information is translated into behavioural responses via the cue-response system is essential (Sih et al. 2013; Ehlman et al. 2019).

1.3.3 How to model adaptive behaviour in IBMs?

"Decision rule: a description (without specifying the underlying neural mechanisms) of the relationship between an internal or external stimulus and the choices an individual will make" – Fawcett et al. (2013).

Adaptive behaviour emerges from a set of rules in IBMs. These rules are contained in a "behaviour sub-model" and determine how the individual(s) make decisions. A wide range

of rules have been implemented in IBMs that vary greatly in complexity (see reviews by Tang and Bennett [2010] and DeAngelis and Diaz [2019]). An individual may be instructed to follow or respond to a particular gradient (a taxis), or to evaluate a sequence of logical rules (if-else statements) where thresholds on causal factors determine the appropriate action(s) to be taken. Such approaches are appealing due to their computational efficiency and because the modeller can "curate" the rules to specifically mimic observed behaviours (Grimm and Railsback 2005).

To simulate behaviours in unpredictable environments that are subjected to feedbacks from individual actions, greater complexity is often required in rules (DeAngelis and Diaz 2019). Such rules may consider multiple cues from both internal and external sources, as well as an individual's capacity to memorise and predict. These rules often employ a fitness-seeking component where the benefits and costs of alternative actions are evaluated prior to acting (e.g. Kristiansen et al. 2009). For example, in state- and prediction-based theory, an individual acts to maximise fitness which is defined as the expected survival from predation and starvation over the time horizon under constant conditions (Railsback and Harvey 2013). Another approach is to evolve rules using techniques from artificial intelligence. For example, reaction norms describing how individual's responds to various stimuli can be evolved using genetic algorithms (e.g. Giske et al. 2013; Quinones et al. 2016; Budaev et al. 2019). In these models, rules are not implemented explicitly, they emerge from a simulated version of natural selection.

1.3.4 Optimal or sub-optimal behaviours?

The optimal strategy for an individual is the one that maximises its fitness (lifetime reproductive success). To find the optimal strategy, an individual must therefore "know" how each decision it makes will affect its ultimate fitness. This assumption entails that environments are predictable and that behaviours are completely flexible, i.e. individuals are free from phenotypic constraints (the phenotypic gambit, Grafen 1984) other than those imposed upon the model (McNamara and Houston 2009). These assumptions underlie dynamic state-variable models (DSVM) which utilise dynamic programming to find optimal strategies in stable environments (Mangel and Clark 1988; Houston and McNamara 1999). In these models, an organism is characterised by a set of state variables which can reflect its biology (e.g. size or gut fullness) and/or environment (e.g. hour or habitat quality). The resulting "rule" is a lookup table that specifies the action(s) an organism should take for each possible value/combination of the state variables.

The assumption of completely flexible behaviours is not met in reality because phenotypic plasticity has associated costs (DeWitt et al. 1998) and individuals are constrained by proximate mechanisms, such as their ability to learn and process information (McNamara and Houston 2009; Fawcett et al. 2012; Giske et al. 2013). The assumption of predictable environments is also rarely met in nature because environments consist of spatiotemporal gradients in variables directly and indirectly related to fitness (e.g. Staaterman et al. 2014; Gallagher et al. 2017; Kohl et al. 2018). Organisms interact with each other in direct (consumptive effects) and indirect (non-consumptive effects) ways that can lead to density-dependent feedbacks and "games" that produce conditions that are not foreseeable. Whilst we do not expect individuals to make optimal decisions, given a history of natural selection in similar environments, they should make decisions that perform well (Todd and Gigerenzer 2007; McNamara and Houston 2007; Fawcett et al. 2013). Therefore, by explicitly representing decision rules, IBMs are well equipped to address realistic

ecological problems that DSVM models are unable to tackle (without substantial simplifications) due to the assumptions outlined above.

Bearing these considerations in mind, an important step in evaluating the performance of decision rules is to compare their emergent properties to the optimal equivalents produced by DSVM models. Such comparisons can reveal (1) deficiencies in simple rule-based models, and (2) how proximate constraints may prevent the optima from being achieved (Hutchinson and Gigerenzer 2005).

1.4 Biophysical IBMs

1.4.1 Particle tracking models

Lagrangian particle tracking algorithms calculate the advection and diffusion of individual tracers in time and space. This approach differs from Eulerian methods which deal with concentrations of particles at fixed spatial points. Lagrangian algorithms can be applied to the output of 3-d hydrodynamic models to calculate the advection and diffusion of the early life-stages of marine organisms. The resulting Lagrangian particle tracking models are powerful tools for understanding connectivity between spawning and nursery grounds because dispersal trajectories are to a large extent dependent upon the direction, magnitude, and variation of ocean currents. These models have been greatly aided by increases in computational efficiency (Gentleman 2002) and have become the predominant tool for understanding the dispersal patterns of marine eggs and larvae (Swearer et al. 2019).

1.4.2 Biological particle tracking models

In a recent review of particle tracking models, Swearer (2019) found that the majority of studies considered larvae to be passive, unresponsive particles. For many species, this is an unrealistic assumption (Shanks 2009; Nanninga and Manica 2018). Key vital rates such as growth and mortality depend upon an individual's environmental exposure (e.g. Houde 1989) and an individual's environmental exposure can be mediated by its behaviour (e.g. Fiksen et al. 2007). For this reason, IBMs are often embedded within particle tracking models to simulate the behaviours of individual larvae or movements of individual eggs. Such coupled models offer the scope to capture many of the interactions that underpin the survival of fish eggs and larvae (Houde 2008; Hare 2014). The hydrodynamic model provides realistic, high resolution information on flow fields and environmental gradients, which are used to advect individuals through a heterogeneous environment. The IBM provides a platform to simulate how individual's respond to changes in the ambient environment and potentially their internal state via behavioural and/or physiological mechanisms.

One of the complaints often levelled at the IBM approach is that their complexity hinders an understanding of how the models actually works, i.e. the mechanisms driving the emergent properties (Grimm 1999). Coupled biophysical IBMs are certainly complex models, they are typically rich in parameters and require extensive sensitivity analyses to understand how the assumptions of the model affect its emergent properties (e.g. Brickman et al., 2007; Peck and Hufnagl, 2012). For example, Kvile et al. (2018) found that interannual variation in circulation patterns had a larger impact on dispersal patterns than model resolution or DVM behaviour. Conversely, North et al. (2008) found that implementing larval behaviours generated spatial patterns of transport more successfully than interannual variation in circulation patterns. These contradictory conclusions

illustrate that dispersal patterns are system specific. From the regional hydrography to the density of an individual egg, biophysical IBMs need to be tailored to the study system to reflect its patterns and processes. Furthermore, dispersal patterns need to be understood in terms of the constraints imposed upon the model and the assumptions underlying its formulation.

A common constraint is the lack of flexibility in the rule that generates larval behaviours. Of the particle tracking models that employ behavioural algorithms, very few employ direct fitness-seeking rules. If the rule is created to mimic an observed behaviour it contributes to fitness in an indirect manner, and it is assumed this observed behaviour occurs in all environments and under all internal states (i.e. it is not plastic). Is this a fair assumption for marine larvae? The active role of behaviour in larval transport has been demonstrated in numerous empirical studies (e.g. Paris and Cowan 2004; Santos et al. 2008; Morgan and Fisher 2010; Paris et al. 2013) and adaptive responses to predation risk and hunger have been demonstrated in laboratory experiments (Fuiman 1994; Skajaa et al. 2003). Implementing direct fitness-seeking rules involves additional parameters and computation time (due to the optimisation module); however, such approaches can yield novel insights into population growth rates and dispersal trajectories due to the flexibility of the behaviours. For instance, Kristiansen et al. (2011) showed that high survival of larval cod was driven by the duration of overlap with prey items rather than the match-mismatch between larval hatching and peak prey concentrations. Regarding drift trajectories, Vikebo et al. (2007) highlighted how individuals with varying levels of "boldness" – the propensity for an individual to take risks – can take vastly different dispersal trajectories.

1.5 Vertical movements of marine organisms

1.5.1 The egg stage

Estimates of the density (or specific gravity) and, to a lesser degree, the size of fish eggs are required to understand how eggs are vertically displaced. It is through the interactions of these traits with the environment that vertical egg distributions are generated (Sundby et al. 1991). However, prior to these interactions, it is necessary to consider the strategies and traits of spawning females (see Murua and Saborido-Rey 2003). For example, the precise spatiotemporal location that eggs are released will influence their environmental exposure which determines their vertical distribution (Checkley et al. 1988; Sundby et al. 2001; Nissling et al. 2017). If eggs are released into the pelagic, they will be advected and diffused, whilst if they are "stuck" to benthic substrate via an adhesive (e.g. herring), they will remain in a fixed position as long as the adhesive remains intact. Furthermore, several studies have highlighted relationships between the physical properties of eggs and maternal traits. Larger females tend to produce more eggs of a larger size. For batch spawners, egg size tends to decrease with each successive batch (Kjesbu et al. 1992; Vallin and Nissling, 2000; Trippel and Neil, 2004). Due to these relationships, the distributions of egg traits are tightly linked to the size-structure of the spawning population. This has important implications for vertical distributions, as well as harvesting strategies (Vallin and Nissling 2000; Barneche et al. 2018) and larval viability (Marteinsdóttir and Steinarsson 1998; Nissling et al. 1998; Marteinsdottir and Begg 2002).

Viewed from an evolutionary perspective, the size and density of fish eggs are traits that have been honed by natural selection to maximise maternal fitness (Jørgensen et al. 2011), i.e. they are adapted to the range of environments experienced by their ancestors. This is

demonstrated by the egg properties of Baltic sea species which inhabit a brackish (as opposed to marine) environment with strong spatial gradients in salinity and oxygen (e.g. Mackenzie et al. 2000). Baltic cod produce large, low density eggs, that ensure the eggs remain above the stressful anoxic layer (Nissling and Westin, 1991; Vallin and Nissling, 2000). This is an adaptation to avoid low oxygen environments, one also seen in Baltic sea flatfish species (Nissling et al. 2017) and other systems with deep anoxic layers (e.g. Sundby et al. 2001). In contrast, the closely related Norwegian coastal cod produces smaller eggs of greater density that generate a pelagic rather than bathypelagic vertical distribution (Jung et al. 2012). Studies that transplanted Baltic sea cod and flounder (*Pleuronectes flesus*) from brackish to marine environments highlighted that egg densities have a strong genetic adaptation to the Baltic environment and limited phenotypic plasticity in novel marine environments (Solemdal 1970, 1973; Nissling and Westin 1997).

Egg density and size show great variation between species (e.g. Pauly and Pullin 1988; Petereit et al. 2014; Sundby and Kristiansen 2015) and considerable variation can also exist at the intraspecific level (e.g. Vallin and Nissling 2000; Jung et al. 2012). Several studies have also highlighted how ontogenetic variation in egg density can have pronounced effects on vertical distributions (Ådlandsvik et al. 2001; Ospina-Álvarez et al. 2012; Petereit et al. 2014), possibly controlling the development and maintenance of mesopelagic egg distributions (Sundby and Kristiansen 2015). Using Atlantic cod as a model organism, Jung et al. (2014) analysed the mechanisms and proposed a generic template for the ontogenetic development of egg density. This involved an initial increase due to water loss, a subsequent decline as the embryo develops, and a final increase prior to hatching (Jung et al. 2014).

In **Paper I**, we sampled the eggs of wild-spawning haddock and saithe. Subsequently, we measured egg density and size through development until hatching. The dataset was combined with archived cod data and used to identify (1) whether there are differences in the physical properties of eggs between the three species, and (2) whether these physical properties change through ontogeny for each species. Summary statistics derived from this study were used as inputs to a 1-dimensional model to test how these observed differences impacted upon vertical distributions in various environmental gradients.

1.5.2 Modelling vertical egg distributions

The vertical position of a marine fish egg that floats freely in the water column is a function of the ambient environment (density and turbulence) and the egg's physical properties (density and size). The difference in density between the egg and the surrounding water determines the egg's buoyancy. In an environment with no vertical mixing, an egg will rise if positively buoyant and sink if negatively buoyant. Turbulence homogenises vertical egg distributions. Vertical gradients in turbulence depend upon wind velocities, wave energy, stratification, and bottom stress. It is typically strongest in the surface mixed layer and weakest at the pycnocline.

Using the concepts outlined above, Sundby (1991) used a one-dimensional modelling approach to illustrate how pelagic, bathypelagic, and demersal egg distributions can result from a variety of biophysical interactions. Two advection-diffusion models were used, one calculated the steady-state distribution of eggs (see Sundby 1983), the other was a numerical solution that simulated the temporal development of egg distributions (see Westgård 1989). Both models are based on a transport equation with advection (or vertical

flux) determined by an eggs terminal velocity – the velocity an egg ascends/descends when the buoyant forces balance the frictional drag – and diffusion modelled by Fick's law using the vertical eddy diffusivity coefficient. Both of these models, as well as alternate numerical schemes and functions for analysing egg distributions were implemented in the MATLAB VertEgg toolbox (Ådlandsvik 1998).

In **Paper I**, the VertEgg toolbox was utilised to model the vertical distributions of cod, haddock, and saithe eggs. The scripts were converted to the R programming language and additional functionality added where required. Specifically, we utilised a Monte Carlo Markov Chain (MCMC) method to incorporate natural variation in egg properties into the model. This was then compared with a mean-only approach to investigate whether the observed interspecific and ontogenetic differences in egg density and diameter (also **Paper I**) led to interspecific and ontogenetic differences in vertical egg distributions along a stratified water column.

The results from **Paper I** informed the design of the vertical egg displacement module in the 3-d Lagrangian particle tracking model developed in **Paper II** (see section 2.3 for details). As the model described above is a Eulerian approach which is not applicable to Lagrangian models, the "binned random walk" (BRW) developed by Thygesen and Ådlandsvik (2007) was utilised. This model can be viewed as a mixed Eulerian-Lagrangian approach that keeps track of an individual's depth bin rather than its precise location.

1.5.3 The larval stage

From large planktivorous sharks to miniscule crustacea larvae, migrations up and down the water column that are in some way synchronised with the day-night cycle are a ubiquitous behavioural feature of marine organisms. Collectively, these diel vertical migrations (DVMs) are potentially the largest daily movement of animal mass (Brierly 2014), they occur in freshwater and marine environments, from the tropics to the high and low latitudes (see Bianchi and Mislan 2016 and Behrenfeld et al. 2019 for global perspectives). An outcome of DVMs is the transport of carbon from the surface to deeper waters, they are therefore a critical component of the biological pump and thus the regulation of ocean carbon storage (Steinberg and Landry 2017; Kelly et al. 2019). Furthermore, by mediating trophic interactions, DVMs are an important structuring force in pelagic ecosystems (Hays 2003; Bollens et al. 2011).

The most common form of DVM includes an ascent at dusk and a descent at dawn (hereafter referred to as "normal DVM"). Other forms include a "reverse DVM" which mirrors the normal form (e.g., Ohman et al. 1983), and a "twilight DVM" with ascents and descents both occurring at dusk and dawn (e.g., Cohen and Forward 2005). Evidence from predator manipulation studies (Bollens and Frost 1991; Ohman 1990) and observational studies (Gliwicz 1986) have highlighted that DVMs are adaptive rather than fixed behaviours. That is, the behaviours expressed, e.g. when to move and in which direction to move, are flexible (to a degree), dependent upon the prevailing environmental conditions. For example, Ohman (1990) observed individual copepods from within a single population performing normal and reverse DVMs (as well as exhibiting no DVM); the former form occurred when the risk of predation increased in daytime (from visually feeding fish), the latter when the risk of predation increased at night time (from nocturnal zooplankton predators).

Predator evasion and energetic gain are widely considered to be the most important ultimate causes of DVMs (Lampert 1989; Hays 2003). Other ultimate causes include the optimisation of metabolic rates which are temperature-dependent, the transport to favourable habitats, and the avoidance of ultraviolet radiation (e.g. Sims et al. 2006; Fischer et al. 2015; Morgan 2014). Furthermore, trade-offs may exist between ultimate goals, Morgan and Anastasia (2008) showed that crab larvae are willing to accept higher predation risks (by ascending in daytime) in order to facilitate emigration from an estuarine environment. There is an extensive list of demonstrated proximate causes of DVMs. This most likely reflects the fact that marine organisms inhabit rich sensory environments and can possess multiple sensory apparatus (see Kingsford et al. 2002 and Leis et al. 2011 for larval fish reviews). However, changes in light intensity are widely regarded to be the principle proximate cause (Reebs 2002; Cohen and Forward 2009; Ringelberg 2010; Mehner 2012). As a cue for DVMs, there are several hypotheses regarding the actual functional form it takes, individuals may sense and follow a particular isolume (a "packet" of light) or swimming activities may be activated above a certain threshold of ambient light (see review of Cohen and Forward 2009). Furthermore, other proximate cues, such as hunger or fish kairomones, may serve to modify photo-behavioural responses (Cohen and Forward 2009; Ringelberg 2010) creating cue-synergies that modify the DVM patterns.

Upon hatching, teleost larvae typically have limited motile and sensory abilities which constrains the migratory abilities of younger larvae. However, the larval phase is characterised by rapid growth and development which means that larvae quickly develop the motion capacity to overcome (at least partially) hydrodynamic processes (Allen et al. 2018; Downie et al. 2020). This is often seen through the onset of DVM patterns with the development of notochord flexion and a subsequent ontogenetic vertical migration – a progressive deepening of the DVM pattern through ontogeny (Lough and Potter 1993; Hurst et al. 2009; Hernandez et al. 2009; Smart et al. 2013). From a behavioural ecology perspective, these changes in migratory patterns through ontogeny are driven by size-dependent gradients in foraging abilities, metabolic demands, and vulnerability to stressors (both abiotic and biotic). The observed behavioural strategies have been honed by these constraints and pressures to best balance the conflicting demands of growth and survival along these gradients. For instance, if mortality rates decline with size, the best strategy is probably to grow as quickly as possible to minimise the cumulative mortality and benefit from the lower mortality rates associated with larger size (Werner and Gilliam 1984; Jørgensen et al. 2013).

1.5.4 Modelling diel vertical migrations

Diel vertical migrations are a classical optimisation problem: how much risk is an individual willing to accept to maintain a healthy state? Optimal foraging theory tackles such questions by assuming that natural selection has honed behavioural strategies that maximise an individual's fitness (Pyke 2019). Solutions are found using "maximisation of a utility" approaches where the utility (or currency) to be maximised is either fitness or a proxy of fitness, such as the net rate of energetic gain (e.g. Charnov et al. 1976). For example, Clarke and Levy (1988) used a dynamic programming approach to model the foraging behaviour of juvenile sockeye salmon. The optimal behavioural strategy was to forage during narrow windows of time ("antipredation windows") that allowed the individual to fulfil its energetic requirements whilst minimising the risk of dying; the optimal strategy did not necessarily lead to maximal growth rates, fitness was maximised by selectively sacrificing growth for safety (Clarke and Levy 1988).

In biophysical IBMs that have environmental gradients that vary in space and time, optimal solutions cannot be found (see section 1.3.3). Behaviours are therefore often implemented via simple "rules of thumb"; an individual may move between adjacent depth bins at night and day or follow a sinusoidal pattern throughout the diel cycle. In the particle tracking model developed in **Paper II**, we simulated DVM using a simple rule where larvae migrated up and down the water column in accordance with the prevailing light regime (Opdal et al. 2011). A simple rule was chosen because simulating trophic interactions was not a goal of **Paper II**, therefore an approach that captured the essence of "normal DVMs" in a speedy algorithm that required minimal data was preferred. However, the drawback of such rules is that they are not fitness-seeking, i.e. behaviours are not driven by an ultimate goal(s). So even if the risk of predation in surface waters at night was far greater than during the day, an individual following this rule would still perform a "normal DVM" pattern, whereas a fitness-seeking approach would probably produce an "inverse DVM".

Ideally, a model of adaptive DVMs would capture the flexibility of DVMs seen in nature and produce realistic predictions regarding the timing and amplitude of migratory behaviours. A useful starting point is the rule that maximises the ratio between growth and mortality (De Robertis 2002). This rule is a useful proxy for fitness (Jørgensen et al. 2013) because it captures the need to survive and feed in a single objective. It was developed to explain ontogenetic shifts in various taxa as a function of mortality and growth rates (Werner and Gilliam 1984). In a constant environment, it optimises lifetime reproductive fitness, i.e. the same as dynamic programming (Sainmont et al. 2015). However, in IBMs with variable environmental gradients, the rule may lead to irrational behaviours that make little sense because the assumptions underpinning its original formulation are violated (reviewed in Railsback et al. 1999). For instance, if growth is negative, the rule will select the action that maximises mortality.

In **Paper III**, we developed an IBM to simulate the risk-sensitive foraging behaviour of a larval cod. As a starting point, we utilised a rule that maximised the **difference** between growth and mortality as a proxy of fitness. By utilising the difference, many of the weaknesses outlined by Railsback et al. (1999) are overcome (Fiksen et al. 2007; Kristiansen et al. 2009). We sequentially added complexity to the rule by including multiple foraging traits, proximate cues from internal and external sources, and length-dependence in the cue-response system. The rule thus captures the ultimate and proximate causes of DVMs in a computationally efficient algorithm that can easily be embedded within ecosystem models. All variants of the rule were evaluated against optimal behaviour to assess their performance.

1.6 From individuals to populations

The survival of early life-stages is largely driven by density-independent processes (e.g. advection to "good" or "bad" habitats). Theoretically this suggests a positive relationship between the number of eggs produced and the number of larvae that successfully settle. Furthermore, it suggests that an increase in the number of (viable) eggs produced increases the resilience of the early-life stages to stochasticity in the density-independent processes. For these reasons, a stock's reproductive potential—its ability to produce viable eggs/larvae that successfully recruit (Marshall et al. 1998; Trippel 1999)—has important implications for first year-class strength. High reproductive potential is provided by a large

abundance of spawners, and diversity in both a stock's age/size structure and its underlying maternal traits (Trippel 1999; Marteinsdóttir and Pardoe 2008).

Exploitation can adversely affect each of these components of a stock's reproductive potential, and thus the survival of early life-stages. Declines in SSB have been linked to reduced recruitment (Barrowman and Myers 1996; MacKenzie et al. 2003). Size- or age-truncation through the removal of older, larger females (i.e. age-truncation) that are more fecund can reduce the production of "better" quality eggs (Marteinsdottir and Steinarsson 1998; Hixon et al. 2014), essentially reducing a stock's reproductive resilience (Lowerre-Barbieri et al. 2014). In accordance with life-history theory, such harvesting regimes create selective pressures that can lead to changes in reproductive traits (e.g. earlier maturation) that negatively influence a stock's reproductive potential (Jørgensen et al. 2007). Whilst the impact of these changes on a stock's ability to recover may be smaller than the prevailing fishing pressure, the magnitude of decline, or natural mortality (Hutchings and Kuparinen 2020), management measure that aim to mitigate such changes are considered essential to maintain intra-stock diversity (Heino et al. 2013) and thus the ability of a stock to produce large numbers of larvae that successfully settle.

1.7 Marine fish stock collapses

"*Fish stock collapse: the reduction of a fish stock by fishing or other causes to levels at which the production is only a negligible proportion of its former levels. The word is normally used when the process is sudden compared with the likely time scale of recovery, if any, but is sometimes used melodramatically for any case of overfishing*" – Cooke (1984).

1.7.1 Exploitation status

Marine fish stock depletions and collapses can have significant impacts on ecosystem resilience, livelihoods, and food security. Characterising the state of marine fish stocks is therefore an important step for rebuilding stocks to sustainable levels and maintaining sustainability where it exists. The most recent assessment of the "State of World Fisheries" by the Food and Agricultural Organisation (FAO) highlighted that, as of 2017, 34% of the world's fish stocks are unsustainable and 21% of the global catch comes from unsustainable stocks (FAO 2020). Both values have increased in time from the 1970s (FAO 2020), although sustainability has generally increased in regions with scientific assessments as opposed to those without (Costello et al. 2012; Hilborn et al. 2020).

The current framework employed by the FAO for the assessment of exploitation status consists of three potential states: overfished (biological), maximally sustainably fished, and underfished (FAO 2020). Stocks are assigned to a state based on four indicators: stock abundance (of primary importance), spawning potential, catch trend, and size/age composition (FAO 2011). This framework is a simplification of the previous criteria, a process (the simplification) which was driven by the need to both reflect uncertainty in stock status and produce assessments that are comparable between stocks that may greatly differ in data availability, biological traits, and harvesting regimes (FAO 2011). The FAO do not include a "collapsed" state in their annual assessments. In part, this is due to uncertainty over the specific level of decline from B_{MSY} (the biomass that can sustain maximum sustainable yield) required for a stock to be collapsed, and also because the rate of biomass decline may be more important than any specific reference value (Garcia et al. 2018). However, distinguishing "collapsed" states from within "overfished" states is of

considerable importance for the formation and allocation of appropriate rebuilding strategies, particularly for stocks that do not have rigorous stock assessments. If production is impaired (a collapse, see below), the mechanisms that lead to population growth have been disrupted. The ecological and socio-economic implications of such an event are potentially far worse than if production is low but the potential growth mechanisms remain intact. The importance of global/regional assessments of the collapsed state is illustrated by the large number of meta-analyses of "collapsed" stocks (e.g. Worm et al. 2006, 2009; Costello et al. 2012; Essington et al. 2015; Pinsky and Byler 2015), and in some instances, the subsequent debate surrounding these analyses (e.g. Branch et al. 2011; Hilborn and Branch 2013; Pauly 2013). A notable feature amongst the previous studies on the "collapsed" state is that a unified quantitative definition does not exist. This has probably contributed to the diverging views of the collapsed state and highlights the need for such a definition, or at least to test whether such a definition is feasible.

1.7.2 Defining the collapsed state

The mathematical theory underlying fish stock collapses was provided by Cook et al. (1997). In fisheries, the replacement line is a function of fisheries mortality and defines the number of y recruits required to replace x SSB in the future. When the slope of the replacement line exceeds the slope of the stock-recruitment relationship, a stock spirals towards the origin as there is no non-zero equilibrium (Cook et al. 1997). A practical problem with this theory is that estimating the slope of the stock-recruitment curve close to zero is often unfeasible due to a lack of observations. This is one of the reasons for the use of "simpler" metrics to identify fish stock collapses. Another (related) reason is that for many of the world's fish stocks, it is simply not possible to establish stock-recruitment relationships due to data limitations or the inability to find a reasonable fit.

From a semantic perspective, the Merriam-Webster dictionary defines "collapse" as "to fall or shrink together abruptly and completely". Implicit in this definition and the biological definition of Cooke (1984) outlined above is that the change in population abundance has occurred over a relatively short period of time (Cumming and Pedersen 2017) and that the prospects of rebuilding the population will take a relatively long period of time. For instance, if a building or a lung collapses, the event is abrupt, and restoration is slow. This definition contrasts with "depletion" which is defined as "to lessen markedly in quantity", a definition that does not imply either "abruptness" or "impairment".

Studies have highlighted relationships between collapse and recovery rates. For instance, using IUCN's decline-rate thresholds as a proxy for collapse, Hutchings (2000) demonstrated that the rate of decline is negatively associated with the rate of recovery (see also Hutchings and Reynolds 2004). The impairment of production is of great importance because it can indicate insufficient management measures, decreased ecosystem resilience, depensatory effects, or that the causes that led to low recruitment persist (Lotze et al. 2011; Neubauer et al. 2013; Perälä and Kuparinen 2017). Petitgas et al. (2010) took the distinction between collapses and depletions a step further by comparing stocks that recovered from collapses/depletions on different timescales. The conclusion Petitgas et al. (2010) reached was that a collapse occurs when biomass loss (a depletion) is accompanied by a breakdown in its contingent (migrant vs resident) structure and habitat-use patterns (spawning and feeding). Approaches that look beyond changes in biomass are likely to uncover the mechanisms underlying collapses and offer more robust classifications (see also Buren et al. 2019); however, they also require greater data that will not be available for many stocks.

In **Paper IV**, we test the hypothesis that the lack of a unified collapse definition has contributed to contrasting perceptions of the state of fish stocks. First, we illustrate through a literature review that a common quantitative definition of fish stock collapse does not exist. Then we propose a definition specifically designed to be applied across multiple stocks in a consistent manner. Subsequently, we test how the classifications of the proposed and existing definitions compare to management thresholds defined as "the stock size below which there is a high risk of reduced recruitment" (thus capturing the essence of "collapse") for data rich stocks.

2 Methods

2.1 Sampling and analysis of gadoid eggs

Eggs from wild-spawning haddock and saithe were sampled aboard commercial fishing vessels in 2012 (Fig. 2). The eggs were fertilized *in vitro*, stored in unique batches (i.e., per female), and reared until hatching at the Marine Research Institute's mariculture laboratory. On multiple days-post-fertilisation (DPF), egg densities were measured using density-gradient columns (Coombs 1981) and egg diameters were measured from high-resolution photographs. The dataset was combined with archived cod data (Guðmundsdóttir 2013). A temperature correction was applied to a subset of the cod data to ensure all density measurements were standardised to 7°C. The dominant ontogenetic stage per species per DPF was then determined (Table 1) using the high-resolution photographs and the classification scheme of Thompson and Riley (1981).

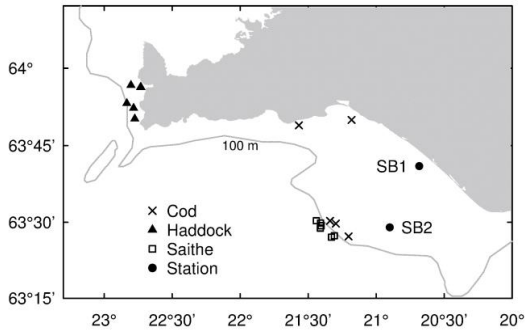

***Figure 2**: Sampling locations for each species. Environmental profiles for modelling (section 2.2) were extracted from a 3-dimensional hydrodynamic model at stations SB1 and SB2.*

A suite of linear mixed effects models were used to analyse the data. Separate models were fit for each response variable (density and diameter). Species, ontogenetic stage, and female length were fixed effects for both responses. Mean diameter per batch was an additional fixed effect for the density models. Batches were nested within species and implemented as a random effect. The procedure for model selection followed Zuur et al. (2009), and post hoc analyses were performed to identify specific contrasts that underlay significant effects.

	Ontogenetic stage				
	IAB	**II**	**III**	**IV**	**V**
Cod	2	5	7	10	13
Haddock	1	3	6	9	12
Saithe	1	3	6	-	9

***Table 1**: The dominant ontogenetic stage for each measurement day (DPF).*

2.2 Modelling gadoid vertical egg distributions

The MATLAB VertEgg toolbox (Ådlandsvik 1998) was used to model the vertical distributions of cod, haddock, and saithe eggs. Vertical profiles of the water column were extracted from the three-dimensional hydrodynamic model CODE (Logemann et al. 2013). Daily profiles consisted of vertical gradients in salinity, temperature and vertical eddy diffusivity for a period that encompassed the spawning activity (and thus the seasonal development in stratification) of all three species (Fig. 3). Profiles were extracted at two stations (Fig. 2): an inshore station (SB1) that lay in the path of the Icelandic Coastal Current, and an offshore station (SB2) that lay in the path of the incoming Atlantic water. All density measurements were converted to salinities of neutral buoyancy using the UNESCO equation of state for seawater (Millero and Poisson 1981).

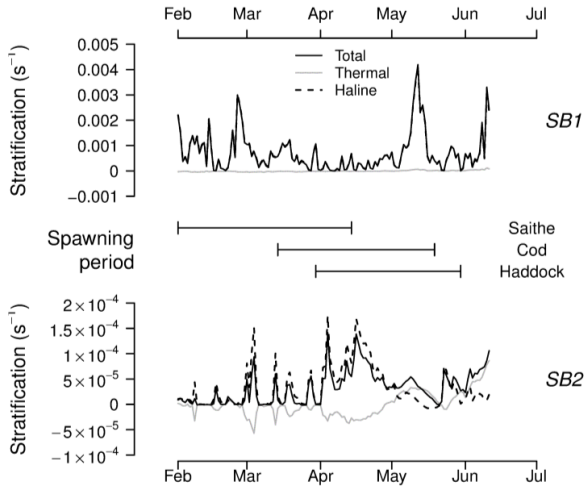

Figure 3*: Time series of stratification at each station in 2006. The water column's buoyancy frequency (N2) from 0–40 m was used as a measure of stratification. This is decomposed into its thermal and haline components (total = thermal + haline). For details on this approach, see Li et al. (2015). The middle panel shows approximate spawning periods for each species.*

For each profile, the steady-state vertical distribution of eggs was computed. This was done at two levels: (1) utilizing the pooled data for each species to examine interspecific differences in vertical distributions; (2) utilizing the stage-specific data for each species to examine intraspecific ontogenetic differences in vertical distributions. To account for natural variation in the physical properties of the eggs, a MCMC procedure was employed. This involved generating 75,000 random samples of the salinity of neutral buoyancy and/or diameter parameters, calculating the steady-state distribution for each sample, and aggregating all distributions by depth interval. This procedure was deployed at the inter- and intraspecific levels and contrasted with mean-only equivalents to understand how accounting for natural variation in egg properties changed the vertical egg distributions. The root-mean-square-deviation (RMSD) was used to compare distributions, this quantified how any two distributions differed in the number of eggs per m^3.

2.3 Biophysical IBM for larval cod

A Lagrangian particle tracking model that utilised high resolution flow fields from the 3-d hydrodynamic model CODE was developed. The model was coupled to an IBM that simulated the early life history of a larval cod, including temperature-dependent development (of the egg and larval stages), vertical displacement of eggs through an advection-diffusion module, and vertical displacement of larval through a DVM module. Simulations were carried out from 1998 to 2012. For each year, one thousand eggs were released per day from mid-March to mid-May, the main spawning period for Icelandic cod (Marteinsdóttir and Björnsson 1999). This procedure was carried out at two spawning grounds that correspond to inshore and offshore sub-components of the main spawning grounds southwest of Iceland (Fig. 4B).

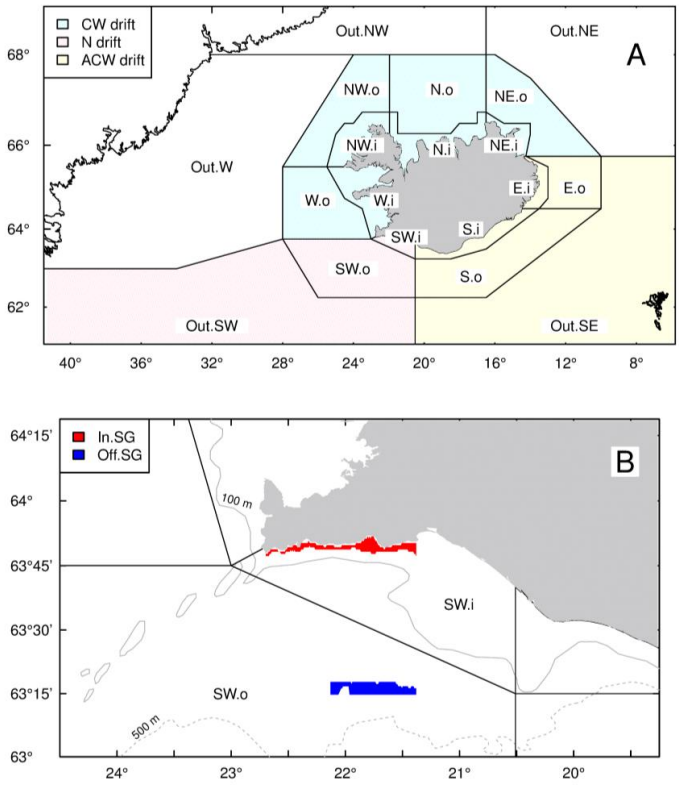

Figure 4*: Panel A shows the division of Icelandic and surrounding waters into distinct regions for analysing connectivity. The regions were divided into inshore and offshore components, identified by the "i" and "o" suffixes respectively. Regions located outside the regional grid have the prefix "Out". To analyse the direction of drifting particles, regions were grouped into clockwise (CW), anticlockwise (ACW) and neutral (N) components, indicated by the different shadings. Panel B shows the inshore (In.SG) and offshore (Off.SG) spawning grounds utilized for the release of particles.*

We created a map of endpoint regions to examine the direction and magnitude of dispersal. This was modified from an existing map (Begg and Marteinsdottir 2000) which was derived from known spawning grounds, 0-group surveys, and bathymetry. The larvae were assigned to a region based on their spatial location after 120 days of drift. This resulted in one connectivity matrix per spawning ground per release date that described the number of larvae that drifted to each endpoint region. The connectivity matrices were then aggregated over various spatial and temporal configurations to examine specific questions. To examine the direction of dispersal, the matrices were pooled into clockwise, anticlockwise, and neutral components (different shadings in Fig. 4A). These were subsequently aggregated over each spawning season to obtain the number of larvae drifting in each direction per year.

2.4 A proximate rule for risk-sensitive foraging

An IBM that simulated the risk-sensitive foraging of a larval cod was developed. The individual resided in a 1-dimensional water column which revolved around a fixed day of the year at an hourly timestep. The environment captured many of the key features a temperate marine larvae would experience including depth-dependent temperature and prey gradients, and ambient light levels that vary with time and depth, generating spatiotemporal gradients in foraging opportunities and predation-risk from visual predators (Fig. 5).

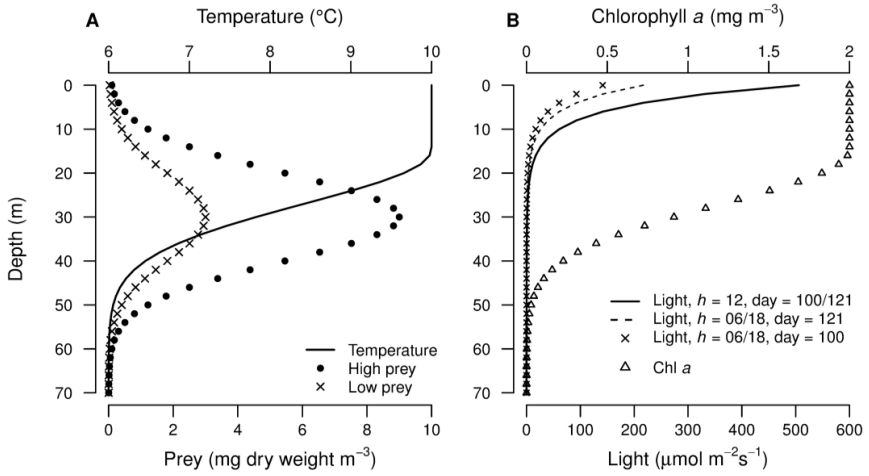

Figure 5*: Key environmental gradients for the model. Panel A shows the vertical gradients in temperature and prey density, including two scenarios for prey density. Panel B shows the vertical gradients in ambient light at midday (1200) and dawn/dusk (0600/1800) for two scenarios: an early date (day 100) and a late date (day 121. The vertical gradient in chlorophyll a is also shown in panel B, this determines how light is attenuated down the water column.*

The larva possessed two foraging traits: habitat selection and foraging activity. Each trait has associated benefits (energetic gain) and costs (mortality) that change through ontogeny. By changing habitat (depth), the larva could utilise the spatiotemporal light gradients to seek food and hide from visual predators (Fig. 6B). As the larva grew, it was more easily detected by visual predators and its visual range increased meaning it could scan a larger volume of water for prey within a timestep (Fig. 6B). Increasing activity levels led to more encounters with both prey items and invertebrate ambush predators such

as jellyfish (Fig. 6A). As the larva grows, it develops improved escape abilities (Fuiman 1994) leading to a gradual decline in predation through ontogeny (Fig. 6A).

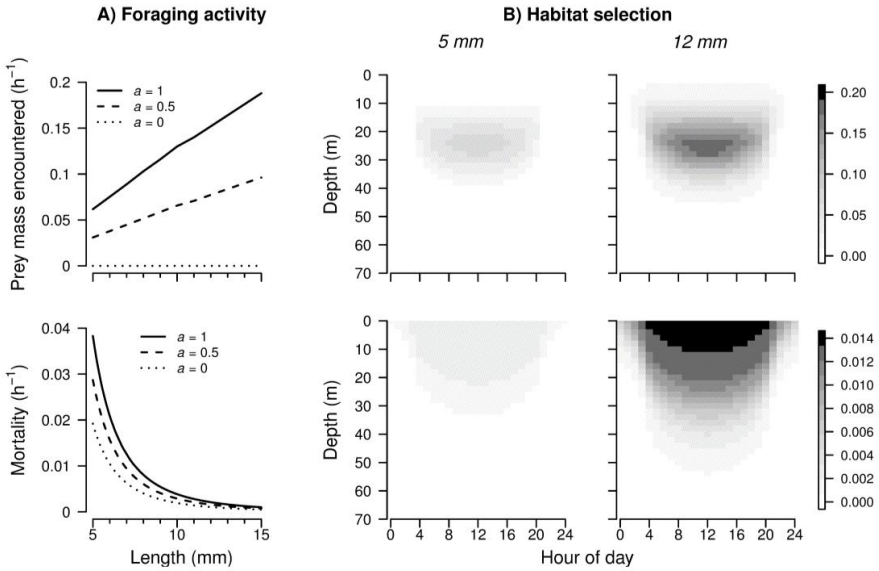

Figure 6*: Shows the benefits (energetic gain, top row) and costs (mortality, bottom row) of the foraging activity (A) and habitat selection (B) traits. For the foraging activity trait, three activity levels (a) are presented that correspond to the foraging speed in body lengths per second. For the habitat selection trait, the interaction between depth and hour is shown for a small (5 mm) and a large (12 mm) larva.*

At the core of the model was a decision-making module that determined the expression of both traits (i.e. where to move and how actively to forage). The module contained a simple fitness-seeking rule that was evaluated at each timestep and selected the "best" behavioural actions given the information provided in the rule. For simplicity, we illustrate how the rule works using the habitat selection trait:

$$z_i = max_z[F_z - m_z].$$

Here, the individual i calculated the difference between weight-specific ingestion F and total mortality m at each potential depth z. The best depth z_i is the grid cell where the difference was maximised. Once found, the larva moved to z_i and time moved forward one hour. We extended this model to include proximate cues that modulated the stimulation to forage:

$z_i = max_z[\theta_i F_z - m_z]$, where $\theta_i = \beta_{1,i} r + \beta_{2,i} l + \beta_{3,i}(1 - S)^{\beta_{4,i}}$.

The proximate cues (θ_i) were implemented in an additive manner and consisted of stimulation from light intensity (l), gut fullness (S), and inherent risk inclination (r). The form of each cue is determined by the parameters β_1-β_4. The resulting rule captures the ultimate goals of energetic gain and predator avoidance, and key proximate mechanisms underlying larval fish foraging behaviours.

An extensive parameter search was conducted to find the fitness-maximising parameters for a number of rules that varied in complexity (Table 2). Fitness was defined as survival at the target length of 15 mm. This procedure was carried out in three additional simplified environments: (1) fixed temperature through depth, (2) fixed concentration of prey through depth, and (3) a fixed background mortality from invertebrates (i.e. mortality did not decline through ontogeny). This allowed us to identify whether environmental gradients constrained the IBM's ability to capture optimal behaviour.

Rule	**Rule component**			
	Adaptive trait		**Proximate cues**	
	$\boldsymbol{a}$	$\boldsymbol{z}$	$\boldsymbol{\theta_i}$	$\boldsymbol{\theta_{i,L}}$
BL strategy	✓	-	-	-
F-M strategy	✓	✓	-	-
FP strategy	✓	✓	✓	-
LdP strategy	✓	✓	✓	✓

Table 2*: Shows the different proximate rules tested and how they differ in their formulation. BL = baseline, F-M = ingestion-mortality, FP = fixed proximate, LdP = length-dependent proximate, a = foraging activity trait, z = habitat selection trait,* θ_i*= proximate cues,* $\theta_{i,L}$*= length-dependent proximate cues.*

To analyse the output, survival per mm and fitness were expressed relative to optimal behaviour which was found using an equivalent DSVM model (Fouzai et al. 2019). The optimal larva **maximised** fitness, whereas the IBM larva **tried to maximise** fitness, and by comparing the two approaches, the strengths and weaknesses of various proximate rules became apparent (see section 1.3.4).

2.5 Evaluation of fish stock collapse definitions

We conducted a literature review to identify existing quantitative definitions of "fish stock collapse". Subsequently, we proposed a new collapse definition that addressed the weaknesses identified in the literature review. The proposed definition captured an abrupt decline to a depleted state. It combined two components of the existing definitions with each one expressed in terms of generation time, allowing its application across multiple stocks in a consistent manner (Fig. 7). Furthermore, we anticipated that the definition's formulation enabled depletions and natural fluctuations to be distinguished from collapses (Fig. 7).

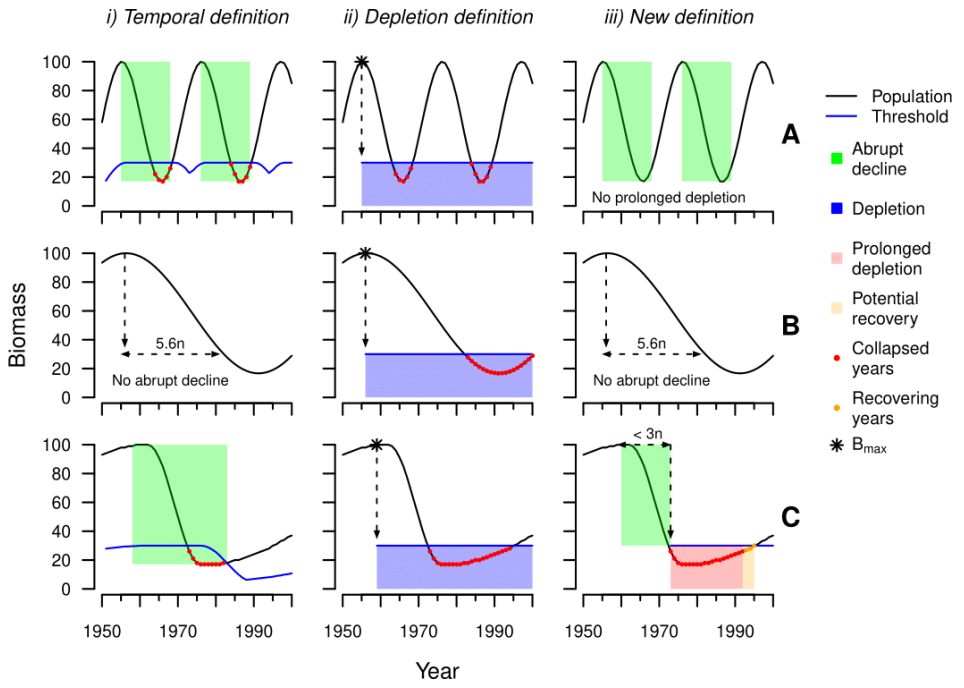

***Figure 7**: Three different collapse criteria (columns i, ii and iii) are applied to three hypothetical stocks (rows A, B and C) to demonstrate how the formulation of a collapse criteria can result in misleading classifications of a stock's state. Stock A fluctuates in a cyclic manner, stock B gradually depletes over a long period of time, stock C rapidly declines and exhibits prolonged depletion following the decline. The first definition (i) classifies a year as collapsed if a 70% decline occurs within three generations (i.e., it captures an abrupt decline). This can misclassify stocks with cyclic dynamics (i, A) because there is no consideration of prolonged depletion. The second definition (ii) classifies a year as collapsed if the stock's biomass falls below 30% of the historical maximum (B_{max}). This definition misclassifies a stock that gradually depletes (B, ii) because the rate of decline is not considered, and it misclassifies a stock with cyclic dynamics (A, ii) because it does not consider prolonged depletion. The proposed definition (iii) classifies a stock as collapsed if a decline of 70% within 3 generations is immediately followed by a period of prolonged depletion where biomass remains below the threshold for a generation. By considering the abrupt decline and prolonged depletion as an interlinked process, the proposed definition can filter out natural fluctuations (A, iii) and gradual depletions (B, iii) from more drastic collapses (C, iii).*

To test the performance of each definition, we extracted time series data for 44 stocks from the ICES stock assessment database (ICES 2019). The criteria for stock selection included: (1) that SSB had dropped below B_{lim} at some point in the time series, and (2) that sufficient years was available to run each definition. The mean age per year was calculated for each stock and used as a proxy for generation time. Each definition was then applied to each stock resulting in 1186 classified time series.

We also carried out a simulation experiment to examine how specific components of collapse definitions perform (see Fig. 7). Definitions were built from four parameters (Table 3) which describe the type of data, how the reference biomass is calculated, the magnitude of decline (from the reference biomass), and duration of prolonged depletion (how many generations biomass must remain below the threshold to be collapsed). All possible permutations of these parameters (270 in total) were then applied to each of the stocks.

Data type	**Ref. Biomass**	**% Decline**	**PD (*n*)**
SSB	Hist. Max	[10, 90, 10]	[0, 2, 0.5]
Catches	Hist. Max within 3*n* (AD)		
	Pop. Mean		

***Table 3**: Parameters and their resolutions used in the simulation experiment where n describes a stock's generation time, PD stands for prolonged depletion and AD stands for abrupt decline. The "% Decline" and "PD (n)" parameters are described in the format [min, max, increment].*

To assess how each definition performed, we compared each classified time series against the SSB < B_{lim} definition (Lindegren et al. 2009) for each stock. Our motivation for this approach was that B_{lim} is determined through dedicated expert groups under standardised guidance outlined by the "precautionary approach to fisheries management" (ICES 2003; Rindorf et al. 2016). Defined as "the stock size below which there is a high risk of reduced recruitment" (ICES 2019), B_{lim} captures the essence of a collapsed state and is thus a suitable benchmark against which to test simple definitions. Such analyses will provide useful baselines for the future application of definitions to data-limited stocks or those without equivalent management reference points. For each comparison we calculated the F_1 score which is a measure of a test's accuracy in binary classification. Defined as the harmonic mean of precision and recall, where precision is the proportion of predicted "collapsed" years that were correct, and recall is the proportion of actual "collapsed" years that were predicted correctly. A value of 1 indicated perfect precision and recall, whilst a value of 0 indicated that a definition's precision and/or recall completely failed.

3 Results and discussion

3.1 Gadoid egg density and size (Paper I)

Distinctive differences in egg density and diameter were found between the three species. Whilst cod and haddock had broadly similar values for both properties, saithe eggs were significantly smaller and less dense (Fig. 8b). These differences were seen at each ontogenetic stage (Fig. 8a).

There is minimal information regarding the egg density for haddock and saithe, therefore this study should provide a useful baseline for further studies on these species. Regarding egg diameters, similar interspecific trends (e.g. Markle and Frost 1985) and species-specific summary statistics from other systems (e.g. Trippel and Neil 2004; Skjæraasen et al. 2017) suggests that the observed interspecific trend is likely to exist across regions.

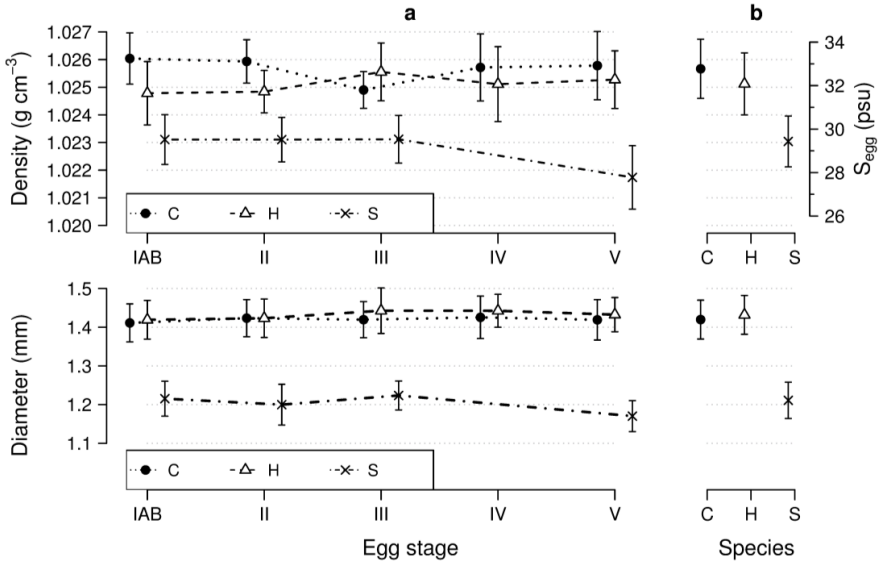

***Figure 8**: The top row shows the mean (±1 standard deviation) egg density and the corresponding salinity of neutral buoyancy (right axis) at 7°C. The bottom row shows the mean (±1 standard deviation) egg diameter. Stage-specific results are presented in panel a. Overall results (pooled over stage) are presented in panel b. For clarity, the points at each stage are staggered from left to right for cod (C), haddock (H) and saithe (S) respectively.*

The ontogenetic changes in diameter were a surprising result given that egg diameters are expected to remain constant through development (Jung et al. 2014). The significant comparisons were most prominent in saithe and, for all species, potentially driven by the small sample sizes. High within-batch correlations for each species highlighted that more robust population estimates could be attained by sampling more females.

The changes in egg density through ontogeny were fairly consistent between batches (individual spawners) for cod and saithe. A decline through ontogeny was seen in all batches for cod which fits the general pattern described by Jung et al. (2014); however, the rate of decline was ~90% quicker than the rate observed by Jung et al. (2014). Although the experimental setup was not appropriate for direct evaluation of the hypothesis proposed by Jung et al. (2004), the consistency of the decline between batches does suggest the existence of a unifying mechanism between spawners. The decline in saithe egg density at the final stage was seen in all batches that remained unhatched. As this was accompanied by a decline in diameter, it implies the loss of material (see Kjesbu et al. 1992 for details). As all the batches were on the cusp of hatching, the enzymatic dissolution of material is a potential explanation for this observation (Hall et al. 2004; Jung et al. 2014), although it should be noted that the confidence in the estimates of saithe egg density and diameter at stage V was considerably lower than all other ontogenetic stages.

3.2 Gadoid vertical egg distributions (Paper I)

Distinctive interspecific differences in the vertical egg distributions were only visible under strongly stratified conditions at the inshore station SB1 (Fig. 9A). In these conditions, saithe eggs occupied a higher position in the water column than cod and haddock (which had similar distributions). In highly stratified environments, vertical distributions were driven by egg buoyancy because vertical mixing was minimal. At the inshore station, stratification was much stronger (~22 times) than at the offshore station. The low salinity surface waters (from freshwater runoff [Fig. 3]) drove the cod and haddock eggs down but not the saithe eggs due to their lower salinity of neutral buoyancy (Fig. 8A). At the offshore station SB2 – which lay outside the path of the coastal current – the surface density under stratified conditions was greater than the egg densities for all species resulting in the majority of eggs for all species residing in the surface grid cell (Fig. 9A). These conclusions were not altered by incorporating the observed ontogenetic changes into the vertical distribution model, highlighting the minimal impact of ontogeny on the vertical egg distributions.

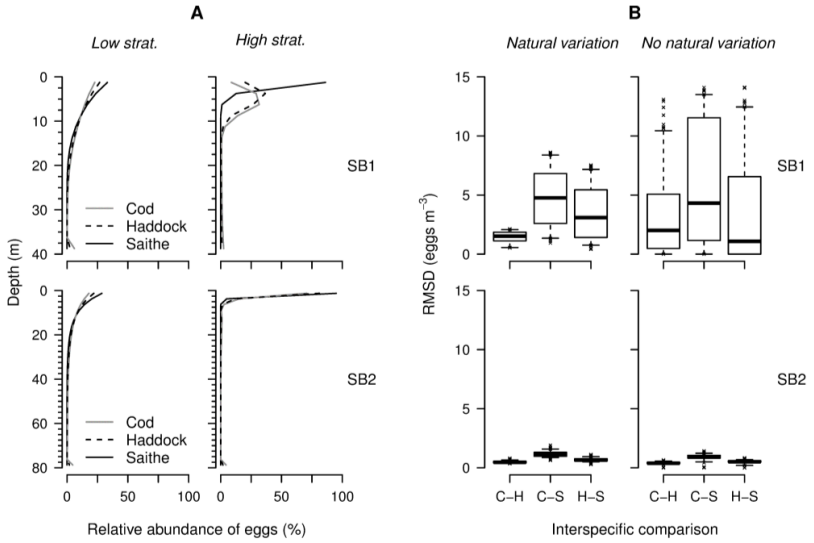

Figure 9*: Column A shows the vertical distributions of eggs for each species in a well-mixed (Low strat.) and a highly stratified (High strat.) environment at the inshore (SB1) and offshore (SB2) stations. Column B shows the interspecific contrasts pooled across all environments when natural variation in egg density is considered and when a mean-only approach is utilized (no natural variation). The RMSD values show the how the vertical egg distributions of cod (C), haddock (H) and saithe (S) differ in eggs per* m^3.

The majority of eggs for all species were positively buoyant highlighting that the ultimate function of the egg traits is to maintain a high position in the water column. For saithe, which spawn earlier in the season and further offshore than cod and haddock, their eggs will ascend quickly and agglomerate in the surface layer. The vertical distribution of eggs determined predominantly through wind-induced turbulence rather than stratification-induced changes in buoyancy. The model suggested a similar pattern for cod and haddock that spawn further offshore. For coastal spawners, vertical distributions will depend on the interaction between freshwater runoff and wind stress. Sub-surface distributions may become evident when the freshwater layer promotes stability and buoyancy in the surface layer becomes negative. Although, even in these cases, the egg distributions will remain pelagic and well within the vertical range of the Icelandic Coastal Current (see Logemann et al. 2013).

Inclusion of natural variation in the salinity of neutral buoyancy into the model had a large impact on both the interspecific and ontogenetic contrasts at the inshore station (Fig. 9B). This was seen in a reduced spread of the RMSD values by cutting down the right-hand tail of the distributions (Fig. 9B). This result highlights that in highly stratified environments (when buoyancy is minimal), utilising mean values to generate vertical distributions can lead to substantial interspecific and ontogenetic differences that are not seen when utilising a distributional approach. This result highlights the importance of including a trait for natural variation in the salinity of neutral buoyancy into biophysical IBMs.

3.3 Dispersal of larval cod (Paper II)

The drift of larvae clockwise around Iceland was evident from both spawning grounds (Fig. 10A, B). However, the proportion of larvae that drifted clockwise was greater and

more stable across years from the inshore spawning ground (Fig. 10C). From the offshore spawning ground, substantial proportions of larvae drifted anticlockwise to endpoints in the SE and in a neutral direction to endpoints SW of the spawning grounds (Fig. 10D). The mechanism underlying these results lies in the situation of each spawning ground in relation to the regional hydrography. The inshore spawning ground lies within the vicinity of the Icelandic Coastal Current which entrains eggs/larvae within its path and transports them to the north of Iceland. The offshore spawning ground is located outside of this current's path, with dispersal trajectories dependent upon the incoming Atlantic water. A bifurcation in drift trajectories was seen with large portions of larvae drifting both anticlockwise along the south coast of Iceland and clockwise to the north of Iceland. Previous particle tracking studies found little variation in the direction of dispersal between sub-components of the main spawning ground (Brickman et al. 2007). However, the spawning grounds in this study were spatially isolated (i.e. not adjacent) with the offshore one representing the outer limits of the main spawning grounds. The results highlight that (1) variation in dispersal trajectories do exist between sub-components of the spawning ground, and (2) that proximity-to-shore is a key explanation of this variation. Both of these conclusions apply at the seasonal level because similar between spawning grounds differences in the direction, magnitude, and stability of dispersal patterns were seen within each year.

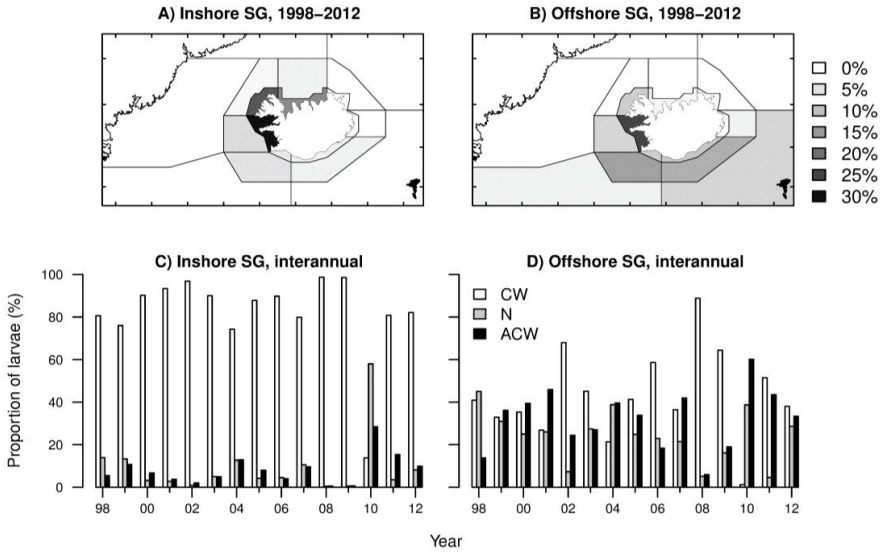

***Figure 10**: Connectivity between spawning grounds and drift endpoints for 120-day old larvae. Panels A and B show the total connectivity (i.e., pooled over years) for the inshore and offshore spawning grounds respectively. Panels C and D show interannual variation in the direction of dispersal from the inshore and offshore spawning grounds respectively. Three directions are shown: clockwise drift (CW), neutral drift (N), and anticlockwise drift (ACW), see Figure 3A for how these directions are defined.*

Pronounced differences in the connectivity matrices between the fixed depth simulations and the reference simulation highlighted that egg and larval vertical movements can significantly alter dispersal trajectories and magnitudes due to current stratification. At 5

m, the proportion of larvae drifting clockwise was similar to the reference simulation; however, the magnitude of clockwise dispersal was far greater. Furthermore, substantial portions of larvae drifted to Greenland, a pattern not seen in any other simulation, highlighting that the drift of larvae to Greenland is depth dependent. In contrast, the magnitude of clockwise dispersal was reduced with the 15 m fixed depth simulations. The differences between the 5 m and 15 m fixed depth simulations highlights that dispersal trajectories and magnitudes were highly sensitive to the DVM module.

3.4 Risk-sensitive foraging of larvae (Paper III)

The best proximate rule was successful in capturing the general behavioural patterns from the optimality model. However, small-scale differences in emergent behaviours throughout ontogeny led to fitness values < 82% of optimised fitness (Fig. 11C). In the reference environment, the largest contribution to this deficit was earlier in ontogeny (5 – 7 mm) when individuals were unable to modulate activity levels to the same degree as the optimal larva (Fig. 11A). In the environments with homogeneous prey concentrations and a fixed mortality rate through ontogeny (Fig. 11B), the larvae performed better from 5 – 7 mm highlighting that the prey gradient and background decline in mortality constrained the larva's ability to mimic optimal behaviour in the reference environment. This was because it was better to take higher risks earlier in ontogeny to reap the benefits of large size sooner, but in the simplified environments the costs of high-risk activities were substantially reduced.

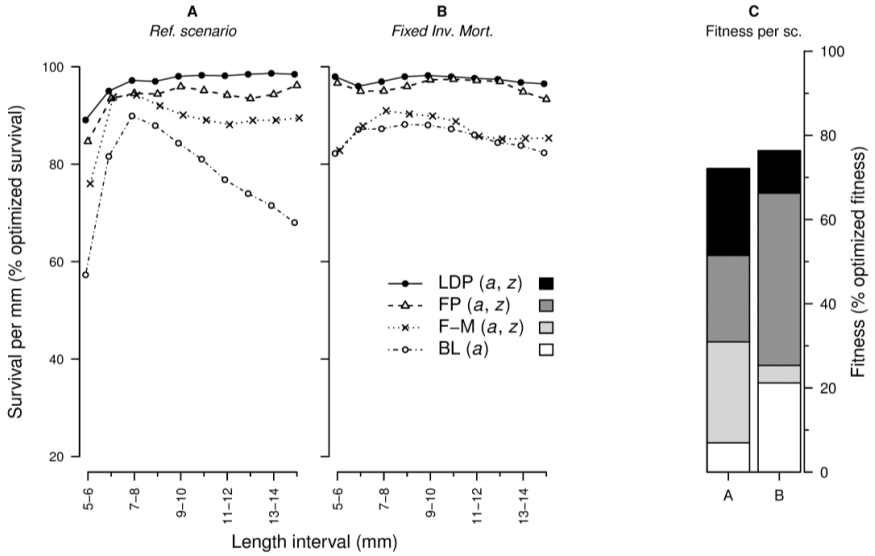

***Figure 11**: Emergent properties from four proximate rules that sequentially increase in complexity. Survival per mm in the reference environment (with all environmental gradients) and the fixed mortality environment is shown in panels A and B respectively. Panel C shows fitness (survival at 15 mm) in the reference (A) and fixed mortality environments (B). Four rules are shown: the baseline strategy (BL) that remains at a fixed depth, the F-M strategy that has both traits but no additional proximate cues, the fixed proximate strategy (FP) that has proximate cues that do not vary through ontogeny, and the length-dependent proximate strategy (LDP). Both survival and fitness measures are expressed as percentages of the optimal equivalents.*

The rule was greatly improved by including additional proximate cues (Fig. 11). These cues provided information to the larva that enabled it to better approximate optimal behaviour. For instance, if a large larva's stomach is partially full at midday, the $F - M$ rule may lead to risky behaviour just because the individual can potentially ingest. In contrast, the optimal decision in such circumstances will more likely minimise the risk of dying at the expense of state (gut content). Introducing additional proximate cues provided the missing information so that the individual was able to make a similar decision to the optimal one (i.e. sacrificing state for safety). Technically, this was achieved when F was scaled to a value close to or equal to zero by stimulation from light intensity and/or gut fullness. In this manner, the proximate cues serve to reduce uncertainty in future conditions by telling the larva to forage only when famished or environmental conditions are favourable. The individual therefore becomes attuned to its immediate environment and internal state in a way that is more consistent with how individuals move and forage in the real world (e.g. Nathan et al. 2008).

The analysis highlighted two further important components of proximate rules. Firstly, as adaptive behaviours will often involve the expression of multiple traits, this needs to be reflected in rules that seek to capture realistic behavioural patterns. For instance, supplementing the activity trait with a trait for habitat selection (or vice versa) provided that larva with a more diverse set of potential actions and greatly improved the rule's performance (Fig. 11). Secondly, incorporating length-dependence into the cue-response system substantially improved the rule, particularly in the reference environment (Fig. 11A). In the environments with higher risk, an ontogenetic shift in the behavioural strategy vector was seen. This allowed the larva to forage in a continual manner when constrained to the surface and in a vigilant manner when it could make use of depth as a refuge by sacrificing state and using light and a nearly empty stomach as a cue for emergence. This result is consistent with the original theory by Werner and Gilliam (1984) that ontogenetic shifts can be described as a function of growth and mortality.

3.5 When is a fish stock collapsed? (Paper IV)

Twenty different time-series-based stock level definitions were found in the literature search. The definitions included a wide variety of formulations and parameter values. Consequently, their ability to reproduce the classifications of the benchmark definition was limited (Fig. 12A). For instance, only 8 definitions (n = 23, 35%) had a median F_1 score greater than zero (Fig. 12B). When broken down, every definition recorded at least one value of zero, whilst only 8 definitions recorded a score of one. The best definition – "25% Hist. Max. SSB" – was the equal best and worst definition in 19 and 9 stocks respectively. These results highlight that both the literature and proposed definitions can capture a "high risk of collapse" in particular stocks but not consistently across stocks (Fig. 12C).

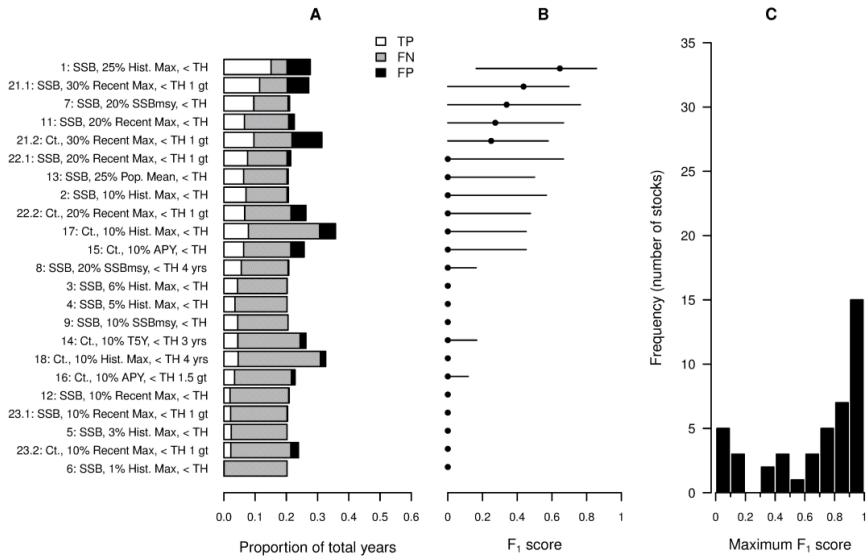

***Figure 12**: Classification success of the literature and proposed collapse definitions. Panel A shows the composition of true positives (TP), false negatives (FN), and false positives (FP) for each definition (pooled over stocks). True positives occur when the test and benchmark (SSB < B_{lim}) definitions both classify a year as collapsed; false negatives occur when the benchmark definition classifies a year as collapsed but the test definition does not, and vice versa for false positives. Panel B shows the median and interquartile range of F_1 scores from across all stocks. Panel C shows the distribution of "best" F_1 scores (one value per stock, irrespective of definition). An F_1 score of one means the definition perfectly captures the classifications of the benchmark (SSB < B_{lim}) definition.*

This conclusion was reinforced by the simulation experiment. The simulated definitions captured more true positives at the expense of false positives leading to an improvement in classification success. However, whilst a higher proportion of definitions (75%) had a median F_1 score greater than one, the best simulated definition ("60% population mean") produced scores of one and zero in 6 and 11 stocks respectively. Considering the combined dataset, we found that classifications are highly sensitive to a definition's formulation and its parameter values (Table 4). These results highlight the same problem as the literature and proposed definitions: that a single definition cannot perform consistently across stocks.

Threshold	**HM**	**AD**	**AD + PD**
70%	38 (0.28)	32 (0.25)	29 (0.18)
80%	31 (0.17)	25 (0.14)	22 (0.09)
90%	15 (0.08)	9 (0.04)	7 (0.02)

***Table 4**: Shows the number of stocks (total = 44) and the proportion of years (across all stocks) classified as "collapsed" according the HM, AD and AD + PD definitions with three different thresholds (rows).*

Developing single collapse criteria involves definition-dependent trade-offs on what a "collapse" as a concept entails (Fig. 7). Characterising the collapses to B_{lim} for each stock utilising the "collapse" parameters in Table 3 clarified why a single definition did not perform well across stocks. Each parameter showed substantial variation, for example, the magnitude of decline varied from 25% to 98% for the HM and AD reference biomasses, whilst the speed of decline from the HM varied from 0.5 to 8.1 generations.

To address the issues raised in these results, we suggest estimating the collapse status of fish stocks using multiple collapse criteria. Including several collapse criteria in stock status analyses and reporting (dis-)agreement among these criteria provides a more robust approach to status categorisations than single collapse criteria assessments. A critical benefit of the multi-definition approach is that using a suite of collapse criteria allows the reporting of uncertainty in the collapse status categorization of fish stocks. In doing so, use of multiple collapse criteria will enhance our ability to interpret seemingly biased (overly optimistic or pessimistic) research results and reduce controversy.

4 Conclusions and future perspectives

Biophysical IBMs are typically rich in parameters, often relying on surrogates or simplifying assumptions when estimates for particular parameters are not available. In **Paper I**, we provided the first (as far as the authors are aware) measurements of the density of haddock and saithe eggs, two species of commercial importance in the North Atlantic. Together with the diameter measurements, this dataset provides species-specific information for use in biophysical models and that provide useful baselines for further observational studies on these two species.

There was no evidence of a unifying mechanism driving the changes in egg density across all three species; however, between batch similarities for cod and saithe suggest that common mechanisms were operating at the species level (**Paper I**). Ultimately, to understand the proximate mechanisms driving the observed interspecific and ontogenetic differences seen in this study, the relative contributions of each of the egg constituents (see Jung et al. 2014) needs to be quantified at the individual level for gadoids in Iceland.

The observed interspecific and ontogenetic differences in density had minimal impact on predicted vertical distributions (**Paper I**). However, a different conclusion would be reached if natural variation in the salinity of neutral buoyancy was not incorporated into the model. By comparing distributional and mean-only approaches, we identified three important features that informed the development of the egg movement module in **Paper II**: (1) egg diameters can be implemented using a single mean value because accounting for natural variation in this parameter did not affect the output; (2) accounting for natural variation in the salinity of neutral buoyancy is essential, particularly in situations where buoyancy will be minimal (e.g. coastal environments); (3) accounting for ontogenetic changes in the salinity of neutral buoyancy is not essential, but only if taking into account natural variation about the overall mean. These features are likely to be common (particularly points 1 and 2) but not necessarily universal due to variation in egg properties between stocks and species. For instance, whether or not ontogenetic variation will have an impact on the vertical distributions of eggs will depend upon the degree of overlap between variances throughout development. Therefore, we suggest that carrying out "virtual" experiments with simpler 1-dimensional vertical distribution models can help identify the level of complexity required for egg movement modules in 3-d biophysical IBMs.

The Lagrangian particle tracking model highlighted that variation in the direction and magnitude of drift exists within the main spawning grounds SW of Iceland (**Paper II**). This variation was not seen in previous particle tracking studies and resulted from a refined discretisation of the spawning grounds. Several studies have distinguished multiple spawning components within the SW spawning grounds (see section 1.2.1). Tying together the outcomes of these studies with particle tracking simulations will help to understand the relative contributions of the various sub-component structures to the relative abundance and spatiotemporal distributions of pelagic larvae and early juveniles. For example, utilising an egg production model that incorporates variation in maternal traits (condition, timing of spawning activity etc) as a basis for initialising the particle

tracking model would link dispersal trajectories to the biological features of each spawning component.

The model in **Paper II** highlighted the importance of running simulations across multiple years and at a high temporal resolution within years. Considering multiple years is essential to capture large-scale changes in ocean current patterns and variables (e.g. temperature) that influence the survival of larvae. Dispersal patterns from the inshore spawning ground were relatively stable across years. In contrast, considerable interannual variation in dispersal patterns was found from the offshore spawning ground. This result highlights that interannual variation in the spatiotemporal distribution of pelagic larvae may be better explained by variations in the incoming Atlantic water than variations in the coastal current. Similar differences in dispersal patterns were seen within each year. Each spawning season could be broken down to clusters of dominant endpoints reflecting consistent (over multiple days) changes in dispersal direction. These were more frequent and extended over a longer period of time from the offshore spawning ground. Running simulations at lower temporal resolutions risks missing certain clusters resulting in an incomplete picture of dispersal. Therefore, releasing large quantities of particles at a high seasonal resolution is essential for particle tracking models to capture variation in dispersal patterns with a high degree of certainty. This is particularly important for species with protracted spawning periods because the environment will exhibit considerable variation over the entire duration of spawning.

The results from **Paper II** also highlighted the sensitivity of dispersal patterns to the vertical movement of particles, particularly larval DVMs. Contrasting fixed-depth simulations with DVMs simulations revealed strong depth stratification in currents that substantially altered the direction and magnitude of dispersal, one of the results of which was vast variation in the connectivity between Iceland and Greenland. This sensitivity highlights the need for studies to provide empirical estimates of key parameters that describe the amplitude and timing of DVMs through ontogeny for gadoids in Iceland. With this information, more realistic models of DVMs can be incorporated into biophysical models and thus more certainty in dispersal patterns will be attained.

In **Paper III**, we showed that is it possible for explicit proximate rules to capture key facets of optimal behaviour, but why is this important? Whilst the fate of marine larvae is to a large extent driven by patterns of circulation, larvae can also exert some control over their growth and dispersal through vertical movements. The marine environment is dynamic with gradients in many variables that vary in space and time. As the traits driving behavioural decisions are heritable, we expect the "good" ones – that operate well across a range of environmental gradients – to persist and increase through generations. The optimal rule is the "best" one, but due to the underlying assumptions required to compute optimal solutions, they cannot be found in biophysical IBMs. However, if a simple proximate rule can produce behaviours that mimic optimal behaviour fairly well across environments, it is likely to represent a strategy that would evolve under the environments tested.

The rule we presented in **Paper III** captures the interplay between proximate cues and ontogeny in a single fitness-seeking objective. In doing so, the rule offers a simple template for any model seeking to capture adaptive foraging in complex spatial gradients. The myopic nature of the rule means it is computationally efficient and thus easily embedded within, or coupled to, biophysical IBMs or ecosystem models to examine trait-mediated interactions (with biotic or abiotic components). Furthermore, the flexibility of

the rule's construction allows multiple cues from multiple sources (both internal and external, direct and indirect) to be integrated in a manner that can capture the complexities involved in individual foraging. Integrating the rule into drift models will be particularly useful for biophysical IBMs that consider a more ecosystem-orientated approach, i.e., with multiple trophic levels. For instance, with the inclusion of a zooplankton layer, the particle tracking model developed in **Paper II** would be well suited to examine the match-mismatch between cod larvae and zooplankton prey at hatching and along drift trajectories. However, quantifying the effects of match-mismatch on 0-group strength would require a presumed relationship between zooplankton abundance and larval growth and/or survival. By incorporating risk-sensitive foraging into such a model, growth and mortality rates (and thus population abundance and distribution) would emerge from the adaptive behaviours of individuals in a more realistic manner. This could yield additional insights into how the degree of match-mismatch shapes the abundance and distribution of cod early life-stages.

The literature review in **Paper IV** found many unique, quantitative fish stock collapse definitions indicating that there is no consensus regarding the choice of analytical approach used to reliably classify the status of a fish stock as collapsed. The subsequent analysis highlighted that collapse classifications are highly sensitive to small changes in a definition's parameters and its overall formulation. Such inconsistencies in collapse definitions and their classifications offers a plausible explanation for disagreement among scientists on the general state of the global fish stocks.

Identifying fish stock collapses using simple criteria is driven by data limitations: the fact that few observations are available to establish stock-recruitment relationships (assuming they exist) at low values of biomass, and that many of the world's fish stocks do not have direct estimates of biomass. The results highlight that extreme caution should be taken when using single fish stock collapse definitions. The motivation for using a particular definition should be described and the fits to each stock should be reported and analysed to ensure they are plausible from a population dynamics perspective. We suggest two approaches to help quantify uncertainty in collapse classifications: (1) using Bayesian approaches to account for uncertainty in biomass estimates by generating distributional thresholds, and (2) utilising multiple collapse definitions that would enable the reporting of uncertainty in collapse definitions which, in turn, would aid the ability to interpret the results.

References

Ådlandsvik, B., 2000. VertEgg – A Toolbox for Simulation of Vertical Distributions of Fish Eggs. Bergen.

Ådlandsvik, B., Coombs, S., Sundby, S., Temple, G., 2001. Buoyancy and vertical distribution of eggs and larvae of blue whiting (Micromesistius poutassou): Observations and modelling. Fish. Res. 50, 59–72. https://doi.org/10.1016/S0165-7836(00)00242-3

Allen, R.M., Metaxas, A., Snelgrove, P.V.R., 2018. Applying movement ecology to marine animals with complex life cycles. Ann. Rev. Mar. Sci. 10, 3.1-3.24. https://doi.org/10.1146/annurev-marine-121916-063134

Amo, L., López, P., Martín, J., 2004. Wall lizards combine chemical and visual cues of ambush snake predators to avoid overestimating risk inside refuges. Anim. Behav. 67, 647–653. https://doi.org/10.1016/j.anbehav.2003.08.005

Armannsson, H., Jonsson, S.T., Neilson, J.D., Marteinsdottir, G., 2007. Distribution and migration of saithe (Pollachius virens) around Iceland inferred from mark-recapture studies. ICES J. Mar. Sci. 64, 1006–1016. https://doi.org/10.1093/icesjms/fsm076

Astthorsson, O.S., Gislason, A., 1998. Environmental conditions, zooplankton, and capelin in the waters north of Iceland. ICES J. Mar. Sci. 55, 808–810.

Astthorsson, O.S., Gislason, A., Jonsson, S., 2007. Climate variability and the Icelandic marine ecosystem. Deep. Res. Part II Top. Stud. Oceanogr. 54, 2456–2477. https://doi.org/10.1016/j.dsr2.2007.07.030

Astthorsson, O.S., Vilhjálmsson, H., 2002. 7 Iceland shelf LME: Decadal assessment and resource sustainability, in: Large Marine Ecosystems. Elsevier, pp. 219–243.

Bailey, K.M., Houde, E.D., 1989. Predation on eggs and larvae of marine fishes and the recruitment problem, in: Advances in Marine Biology. Elsevier, pp. 1–83.

Bardarson, H., McAdam, B.J., Thorsteinsson, V., Hjorleifsson, E., Marteinsdottir, G., 2017. Otolith shape differences between ecotypes of Icelandic cod (Gadus morhua) with known migratory behaviour inferred from data storage tags. Can. J. Fish. Aquat. Sci. 74, 2122–2130. https://doi.org/10.1139/cjfas-2016-0307

Barneche, D.R., Robertson, D.R., White, C.R., Marshall, D.J., 2018. Fish reproductive-energy output increases disproportionately with body size. Science (80-.). 360, 642–645.

Barrowman, N.J., Myers, R.A., 1996. Is fish recruitment related to spawner abundance. Fish. Bull 94, 707–724.

Begg, G.A., Marteinsdottir, G., 2002. Environmental and stock effects on spatial distribution and abundance of mature cod Gadus morhua. Mar. Ecol. Prog. Ser. 229, 245–262. https://doi.org/10.3354/meps229245

Begg, G.A., Marteinsdottir, G., 2000. Spawning origins of pelagic juvenile cod Gadus morhua inferred from spatially explicit age distributions: Potential influences on year-class strength and recruitment. Mar. Ecol. Prog. Ser. 202, 193–217. https://doi.org/10.3354/meps202193

Behrenfeld, M.J., Gaube, P., Della Penna, A., O'Malley, R.T., Burt, W.J., Hu, Y., Bontempi, P.S., Steinberg, D.K., Boss, E.S., Siegel, D.A., Hostetler, C.A., Tortell, P.D., Doney, S.C., 2019. Global satellite-observed daily vertical migrations of ocean animals. Nature 576, 257–261. https://doi.org/10.1038/s41586-019-1796-9

Bianchi, D., Mislan, K.A.S., 2016. Global patterns of diel vertical migration times and velocities from acoustic data. Limnol. Oceanogr. 61, 353–364. https://doi.org/10.1002/lno.10219

Bollens, S.M., Frost, B.W., 1991. Diel vertical migration in zooplankton: rapid individual response to predators. J. Plankton Res. 13, 1359–1365.

Bollens, S.M., Rollwagen-Bollens, G., Quenette, J.A., Bochdansky, A.B., 2011. Cascading migrations and implications for vertical fluxes in pelagic ecosystems. J. Plankton Res. 33, 349–355. https://doi.org/10.1093/plankt/fbq152

Bolnick, D.I., Amarasekare, P., Araújo, M.S., Bürger, R., Levine, J.M., Novak, M., Rudolf, V.H.W., Schreiber, S.J., Urban, M.C., Vasseur, D.A., 2011. Why intraspecific trait variation matters in community ecology. Trends Ecol. Evol. 26, 183–192. https://doi.org/10.1016/j.tree.2011.01.009

Bonanomi, S., Overgaard Therkildsen, N., Retzel, A., Berg Hedeholm, R., Pedersen, M.W., Meldrup, D., Pampoulie, C., Hemmer-Hansen, J., Grønkjaer, P., Nielsen, E.E., 2016. Historical DNA documents long-distance natal homing in marine fish. Mol. Ecol. 25, 2727–2734. https://doi.org/10.1111/mec.13580

Bonanomi, S., Pellissier, L., Therkildsen, N.O., Hedeholm, R.B., Retzel, A., Meldrup, D., Olsen, S.M., Nielsen, A., Pampoulie, C., Hemmer-Hansen, J., Wisz, M.S., Grønkjær, P., Nielsen, E.E., 2015. Archived DNA reveals fisheries and climate induced collapse of a major fishery. Sci. Rep. 5, 1–8. https://doi.org/10.1038/srep15395

Boyra, G., Rueda, L., Coombs, S.H., Sundby, S., Ådlandsvik, B., Santos, M., Uriarte, A., 2003. Modelling the vertical distribution of eggs of anchovy (Engraulis encrasicolus) and sardine (Sardina pilchardus). Fish. Oceanogr. 12, 381–395. https://doi.org/10.1046/j.1365-2419.2003.00260.x

Branch, T.A., Jensen, O.P., Ricard, D., Ye, Y., Hilborn, R., 2011. Contrasting Global Trends in Marine Fishery Status Obtained from Catches and from Stock Assessments. Conserv. Biol. 25, 777–786. https://doi.org/10.1111/j.1523-1739.2011.01687.x

Brickman, D., Marteinsdottir, G., Logemann, K., Harms, I.H., 2007. Drift probabilities for Icelandic cod larvae. ICES J. Mar. Sci. 64, 49–59. https://doi.org/10.1093/icesjms/fsl019

Brierley, A.S., 2014. Diel vertical migration. Curr. Biol. 24, R1074–R1076. https://doi.org/10.1016/j.cub.2014.08.054

Budaev, S., Jørgensen, C., Mangel, M., Eliassen, S., Giske, J., 2019. Decision-Making From the Animal Perspective: Bridging Ecology and Subjective Cognition. Front.

Ecol. Evol. 7, 1–14. https://doi.org/10.3389/fevo.2019.00164

Buren, A.D., Murphy, H.M., Adamack, A.T., Davoren, G.K., Koen-Alonso, M., Montevecchi, W.A., Mowbray, F.K., Pepin, P., Regular, P.M., Robert, D., Rose, G.A., Stenson, G.B., Varkey, D., 2019. The collapse and continued low productivity of a keystone forage fish species. Mar. Ecol. Prog. Ser. 616, 155–170. https://doi.org/10.3354/meps12924

Chambers, C., Carothers, C., 2017. Thirty years after privatization: A survey of Icelandic small-boat fishermen. Mar. Policy 80, 69–80. https://doi.org/10.1016/j.marpol.2016.02.026

Chambers, R.C., 1993. Phenotypic Variability in Fish Populations and Its Representation in Individual-Based Models. Trans. Am. Fish. Soc. 122, 404–414. https://doi.org/10.1577/1548-8659(1993)122<0404:PVIFPA>2.3.CO;2

Charnov, E.L., 1976. Optimal foraging: the marginal value theorem. Theor. Popul. Ecol. 9, 129–136.

Checkley, D.M., Raman, S., Maillet, G.L., Mason, K.M., 1988. Winter storm effects on the spawning and larval drift of a pelagic fish. Nature 335, 346–348.

China, V., Holzman, R., 2014. Hydrodynamic starvation in first-feeding larval fishes. Proc. Natl. Acad. Sci. U. S. A. 111, 8083–8088. https://doi.org/10.1073/pnas.1323205111

Clark, C.W., Levy, D.A., 1988. Diel Vertical Migrations by Juvenile Sockeye Salmon and the Antipredation Window. Am. Nat. 131, 271–290. https://doi.org/10.1126/science.26.678.918

Cohen, J.H., Forward Jr, R.B., 2009. Zooplankton diel vertical migration: a review of proximate control. Oceanogr. Mar. Biol. An Annu. Rev. 47.

Cohen, J.H., Forward, R.B., 2005. Diel vertical migration of the marine copepod Calanopia americana. I. Twilight DVM and its relationship to the diel light cycle. Mar. Biol. 147, 387–398. https://doi.org/10.1007/s00227-005-1569-x

Cook, R.M., Sinclair, A., Stefánsson, G., 1997. Potential collapse of North Sea cod stocks. Nature. https://doi.org/10.1038/385521a0

Cooke, J.G., 1984. Glossary of technical terms. Exploit. Mar. Communities 341.

Coombs, S.H., 1981. A density-gradient column for determining the specific gravity of fish eggs, with particular reference to eggs of the mackerel Scomber scombrus. Mar. Biol. 63, 101–106. https://doi.org/10.1007/BF00394667

Costello, C., Ovando, D., Hilborn, R., Gaines, S.D., Deschenes, O., Lester, S.E., 2012. Status and solutions for the world's unassessed fisheries. Science (80-.). 338, 517–520. https://doi.org/10.1126/science.1223389

Cumming, G.S., Peterson, G.D., 2017. Unifying Research on Social–Ecological Resilience and Collapse. Trends Ecol. Evol. 32, 695–713. https://doi.org/10.1016/j.tree.2017.06.014

De Robertis, A., 2002. Size-dependent visual predation risk and the timing of vertical migration: An optimization model. Limnol. Oceanogr. 47, 925–933.

DeAngelis, D.L., Diaz, S.G., 2019. Decision-making in agent-based modeling: A current review and future prospectus. Front. Ecol. Evol. 6, 237.

DeAngelis, D.L., Grimm, V., 2014. Individual-based models in ecology after four decades. F1000Prime Rep. 6. https://doi.org/10.12703/P6-39

DeWitt, T.J., Sih, A., Wilson, D.S., 1998. Costs and limits of phenotypic plasticity. Trends Ecol. Evol. 13, 77–81.

Dickson, R.R., Brander, K.M., 1993. Effects of a changing windfield on cod stocks of the North Atlantic. Fish. Oceanogr. 2, 124–153.

Dos Santos, A., Santos, A.M.P., Conway, D.V.P., Bartilotti, C., Lourenço, P., Queiroga, H., 2008. Diel vertical migration of decapod larvae in the Portuguese coastal upwelling ecosystem: Implications for offshore transport. Mar. Ecol. Prog. Ser. 359, 171–183. https://doi.org/10.3354/meps07341

Downie, A.T., Illing, B., Faria, A.M., Rummer, J.L., 2020. Swimming performance of marine fish larvae: review of a universal trait under ecological and environmental pressure. Rev. Fish Biol. Fish. 30, 93–108. https://doi.org/10.1007/s11160-019-09592-w

Ehlman, S.M., Trimmer, P.C., Sih, A., 2019. Prey responses to exotic predators: Effects of old risks and new cues. Am. Nat. 193, 575–587. https://doi.org/10.1086/702252

Elvarsson, B.Þ., Agnarsson, S., Guðmundsdóttir, S., Viðarsson, J., 2020. Using multi-criteria analysis the assess impacts of change in ecosystem-based fisheries management: The case of the Icelandic cod. Mar. Policy 103825.

Essington, T.E., Moriarty, P.E., Froehlich, H.E., Hodgson, E.E., Koehn, L.E., Oken, K.L., Siple, M.C., Stawitz, C.C., 2015. Fishing amplifies forage fish population collapses. Proc. Natl. Acad. Sci. U. S. A. 112, 6648–6652. https://doi.org/10.1073/pnas.1422020112

FAO, 2020. The State of World Fisheries and Aquaculture 2020. Sustainability in action. Rome.

FAO, 2011. Review of the state of world marine fishery resources. FAO Fisheries and Aquaculture Technical Paper No. 569. Rome, FAO. 2011. 334 pp.

Fawcett, T.W., Hamblin, S., Giraldeau, L.A., 2013. Exposing the behavioral gambit: The evolution of learning and decision rules. Behav. Ecol. 24, 2–11. https://doi.org/10.1093/beheco/ars085

Fernandes, P.G., Cook, R.M., 2013. Reversal of fish stock decline in the Northeast Atlantic. Curr. Biol. 23, 1432–1437. https://doi.org/10.1016/j.cub.2013.06.016

Fiksen, Ø., Jørgensen, C., 2011. Model of optimal behaviour in fish larvae predicts that food availability determines survival, but not growth. Mar. Ecol. Prog. Ser. 432, 207–219. https://doi.org/10.3354/meps09148

Fiksen, Ø., Jørgensen, C., Kristiansen, T., Vikebø, F., Huse, G., 2007. Linking behavioural ecology and oceanography: Larval behaviour determines growth, mortality and dispersal. Mar. Ecol. Prog. Ser. 347, 195–205. https://doi.org/10.3354/meps06978

Fischer, J.M., Olson, M.H., Theodore, N., Williamson, C.E., Rose, K.C., Hwang, J., 2015.

Diel vertical migration of copepods in mountain lakes: The changing role of ultraviolet radiation across a transparency gradient. Limnol. Oceanogr. 60, 252–262. https://doi.org/10.1002/lno.10019

Fouzai, N., Opdal, A.F., Jørgensen, C., Fiksen, Ø., 2019. Dying from the lesser of three evils: facilitation and non-consumptive effects emerge in a model with multiple predators. Oikos 128, 1307–1317. https://doi.org/10.1111/oik.05631

Frank, K.T., Petrie, B., Choi, J.S., Leggett, W.C., 2005. Ecology: Trophic cascades in a formerly cod-dominated ecosystem. Science (80-.). 308, 1621–1623. https://doi.org/10.1126/science.1113075

Fuiman, L.A., 1994. The interplay of ontogeny and scaling in the interactions of fish larvae and their predators. J. Fish Biol. 45, 55–79.

Gallagher, A.J., Creel, S., Wilson, R.P., Cooke, S.J., 2017. Energy Landscapes and the Landscape of Fear. Trends Ecol. Evol. 32, 88–96. https://doi.org/10.1016/j.tree.2016.10.010

Garcia, S.M., Ye, Y., Rice, J., Charles, A., 2018. Rebuilding of marine fisheries. Part 1: Global review, FAO Fisheries and Aquaculture Technical Paper No. 630/1. FAO, ROME.

Garrido, S., Ben-Hamadou, R., Santos, A.M.P., Ferreira, S., Teodósio, M.A., Cotano, U., Irigoien, X., Peck, M.A., Saiz, E., Re, P., 2015. Born small, die young: Intrinsic, size-selective mortality in marine larval fish. Sci. Rep. 5, 17065.

Gentleman, W., 2002. A chronology of plankton dynamics in silico: How computer models have been used to study marine ecosystems. Hydrobiologia 480, 69–85. https://doi.org/10.1023/A:1021289119442

Giske, J., Eliassen, S., Fiksen, Ø., Jakobsen, P.J., Aksnes, D.L., Jørgensen, C., Mangel, M., 2013. Effects of the emotion system on adaptive behavior. Am. Nat. 182, 689–703. https://doi.org/10.1086/673533

Gislason, A., Astthorsson, O.S., Gudfinnsson, H., 1994. Phytoplankton, Calanus finmarchicus, and fish eggs southwest of Iceland, 1990-1992. ICES Mar. Sci. Symp. 198, 423–429.

Gislason, A., Logemann, K., Marteinsdottir, G., 2016. The cross-shore distribution of plankton and particles southwest of Iceland observed with a Video Plankton Recorder. Cont. Shelf Res. 123, 50–60. https://doi.org/10.1016/j.csr.2016.04.004

Gliwicz, M.Z., 1986. Predation and the evolution of vertical migration in zooplankton. Nature 320, 746–748.

Grabowski, T.B., Boswell, K.M., McAdam, B.J., Wells, R.J.D., Marteinsdóttir, G., 2012. Characterization of Atlantic Cod Spawning Habitat and Behavior in Icelandic Coastal Waters. PLoS One 7. https://doi.org/10.1371/journal.pone.0051321

Grabowski, T.B., Thorsteinsson, V., McAdam, B.J., Marteinsdóttir, G., 2011. Evidence of segregated spawning in a single marine fish stock: Sympatric divergence of ecotypes in Icelandic cod? PLoS One 6. https://doi.org/10.1371/journal.pone.0017528

Grafen, A., 1984. Natural selection, kin selection and group selection. Behav. Ecol. An Evol. approach 2, 62–84.

Grimm, V., 1999. Ten years of individual-based modelling in ecology: What have we learned and what could we learn in the future? Ecol. Modell. 115, 129–148. https://doi.org/10.1016/S0304-3800(98)00188-4

Grimm, V., Railsback, S.F., 2005. Individual-based modeling and ecology. Princeton university press.

Guðmundsdóttir, L.Ó., 2013. Intra-Stock Diversity in Egg Specific Gravity of Atlantic Cod in Icelandic Waters. University of Iceland.

Hall, T.E., Smith, P., Johnston, I.A., 2004. Stages of Embryonic Development in the Atlantic Cod Gadus morhua. J. Morphol. 259, 255–270. https://doi.org/10.1002/jmor.10222

Hammerschlag, N., Schmitz, O.J., Flecker, A.S., Lafferty, K.D., Sih, A., Atwood, T.B., Gallagher, A.J., Irschick, D.J., Skubel, R., Cooke, S.J., 2019. Ecosystem Function and Services of Aquatic Predators in the Anthropocene. Trends Ecol. Evol. 34, 369–383. https://doi.org/10.1016/j.tree.2019.01.005

Hare, J.A., 2014. The future of fisheries oceanography lies in the pursuit of multiple hypotheses. ICES J. Mar. Sci. 71, 2343–2356.

Hays, G.C., 2003. A review of the adaptive significance and ecosystem consequences of zooplankton diel vertical migrations. Hydrobiologia 503, 163–170. https://doi.org/10.1023/B:HYDR.0000008476.23617.b0

Heino, M., Baulier, L., Boukal, D.S., Ernande, B., Johnston, F.D., Mollet, F.M., Pardoe, H., Therkildsen, N.O., Uusi-Heikkilä, S., Vainikka, A., others, 2013. Can fisheries-induced evolution shift reference points for fisheries management? ICES J. Mar. Sci. 70, 707–721.

Hernandez, F.J., Hare, J.A., Fey, D.P., 2009. Evaluating diel, ontogenetic and environmental effects on larval fish vertical distribution using generalized additive models for location, scale and shape. Fish. Oceanogr. 18, 224–236. https://doi.org/10.1111/j.1365-2419.2009.00508.x

Hilborn, R., Amoroso, R.O., Anderson, C.M., Baum, J.K., Branch, T.A., Costello, C., De Moor, C.L., Faraj, A., Hively, D., Jensen, O.P., Kurota, H., Little, L.R., Mace, P., McClanahan, T., Melnychuk, M.C., Minto, C., Osio, G.C., Parma, A.M., Pons, M., Segurado, S., Szuwalski, C.S., Wilson, J.R., Ye, Y., 2020. Effective fisheries management instrumental in improving fish stock status. Proc. Natl. Acad. Sci. U. S. A. 117, 2218–2224. https://doi.org/10.1073/pnas.1909726116

Hixon, M.A., Johnson, D.W., Sogard, S.M., 2014. BOFFFFs: on the importance of conserving old-growth age structure in fishery populations. ICES J. Mar. Sci. 71, 2171–2185.

Hjort, J., 1926. Fluctuations in the year classes of important food fishes. J. Cons. int. Explor. Mer 1, 5–38.

Hjort, J., 1914. Fluctuations in the great fisheries of northern Europe viewed in the light of biological research. Rapp. P.-V. Reun. Cons. Int. Explo. Mer 20, 1–228.

Houde, E.D., 2008. Emerging from Hjort's shadow. J. Northwest Atl. Fish. Sci. 41, 53–70. https://doi.org/10.2960/J.v41.m634

Houde, E.D., 1989. Comparative growth, mortality, and energetics of marine fish larvae: temperature and implied latitudinal effects. Fish. Bull. 87, 471–495.

Houde, E.D., 1987. Fish early life dynamics and recruitment variability. Am. Fish. Soc. Symp. 2, 17–29.

Houston, A.I., McNamara, J.M., Hutchinson, J.M.C., 1993. General results concerning the trade-off between gaining energy and avoiding predation. Philos. Trans. R. Soc. B Biol. Sci. 341, 375–397.

Houston, A.I., McNamara, J.M., others, 1999. Models of adaptive behaviour: an approach based on state. Cambridge University Press.

Hurst, T.P., Cooper, D.W., Scheingross, J.S., Seale, E.M., Laurel, B.J., Spencer, M.L., 2009. Effects of ontogeny, temperature, and light on vertical movements of larval pacific cod (Gadus macrocephalus). Fish. Oceanogr. 18, 301–311. https://doi.org/10.1111/j.1365-2419.2009.00512.x

Huston, M., DeAngelis, D., Post, W., 1988. New computer models unify ecological theory. Bioscience 38, 682–691.

Hutchings, J.A., 2015. Thresholds for impaired species recovery. Proc. R. Soc. B Biol. Sci. 282. https://doi.org/10.1098/rspb.2015.0654

Hutchings, J.A., 2000. Collapse and recovery of marine fishes. Nature 406, 882–885.

Hutchings, J.A., Kuparinen, A., 2020. Implications of fisheries-induced evolution for population recovery: Refocusing the science and refining its communication. Fish Fish. 21, 453–464. https://doi.org/10.1111/faf.12424

Hutchings, J.A., Myers, R.A., 1994. What Can Be Learned from the Collapse of a Renewable Resource? Atlantic Cod, Gadus morhua, of Newfoundland and Labrador. Can. J. Fish. Aquat. Sci. 51, 2126–2146.

Hutchings, J.A., Reynolds, J.D., 2004. Marine fish population collapses: Consequences for recovery and extinction risk. Bioscience 54, 297–309. https://doi.org/10.1641/0006-3568(2004)054[0297:MFPCCF]2.0.CO;2

Hutchinson, J.M.C., Gigerenzer, G., 2005. Simple heuristics and rules of thumb: Where psychologists and behavioural biologists might meet. Behav. Processes 69, 97–124. https://doi.org/10.1016/j.beproc.2005.02.019

ICES, 2019a. ICES Stock Assessment Database [accessed 1st January 2019].

ICES, 2019b. Advice basis 2019. Rep. ICES Advis. Committee, 2019. section 1.2. https://doi.org/https://doi.org/10.17895/ices.advice. 5757

ICES, 2017. ICES fisheries management reference points for category 1 and 2 stocks, in: ICES Advice Technical Guidelines. Copenhagen, Denmark, p. 19. https://doi.org/10.17895/ices.pub.3036

ICES, 2005. Spawning and life history information for North Atlantic cod stocks. ICES Coop. Res. Rep. 152.

Jakobsson, J., Stefánsson, G., 1998. Rational harvesting of the cod-capelin-shrimp complex in the Icelandic marine ecosystem. Fish. Res. 37, 7–21. https://doi.org/10.1016/S0165-7836(98)00123-4

Jónsdóttir, Ingibjörg G., Campana, S.E., Marteinsdottir, G., 2006. Otolith shape and temporal stability of spawning groups of Icelandic cod (Gadus morhua L.). ICES J. Mar. Sci. 63, 1501–1512. https://doi.org/10.1016/j.icesjms.2006.05.006

Jónsdóttir, I. G., Campana, S.E., Marteinsdottir, G., 2006. Stock structure of Icelandic cod Gadus morhua L. based on otolith chemistry. J. Fish Biol. 69, 136–150. https://doi.org/10.1111/j.1095-8649.2006.01271.x

Jónsson, G., Pálsson, J., 2013. Íslenski fiskar (e. Icelandic fish). Mál og Menn. Reykjavik, Icel. 493.

Jónsson, J., 1994. Fisheries off Iceland, 1600-1900. ICES Mar. Sci. Symp. 198, 3–16.

Jónsson, S., Valdimarsson, H., 2012. Water mass transport variability to the North Icelandic shelf, 1994--2010. ICES J. Mar. Sci. 69, 809–815.

Jónsson, S., Valdimarsson, H., 2005. The flow of Atlantic water to the North Icelandic Shelf and its relation to the drift of cod larvae. ICES J. Mar. Sci. 62, 1350–1359. https://doi.org/10.1016/j.icesjms.2005.05.003

Jørgensen, C., Auer, S.K., Reznick, D.N., 2011. A model for optimal offspring size in fish, including live-bearing and parental effects. Am. Nat. 177. https://doi.org/10.1086/659622

Jørgensen, C., Enberg, K., Dunlop, E.S., Arlinghaus, R., Boukal, D.S., Brander, K., Ernande, B., Gårdmark, A., Johnston, F., Matsumura, S., Pardoe, H., Raab, K., Silva, A., Vainikka, A., Dieckmann, U., Heino, M., Rijnsdorp, A.D., 2007. Ecology: Managing evolving fish stocks. Science (80-.). 318, 1247–1248. https://doi.org/10.1126/science.1148089

Jørgensen, C., Opdal, A.F., Fiksen, Ø., 2014. Can behavioural ecology unite hypotheses for fish recruitment? ICES J. Mar. Sci. 71, 909–917. https://doi.org/10.1093/icesjms/fst083

Jung, K.M., Folkvord, A., Kjesbu, O.S., Agnalt, A.L., Thorsen, A., Sundby, S., 2012. Egg buoyancy variability in local populations of Atlantic cod (Gadus morhua). Mar. Biol. 159, 1969–1980. https://doi.org/10.1007/s00227-012-1984-8

Jung, K.M., Folkvord, A., Kjesbu, O.S., Sundby, S., 2014. Experimental parameterisation of principal physics in buoyancy variations of marine teleost eggs. PLoS One 9. https://doi.org/10.1371/journal.pone.0104089

Kelly, T.B., Davison, P.C., Goericke, R., Landry, M.R., Ohman, M.D., Stukel, M.R., 2019. The Importance of Mesozooplankton Diel Vertical Migration for Sustaining a Mesopelagic Food Web. Front. Mar. Sci. 6, 1–18. https://doi.org/10.3389/fmars.2019.00508

Kingsford, M.J., Leis, J.M., Shanks, A., Lindeman, K.C., Morgan, S.G., Pineda, J., 2002. Sensory environments, larval abilities and local self-recruitment. Bull. Mar. Sci. 70, 309–340.

Kjesbu, O.S., Krivit, H., Sundby, S., Solemdal, P., 1992. Buoyancy variations in eggs of cod in relation to chorion thickness and egg size theory and observations. J. Fish Biol. 41, 581–599.

Kohl, M.T., Stahler, D.R., Metz, M.C., Forester, J.D., Kauffman, M.J., Varley, N., White,

P.J., Smith, D.W., MacNulty, D.R., 2018. Diel predator activity drives a dynamic landscape of fear. Ecol. Monogr. 88, 638–652. https://doi.org/10.1002/ecm.1313

Kristiansen, T., Drinkwater, K.F., Lough, R.G., Sundby, S., 2011. Recruitment variability in North Atlantic cod and match-mismatch dynamics. PLoS One 6. https://doi.org/10.1371/journal.pone.0017456

Kristiansen, T., Jørgensen, C., Lough, R.G., Vikebø, F., Fiksen, Ø., 2009. Modeling rule-based behavior: Habitat selection and the growth-survival trade-off in larval cod. Behav. Ecol. 20, 490–500. https://doi.org/10.1093/beheco/arp023

Kurlansky, M., 2011. Cod: a biography of the fish that changed the world. Vintage Canada.

Kuroda, H., Takahashi, D., Mitsudera, H., Azumaya, T., Setou, T., 2014. A preliminary study to understand the transport process for the eggs and larvae of Japanese Pacific walleye pollock Theragra chalcogramma using particle-tracking experiments based on a high-resolution ocean model. Fish. Sci. 80, 127–138. https://doi.org/10.1007/s12562-014-0717-y

Kvile, K.Ø., Romagnoni, G., Dagestad, K.F., Langangen, Ø., Kristiansen, T., 2018. Sensitivity of modelled North Sea cod larvae transport to vertical behaviour, ocean model resolution and interannual variation in ocean dynamics. ICES J. Mar. Sci. 75, 2413–2424. https://doi.org/10.1093/icesjms/fsy039

Laland, K.N., Sterelny, K., Odling-Smee, J., Hoppitt, W., Uller, T., 2011. Cause and effect in biology revisited: Is Mayr's proximate-ultimate dichotomy still useful? Science (80-.). 334, 1512–1516. https://doi.org/10.1126/science.1210879

Lampert, W., 1989. The Adaptive Significance of Diel Vertical Migration of Zooplankton. Funct. Ecol. 3, 21–27. https://doi.org/10.2307/2389671

Leggett, W.C., Deblois, E., 1994. Recruitment in marine fishes: Is it regulated by starvation and predation in the egg and larval stages? Netherlands J. Sea Res. 32, 119–134. https://doi.org/10.1016/0077-7579(94)90036-1

Leis, J.M., Siebeck, U., Dixson, D.L., 2011. How nemo finds home: The neuroecology of dispersal and of population connectivity in larvae of marine fishes. Integr. Comp. Biol. 51, 826–843. https://doi.org/10.1093/icb/icr004

Lima, S.L., Dill, L.M., 1990. Behavioral decisions made under the risk of predation: a review and prospectus. Can. J. Zool.

Lindegren, M., Möllmann, C., Nielsen, A., Stenseth, N.C., 2009. Preventing the collapse of the Baltic cod stock through an ecosystem-based management approach. Proc. Natl. Acad. Sci. U. S. A. 106, 14722–14727. https://doi.org/10.1073/pnas.0906620106

Link, J.S., Bogstad, B., Sparholt, H., Lilly, G.R., 2009. Trophic role of Atlantic cod in the ecosystem. Fish Fish. 10, 58–87. https://doi.org/10.1111/j.1467-2979.2008.00295.x

Logemann, K., Ólafsson, J., Snorrason, Á., Valdimarsson, H., Marteinsdóttir, G., 2013. The circulation of Icelandic waters - A modelling study. Ocean Sci. 9, 931–955. https://doi.org/10.5194/os-9-931-2013

Lotze, H.K., Coll, M., Magera, A.M., Ward-Paige, C., Airoldi, L., 2011. Recovery of

marine animal populations and ecosystems. Trends Ecol. Evol. 26, 595–605. https://doi.org/10.1016/j.tree.2011.07.008

Lough, R.G., Potter, D.C., 1993. Vertical distribution patterns and diel migrations of larval and juvenile haddock Melanogrammus aeglefinus and Atlantic cod Gadus morhua on Georges Bank. Fish. Bull. 91, 281–303.

Lowerre-Barbieri, S., DeCelles, G., Pepin, P., Catalán, I.A., Muhling, B., Erisman, B., Cadrin, S.X., Alós, J., Ospina-Alvarez, A., Stachura, M.M., Tringali, M.D., Burnsed, S.W., Paris, C.B., 2017. Reproductive resilience: a paradigm shift in understanding spawner-recruit systems in exploited marine fish. Fish Fish. 18, 285–312. https://doi.org/10.1111/faf.12180

MacKenzie, B.R., Hinrichsen, H.-H., Plikshs, M., Wieland, K., Zezera, A.S. 2000, 2000. Quantifying environmental heterogeneity: habitat size necessary for successful development of cod Gadus morhua eggs in the Baltic Sea. Mar. Ecol. Prog. Ser. 193, 143–156.

MacKenzie, B.R., Miller, T.J., Cyr, S., C., L.W., 1994. Evidence for a dome-shaped relationship between turbulence and larval fish ingestion rates. Limnol. Oceanogr. 39, 1790–1799.

MacKenzie, B.R., Myers, R.A., Bowen, K.G., 2003. Spawner-recruit relationships and fish stock carrying capacity in aquatic ecosystems. Mar. Ecol. Prog. Ser. 248, 209–220.

Mangel, M., Clark, C.W., others, 1988. Dynamic modeling in behavioral ecology. Princeton University Press.

Markle, D.F., Frost, L.-A., 1985. Comparative morphology, seasonality, and a key to planktonic fish eggs from the Nova Scotian shelf. Can. J. Zool. 63, 246–257. https://doi.org/10.1139/z85-038

Marshall, C.T., Kjesbu, O.S., Yaragina, N.A., Solemdal, P., Ulltang, O., 1998. Is spawner biomass a sensitive measure of the reproductive and recruitment potential of Northeast Arctic cod? Can. J. Fish. Aquat. Sci. 55, 1766–1783. https://doi.org/10.1139/f98-062

Marshall, C.T., Needle, C.L., Thorsen, A., Kjesbu, O.S., Yaragina, N.A., 2006. Systematic bias in estimates of reproductive potential of an Atlantic cod (Gadus morhua) stock: implications for stock recruit theory and management. Can. J. Fish. Aquat. Sci. 63, 980–994.

Marteinsdottir, G., Begg, G.A., 2002. Essential relationships incorporating the influence of age, size and condition on variables required for estimation of reproductive potential in Atlantic cod Gadus morhua. Mar. Ecol. Prog. Ser. 235, 235–256. https://doi.org/10.3354/meps235235

Marteinsdottir, G., Gudmundsdottir, A., Thorsteinsson, V., Stefansson, G., 2000a. Spatial variation in abundance, size composition and viable egg production of spawning cod (Gadus morhua L.) in Icelandic waters. ICES J. Mar. Sci. 57, 824–830. https://doi.org/10.1006/jmsc.2000.0568

Marteinsdottir, G., Gunnarsson, B., Suthers, I.M., 2000b. Spatial variation in hatch date distributions and origin of pelagic juvenile cod in icelandic waters. ICES J. Mar. Sci. 57, 1182–1195. https://doi.org/10.1006/jmsc.2000.0880

Marteinsdøttir, G., Björnsson, H., 1999. Time and Duration of Spawning of Cod in Icelandic Waters. ICES C. Y:34, 1–14.

Marteinsdóttir, G., Pardoe, H., 2008. Effects of fishing on inter and intra stock diversity of marine resources, in: Fisheries for Global Welfare and Environment, 5th World Fisheries Congress 2008. pp. 27–43.

Marteinsdottir, G., Steinarsson, A., 1998. Maternal influence on the size and viability of Iceland cod Gadus morhua eggs and larvae. J. Fish Biol. 52, 1241–1258. https://doi.org/10.1006/jfbi.1998.0670

Marteinsdottir, G., Thorarinsson, K., 1998. Improving the stock-recruitment relationship in Icelandic cod (Gadus morhua) by including age diversity of spawners. Can. J. Fish. Aquat. Sci. 55, 1372–1377. https://doi.org/10.1139/f98-035

Mayr, E., 1961. Cause and effect in biology. Science (80-.). 134, 1501–1506.

McGinty, N., Guðmundsson, K., Ágústsdóttir, K., Marteinsdóttir, G., 2016. Environmental and climactic effects of chlorophyll-a variability around Iceland using reconstructed satellite data fields. J. Mar. Syst. 163, 31–42. https://doi.org/10.1016/j.jmarsys.2016.06.005

McGurk, M.D., 1986. Natural mortality of marine pelagic fish eggs and larvae: role of spatial patchiness. Mar. Ecol. Prog. Ser. 34, 227–242.

McNamara, J.M., Houston, A.I., 2009. Integrating function and mechanism. Trends Ecol. Evol. 24, 670–675. https://doi.org/10.1016/j.tree.2009.05.011

Mehner, T., 2012. Diel vertical migration of freshwater fishes - proximate triggers, ultimate causes and research perspectives. Freshw. Biol. 57, 1342–1359. https://doi.org/10.1111/j.1365-2427.2012.02811.x

Millero, F.J., Poisson, A., 1981. International one-atmosphere equation of state of seawater. Deep Sea Res. Part A, Oceanogr. Res. Pap. 28A, 625–629. https://doi.org/10.1016/0198-0149(81)90122-9

Morgan, S.G., 2014. Behaviorally Mediated Larval Transport in Upwelling Systems. Adv. Oceanogr. 2014, 1–17. https://doi.org/10.1155/2014/364214

Morgan, S.G., Anastasia, J.R., 2008. Behavioral tradeoff in estuarine larvae favors seaward migration over minimizing visibility to predators. Proc. Natl. Acad. Sci. U. S. A. 105, 222–227. https://doi.org/10.1073/pnas.0704725105

Morgan, S.G., Fisher, J.L., 2010. Larval behavior regulates nearshore retention and offshore migration in an upwelling shadow and along the open coast. Mar. Ecol. Prog. Ser. 404, 109–126. https://doi.org/10.3354/meps08476

Munoz, N.E., Blumstein, D.T., 2012. Multisensory perception in uncertain environments. Behav. Ecol. 23, 457–462. https://doi.org/10.1093/beheco/arr220

Murua, H., Saborido-Rey, F., 2003. Female reproductive strategies of marine fish species of the North Atlantic. J. Northwest Atl. Fish. Sci. 33, 23–31. https://doi.org/10.2960/J.v33.a2

Nanninga, G.B., Manica, A., 2018. Larval swimming capacities affect genetic differentiation and range size in demersal marine fishes. Mar. Ecol. Prog. Ser. 589, 1–

12. https://doi.org/10.3354/meps12515

Nathan, R., Getz, W.M., Revilla, E., Holyoak, M., Kadmon, R., Saltz, D., Smouse, P.E., 2008. A movement ecology paradigm for unifying organismal movement research. Proc. Natl. Acad. Sci. U. S. A. 105, 19052–19059.

Neubauer, P., Jensen, O.P., Hutchings, J.A., Baum, J.K., 2013. Resilience and recovery of overexploited marine populations. Science (80-.). 340, 347–349. https://doi.org/10.1126/science.1230441

Nissling, A., Larsson, R., Vallin, L., Frohlund, K., 1998. Assessment of egg and larval viability in cod, Gadus morhua: methods and results from an experimental study. Fish. Res. 38, 169–186.

Nissling, A., Nyberg, S., Petereit, C., 2017. Egg buoyancy of flounder, Platichthys flesus, in the Baltic Sea—adaptation to salinity and implications for egg survival. Fish. Res. 191, 179–189. https://doi.org/10.1016/j.fishres.2017.02.020

Nissling, A., Westin, L., 1997. Salinity requirements for successful spawning of Baltic and Belt Sea cod and the potential for cod stock interactions in the Baltic Sea. Mar. Ecol. Prog. Ser. 152, 261–271.

Nissling, A., Westin, L., 1991. Egg buoyancy of Baltic cod (Gadus morhua) and its implications for cod stock fluctuations in the Baltic. Mar. Biol. 111, 33–35. https://doi.org/10.1007/BF01986342

North, E.W., Schlag, Z., Hood, R.R., Li, M., Zhong, L., Gross, T., Kennedy, V.S., 2008. Vertical swimming behavior influences the dispersal of simulated oyster larvae in a coupled particle-tracking and hydrodynamic model of Chesapeake Bay. Mar. Ecol. Prog. Ser. 359, 99–115. https://doi.org/10.3354/meps07317

Ohman, M.D., 1990. The Demographic Benefits of Diel Vertical Migration of Zooplankton. Ecol. Monogr. 60, 257–281.

Ohman, M.D., Frost, B.W., Cohen, E.B., 1983. Reverse Diel Vertical Migration: An Escape from Invertebrate Predators. Science (80-.). 220, 1404–1407.

Ólafsdóttir, G.Á., Westfall, K.M., Edvardsson, R., Pálsson, S., 2014. Historical DNA reveals the demographic history of Atlantic cod (Gadus morhua) in medieval and early modern Iceland. Proc. R. Soc. B Biol. Sci. 281. https://doi.org/10.1098/rspb.2013.2976

Olafsson, J., 1985. Recruitment of Icelandic haddock and cod in relation to variability in the physical environment. ICES C. G:59, 10.

Opdal, A.F., Vikebø, F.B., Fiksen, Ø., 2011. Parental migration, climate and thermal exposure of larvae: Spawning in southern regions gives Northeast Arctic cod a warm start. Mar. Ecol. Prog. Ser. 439, 255–262. https://doi.org/10.3354/meps09335

Ospina-álvarez, A., Palomera, I., Parada, C., 2012. Changes in egg buoyancy during development and its effects on the vertical distribution of anchovy eggs. Fish. Res. 117–118, 86–95. https://doi.org/10.1016/j.fishres.2011.01.030

Ottersen, G., Bogstad, B., Yaragina, N.A., Stige, L.C., Vikebø, F.B., Dalpadado, P., 2014. A review of early life history dynamics of Barents Sea cod (Gadus morhua). ICES J. Mar. Sci. 71, 2064–2087.

Pampoulie, C., Ruzzante, D.E., Chosson, V., Jörundsdóttir, T.D., Taylor, L., Thorsteinsson, V., Daníelsdóttir, A.K., Marteinsdóttir, G., 2006. The genetic structure of Atlantic cod (Gadus morhua) around Iceland: Insight from microsatellites, the Pan I locus, and tagging experiments. Can. J. Fish. Aquat. Sci. 63, 2660–2674. https://doi.org/10.1139/F06-150

Parada, C., Van Der Lingen, C.D., Mullon, C., Penven, P., 2003. Modelling the effect of buoyancy on the transport of anchovy (Engraulis capensis) eggs from spawning to nursery grounds in the southern Benguela: An IBM approach. Fish. Oceanogr. 12, 170–184. https://doi.org/10.1046/j.1365-2419.2003.00235.x

Paris, C.B., Atema, J., Irisson, J.O., Kingsford, M., Gerlach, G., Guigand, C.M., 2013. Reef Odor: A Wake Up Call for Navigation in Reef Fish Larvae. PLoS One 8, 1–8. https://doi.org/10.1371/journal.pone.0072808

Paris, C.B., Cowen, R.K., 2004. Direct evidence of a biophysical retention mechanism for coral reef fish larvae. Limnol. Oceanogr. 49, 1964–1979. https://doi.org/10.4319/lo.2004.49.6.1964

Pauly, D., Pullin, R.S.V., 1988. Hatching time in spherical, pelagic, marine fish eggs in response to temperature and egg size. Environ. Biol. Fishes 22, 261–271. https://doi.org/10.1007/BF00004892

Peck, M.A., Hufnagl, M., 2012. Can IBMs tell us why most larvae die in the sea? Model sensitivities and scenarios reveal research needs. J. Mar. Syst. 93, 77–93. https://doi.org/10.1016/j.jmarsys.2011.08.005

Perälä, T., Kuparinen, A., 2017. Detection of Allee effects in marine fishes: Analytical biases generated by data availability and model selection. Proc. R. Soc. B Biol. Sci. 284. https://doi.org/10.1098/rspb.2017.1284

Petereit, C., Hinrichsen, H.H., Franke, A., Köster, F.W., 2014. Floating along buoyancy levels: Dispersal and survival of western Baltic fish eggs. Prog. Oceanogr. 122, 131–152. https://doi.org/10.1016/j.pocean.2014.01.001

Petitgas, P., Secor, D.H., McQuinn, I., Huse, G., Lo, N., 2010. Stock collapses and their recovery: Mechanisms that establish and maintain life-cycle closure in space and time. ICES J. Mar. Sci. 67, 1841–1848. https://doi.org/10.1093/icesjms/fsq082

Petursdottir, G., Begg, G.A., Marteinsdottir, G., 2006. Discrimination between Icelandic cod (Gadus morhua L.) populations from adjacent spawning areas based on otolith growth and shape. Fish. Res. 80, 182–189. https://doi.org/10.1016/j.fishres.2006.05.002

Pinsky, M.L., Byler, D., 2015. Fishing, fast growth and climate variability increase the risk of collapse. Proc. R. Soc. B Biol. Sci. 282, 1–9. https://doi.org/10.1098/rspb.2015.1053

Pyke, G., 2019. Optimal foraging theory: An introduction, in: Encyclopedia of Animal Behavior. Elsevier Academic Press, pp. 111–117.

Quiñones, A.E., van Doorn, G.S., Pen, I., Weissing, F.J., Taborsky, M., 2016. Negotiation and appeasement can be more effective drivers of sociality than kin selection. Philos. Trans. R. Soc. B Biol. Sci. 371, 20150089.

Railsback, S.F., Harvey, B.C., 2013. Trait-mediated trophic interactions: Is foraging

theory keeping up? Trends Ecol. Evol. 28, 119–125. https://doi.org/10.1016/j.tree.2012.08.023

Railsback, S.F., Lamberson, R.H., Harvey, B.C., Duffy, W.E., 1999. Movement rules for individual-based models of stream fish. Ecol. Modell. 123, 73–89. https://doi.org/10.1016/S0304-3800(99)00124-6

Reebs, S.G., 2002. Plasticity of diel and circadian activity rhythms in fishes. Rev. Fish Biol. Fish. 12, 349–371. https://doi.org/10.1023/A:1025371804611

Rindorf, A., Cardinale, M., Shephard, S., De Oliveira, J.A.A., Hjorleifsson, E., Kempf, A., Luzenczyk, A., Millar, C., Miller, D.C.M., Needle, C.L., Simmonds, J., Vinther, M., 2017. Fishing for MSY: Using "pretty good yield" ranges without impairing recruitment. ICES J. Mar. Sci. 74, 525–534. https://doi.org/10.1093/icesjms/fsw111

Ringelberg, J., 2010. Diel Vertical Migration in Lakes, in: Diel Vertical Migration of Zooplankton in Lakes and Oceans. Springer, pp. 171–215.

Robichaud, D., Rose, G.A., 2004. Migratory behaviour and range in Atlantic cod: inference from a century of tagging. Fish Fish. 5, 185–214.

Sainmont, J., Andersen, K.H., Thygesen, U.H., Fiksen, Ø., Visser, A.W., 2015. An effective algorithm for approximating adaptive behavior in seasonal environments. Ecol. Modell. 311, 20–30. https://doi.org/10.1016/j.ecolmodel.2015.04.016

Salvanes, A.G.V., Skjæraasen, J.E., Nilsen, T., 2004. Sub-populations of coastal cod with different behaviour and life-history strategies. Mar. Ecol. Prog. Ser. 267, 241–251.

Schopka, S.A., 1994. Fluctuations in the cod stock off Iceland during the twentieth century in relation to changes in the fisheries and environment. ICES Mar. Sci. Symp. 198, 175–193.

Shanks, A.L., 2009. Pelagic larval duration and dispersal distance revisited. Biol. Bull. 216, 373–385. https://doi.org/10.2307/25548167

Sih, A., 2013. Understanding variation in behavioural responses to human-induced rapid environmental change: A conceptual overview. Anim. Behav. 85, 1077–1088. https://doi.org/10.1016/j.anbehav.2013.02.017

Sims, D.W., Wearmouth, V.J., Southall, E.J., Hill, J.M., Moore, P., Rawlinson, K., Hutchinson, N., Budd, G.C., Righton, D., Metcalfe, J.D., Nash, J.P., Morritt, D., 2006. Hunt warm, rest cool: Bioenergetic strategy underlying diel vertical migration of a benthic shark. J. Anim. Ecol. 75, 176–190. https://doi.org/10.1111/j.1365-2656.2005.01033.x

Sinclair, M., 1988. Marine populations. An essay on population regulation and speciation. Washington Sea Grant Program. University of Washington Press, Seattle.

Skajaa, K., Fernö, A., Folkvord, A., 2003. Swimming, feeding and predator avoidance in cod larvae (Gadus morhua L.): trade-offs between hunger and predation risk, in: The Big Fish Bang: Proceedings of the 26th Annual Larval Fish Conference. pp. 105–121.

Skjæraasen, J.E., Devine, J.A., Godiksen, J.A., Fonn, M., Otterå, H., Kjesbu, O.S., Norberg, B., Langangen, Ø., Karlsen, Ø., 2017. Timecourse of oocyte development in saithe Pollachius virens. J. Fish Biol. 90, 109–128. https://doi.org/10.1111/jfb.13161

Smart, T.I., Siddon, E.C., Duffy-Anderson, J.T., 2013. Vertical distributions of the early life stages of walleye pollock (Theragra chalcogramma) in the Southeastern Bering Sea. Deep. Res. Part II Top. Stud. Oceanogr. 94, 201–210. https://doi.org/10.1016/j.dsr2.2013.03.030

Solemdal, P., 1973. Transfer of Baltic flatfish to a marine environment and the long term effects on reproduction. Oikos Suppl. 15, 268–276.

Solemdal, P., 1970. Intraspecific Variations in size, buoyancy and growth of eggs and early larvae of Arcto-Norweign Cod, Gadus morhua L., due to parental and environmental effects. ICES C. F:28, 1–12.

Somarakis, S., Tsoukali, S., Giannoulaki, M., Schismenou, E., Nikolioudakis, N., 2019. Spawning stock, egg production and larval survival in relation to small pelagic fish recruitment. Mar. Ecol. Prog. Ser. 617–618, 113–136. https://doi.org/10.3354/meps12642

Staaterman, E., Paris, C.B., DeFerrari, H.A., Mann, D.A., Rice, A.N., D'Alessandro, E.K., 2014. Celestial patterns in marine soundscapes. Mar. Ecol. Prog. Ser. 508, 17–32. https://doi.org/10.3354/meps10911

Stein, M., Borovkov, V.A., 2004. Greenland cod (Gadus morhua): Modeling recruitment variation during the second half of the 20th century. Fish. Oceanogr. 13, 111–120. https://doi.org/10.1046/j.1365-2419.2003.00280.x

Steinberg, D.K., Landry, M.R., 2017. Zooplankton and the Ocean Carbon Cycle. Ann. Rev. Mar. Sci. 9, 413–444. https://doi.org/10.1146/annurev-marine-010814-015924

Stillman, R.A., Railsback, S.F., Giske, J., Berger, U., Grimm, V., 2015. Making predictions in a changing world: The benefits of individual-based ecology. Bioscience 65, 140–150. https://doi.org/10.1093/biosci/biu192

Sundby, S., 1997. Turbulence and ichthyoplankton: Influence on vertical distributions and encounter rates. Sci. Mar. 61, 159–176.

Sundby, S., 1991. Factors affecting the vertical distribution of eggs, in: ICES Marine Science Symposia. pp. 33–38.

Sundby, S., 1983. A one-dimensional model for the vertical distribution of pelagic fish eggs in the mixed layer. Deep Sea Res. Part A, Oceanogr. Res. Pap. 30, 645–661. https://doi.org/10.1016/0198-0149(83)90042-0

Sundby, S., Boyd, A.J., Hutchings, L., O'Toole, M.J., Thorisson, K., Thorsen, A., 2001. Interaction between Cape hake spawning and the circulation in the Northern Benguela upwelling ecosystem. African J. Mar. Sci. 23, 317–336.

Sundby, S., Kristiansen, T., 2015. The principles of buoyancy in Marine Fish Eggs and their vertical distributions across the World Oceans. PLoS One 10, 1–23. https://doi.org/10.1371/journal.pone.0138821

Swearer, S.E., Treml, E.A., Shima, J.S., 2019. A Review of Biophysical Models of Marine Larval Dispersal, in: Oceanography and Marine Biology. Taylor & Francis.

Takasuka, A., Aoki, I., Mitani, I., 2003. Evidence of growth-selective predation on larval Japanese anchovy Engraulis japonicus in Sagami Bay. Mar. Ecol. Prog. Ser. 252, 223–238.

Takasuka, A., Yoneda, M., Oozeki, Y., 2019. Density dependence in total egg production per spawner for marine fish. Fish Fish. 20, 125–137.

Tang, W., Bennett, D.A., 2010. Agent-based modeling of animal movement: a review. Geogr. Compass 4, 682–700.

Therkildsen, N.O., Hemmer-Hansen, J., Hedeholm, R.B., Wisz, M.S., Pampoulie, C., Meldrup, D., Bonanomi, S., Retzel, A., Olsen, S.M., Nielsen, E.E., 2013. Spatiotemporal SNP analysis reveals pronounced biocomplexity at the northern range margin of Atlantic cod Gadus morhua. Evol. Appl. 6, 690–705. https://doi.org/10.1111/eva.12055

Thompson, B.M., Riley, J.D., 1981. Egg and larval development studies in the North Sea cod (Gadus morhua L.). Rapp. P.-V. Reun. Cons. Int. Explo. Mer 178, 553–559.

Thordardottir, T., 1984. Primary production north of Iceland in relation to water masses in May--June 1970--1980. ICES C. 50, 20.

Thórdardóttir, T., 1986. Timing and duration of spring blooming south and southwest of Iceland, in: The Role of Freshwater Outflow in Coastal Marine Ecosystems. Springer, pp. 345–360.

Thygesen, U.H., Ådlandsvik, B., 2007. Simulating vertical turbulent dispersal with finite volumes and binned random walks. Mar. Ecol. Prog. Ser. 347, 145–153. https://doi.org/10.3354/meps06975

Todd, P.M., Gigerenzer, G., 2007. Environments that make us smart: Ecological rationality. Curr. Dir. Psychol. Sci. 16, 167–171. https://doi.org/10.1111/j.1467-8721.2007.00497.x

Trippel, E.A., 1999. Estimation of stock reproductive potential: History and challenges for Canadian Atlantic gadoid stock assessments. J. Northwest Atl. Fish. Sci. 25, 61–81. https://doi.org/10.2960/J.v25.a6

Trippel, E.A., Neil, S.R.E., 2004. Maternal and seasonal differences in egg sizes and spawning activity of northwest Atlantic haddock (Melanogrammus aeglefinus) in relation to body size and condition. Can. J. Fish. Aquat. Sci. 61, 2097–2110. https://doi.org/10.1139/F04-125

Valdimarsson, H., Astthorsson, O.S., Palsson, J., 2012. Hydrographic variability in Icelandic waters during recent decades and related changes in distribution of some fish species. ICES J. Mar. Sci. 69, 816–825.

Valdimarsson, H., Malmberg, S., 1999. Near-surface circulation in Icelandic waters derived from satellite tracked drifters. Rit Fiskid. 16, 23–39.

Vallin, L., Nissling, A., 2000. Maternal effects on egg size and egg buoyancy of Baltic cod, Gadus morhua, implications for stock structure effects on recruitment. Fish. Res. 49, 21–37. https://doi.org/10.1016/s0165-7836(00)00194-6

Vikebø, F., Jørgensen, C., Kristiansen, T., Fiksen, Ø., 2007. Drift, growth, and survival of larval Northeast Arctic cod with simple rules of behaviour. Mar. Ecol. Prog. Ser. 347, 207–219. https://doi.org/10.3354/meps06979

Violle, C., Enquist, B.J., McGill, B.J., Jiang, L., Albert, C.H., Hulshof, C., Jung, V., Messier, J., 2012. The return of the variance: Intraspecific variability in community

ecology. Trends Ecol. Evol. 27, 244–252. https://doi.org/10.1016/j.tree.2011.11.014

Vollset, K.W., Catalán, I.A., Fiksen, Ø., Folkvord, A., 2013. Effect of food deprivation on distribution of larval and early juvenile cod in experimental vertical temperature and light gradients. Mar. Ecol. Prog. Ser. 475, 191–201. https://doi.org/10.3354/meps10129

Werner, E.E., Anholt, B.R., 1993. Ecological consequences of the trade-off between growth and mortality rates mediated by foraging activity. Am. Nat. 142, 242–272.

Werner, E.E., Gilliam, J.F., 1984. The ontogenetic niche and species interaction in size-structured populations. Annu. Rev. Ecol. Syst. 15, 393–425.

Westgård, T., 1989. Two models of the vertical distribution of pelagic fish eggs in the turbulent upper layer of the ocean. Rapp. P.-v. Reun. Cons. int. Explor. Mer 191, 195–200.

Wieland, K., Hovgård, H., 2002. Distribution and drift of Atlantic cod (Gadus morhua) eggs and larvae in Greenland offshore waters. J. Northwest Atl. Fish. Sci. 30, 61–76. https://doi.org/10.2960/j.v30.a4

Worm, B., Barbier, E.B., Beaumont, N., Duffy, J.E., Folke, C., Halpern, B.S., Jackson, J.B.C., Lotze, H.K., Micheli, F., Palumbi, S.R., Sala, E., Selkoe, J.J.S., Watson, R., 2006. Impacts of Biodiversity Loss on Ocean Ecosystem Services. Science (80-.). 314, 787–791. https://doi.org/10.1126/science.1132294

Worm, B., Hilborn, R., Baum, J.K., Branch, T.A., Collie, J.S., Costello, C., Fogarty, M.J., Fulton, E.A., Hutchings, J.A., Jennings, S., Jensen, O.P., Lotze, H.K., Mace, P.M., McClanahan, T.R., Minto, C., Palumbi, S.R., Parma, A.M., Ricard, D., Rosenberg, A.A., Watson, R., Zeller, D., 2009. Rebuilding Global Fisheries. Science (80-.). 325, 578–585. https://doi.org/10.1126/science.1173146

Zhai, L., Gudmundsson, K., Miller, P., Peng, W., Gufinnsson, H., Debes, H., Hátún, H., White, G.N., Hernández Walls, R., Sathyendranath, S., Platt, T., 2012. Phytoplankton phenology and production around Iceland and Faroes. Cont. Shelf Res. 37, 15–25. https://doi.org/10.1016/j.csr.2012.01.013

Zuur, A., Ieno, E.N., Walker, N., Saveliev, A.A., Smith, G.M., 2009. Mixed effects models and extensions in ecology with R. Springer Science & Business Media.

Paper I

Paper I

Egg size and density estimates for three gadoids in Icelandic waters and their implications for the vertical distribution of eggs along a stratified water column

William E. Butler, Lovísa Ó. Guðmundsdóttir, Kai Logemann, Tom J. Langbehn, and Guðrún Marteinsdóttir.

Published in the *Journal of Marine Systems* 204 (2020): 103290.

Author contributions: WB and GM jointly conceived the study idea. GM supervised the project. WB and TL carried out the sampling and laboratory experiments for haddock and saithe. LG carried out the sampling and laboratory experiments for cod. WB programmed the VertEgg model in R. WB performed all analyses. KL wrote a Fortran program for the extraction of environmental profiles from the 3-D hydrodynamic model CODE. WB prepared the initial manuscript. All authors contributed to revisions.

Journal of Marine Systems 204 (2020) 103290

Contents lists available at ScienceDirect

Journal of Marine Systems

journal homepage: www.elsevier.com/locate/jmarsys

Egg size and density estimates for three gadoids in Icelandic waters and their implications for the vertical distribution of eggs along a stratified water column

W.E. Butler[a,*], L.Ó. Guðmundsdóttir[a], K. Logemann[b], T.J. Langbehn[c], G. Marteinsdóttir[a]

[a] MARICE, Faculty of Life and Environmental Sciences, University of Iceland, Askja, Sturlugata 7, 101 Reykjavik, Iceland
[b] Institute of Coastal Research, Helmholtz-Zentrum Geesthacht, Max-Planck-Straße 1, 21502 Geesthacht, Germany
[c] Department of Biological Sciences, University of Bergen, Thormøhlensgate 53B, 5020 Bergen, Norway

ARTICLE INFO

Keywords:
Fish eggs
Vertical distribution
Buoyancy
Density measurement
Gadoid
Biophysical model
North Atlantic, Iceland

ABSTRACT

The vertical distribution of fish eggs can have important consequences for recruitment through its influence on dispersal trajectories and thus connectivity between spawning and nursery locations. Egg density and size are key parameters for the modelling of vertical egg distributions, both of which show variation at the species level, as well as between and within individuals (i.e., through ontogeny). We conducted laboratory experiments on the eggs of wild-spawning cod, haddock and saithe from Icelandic waters to estimate these parameters throughout ontogeny. Subsequently, this information was used in a 1-dimensional model to generate vertical distributions for each species along a stratified water column. Saithe eggs were significantly smaller and less dense than cod and haddock eggs. Cod eggs were slightly denser than haddock eggs in the first ontogenetic stage but statistically similar in the later stages. No significant differences were found between the egg diameters of cod and haddock. For each species, both parameters changed significantly through ontogeny. Yet despite these significant results, the 1-d model suggests that neither the interspecific nor ontogenetic differences would have a significant impact on the vertical egg distributions. Only under highly stratified conditions, when buoyancy is minimised due to the freshwater layer, do distributional differences become evident. In such situations, incorporating intraspecific variation in egg density into the model substantially reduced the distributional differences and this is highlighted as an important consideration for the modelling of pelagic vertical egg distributions.

1. Introduction

Owing to variation in the direction and amplitude of currents throughout the water column, plankton separated by small vertical distances can take vastly different drift trajectories. For pelagic fish eggs, this can lead to variation in the quality of habitat during the first feeding "critical period" (Hjort, 1914) and in the transport success to suitable nursery grounds (Parada et al., 2003; Huret et al., 2007; Kuroda et al., 2014; Santos et al., 2018). Knowledge of the vertical distributions of eggs and how they change along environmental gradients is therefore an important precursor to understanding the viability of early life-stages and subsequently populations. This entails consideration of how an egg's physical properties (or traits) interact with the prevailing abiotic conditions (Sundby, 1983, 1991). Biophysical models—which couple individual-based models (IBMs) to hydrodynamic models—are a widely used method to examine the dispersal of early life-stages (Fiksen et al., 2007; Staaterman and Paris, 2014). Flow fields from the hydrodynamic model advect individuals through heterogeneous, dynamic environments, whilst IBMs provide a platform to simulate how individuals respond to the prevailing environment. The key strength of IBMs is that they simulate populations of unique individuals, and through the interactions of these individuals with each other and the environment, populations properties emerge (Huston et al., 1988; Grimm and Railsback, 2005). For pelagic fish eggs, variation in traits that affect vertical positioning can ultimately lead to variation in key emergent properties including growth and mortality rates, and the spatiotemporal location at hatching (e.g., Hinrichsen et al., 2016).

Egg density (or specific gravity) and, to a lesser degree, size are important physical properties for the modelling of vertical egg distributions (Sundby, 1983; Ådlandsvik, 2000; Petitgas et al., 2006) and individual dispersal trajectories (Thygesen and Ådlandsvik, 2007). Naturally, these properties show great variation between species (e.g. Pauly and Pullin, 1988; Petereit et al., 2014; Sundby and Kristiansen,

* Corresponding author.
E-mail address: will.butler42@gmail.com (W.E. Butler).

https://doi.org/10.1016/j.jmarsys.2019.103290
Received 10 September 2019; Received in revised form 6 December 2019; Accepted 17 December 2019
Available online 20 December 2019

2015). Considerable variation can also exist between stocks of the same species (e.g. Thorsen et al., 1996) with important consequences for the survival of progeny. For example, the large size and low density of Baltic cod eggs ensure they remain above the stressful anoxic layer (Nissling and Westin, 1991; Vallin and Nissling, 2000). This is an adaptation to avoid low oxygen environments, one also seen in flatfish species (Nissling et al., 2017) and the spawning strategies of Cape hake females (Sundby et al., 2001). In contrast, the closely related Norwegian coastal cod produce smaller eggs of greater density that generate a pelagic rather than bathypelagic vertical distribution (Jung et al., 2012) which can lead to retention of offspring in local fjords, and thus a degree of segregation between spawning sub-populations (Ciannelli et al., 2010; Myksvoll et al., 2011, 2014). Furthermore, several studies have highlighted how ontogenetic variation in egg density (e.g., Jung et al., 2012) can have pronounced effects on vertical distributions (Ådlandsvik et al., 2001; Ospina-Álvarez et al., 2012; Petereit et al., 2014), possibly controlling the development and maintenance of mesopelagic egg distributions (Sundby and Kristiansen, 2015).

In Icelandic waters, the main spawning grounds for Atlantic cod (*Gadus morhua*), haddock (*Melanogrammus aeglefinus*) and saithe (*Pollachius virens*) are in the southwest. Despite spatial and temporal overlap in spawning activity, there are distinct differences between the three species. The most notable of these differences is the sequential nature of spawning activity in time, with saithe spawning from late January to mid-March (Jónsson and Pálsson, 2013), cod from mid-March to mid-May (Marteinsdóttir and Björnsson, 1999), and haddock from early April to late May (Jónsson and Pálsson, 2013). From a spatial perspective, a sequential pattern is also seen with the distance-to-shore from the main spawning grounds increasing from cod and haddock (Marteinsdottir et al., 2000) to saithe (Armannsson et al., 2007). These interspecific differences in spawning activity will generate environmental exposures for eggs/larvae that vary between the three species. In particular, distance-to-shore may have a large influence on early life stage survival due to the influence of freshwater runoff which is hypothesized to be tightly linked to recruitment success in two ways. Firstly, the presence of coastal water stabilises the water column, providing conditions to initiate the early phytoplankton bloom in coastal waters (Thórdardóttir, 1986) which has been correlated with key prey items for gadoid larvae (e.g., Gislason et al., 1994). Secondly, through its influence on the Icelandic Coastal Current which is primarily driven by entrained runoff (Logemann et al., 2013) and thought to play a crucial role in the transportation of gadoid larvae to the preferred nursery habitats in the north (Olafsson, 1985; Begg and Marteinsdottir, 2002; Brickman et al., 2007; Jonasson et al., 2009).

In this study, we conducted laboratory experiments to measure the density and diameter of wild-spawning cod, haddock and saithe eggs. Subsequently, we used a one-dimensional advection-diffusion model to examine how these properties affect the vertical positioning of eggs in environmental gradients that encompass the range of realistic abiotic conditions for each species. The overall objectives of the laboratory experiments are to: (1) assess whether there are differences in the physical properties of eggs between the three species, and (2) assess whether these physical properties change through ontogeny for each species. Subsequently, the vertical distribution model is used to evaluate what impacts these differences and changes have on the vertical distribution of eggs along a stratified water column, and to examine how these impacts vary when accounting for intraspecific natural variation in the physical egg properties.

2. Materials and methods

2.1. Sampling procedure

Samples were collected aboard commercial fishing vessels at known spawning grounds in southwest Iceland (Fig. 1 and Table 1). Haddock and saithe were sampled in 2012 and combined with archived cod data from 2010 (Guðmundsdóttir, 2013). The procedure for collecting, fertilising and storing eggs followed those applied in previous studies in Icelandic waters (Marteinsdottir and Begg, 2002; Guðmundsdóttir, 2013). Eggs were stripped from freely running females and stored in separate 1 l plastic beakers, hereafter referred to as batches. Each batch was fertilised in vitro by applying fresh milt to the eggs, stirring, and adding fresh seawater. Although effort was made to cross-fertilise individual males and females, this was not always possible due to a scarcity of running males. In such cases, prompt fertilisation was prioritised and the milt from an individual male was used to fertilise up to three females (from the same haul). After fertilisation, organic debris was removed to avoid contamination, and to ensure batches were adequately oxygenated, water changes were conducted at 30 min post-fertilisation and subsequently at regular intervals never exceeding 3 h. The temperature of each batch was continuously monitored to ensure congruence with the ambient seawater (6–7 °C) by applying/removing ice surrounding each batch. All sampled fish were tagged and stored until morphological measurements could be taken. Total length (L) and total weight (W) were measured to the nearest centimetre and gram respectively. Weight measurements could not be taken for haddock.

Upon landing, samples were immediately transferred to the mariculture laboratory at Staður, Grindavík. Each batch was transferred to a 25-l hatching silo with running water pumped from the neighbouring sea. If hatching silos were not available, batches were stored in a temperature-regulated room using 6-l plastic cylinders filled with fresh seawater and aeration stones. In these cases, water changes were conducted daily until 3 days post-fertilisation (DPF), and at every measurement day thereafter. Temperature was kept at 7 ± 0.2 °C which, based on oceanographic monitoring at stations SB1 and SB2 (www.hafro.is/Sjora), adequately reflected the surface temperatures the eggs would likely experience in the wild (see Huret et al., 2016).

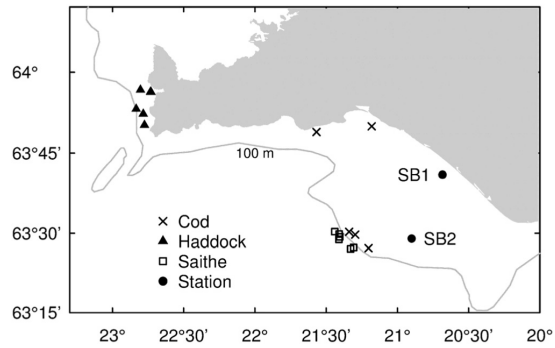

Fig. 1. Sampling locations for each species. Environmental profiles for modelling were extracted from a 3-dimensional hydrodynamic model at stations SB1 and SB2.

Table 1
Table showing the sampling dates, gear types and the number of spawning females sampled (n) whose eggs survived the duration of the experiments. The overall mean, standard deviation and range of female lengths (L) are shown for each species at each sampling date.

Species	Gear type	Date	n	$\bar{L}$ ± SD (cm)	Range (cm)
Cod	Gillnet	07/04/2010	4	97 ± 3.2	93–100
		13/04/2010	6	83 ± 6.1	74–90
Haddock	Danish seine	30/04/2012	9	50 ± 4.2	43–56
Saithe	Gillnet	10/04/2012	6	88.5 ± 5.1	81–94
		13/04/2012	8	97 ± 11.3	87–115

2.2. Egg density and diameter measurements

Egg density (ρ_{egg}) was measured using density gradient columns, following the protocol set out by Coombs (1981). Low and high saline solutions, corresponding to salinities of approximately 24.3‰ and 47.3‰ respectively, were prepared using de-ionised water and NaCl, and subsequently mixed to create a linear density gradient. The end-points were determined in a pilot study using eggs from captive cod and were chosen to encompass the range of neutral buoyancies displayed by the eggs and two sets of calibration beads (Martin Instrument, Inc). For beads not calibrated at 7 °C, a temperature adjustment was provided by Martin Instrument to account for the discrepancy. Density gradients were calibrated at the beginning of each measurement day and whenever new columns were created. The latter instance occurred every second measurement day unless calibrations suggested the density gradient was not linear ($r < 0.99$), the columns were physically disturbed, or eggs/larvae were not captured by the ascending basket.

Measurement days were synchronised between haddock and saithe but unsynchronised with cod. This was due to the sampling regime where opportunities to sample were dependent on the schedule of commercial fishing vessels. On each measurement day, random samples of eggs from each batch were gently placed into the top of the column. Eggs were given a minimum of 30 min (determined in the pilot study) to reach neutral buoyancy, but if visual inspection deemed them to still be adjusting their depth, they were re-checked at 15-min intervals until neutral buoyancy was achieved. By and large, 30 min was adequate for saithe, whilst 45–60 min was appropriate for haddock eggs. Measurements ceased when 50% of the surviving eggs in a batch had hatched. This was estimated by assessing random samples from the hatching silos under the microscope.

A subsample of the archived cod data was measured at 6 °C and 8 °C, therefore we employed a temperature correction using the UNESCO equation of state for seawater (Millero and Poisson, 1981) to standardise all density measurements at 7 °C. Subsequently, the same equation was used to calculate each egg's corresponding salinity of neutral buoyancy (S_{egg}) for use in the advection diffusion model.

Random samples of ten eggs per batch per measurement day were used to estimate egg diameters (D) and assess their quality and development. This was carried out independently of the density experiments. To obtain high resolution photographs, we deployed a Pixxelink PL-A662 camera attached to a Leica MZ95 stereomicroscope. Camera settings were individually calibrated to the eggs to obtain the maximal picture quality at a resolution of 1280 × 1024 pixels. For each batch at each measurement day, the camera was calibrated with a microscale allowing measurements of egg diameter to the nearest micrometre using the free domain image processing and analysing software ImageJ 1.45 (Schneider et al., 2012). The samples were staged according to the classification scheme developed by Thompson and Riley (1981) with the minor adjustment that stages IA and IB were pooled together (IAB). For each DPF, the data was pooled over batches and the dominant ontogenetic stage identified. This resulted in a unique ontogenetic stage for each measurement day per species (Table 2).

2.3. Statistical analyses

Mixed effects models were used to model egg density as a response to egg stage *ES* (ordered factor, see Table 2), female length L (covariate), batch B (factor), species Sp (factor), and mean diameter per batch $\overline{D}_B$ (covariate). Egg diameter was modelled as a response to the same explanatory variables excluding $\overline{D}_B$. Because the statistical procedures were identical for both responses, we solely focus on ρ_{egg} here. Batches were unique to each species, therefore a mixed effects modelling approach was used with B treated as a random effect. This allowed for correlations between individuals of the same species (see Zuur et al., 2009) and facilitated general conclusions about females within species rather than conclusions about the specific females sampled. A suite of linear mixed-effects models were fit using the nlme R package (Pinheiro et al., 2019). Species-specific models were fit with *ES*, L and $\overline{D}_B$ as additive explanatory variables (i.e., $ES + L + \overline{D}_B$). The species factor was introduced to test for significant interactions between species and each explanatory variable (i.e., $Sp{\bullet}ES + Sp{\bullet}L + Sp{\bullet}\overline{D}_B$). Differences between the inshore and offshore sampling sites (Fig. 1) for cod were tested by expanding the Sp factor to four levels (cod_{In}, cod_{Off}, haddock and saithe). Intraclass correlation coefficients (ICCs) were calculated to understand the proportion of random-effect variance explained by B; high values indicated strong correlations between individual eggs from the same batch, and vice versa (Zuur et al., 2009; Nakagawa and Schielzeth, 2010).

Prior to fitting the models, the protocol for data exploration set out by Zuur et al. (2010) was followed to visualise relationships between variables, identify outliers, heteroscedasticity and non-normality. Subsequently, the stepwise model selection procedure recommended by Zuur et al. (2009) was followed to obtain the optimal model structure and test the significance of explanatory variables/interactions. This involved using the Akaike- and Bayesian Information Criteria (AIC and BIC) and the log-likelihood ratio to test the goodness of fit between models. Starting with the full model, the optimal random structure was identified by comparing models fit by restricted maximum likelihood estimation (REML). This step included testing whether a mixed effects model performed better than an ordinary linear regression (fit using the "gls" function). The optimal fixed structure was then identified by comparing models fit by Maximum Likelihood. The final optimal model was presented using REML fits. At each step, normalised residuals were plotted against fitted values and all explanatory variables to check whether model assumptions were violated at each stage of the process. Heteroscedasticity was present for both response variables, so variance structures were employed to achieve homoscedasticity (using the "varIdent" function), these allowed the spread of residuals to vary between levels of a grouping factor (see Zuur et al., 2009). This method was more effective at stabilising the variances than transformations. The optimal structure for ρ_{egg} and D allowed for different variances at each level of the $Sp \cdot ES$ interaction. Post hoc analyses were carried out using the emmeans R package (Lenth, 2019). Contrasts between species at each specific *ES* were generated to examine interspecific differences. Contrasts were also generated for each successive *ES* comparison (i.e., IAB-II, II-III etc) to examine changes through ontogeny within each species.

Table 2
The dominant ontogenetic stage for each measurement day (DPF).

	Ontogenetic stage				
	IAB	II	III	IV	V
Cod	2	5	7	10	13
Haddock	1	3	6	9	12
Saithe	1	3	6	–	9

2.4. Vertical egg distribution model

The MATLAB VertEgg toolbox (Ådlandsvik, 2000) was used to model the vertical distribution of gadoid eggs. The toolbox contains analytical and numerical solutions to Sundby's (1983) one-dimensional vertical distribution model. The model is based on a transport equation, with the vertical flux determined by the egg's terminal velocity—the velocity an egg ascends/descends when the buoyant forces balance the frictional drag—and diffusion modelled by Fick's law using the vertical eddy diffusivity coefficient. The toolbox was converted to the R programming language and additional functionality added where required. The theory behind the model and its solutions is detailed in Sundby (1983), Westgård (1989), and Ådlandsvik, (2000).

2.5. Environmental gradients

Vertical profiles of the water column were extracted from the three-dimensional hydrodynamic model CODE (Cartesian coordinates Ocean model with three-Dimensional adaptive mesh refinement and primitive Equations [Logemann et al., 2013]). In Icelandic waters, CODE has a maximum horizontal and vertical resolution of 1 km and 2.5 m respectively. Freshwater runoff from 46 Icelandic watersheds, estimated by the hydrological model WaSiM (Schulla and Jasper, 2007), are assimilated together with 16,802 CTD profiles to provide a detailed simulation of the regional hydrography of Icelandic waters (Logemann et al., 2013). The model is fully documented in Logemann et al. (2012) and results from recent simulations covering the period between 1992 and 2006 are detailed in Logemann et al. (2013). Output from CODE is stored at 3 hourly intervals and at irregular depth intervals (due to the adaptive mesh refinement, see Logemann et al., 2012), therefore all variables of interest were linearly interpolated along depth to obtain values at 2.5 m intervals. These included temperature T (°C), potential temperature θ (°C), salinity S (psu), in situ density ρ (kg m^{-3}), potential density ρ_θ (kg m^{-3}), and vertical eddy diffusivity K (m^2 s^{-1}).

Vertical profiles were extracted at two locations (Fig. 1) at 00:00 UTC each day in 2006 for a period encompassing the spawning activities of all three species plus an additional 12 days (hatching time for haddock, Table 2) to account for unhatched eggs when spawning has ceased. These locations are part of the Marine Research Institute's annual monitoring programme for hydrography and biological productivity. Situated approximately 5 km offshore, SB1 is 40 m deep and in the path of the freshwater-driven Icelandic Coastal Current. Station SB2 is approximately 25 km offshore, 80 m deep and in the path of incoming Atlantic water. The spawning season of 2006 provided a suitable array of vertical density gradients (from well-mixed to highly stratified) to examine how stratification affects the vertical distribution of eggs.

To estimate the stratification for each vertical profile, we calculated an approximation of the Brunt-Väisälä frequency N^2 (s^{-1}) over the upper 40 m of the water column (see Li et al., 2015; Fig. S1). An exceptionally strong correlation (r_s = 0.98) between N^2 calculated over 40 m and 80 m at station SB2 suggests that constraining N^2 to the upper 40 m adequately captures the water column's stratification.

2.6. Model simulations

For each daily vertical profile, we found the steady-state solution (φ) to the advection diffusion equation using the "sstate" function from the VertEgg toolbox (equation 2.45 in Ådlandsvik, 2000). The "eggvelst" function was used to calculate the terminal velocities. Due to the variable temperature gradients, these were calculated using the S_{egg} values derived from the empirical dataset (see Section 2.2). To account for natural variation in the physical egg properties, we carried out Monte Carlo Markov Chain (MCMC) simulations. This involved generating 75,000 random samples of S_{egg} and/or D, calculating φ for each sample, summing all distributions by depth interval, and normalising the aggregated distribution to obtain the relative abundance of eggs per grid cell, φ^*. Random samples were generated by assuming Gaussian distributions characterised by the species-specific means and standard deviations from the laboratory measurements (Fig. 3), a reasonable assumption based on evidence from the observed dataset. Random samples were generated for S_{egg} and D independently (i.e., one variable was randomly generated whilst the other was fixed at its mean). To test the sensitivity of this assumption, simulations were also carried out by assuming a linear relationship between both variables based on a linear model. The MCMC simulations were carried out using summary statistics for each species pooled over stage (Fig. 3b), and for each individual stage within species to assess variation through ontogeny (Fig. 3a). Convergence between the normalised distribution and key descriptors of the vertical egg distribution (see below) at i and i-1 was used to gauge the number of simulations required to adequately account for natural variation in S_{egg} and D.

2.7. Model analyses

The output comprised the number of eggs per grid cell (grid cell thickness = 2.5 m) with a total of 100 eggs in the water column. Subsequently, we calculated the median depth $\tilde{z}$ (m) of the distribution and several percentiles to describe its spread. The median was preferred as a measure of central tendency as the distribution of eggs was often highly skewed. To compare distributions, the root-mean-square deviation RMSD (eggs m^{-3}) was calculated. This showed how two distributions differed in number of eggs per grid cell. To quantify interspecific differences in vertical egg distributions, the RMSD between $\varphi_C{}^*$ and $\varphi_H{}^*$ ($RMSD_{C\cdot H\cdot}$), $\varphi_C{}^*$ and $\varphi_S{}^*$ ($RMSD_{C\cdot S\cdot}$), and $\varphi_H{}^*$ and $\varphi_S{}^*$ ($RMSD_{H\cdot S\cdot}$) was computed for each daily profile. To quantify ontogenetic differences in vertical egg distributions, the RMSD was computed between the species-specific distributions ($\varphi_C{}^*$, $\varphi_H{}^*$ and $\varphi_S{}^*$) and the stage-specific distributions for the corresponding species (e.g., for cod, $RMSD_{C\cdot C_{IAB}{}^*} = \varphi_C{}^*$ *vs* $\varphi_{C_{IAB}}{}^*$). For both the interspecific and ontogenetic comparisons, equivalent RMSD's were calculated for the analytical solutions without the MCMC procedure, these are denoted in a similar manner but without the asterisk superscript (e.g., $RMSD_{CC_{IAB}} = \varphi_C$ *vs* $\varphi_{C_{IAB}}$). To assess how the magnitude of interspecific or ontogenetic differences in vertical egg distribution changed when accounting for the natural variation in physical egg properties, RMSD's were computed between the egg distributions generated with and without the MCMC procedure (e.g., $RMSD_{C\cdot C} = \varphi_C{}^*$ *vs* φ_C).

3. Results

3.1. Empirical analyses

3.1.1. Egg density

The *Sp*: *ES* interaction was highly significant (L = 515, df = 1, $p < .001$). Saithe eggs were significantly less dense than haddock and cod eggs at each stage (Fig. 3a; $p < .001$). Cod eggs were significantly denser than haddock eggs at stage IAB ($p < .01$); however, both species had statistically similar densities from stages II–V (Fig. 3a; $p > .05$). Within species, cod egg density had a significant decrease between stages II and III ($p < .001$) which was followed by a significant increase between stages III and IV ($p < .001$), a trend seen at both sampling sites (Table 3). Conversely for haddock, there was a significant increase in egg density at stage III (Fig. 3a; $p < .001$) which was followed by a significant decline in density at stage IV ($p < .001$). Saithe egg density decreased prior to hatching (stage V, Fig. 3a) and this stage was significantly less dense than all other stages ($p < .001$). Stage IAB was also significantly less dense than stages II ($p < .05$); however, this was likely due to the model underestimating egg density at stage IAB for saithe as both stages had similar means and spreads (Fig. 3a; Table 3). For each species, all other between-stage comparisons were not significant ($p > .05$).

The cod eggs sampled offshore had a higher density than the coastal cod at each stage (Table 3). However, none of these differences were statistically significant ($p > .05$) so it was concluded that cod had similar densities at each sampling site. The *Sp*: $\overline{D}_B$ interaction was significant (L = 148, df = 1, $p < .001$) suggesting that egg diameter is an important predictor of egg density. For each species comparison, the density-diameter gradients were significantly different ($p < .001$). A negative slope was found for cod and positive slopes for haddock and saithe (Fig. 4). Neither the *Sp*: L interaction nor the length main effect were significant (L = 5, df = 1, p = .077; L = 0.7, df = 1, p = .4) highlighting that no relationship was found between egg density and L for any species.

Incorporating batch as a random intercept substantially improved the model (L = 2027, df = 1, $p < .001$). The optimal random structure

Table 3
Egg density (g cm^{-3}; at 7 °C) and diameter (mm) summary statistics for each species, including for the cod sampled inshore (Cod_{In}) and offshore (Cod_{Off}). The mean, standard error (SE [$\times 10^4$]), number of individual egg measurements (n), and intraclass correlation coefficients derived from the optimal statistical model are presented. ICCs were not computed for the inshore/offshore cod components because no significant differences in either egg density or diameter were found between these components.

		Density				Diameter			
Species	ES	Mean	SE	n	ICC	Mean	SE	n	ICC
Cod	IAB	1.0260	0.522	316	0.51	1.4112	49.16	100	0.82
	II	1.0259	0.426	340	0.53	1.4235	48.04	100	0.82
	III	1.0249	0.361	337	0.51	1.4196	46.64	100	0.83
	IV	1.0257	0.557	474	0.25	1.4255	54.89	100	0.72
	V	1.0258	0.801	238	0.32	1.4191	58.34	80	0.86
Cod_{In}	IAB	1.0256	0.178	133	–	1.4001	88.43	40	–
	II	1.0258	0.413	97	–	1.4052	84.97	40	–
	III	1.0249	0.607	114	–	1.4079	90.17	40	–
	IV	1.0253	1.501	131	–	1.4121	106.0	40	–
	V	1.0255	0.876	62	–	1.3813	143.9	20	–
Cod_{Off}	IAB	1.0264	0.798	183	–	1.4185	55.52	60	–
	II	1.0260	0.568	243	–	1.4356	51.42	60	–
	III	1.0249	0.449	223	–	1.4273	47.38	60	–
	IV	1.0259	0.491	343	–	1.4345	56.02	60	–
	V	1.0259	1.030	176	–	1.4317	52.71	60	–
Haddock	IAB	1.0248	0.559	421	0.26	1.4193	52.99	89	0.52
	II	1.0248	0.428	320	0.66	1.4232	52.31	90	0.62
	III	1.0256	0.497	442	0.65	1.4428	62.41	89	0.61
	IV	1.0251	0.844	258	0.16	1.4425	45.38	88	0.77
	V	1.0253	0.621	282	0.19	1.4326	47.33	87	0.78
Saithe	IAB	1.0231	0.344	683	0.45	1.2153	39.17	133	0.67
	II	1.0231	0.277	840	0.70	1.2000	44.96	137	0.58
	III	1.0231	0.352	601	0.46	1.2237	31.57	140	0.74
	V	1.0217	1.070	115	0.22	1.1703	89.39	20	0.65

included a random intercept (variance = 4.29 × 10^{-7} g cm^{-3}), incorporating a random slope per species did not improve the model (L = 1.14, df = 1, p = .95). The ICCs highlight that between-batch variation was greater than within-batch variation at stages IAB–III for cod, stages II–III for haddock, and stage II for saithe (Table 3). Notably, correlations between individual egg densities were lowest later in ontogeny for each species (Table 3).

3.1.2. Egg diameter

The mean egg diameter per stage for saithe was consistently lower than cod and haddock (Fig. 3a). This was highlighted by a highly significant *Sp*: *ES* interaction (L = 80, df = 1, p < .001). Saithe eggs were significantly smaller than haddock and cod eggs at each stage (p < .001) whilst no significant differences (p > .05) were found between haddock and cod eggs. Within cod, the only significant change in diameter through ontogeny was an increase between stages IAB and II (p < .001). For haddock, diameter increased significantly between stages II and III (p < .001) and to a less extent between stages IV and V (p < .05; Table 3). In contrast, the diameter of saithe eggs fluctuated significantly between each ontogenetic stage (Fig. 3a; p < .005 for IAB-II, p < .001 for the other contrasts).

The cod sampled at the coastal site had consistently smaller diameters than the cod sampled further offshore (Table 3). However, none of the stage-specific differences between sampling sites were significant (p > .05). The *Sp*: L was significant (L = 6, df = 1, p = .041) but the haddock: length effect was the only one that differed from zero (p = .027) with smaller females producing larger eggs. None of the interspecific contrasts were significant (p > .05) suggesting that the diameter-length trends were similar between species. Although removing the cod female which had the smallest diameter across stages (Fig. 2) led to a significant contrast in the diameter-length trend between cod and haddock with smaller cod producing smaller eggs.

Incorporating batch as a random intercept substantially improved the model (L = 1466, df = 1, p < .001). The optimal random structure included a random intercept (variance = 0.0017 mm), including a random slope per species did not improve the model (L = 1.046, df = 1, p = .96). The ICCs indicate substantial correlations within batches for each level of the *Sp*: *ES* interaction (Table 3) with the between-batch variation always exceeding the within-batch variation.

3.2. Vertical distribution model

3.2.1. Terminal velocities

Pooling the data over *ES*, saithe had the highest terminal velocity (Fig. 5). Taken alone, the smaller diameter of saithe eggs would suggest a lower terminal velocity. However, this effect was overridden by their lower densities (Fig. 3b), which always ensured higher ascent speeds. The greater importance of density in determining terminal velocities was exemplified by comparing the distributions of terminal velocities between the two parameters. For all species, the range of diameters led to a much smaller range of terminal velocities than the range of densities (Fig. 5).

3.2.2. Interspecific differences in vertical egg distribution

At each station, the interspecific differences in egg distributions were maximised under stratified conditions (Table 4a) with minimal vertical mixing (Fig. 6). However, it was only under strongly stratified conditions at SB1 that distinctive interspecific differences were visible (Fig. 6, HS). These differences were driven by the distribution of saithe eggs (i.e., cod and haddock had similar distributions), demonstrated by the substantially higher RMSD values for the saithe comparisons (Table 4a). In low mixing scenarios, the egg's buoyancy (the density difference between the egg and the ambient water [$\Delta\rho = \rho_{egg} - \rho$]) became the predominant factor determining the vertical egg distribution. At SB1, the surface density (1.023 g cm^{-3}) is sufficiently low to drive down the cod (84% of eggs between 0 m and 10 m with 50% at 6 m) and haddock (92% of eggs between 0 m and 10 m with 50% at 4.5 m) eggs but not the saithe eggs which agglomerated in the surface grid cell (87% of eggs with 50% at 1.25 m) due to their lower density (Fig. 3). At SB2, surface density under stratified conditions was 1.027 g cm^{-3} which is substantially greater than all egg densities (Fig. 3) leading to 71%, 81% and 95% of eggs residing in the surface grid cell for cod, haddock and saithe respectively (Fig. 6), hence the lower interspecific differences (Table 4a).

At SB2, all interspecific comparisons were substantially less than the LS–HS comparisons demonstrating that the environment (particularly K) was the most important factor in determining the vertical egg distributions at this location (Table 4b). At SB1, changing species from either cod or haddock to saithe had a larger impact on the vertical egg distribution than changing the environment, but this is only under HS conditions (Table 4b). The HS-LS RSMD values were all greater than interspecific comparisons in the well-mixed scenarios (LS, Table 4b), which emphasised the homogenising effect of turbulence in these scenarios.

At SB1, interspecific differences increased linearly, and then decreased slightly before plateauing (Fig. 7). The HS environment presented in Fig. 6 is located at or close to the peaks for all the comparisons in Fig. 7. As stratification increased beyond this point, a higher proportion of saithe eggs are driven down from the surface grid cell due to the lower ambient density, thus leading to the dip in RMSD values for the saithe comparisons. At SB2, although a positive linear relationship was seen between all interspecific differences and stratification, the RMSD values were negligible when compared to SB1 (Fig. 7).

3.2.3. Ontogenetic differences in vertical egg distribution

Whilst the *Sp*: *ES* interaction was a significant predictor of egg density, incorporating the ontogenetic changes into the vertical distribution model revealed little impact of ontogeny on the vertical distribution of eggs (Fig. 8). For cod, the decrease in density at stage III

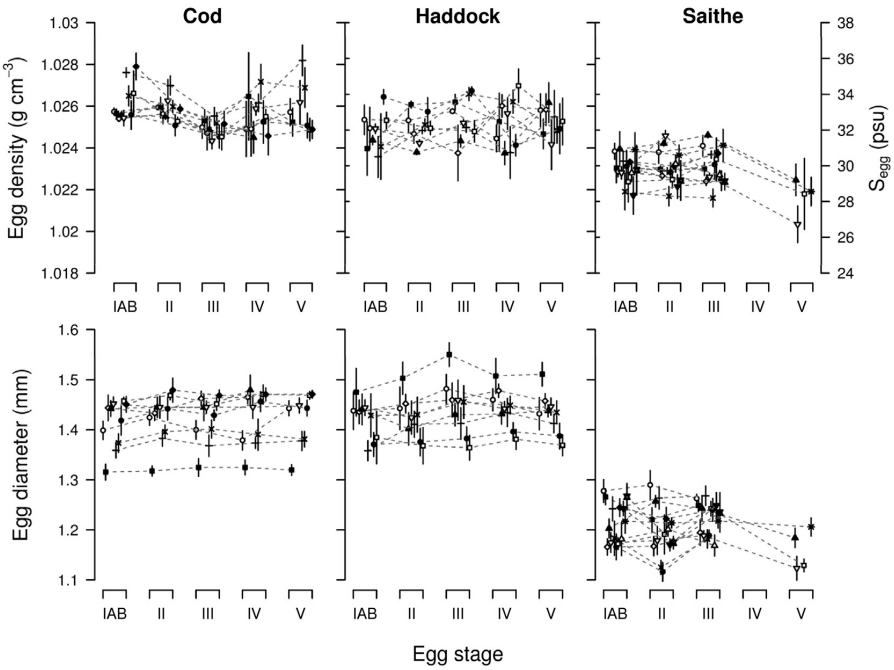

Fig. 2. The top row shows the mean (± 1 standard deviation) egg density and the corresponding salinity of neutral buoyancy (right axis) at 7 °C. The bottom row shows the mean (± 1 standard deviation) diameter at each ontogenetic stage for each batch. Each batch is represented by a unique symbol across stages.

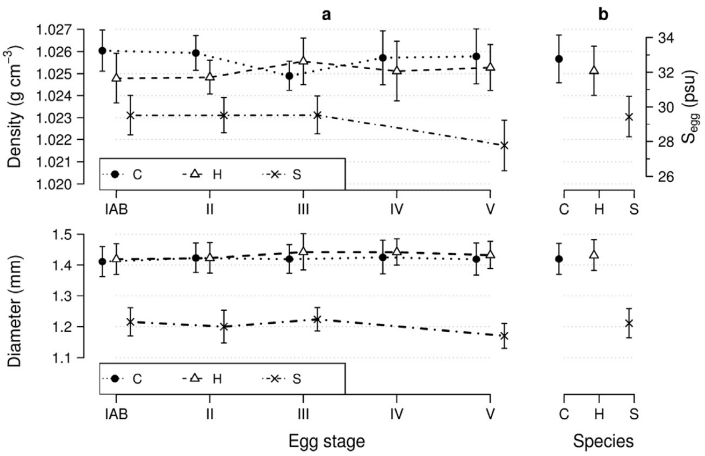

Fig. 3. The top row shows the mean (± 1 standard deviation) egg density and the corresponding salinity of neutral buoyancy (right axis) at 7 °C. The bottom row shows the mean (± 1 standard deviation) egg diameter. Stage-specific results are presented in panel a. Overall results (pooled over stage) are presented in panel b. For clarity, the points at each stage are staggered from left to right for cod (C), haddock (H) and saithe (S) respectively.

(Fig. 3a) led to an $RMSD_{C\text{-}C_{III}}$ of 3.98 eggs m^{-3} and a decrease in $\tilde{z}$ from 4.00 to 1.25 m. This was substantially greater than any other stage and driven by a greater accumulation of eggs in the surface layer (Fig. 8). A similar pattern is seen for saithe where the decrease in density at stage V (Fig. 3a) leads to a greater abundance of eggs in the surface grid cell as opposed to the 2.5–5 m grid cell in the baseline ($RMSD_{S\text{-}S_V}$ = 4.53 eggs m^{-3}; $\tilde{z}$ decreased from 2.98 to 1.25 m). Conversely, the increase in density at stage III for haddock leads to a reduced abundance in the surface grid cell ($\tilde{z}$ increased from 1.25 to 3.49 m); however, the magnitude of change from the baseline ($RMSD_{H\text{-}H_{III}}$ = 1.73 eggs m^{-3}) is smaller than the changes seen within cod and saithe. For haddock and saithe, all the ontogenetic comparisons were smaller than the LS-HS comparison, whilst for the cod, the RMSD at stage III was slightly larger (Fig. 8 and Table 4a).

Out of the 396 simulations (132 days multiplied by 3 species) run at SB1, the grid cell containing the egg maxima changed depth through ontogeny on 62 occasions (38 cod, 22 haddock and 2 saithe comparison). Of these 62, on only two occurrences did the depth change by greater than one grid cell. This, together with the RMSD's (Fig. 8) highlights the minimal impact that ontogenetic variation has on φ.

At station SB2, the range of RMSDs found through ontogeny were 0.12–1.42 eggs m^{-3} for cod, 0.00–0.61 eggs m^{-3} for haddock, and 0.00–0.52 eggs m^{-3} for saithe (Fig. S2). These values are comparable to the interspecific RMSD's which are all < 2 eggs m^{-3} (Fig. 7) and are considerably lower than the LS–HS comparisons (Table 4b), further highlighting that at station SB2 the environment had a greater impact

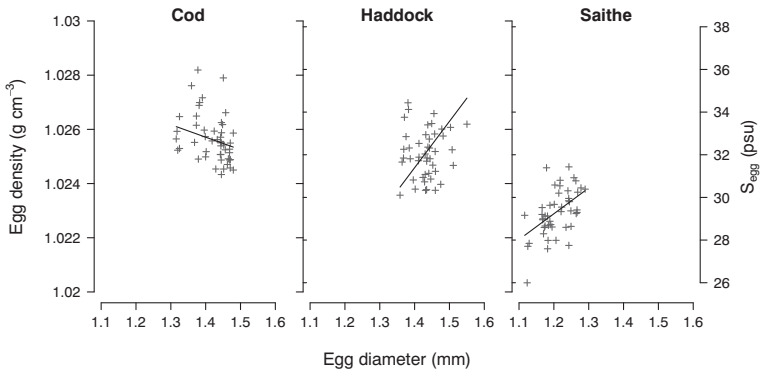

Fig. 4. The relationship between egg density and diameter for each species. The corresponding salinity of neutral buoyancy at 7 °C is shown on the right axis. The data points (+) represent the mean densities and diameters per batch per egg stage. The solid lines are model predictions across the range of diameters for each species.

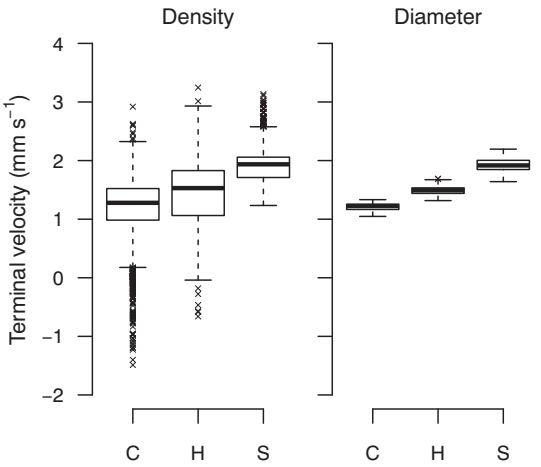

Fig. 5. Boxplots showing the distribution of terminal velocities calculated from the empirical egg density and diameter datasets (both pooled over *ES*) for cod (C), haddock (H) and saithe (S). When considering density, diameter was held constant at the species-specific mean, and vice versa. The median (central solid line), interquartile range (box limits) and 5th–95th percentiles (whisker limits) are shown. The points outlying the whiskers reflect the tails of the distribution. The environment's ambient density, temperature and molecular viscosity are assumed constant throughout the water column and equal to the means across time and both hydrological stations, 1027.6 kg m^{-3}, 7 °C and 1.5×10^{-3} kg m^{-1} s^{-1} respectively.

on egg distributions than either the species or the *ES* parameters. The grid cell containing the egg maxima did not change through ontogeny for any of the species in any environment at SB2.

3.2.4. Natural variation in egg density

For each interspecific comparison (Fig. 9, top row), accounting for natural variation in egg density reduced the spread of RMSD's by cutting down the right-hand tail of the distribution (i.e., the higher RMSD values). This was most noticeable for the C–H comparison where the range of RMSD's was reduced from 0.00–13.08 eggs m^3 to 0.53–2.13 eggs m^3 by incorporating distributional information on S_{egg}. This highlights the similarities in the distributions of S_{egg} between the two species (Fig. 3b). The saithe comparisons remained larger than the C–H comparison owing to the larger differences in the distributions of S_{egg} (Fig. 3b). The ranges were reduced from 0.00–14.09 eggs m^3 to 0.95–8.61 eggs m^3 for the C–S comparison, and 0.00–14.11 eggs m^3 to 0.41–7.53 eggs m^3 for the H–S comparison. On average, the differences between the two approaches were 1.70, 1.11 and 0.05 eggs m^3 for C–H, C–S and H–S respectively. This highlights the impact of stratification. In HS environments, using mean-only values will generate substantial interspecific differences in φ; however, these are substantially reduced when considering distributions of S_{egg} (Table 4). Under LS conditions (the majority of environments, Fig. 7), the MCMC procedure had little impact on φ because of the homogenising effect of turbulence (Table 4).

Accounting for natural variation in egg density substantially reduced the RMSDs characterising the ontogenetic comparisons for cod and haddock (Fig. 9). These reductions highlight that the differences between stage-specific φ and overall species-specific φ are minimised when accounting for natural variation in S_{egg} at each stage (also shown in Fig. 8). For saithe, the RMSD values did not change substantially when the MCMC procedure was used. Only at stage V were differences between stage-specific values and overall mean values seen (Fig. 9), and the MCMC procedure had minimal impact here suggesting that buoyancy ($\Delta\rho$) is high whether or not natural variation in S_{egg} is included.

At station SB2, the MCMC procedure had minimal impact on either the interspecific or ontogenetic differences. Whilst the RMSD's are typically higher when accounting for natural variation (Table 4; Fig. S3), the differences between the two approaches were sufficiently small to be considered negligible. For example, testing across the stratification gradient, the maximum absolute difference between the RMSD's was 0.52, 1.04 and 0.61 eggs m^{-3} for the C–H, C–S and H–S respectively and the mean differences were 0.08, 0.25 and 0.16 eggs m^{-3} respectively.

3.2.5. Sensitivity analyses

Sensitivity analyses showed that variation in neither egg diameter nor vertical molecular viscosity are important in determining the vertical distribution of eggs. Comparing with the baseline distribution for each species at each station, all RMSDs were below 0.07 eggs m^{-3} when assuming a linear relationship between egg density and diameter, and below 0.11 eggs m^{-3} when vertical gradients in molecular viscosity were incorporated. The model was also run with measured cod egg density parameters from 1996 (Marteinsdottir and Begg, 2002). Distributional differences were larger at SB1 (max RMSD = 3.89 eggs m^{-3}; mean RMSD = 2.54 eggs m^{-3}) than SB2 (max RMSD = 1.35 eggs m^{-3}; mean RMSD = 0.80 eggs m^{-3}). At SB1, $\tilde{z}$ was on average 1.25 m deeper in the baseline simulations whilst its interquartile range was 2.39 m larger, reflecting the heavier eggs found in the current study. However, in both simulations the egg maximum was located within 0–10 m and on only 27/132 occasions did it differ between the simulations (only by one grid cell in each instance). At SB2, the surface grid cell always contained the egg maximum in both simulations.

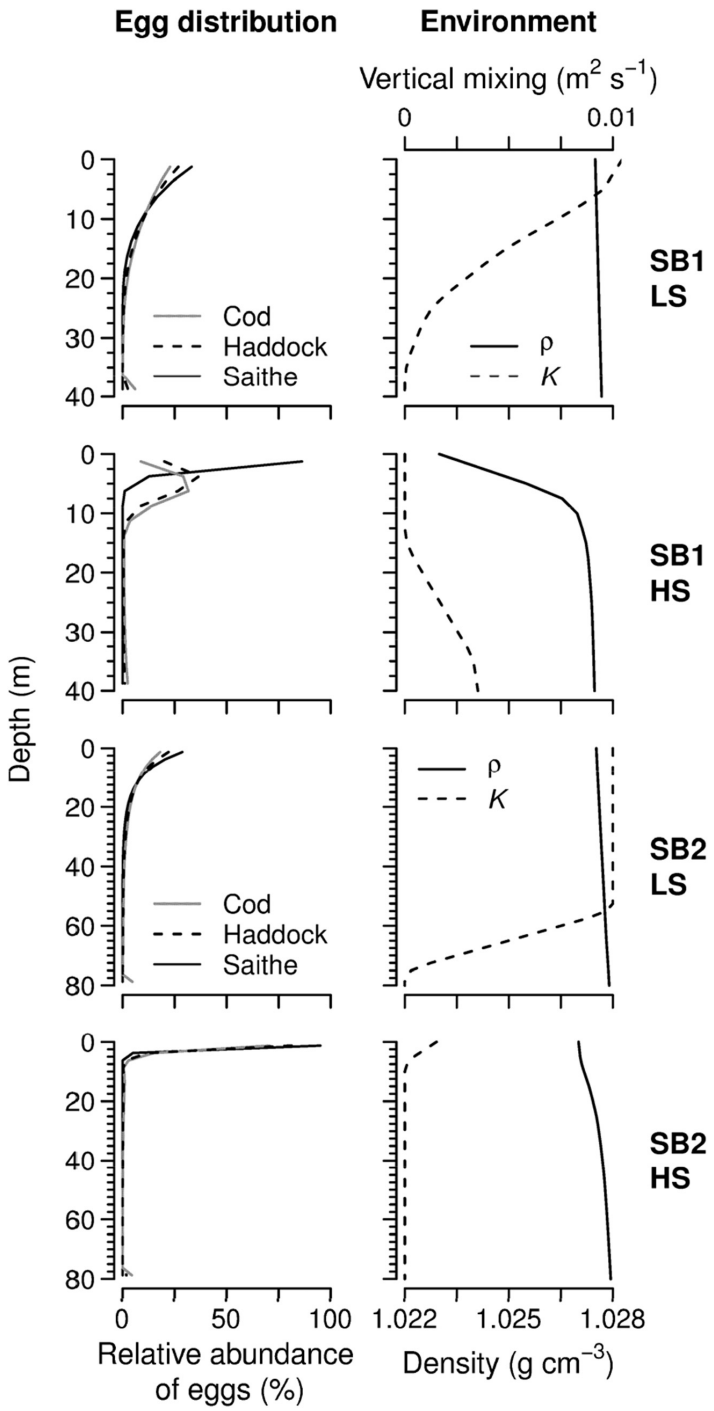

Fig. 6. Modelled vertical egg distributions (left-hand column) in highly stratified (HS) and well-mixed (i.e., low stratification, LS) conditions at both stations. The corresponding environmental gradients are shown in the right-hand column, K = vertical eddy diffusivity, ρ = ambient density.

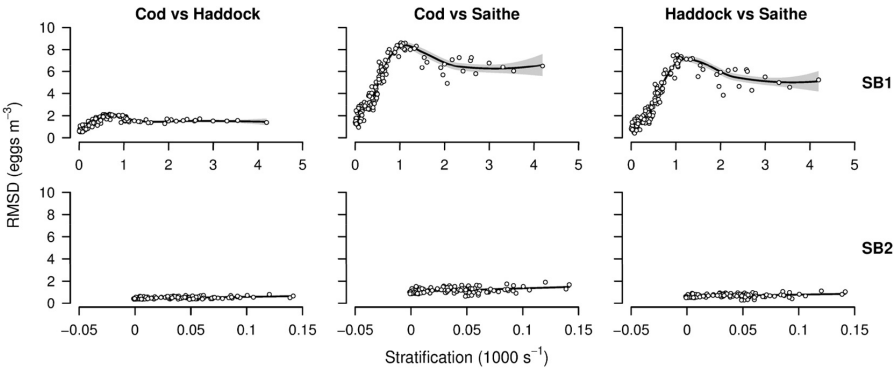

Fig. 7. RMSD values for each species comparison against total stratification N^2 (×1000) for the coastal (SB1) and offshore (SB2) stations. Loess model fits (solid line) and 95% confidence intervals (grey shaded area) are presented for each comparison.

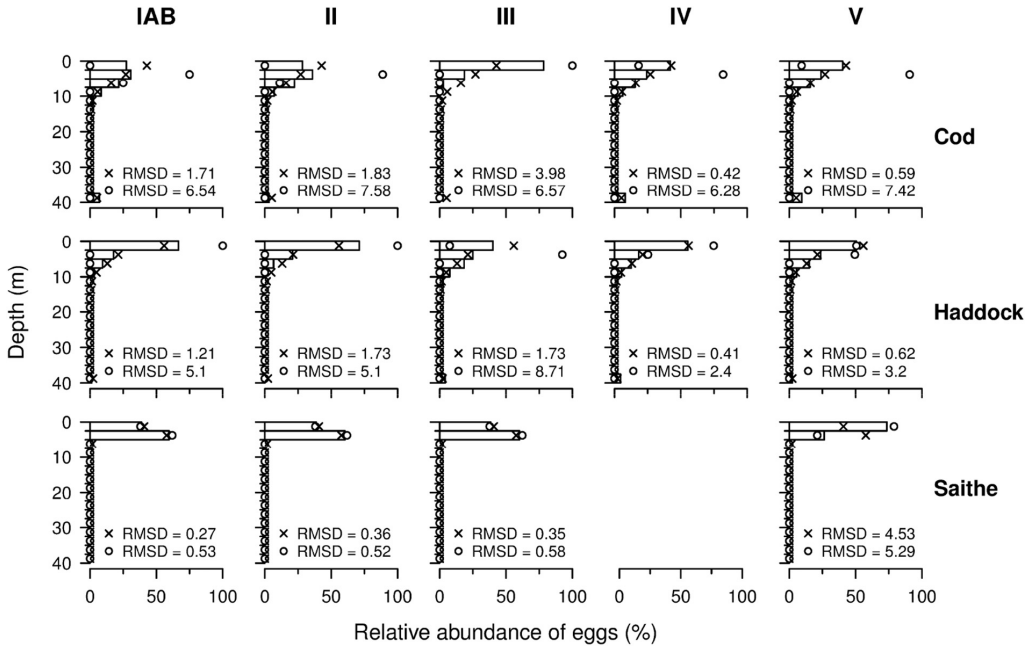

Fig. 8. Modelled relative abundance of eggs per grid cell at station SB1 for each species (different rows) at each ontogenetic stage (different columns). The bars indicate the relative abundance of eggs calculated using the stage-specific data for S_{egg} and D, i.e., $\varphi_{C_{IAB}}{}^{*}$ in the top left panel. The circles show the equivalent distribution calculated without the MCMC procedure, i.e., $\varphi_{C_{IAB}}$ in the top left panel. The crosses denote the baseline distribution, calculated from species-specific data pooled over *ES* ($\varphi_C{}^{*}$, $\varphi_H{}^{*}$ and $\varphi_S{}^{*}$), these distributions do not change per stage. The RMSD values at the bottom of each panel show the difference in eggs per m^3 between stage-specific distributions (the bars) and both the other distributions. Results are presented for the environments that maximised the intraspecific differences for each species (4th June for cod, 30th and 16th of May for haddock and saithe respectively).

4. Discussion

4.1. Interspecific differences

Distinctive differences were found between the three species in egg density and diameter. Whilst cod and haddock had similar values for both properties, saithe eggs were significantly smaller and less dense. Considering diameters, similar interspecific trends are shown in Breder and Rosen (1966) and Markle and Frost (1985) and have also been found in Icelandic waters (Fridgeirsson, 1978; Gislason et al., 1994). Furthermore, the size intervals observed in this study are largely comparable with the literature. For cod, the overall mean and standard deviation (1.42 ± 0.05 mm) is similar to the values obtained by Marteinsdottir and Steinarsson (1998) for freely running females sampled from southwest Iceland, though stage IV spawners had smaller eggs (1.34 ± 0.05 mm). For haddock, the range of diameters (1.31–1.57 mm) encompassed and extended upon the range (1.37–1.53 mm) found by Trippel and Neil (2004) for the northwest Atlantic haddock. Whilst for saithe, the mean (1.21 mm) and range (1.08–1.34 mm) were similar to the values (1.17 mm, 1.04–1.31 mm) found by Skjæraasen et al. (2017) for the North Sea stock.

Regarding egg densities, there is little egg density data available for haddock and saithe, although unpublished data from the Marine Research Institute in Norway suggests that cod and haddock have

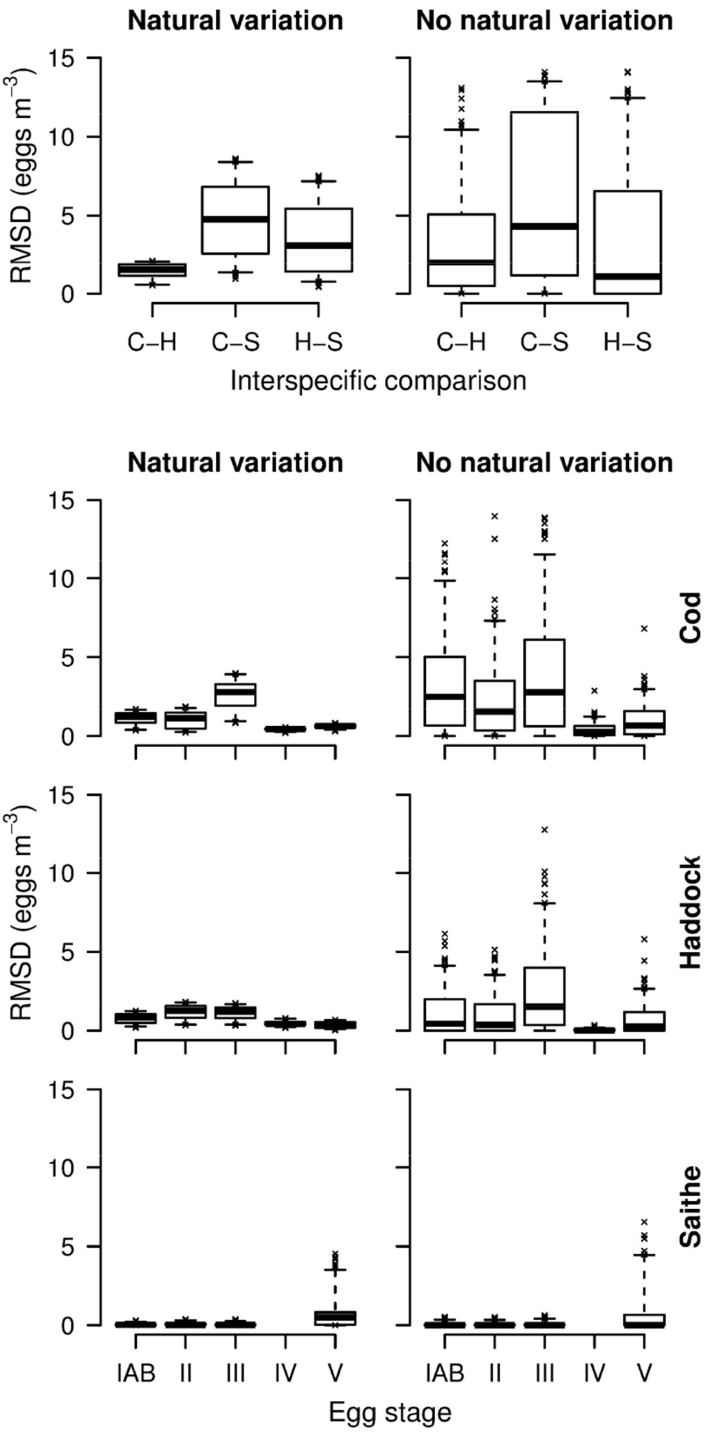

Fig. 9. Interspecific and ontogenetic differences at station SB1 are contrasted between the MCMC simulations that account for natural variation in S_{egg} (left column) and the analytical solution that assumes a single stage-specific density (right column). The top row shows the interspecific differences in egg distributions. The lower three rows show the ontogenetic comparisons between the baseline (pooled over *ES*) and the stage-specific vertical distributions for each species, i.e., for stage IAB cod eggs, the left panel shows $RMSD_{C\text{-}C_{IAB}}$, whilst the right panel shows $RMSD_{CC_{IAB}}$.

Table 4
RMSD values (eggs m^{-3}) for the egg distributions in Fig. 6. The left-hand table (A) shows the interspecific comparisons. The right-hand table (B) shows comparisons for each species between the low- and high-stratification environments. The values in brackets show the equivalent RMSD's when vertical distributions are generated from the analytical solution without the MCMC procedure.

(a)	SB1		SB2		(b)	SB1	SB2
	LS	HS	LS	HS		LS – HS	LS – HS
C-H	0.60 (0.48)	1.57 (6.75)	0.41 (0.37)	0.80 (0.65)	C	2.67 (7.19)	3.90 (4.79)
C-S	1.41 (1.15)	8.62 (13.02)	1.00 (0.89)	1.90 (1.24)	H	2.29 (5.78)	4.39 (5.01)
H-S	0.82 (0.68)	7.53 (12.47)	0.60 (0.52)	1.11 (0.59)	S	5.81 (7.41)	5.03 (5.09)

similar densities (Castaño-Primo et al., 2014), a trend also found in this study. The data obtained in this study should therefore serve as useful baselines for future research on these two species.

For cod, a comparison with the results obtained by Marteinsdottir and Begg (2002) shows that the eggs of spawners in southwest Iceland at 5 DPF were less dense in 1996 (mean = 1.0247 g cm^{-3}; range = 1.0226–1.0266 g cm^{-3}) than 2010 (mean = 1.0259 g cm^{-3}; range = 1.0247–1.0278 g cm^{-3}). However, the results are not directly comparable due to the sampling regimes; Marteinsdottir and Begg (2002) sampled a far greater number of females that encompassed the complete spawning season and multiple spawning stages, whilst the current results are based on point estimates using far smaller sample sizes. Given that the size-structure of the spawning cod varies with proximity-to-shore (Marteinsdottir et al., 2000) and throughout the spawning season (Marteinsdóttir and Björnsson, 1999), the spot-sampling conducted in this study will be subject to biases with regards to the life-history traits of the spawning females. Furthermore, discrepancies between the two studies may be due to interannual variation (e.g., Petitgas et al., 2006; Petereit et al., 2009) which has been observed in relationships between maternal traits and egg properties of Icelandic cod (Marteinsdottir and Begg, 2002), or due to the complex sub-stock structure of Icelandic cod where multiple spawning components have been distinguished within the main spawning grounds (e.g., Marteinsdottir et al., 2000; Jónsdóttir et al., 2006; Petursdottir et al., 2006; Grabowski et al., 2011). This is discussed further in Guðmundsdóttir (2013) and requires research to test whether egg density is an appropriate discriminator of spawning components.

A limitation of the study was that the females were not staged, so it was not possible to standardise the datasets by batch number. All the species examined are batch spawners (Murua and Saborido-Rey, 2003), and with each successive batch, egg diameters have been shown to decrease for each the study species (e.g., Vallin and Nissling, 2000; Trippel and Neil, 2004; Skjæraasen et al., 2017) including the Icelandic cod stock (Marteinsdottir and Steinarsson, 1998; Marteinsdottir and Begg, 2002). Although relationships have been established (e.g., Kjesbu et al., 1992; Nissling et al., 1994), Marteinsdottir and Begg (2002) found no significant differences in egg density between batches. However, the lack of stage-data (and whether fish are recruit or repeat spawners, see Kjesbu et al., 1992, 1996) may be a confounding factor in the analyses. Ultimately, to understand the proximate mechanisms driving the interspecific and ontogenetic differences seen in this study, the relative contributions of each of the egg constituents (see Jung et al., 2014) across batches needs to be quantified for gadoids in Iceland.

4.2. Ontogenetic variation

Egg stage was a significant predictor of both egg density and diameter. Given that egg diameters are expected to remain constant throughout ontogeny (Jung et al., 2014), this was a surprising result. Linear models with "batch" as a fixed explanatory factor revealed that 5/10, 5/9 and 11/14 batches had at least one significant difference in diameter between stages for cod, haddock and saithe respectively ($p < .05$; Fig. 2), although the changes were small relative to the interspecific comparisons (particularly those involving saithe). The significant differences were most prominent in saithe with 18/32 of the comparisons tested significant, whereas 5/38 and 8/36 significant comparisons were found in cod and haddock respectively. These results may reflect the small sample size ($n = 10$) which was used to ensure adequate numbers of eggs remained for the density experiments. Furthermore, high within-batch correlations (Table 3) for each species highlight that more robust population estimates could be attained by sampling more females.

Ontogenetic changes in egg density have been observed for several species (e.g., Sundby et al., 2001; Coombs et al., 2004; Ospina-Álvarez et al., 2012; Nissling et al., 2017) including both Atlantic and Baltic cod stocks (Nissling and Westin, 1991; Jung et al., 2012, 2014). Based on developmental trends in egg specific gravity across three local populations of Atlantic cod, Jung et al. (2012, 2014) suggested a generic pattern for the ontogenetic development of egg specific gravity in pelagic fish eggs, the main characteristic of which was a gradual decline in ρ_{egg} from 4 to 11 DPF. Whilst the experimental setup was not appropriate for the direct evaluation of this hypothesis because individual eggs were not continuously monitored as they were in Jung et al. (2012, 2014), a significant decline through ontogeny was seen in all cod batches. The lowest density was recorded at stage III for 7/10 cod batches and stage IV for 3/10 batches, and the rate of decline from maximum ρ_{egg} (stage IAB or II) to minimum ρ_{egg} (stage III or IV) ranged from 0.0001–0.001 g cm^{-3} day^{-1} with a mean of 0.00038 g cm^{-3} day^{-1} which is ~90% faster than the rate described by Jung et al. (2014).

Excluding one batch, saithe eggs were relatively stable from stage IAB to stage III (Fig. 2; Table 3), whilst the decrease in ρ_{egg} at stage V was seen (and significant) for all batches that remained unhatched ($n = 4$; Fig. 2). This decline does not fit the general picture of increasing density prior to hatching found for Atlantic and Baltic cod (Nissling and Westin, 1991; Jung et al., 2012; Jung et al., 2014), and blue whiting (Ådlandsvik et al., 2001), and is further complicated by all four batches also showing a decrease in diameter (3/4 significant; Fig. 2). Conservation of egg mass implies that as egg volume increases, its density will decrease (see Kjesbu et al., 1992 for details), so a decrease in both volume and density implies a loss of material. Hall et al. (2004) describe the weakening of the chorion due to a hatching enzyme just prior to hatching, and the enzymatic dissolution of material was suggested as a potential cause of the chorion thinning observed for Norwegian Coastal cod at this stage (Jung et al., 2014), though this was considered to be of little significance in determining the chorion mass and thus ρ_{egg} (Jung et al., 2014). The saithe batches measured at stage V were all on the cusp of hatching, so this is a potential explanation for the observed density decrease in saithe eggs. It should also be noted that the three batches that displayed significant declines in diameter at stage V all had small sample sizes ($n = 2$, 4 and 6; $n = 8$ for the non-significant batch) so the confidence in these estimates is low (Table 3). Furthermore, at the species level, the standard error of ρ_{egg} at stage V was approximately three times greater than the other stages highlighting greater uncertainty in the mean (Table 3). Further work is required to determine whether the observed trend is a general pattern for saithe eggs and to examine the relative contributions of egg constituents prior to hatching. In general, the commonalities outlined above for cod and saithe suggest that a unifying mechanism exists; however, the results for haddock were more ambiguous with a variety of ontogenetic patterns found (Fig. 2).

4.3. Implications for the vertical distribution of eggs

The mean densities corresponded to salinities of neutral buoyancy

(S_{egg}) of approximately 32.8, 32.1 and 29.4 PSU at 7 °C for cod, haddock and saithe respectively. Thus, the majority of eggs for all three species were positively buoyant suggesting that the ultimate function of the egg traits is to maintain a high position in the water column. Exceptions occurred at the right tails of the haddock and cod distributions where S_{egg} exceeded 35.2 PSU. The model suggested that differences between φ_C and φ_H will be minimal (Fig. 9), irrespective of the strength of stratification (Fig. 7). Fridgeirsson (1984) observed surface agglomerations of cod and haddock eggs under calm conditions in southwest Iceland using a hydraulic pump in May 1981. Eggs of both species were found at all sampled depths (0–35 m) with the vertical distributions appearing more similar to the distributions under well-mixed conditions presented in Fig. 6. This suggests that the model may be underestimating the spread of eggs; however, without detailed information on the prevailing environmental gradients (particularly K) at the time of Fridgeirsson's study, it is not possible to test the model with these observed distributions. Interspecific differences were also noted by Fridgeirsson (1984) with late-stage haddock eggs having a deeper distribution than the cod equivalents, with an RMSD of 5.55 eggs m^{-3}. Whilst our study suggests a converse pattern as the cod eggs are slightly denser, the densities at stage V were statistically similar between the two species, so it is entirely plausible that owing to various sources of natural variation in egg density (discussed above), sampling that is restricted in time and space (i.e., a snapshot of the system) may capture haddock eggs that are slightly denser than cod eggs.

For each species, the observed ontogenetic changes in egg density had little to no impact on the vertical egg distribution when compared to using the overall mean. With only minor shifts in the concentration of eggs within the upper layer (0–10 m) when mixing was minimal, it is highly unlikely that ontogenetic changes in ρ_{egg}/S_{egg} will have a large impact on dispersal trajectories. Whilst Fridgeirsson (1984) observed a gradual increase in the depth of φ_C through development, the egg maximum concentration was always found at the surface, which is largely in agreement with the model output (100% in the surface at SB2; 67%, 20% and 11% at 0.0–2.5 m, 2.5–5.0 m and 5.0–7.5 m at SB1 respectively). As noted above, monitoring individual eggs continuously would provide a more "complete" picture of ρ_{egg}/S_{egg} development and how φ changes accordingly. This was done for Norwegian coastal cod subpopulations by Myksvoll et al. (2014) who developed an ontogenetic function for S_{egg} (which incorporated intraspecific variation) based on the continuous measurements from Jung et al. (2012). It was concluded that the ontogenetic function was not an important factor for the horizontal dispersion of eggs (Myksvoll et al., 2014).

Stratification over the entire spawning period was dominated by haline controls at both stations and was on average 22–23 times stronger at SB1 (Fig. S1). In general, the thermocline develops mid-late May in southern Icelandic waters (Thórdardóttir, 1986; SB2 in Fig. S1). Therefore, stratification throughout the spawning periods for each species will be predominantly determined by the interaction between freshwater runoff and wind stress. This varies considerably on an interannual basis (Thórdardóttir, 1986; Gislason et al., 1994), as does the horizontal extent of stratification (Gislason et al., 2016). For saithe, which spawn earlier in the season (Gislason et al., 1994; Jónsson and Pálsson, 2013) and further offshore than cod and haddock, the eggs will ascend quickly and agglomerate in the surface layer. And the model suggests similar patterns for cod and haddock that spawn further offshore in deeper waters (e.g., Marteinsdottir et al., 2000). For coastal spawners, sub-surface distributions may become evident when the freshwater layer promotes stability. Although, in these cases, the egg distributions remain pelagic with the majority of eggs found just below the surface and well within the vertical range of the Icelandic Coastal Current which extends from the surface to 10–30 m deep (Logemann et al., 2013).

4.4. Model assumptions

Solely focusing on the steady-state distribution does not allow inference regarding the temporal development of the vertical egg distributions. Whether or not the steady-state is achieved will depend on the 'characteristic time' of the system. If this exceeds the egg duration, the steady-state will not be achieved, and vice versa. If the steady-state is not achieved then the vertical distribution of eggs will be largely influenced by the initialisation depth (Sundby, 1991; Petitgas et al., 2006). Simulations using the numerical schemes in the VertEgg toolbox (Ådlandsvik, 2000) suggested that the "characteristic time" will be less that the egg duration under the HS and LS conditions presented in Fig. 6. However, whether this is the case for the early developmental stages requires further simulations, especially for individuals spawning at great depths as reported for particular spawning components of each study species (e.g., Grabowski et al., 2011; Jónsson and Pálsson, 2013).

The vertical distribution model assumed that an egg's buoyancy is unaffected by the surrounding environment. In reality, chorion permeability means an egg's perivitelline space maintains neutral buoyancy in relation to the ambient seawater (Sundby and Kristiansen, 2015), the effect of which can adjust an egg's density towards that of the surrounding fluid (e.g., Coombs et al., 1985; Nissling and Vallin, 1996). However, this effect is likely to be more pronounced for species with a large perivitelline volume (e.g., sardine, > 80% egg volume) and a primary consideration when utilising density gradient columns to measure egg densities for such species (Coombs et al., 1985, 2004; Boyra et al., 2003; Huret et al., 2016). Jung et al. (2014) obtained a range of 9% to 18% for Norwegian Atlantic cod perivitelline volume and showed that the influence of this range on overall ρ_{egg} was small compared to chorion volume fractions and the specific gravity of the yolk + embryo. The model also assumed that the thermal expansion of fish eggs is equal to that of the ambient seawater. Sundby and Kristiansen (2015) showed that whilst this is not strictly true, the discrepancy between the two is sufficiently small to be considered negligible for a variety of species (including Atlantic cod).

4.5. Implications for coupled biophysical models

Our results emphasise that accounting for intraspecific variation in ρ_{egg}/S_{egg} is an important consideration when modelling the vertical distribution of pelagic fish eggs, particularly in situations where buoyancy is marginal. This conclusion is in line with other studies that have examined how intraspecific variation in ρ_{egg}/S_{egg} affects φ, for example, Boyra et al. (2003) found that including distributions of ρ_{egg} substantially improved the model's fit to observed distributions of anchovy and sardine eggs. By comparing mean-only with distributional approaches, our results have highlighted specific instances where mean-only approaches may fail to truly represent the population. For instance, distribution differences in φ across ontogeny are substantially reduced when intraspecific variation is accounted for (Fig. 9). Whether or not ontogenetic variation will have an impact on the vertical distributions of eggs will depend upon the degree of overlap between variances throughout development, and how this compares to the ambient salinity. When there is considerable overlap between stages and all stages are positively buoyant (as in the study species), it is unlikely that the ontogenetic changes will impact φ if intraspecific variation is considered. More crucially, simulations based on mean-only values may lead to exaggerations in the magnitude and extent of changes in φ due to ontogenetic changes in ρ_{egg}/S_{egg}. When coupled to a spatially explicit hydrodynamic model, this could lead to misleading estimates of dispersal trajectories and magnitudes (assuming there is vertical variation in flow vectors), and thus connectivity. In Icelandic waters, this situation is likely to arise at coastal spawning grounds within proximity of the Icelandic Coastal Current. However, the implications extend to any system where buoyancy is small. For example, the aforementioned studies that consider mesopelagic egg distributions, where fine-scale

changes in buoyancy arise from ontogenetic changes in ρ_{egg}/S_{egg} (Ådlandsvik et al., 2001; Sundby et al., 2001; Ospina-Álvarez et al., 2012).

Carrying out such "virtual" experiments can be a useful tool for designing biophysical models by identifying the degree of complexity required in egg movement modules. Implementing distributional inputs requires a priori knowledge of the variable(s) probability distribution. From a coding perspective this is simple enough, however, owing to spatial-temporal variation in the physical properties of eggs, the parameters describing the distributions ought to reflect the egg properties at the simulation's time and space (see Petitgas et al., 2006), a concern that is also relevant when using mean-only values. Assuming a Gaussian distribution appears to be a reasonable assumption for D and S_{egg} based on visual inspection of histograms and qqplots, as was found by Goarant et al. (2007) for the neutral buoyancies of anchovy. That φ is far less sensitive to D than S_{egg} is well established in the literature (e.g., Sundby, 1983; Petitgas et al., 2006) and the results of the sensitivity analysis confirm this for each of the study species. Therefore, holding D at its mean level whilst allowing for variation in S_{egg} is a reasonable assumption to make. Although if strong, robust relationships exist between both variables, natural variation in both traits could be accounted for when initialising individuals in biophysical models.

Supplementary data to this article can be found online at https://doi.org/10.1016/j.jmarsys.2019.103290.

Data availability

The raw egg density and diameter data are available at Mendeley data (https://doi.org/10.17632/mz6vvzxdt5.1). The complete VertEgg toolbox (Ådlandsvik, 2000) translated into the R programming language is freely available at https://github.com/willbutler42/VertEgg-R.

Acknowledgements

This study is a product of the Nordic Centre for Research on Marine Ecosystems and Resources under Climate Change (NorMER), which is funded by the Norden Top-Level Research Initiative sub-programme 'Effect Studies and Adaptation to Climate Change'. We would like to thank the captain and crew of the "Friðrik Sigurðsson ÁR", "Kristbjörg ÍS 177", "Kristbjörg VE-71" and "Örn KE 14" for their hospitality and help whilst sampling in the field. We also thank the staff at the Marine Research Institute's Mariculture Laboratory at Staður for their technical assistance and hospitality whilst conducting laboratory experiments. Finally, we thank Professor Steven Campana for helpful comments on the manuscript and Dr. Pamela Woods for her assistance on sampling trips.

Author contributions

WB and GM jointly conceived the study idea. GM supervised the project. WB and TL carried out the sampling and laboratory experiments for haddock and saithe. LG carried out the sampling and laboratory experiments for cod. WB programmed the VertEgg model in R. WB performed all analyses. KL wrote a Fortran program for the extraction of environmental profiles from the 3-D hydrodynamic model CODE. WB prepared the initial manuscript. All authors contributed to revisions.

References

Ådlandsvik, B., 2000. VertEgg – A Toolbox for Simulation of Vertical Distributions of Fish Eggs. (Bergen).

Ådlandsvik, B., Coombs, S., Sundby, S., Temple, G., 2001. Buoyancy and vertical distribution of eggs and larvae of blue whiting (*Micromesistius poutassou*): observations and modelling. Fish. Res. 50 (1–2), 59–72. https://doi.org/10.1016/S0165-7836(00)00242-3.

Armannsson, H., Jonsson, S.T., Neilson, J.D., Marteinsdottir, G., 2007. Distribution and migration of saithe (*Pollachius virens*) around Iceland inferred from mark-recapture studies. ICES J. Mar. Sci. 64 (5), 1006–1016. https://doi.org/10.1093/icesjms/fsm076.

Begg, G.A., Marteinsdottir, G., 2002. Environmental and stock effects on spawning origins and recruitment of cod Gadus morhua. Mar. Ecol. Prog. Ser. 229, 263–277. https://doi.org/10.3354/meps229263.

Boyra, G., Rueda, L., Coombs, S.H., Sundby, S., Ådlandsvik, B., Santos, M., Uriarte, A., 2003. Modelling the vertical distribution of eggs of anchovy (Engraulis encrasicolus) and sardine (Sardina pilchardus). Fish. Oceanogr. 12 (4–5), 381–395. https://doi.org/10.1046/j.1365-2419.2003.00260.x.

Breder, C., Rosen, D., 1966. Modes of Reproduction in Fishes. Natural History Press, Garden City, NY Retrieved from. http://agris.fao.org/agris-search/search.do?recordID=US201300482962.

Brickman, D., Marteinsdottir, G., Logemann, K., Harms, I.H., 2007. Drift probabilities for Icelandic cod larvae. ICES J. Mar. Sci. 64 (2002), 49–59.

Castaño-Primo, R., Vikebø, F.B., Sundby, S., 2014. A model approach to identify the spawning grounds and describing the early life history of Northeast Arctic haddock (Melanogrammus aeglefinus). ICES J. Mar. Sci. 71 (9), 2505–2514. https://doi.org/10.1093/icesjms/fsu078. (Original).

Ciannelli, L., Knutsen, H., Olsen, E.M., Espeland, S.H., Asplin, L., Jelmert, A., Stenseth, N.C., 2010. Small-scale genetic structure in a marine population in relation to water circulation and egg characteristics. Ecology 91 (10), 2918–2930.

Coombs, S.H., 1981. A density-gradient column for determining the specific gravity of fish eggs, with particular reference to eggs of the mackerel *Scomber scombrus*. Mar. Biol. 63 (1), 101–106. https://doi.org/10.1007/BF00394667.

Coombs, S.H., Fosh, C.A., Keen, M.A., 1985. The buoyancy and vertical distribution of eggs of sprat (Sprattus sprattus) and pilchard (Sardina pilchardus). J. Mar. Biol. Assoc. U. K. 65, 461–474.

Coombs, S.H., Boyra, G., Rueda, L.D., Uriarte, A., Santos, M., Conway, D.V.P., Halliday, N.C., 2004. Buoyancy measurements and vertical distribution of eggs of sardine (*Sardina pilchardus*) and anchovy (*Engraulis encrasicolus*). Mar. Biol. 145, 959–970. https://doi.org/10.1007/s00227-004-1389-4.

Fiksen, Ø., Jørgensen, C., Kristiansen, T., Vikebø, F., Huse, G., 2007. Linking behavioural ecology and oceanography: larval behaviour determines growth, mortality and dispersal. Mar. Ecol. Prog. Ser. 347, 195–205. https://doi.org/10.3354/meps06978.

Fridgeirsson, E., 1978. Embryonic development of five species of gadoid fishes in Icelandic waters. Rit Fiskideildar 5 (6), 1–68.

Fridgeirsson, E., 1984. Cod larvae sampling with a large pump off SW-Iceland. In: Dahl, E., Danielssen, D.S., Moksness, E., Solemdal, P. (Eds.), The Propagation of Cod *Gadus morhua* L, 1st ed. Flødevigen rapportser, Reykjavik, pp. 317–333.

Gislason, A., Astthorsson, O.S., Gudfinnsson, H., 1994. Phytoplankon, (*Calanus finmarchicus*), and fish eggs southwest of Iceland, 1990-1992. ICES Mar. Sci. Symp. 198, 423–429.

Gislason, A., Logemann, K., Marteinsdottir, G., 2016. The cross-shore distribution of plankton and particles southwest of Iceland observed with a video plankton recorder. Cont. Shelf Res. 123, 50–60. https://doi.org/10.1016/j.csr.2016.04.004.

Goarant, A., Petitgas, P., Bourriau, P., 2007. Anchovy (*Engraulis encrasicolus*) egg density measurements in the Bay of Biscay: evidence for the spatial variation in egg density with sea surface salinity. Mar. Biol. 151 (5), 1907–1915. https://doi.org/10.1007/s00227-007-0624-1.

Grabowski, T.B., Thorsteinsson, V., McAdam, B.J., Marteinsdóttir, G., 2011. Evidence of segregated spawning in a single marine fish stock: sympatric divergence of ecotypes in Icelandic cod? PLoS One 6 (3), e17528. https://doi.org/10.1371/journal.pone.0017528.

Grimm, V., Railsback, S.F., 2005. Individual-Based Modeling and Ecology. Princeton University Press, Princeton, NJ.

Guðmundsdóttir, L., 2013. Intra-Stock Diversity in Egg Specific Gravity of Atlantic Cod in Icelandic Waters. University of Iceland.

Hall, T.E., Smith, P., Johnston, I.A., 2004. Stages of embryonic development in the Atlantic cod *Gadus morhua*. J. Morphol. 259 (3), 255–270. https://doi.org/10.1002/jmor.10222.

Hinrichsen, H.-H., Lehmann, A., Petereit, C., Nissling, A., Ustups, D., Bergström, U., Hüssy, K., 2016. Spawning areas of eastern Baltic cod revisited: using hydrodynamic modelling to reveal spawning habitat suitability, egg survival probability, and connectivity patterns. Prog. Oceanogr. 143, 13–25. https://doi.org/10.1016/j.pocean.2016.02.004.

Hjort, J., 1914. Fluctuations in the great fisheries of northern Europe viewed in the light of biological research. Rapp. P.-v. Reun. Cons. Perm. Int. Explor. Mer 20, 1–228.

Huret, M., Runge, J.A., Chen, C., Cowles, G., Xu, Q., Pringle, J.M., 2007. Dispersal modeling of fish early life stages: sensitivity with application to Atlantic cod in the western Gulf of Maine. Mar. Ecol. Prog. Ser. 347, 261–274. https://doi.org/10.3354/meps06983.

Huret, M., Bourriau, P., Gatti, P., Dumas, F., Petitgas, P., 2016. Size, permeability and buoyancy of anchovy (*Engraulis encrasicolus*) and sardine (*Sardina pilchardus*) eggs in relation to their physical environment in the Bay of Biscay. Fish. Oceanogr. 25 (6), 582–597. https://doi.org/10.1111/fog.12174.

Huston, M., DeAngelis, D., Post, W., 1988. New computer models unify ecological theory. Bioscience 38 (10), 682–691.

Jonasson, J.P., Gunnarsson, B., Marteinsdottir, G., 2009. Abundance and growth of larval and early juvenile cod (*Gadus morhua*) in relation to variable environmental conditions west of Iceland. Deep-Sea Research Part II: Topical Studies in Oceanography 56 (21 – 22), 1992–2000. https://doi.org/10.1016/j.dsr2.2008.11.010.

Jónsdóttir, I.G., Campana, S.E., Marteinsdottir, G., 2006. Otolith shape and temporal stability of spawning groups of Icelandic cod (*Gadus morhua* L.). ICES J. Mar. Sci. 63 (8), 1501–1512. https://doi.org/10.1016/j.icesjms.2006.05.006.

Jónsson, G., Pálsson, J., 2013. Íslenskir Fiskar (Icelandic Fishes), 2nd ed. Mál og Menning, Reykjavík.
Jung, K.-M., Folkvord, A., Kjesbu, O.S., Agnalt, A.L., Thorsen, A., Sundby, S., 2012. Egg buoyancy variability in local populations of Atlantic cod (Gadus morhua). Mar. Biol. 159 (9), 1969–1980. https://doi.org/10.1007/s00227-012-1984-8.
Jung, K.-M., Folkvord, A., Kjesbu, O.S., Sundby, S., 2014. Experimental parameterisation of principal physics in buoyancy variations of marine teleost eggs. PLoS One 9 (8), e104089. https://doi.org/10.1371/journal.pone.0104089.
Kjesbu, O.S., Kryvi, H., Sundby, S., Solemdal, P., 1992. Buoyancy variation in eggs of Atlantic cod (*Gadus morhua* L.) in relation to chorion thickness and egg size: theory and observations. J. Fish Biol. 41, 581–599.
Kjesbu, O.S., Solemdal, P., Bratland, P., Fonn, M., 1996. Variation in annual egg production in individual captive Atlantic cod (*Gadus morhua*). Can. J. Fish. Aquat. Sci. 53 (3), 610–620. https://doi.org/10.1139/cjfas-53-3-610.
Kuroda, H., Takahashi, D., Mitsudera, H., Azumaya, T., Setou, T., 2014. A preliminary study to understand the transport process for the eggs and larvae of Japanese Pacific walleye pollock *Theragra chalcogramma* using particle-tracking experiments based on a high-resolution ocean model. Fish. Sci. 80 (2), 127–138. https://doi.org/10.1007/s12562-014-0717-y.
Lenth, R., 2019. emmeans: estimated marginal means, aka least-squares means. Retrieved from. https://cran.r-project.org/package=emmeans.
Li, Y., Fratantoni, P.S., Chen, C., Hare, J.A., Sun, Y., Beardsley, R.C., Ji, R., 2015. Spatio-temporal patterns of stratification on the Northwest Atlantic shelf. Prog. Oceanogr. 134, 123–137. https://doi.org/10.1016/j.pocean.2015.01.003.
Logemann, K., Olafsson, J., Marteinsdóttir, G., 2012. Modelling the hydrography of Icelandic waters from 1992 to 2006. MARICE-E-report MER-13-2012. Reykjavik. Retrieved from. http://www.marice.is/ereports/MER-13-2012.pdf.
Logemann, K., Ólafsson, J., Snorrason, Á., Valdimarsson, H., Marteinsdóttir, G., 2013. The circulation of Icelandic waters - a modelling study. Ocean Sci. 9 (5), 931–955. https://doi.org/10.5194/os-9-931-2013.
Markle, D.F., Frost, L.-A., 1985. Comparative morphology, seasonality, and a key to planktonic fish eggs from the Nova Scotian shelf. Can. J. Zool. 63 (2), 246–257. https://doi.org/10.1139/z85-038.
Marteinsdottir, G., Begg, G.A., 2002. Essential relationships incorporating the influence of age, size and condition on variables required for estimation of reproductive potential in Atlantic cod *Gadus morhua*. Mar. Ecol. Prog. Ser. 235, 235–256. https://doi.org/10.3354/meps235235.
Marteinsdottir, G., Steinarsson, A., 1998. Maternal influence on the size and viability of Iceland cod *Gadus morhua* eggs and larvae. J. Fish Biol. 52 (6), 1241–1258. https://doi.org/10.1111/j.1095-8649.1998.tb00969.x.
Marteinsdóttir, G., Björnsson, H., 1999. Time and duration of spawning of cod in Icelandic waters. ICES CM, Y 34, 1–14.
Marteinsdottir, G., Gudmundsdottir, A., Thorsteinsson, V., Stefansson, G., 2000. Spatial variation in abundance, size composition and viable egg production of spawning cod (Gadus morhua L.) in Icelandic waters. ICES J. Mar. Sci. 57 (4), 824–830. https://doi.org/10.1006/jmsc.2000.0568.
Millero, F.J., Poisson, A., 1981. International one-atmosphere equation of state of seawater. Deep Sea Research Part A. Oceanographic Research Papers 28 (6), 625–629. https://doi.org/10.1016/0198-0149(81)90122-9.
Murua, H., Saborido-Rey, F., 2003. Female reproductive strategies of marine fish species of the North Atlantic. J. Northwest Atl. Fish. Sci. 33, 23–31. https://doi.org/10.2960/J.v33.a2.
Myksvoll, M.S., Sundby, S., Ådlandsvik, B., Vikebø, F.B., 2011. Retention of coastal cod eggs in a fjord caused by interactions between egg buoyancy and circulation pattern. Marine and Coastal Fisheries 3 (1), 279–294. https://doi.org/10.1080/19425120.2011.595258.
Myksvoll, M.S., Jung, K.-M., Albretsen, J., Sundby, S., 2014. Modelling dispersal of eggs and quantifying connectivity among Norwegian coastal cod subpopulations. ICES J. Mar. Sci. 71 (4), 957–969. https://doi.org/10.1093/icesjms/fst022 Contribution.
Nakagawa, S., Schielzeth, H., 2010. Repeatability for Gaussian and non-Gaussian data: a practical guide for biologists. Biol. Rev. 85 (4), 935–956. https://doi.org/10.1111/j.1469-185X.2010.00141.x.
Nissling, A., Vallin, L., 1996. The ability of Baltic cod eggs to maintain neutral buoyancy and the opportunity for survival in fluctuating conditions in the Baltic Sea. J. Fish Biol. 48, 217–227.
Nissling, A., Westin, L., 1991. Egg buoyancy of Baltic cod (*Gadus morhua*) and its implications for cod stock fluctuations in the Baltic. Mar. Biol. 111 (1), 33–35. https://doi.org/10.1007/BF01986342.
Nissling, A., Kryvi, H., Vallin, L., 1994. Variation in egg buoyancy of Baltic cod *Gadus morhua* and its implications for egg survival in prevailing conditions in the Baltic Sea. Mar. Ecol. Prog. Ser. 110 (1), 67–74. https://doi.org/10.3354/meps110067.
Nissling, A., Nyberg, S., Petereit, C., 2017. Egg buoyancy of flounder, Platichthys flesus, in the Baltic Sea—adaptation to salinity and implications for egg survival. Fish. Res. 191, 179–189. https://doi.org/10.1016/j.fishres.2017.02.020.
Olafsson, J., 1985. Recruitment of Icelandic haddock and cod in relation to variability in the physical environment. ICES CM, G 59, 10.
Ospina-Álvarez, A., Palomera, I., Parada, C., 2012. Changes in egg buoyancy during development and its effects on the vertical distribution of anchovy eggs. Fish. Res. 117–118, 86–95. https://doi.org/10.1016/j.fishres.2011.01.030.
Parada, C., Van Der Lingen, C.D., Mullon, C., Penven, P., 2003. Modelling the effect of buoyancy on the transport of anchovy (*Engraulis capensis*) eggs from spawning to nursery grounds in the southern Benguela: an IBM approach. Fish. Oceanogr. 12 (3), 170–184. https://doi.org/10.1046/j.1365-2419.2003.00235.x.
Pauly, D., Pullin, R.S.V., 1988. Hatching time in spherical, pelagic, marine fish eggs in response to temperature and egg size. Environ. Biol. Fish 22 (4), 261–271.
Petereit, C., Hinrichsen, H., Voss, R., Kraus, G., Freese, M., Clemmesen, C., 2009. The influence of different salinity conditions on egg buoyancy and development and yolk sac larval survival and morphometric traits of Baltic Sea sprat (Sprattus sprattus balticus Schneider). Sci. Mar. 73 (S1), 59–72. https://doi.org/10.3989/scimar.2009.73s1059.
Petereit, C., Hinrichsen, H.-H., Franke, A., Köster, F.W., 2014. Floating along buoyancy levels: dispersal and survival of western Baltic fish eggs. Prog. Oceanogr. 122, 131–152. https://doi.org/10.1016/j.pocean.2014.01.001.
Petitgas, P., Magri, S., Lazure, P., 2006. One-dimensional biophysical modelling of fish egg vertical distributions in shelf seas. Fish. Oceanogr. 15 (5), 413–428. https://doi.org/10.1111/j.1365-2419.2006.00409.x.
Petursdottir, G., Begg, G.A., Marteinsdottir, G., 2006. Discrimination between Icelandic cod (*Gadus morhua* L.) populations from adjacent spawning areas based on otolith growth and shape. Fish. Res. 80 (2–3), 182–189. https://doi.org/10.1016/j.fishres.2006.05.002.
Pinheiro, J., Bates, D., DebRoy, S., Sarkar, D., Team, R.C., 2019. nlme: linear and nonlinear mixed effects models. Retrieved from. https://cran.r-project.org/package=nlme.
Santos, A.M.P., Nieblas, A.-E., Verley, P., Teles-Machado, A., Bonhommeau, S., Lett, C., Peliz, A., 2018. Sardine (*Sardina pilchardus*) larval dispersal in the Iberian upwelling system, using coupled biophysical techniques. Prog. Oceanogr. 162, 83–97. https://doi.org/10.1016/j.pocean.2018.02.011.
Schneider, C.A., Rasband, W.S., Eliceiri, K.W., 2012. NIH image to ImageJ: 25 years of image analysis. Nat. Methods 9 (7), 671–675. https://doi.org/10.1038/nmeth.2089.
Schulla, J., Jasper, K., 2007. Model description WaSiM-ETH. Zürich. Retrieved from. http://www.wasim.ch/downloads/doku/wasim/wasim_2007_en.pdf.
Skjæraasen, J.E., Devine, J.A., Godiksen, J.A., Fonn, M., OtterÅ, H., Kjesbu, O.S., Karlsen, Ø., 2017. Timecourse of oocyte development in saithe *Pollachius virens*. J. Fish Biol. 90 (1), 109–128. https://doi.org/10.1111/jfb.13161.
Staaterman, E., Paris, C.B., 2014. Modeling larval fish navigation: the way forward. ICES J. Mar. Sci. 71 (4), 918–924. https://doi.org/10.1093/icesjms/fst103.
Sundby, S., 1983. A one-dimensional model for the vertical distribution of pelagic fish eggs in the mixed layer. Deep Sea Research Part A, Oceanographic Research Papers 30 (6), 645–661. https://doi.org/10.1016/0198-0149(83)90042-0.
Sundby, S., 1991. Factors effecting the vertical distribution of eggs. ICES Mar. Sci. Symp. 192, 33–38.
Sundby, S., Kristiansen, T., 2015. The principles of buoyancy in marine fish eggs and their vertical distributions across the world oceans. PLoS One 10 (10), e0138821. https://doi.org/10.1371/journal.pone.0138821.
Sundby, S., Boyd, A.J., Hutchings, L., Toole, M.J.O., Thorisson, K., Thorsen, A., 2001. Interaction between cape hake spawning and the circulation in the northern Benguela upwelling ecosystem. S. Afr. J. Mar. Sci. 23, 317–336.
Thompson, B.M., Riley, J.D., 1981. Egg and larval development studies in the north sea cod (*Gadus morhua* L.). Rapp. Proc.-V.Réun. Cons. Int. Explor. Mer. 178, 553–559.
Thórdardóttir, T., 1986. Timing and duration of spring blooming south and southwest of Iceland. In: Skreslet, S. (Ed.), The Role of Freshwater Outflow in Coastal Marine Ecosystems. Springer Berlin Heidelberg, Berlin, Heidelberg, pp. 345–360. https://doi.org/10.1007/978-3-642-70886-2_25.
Thorsen, A., Kjesbu, O.S., Fyhn, H.J., Solemdal, P., 1996. Physiological mechanisms of buoyancy in eggs from brackish water cod. J. Fish Biol. 48 (3), 457–477. https://doi.org/10.1111/j.1095-8649.1996.tb01440.x.
Thygesen, U.H., Ådlandsvik, B., 2007. Simulating vertical turbulent dispersal with finite volumes and binned random walks. Mar. Ecol. Prog. Ser. 347, 145–153. https://doi.org/10.3354/meps06975.
Trippel, E.A., Neil, S.R.E., 2004. Maternal and seasonal differences in egg sizes and spawning activity of Northwest Atlantic haddock (*Melanogrammus aeglefinus*) in relation to body size and condition. Can. J. Fish. Aquat. Sci. 61 (11), 2097–2110. https://doi.org/10.1139/f04-125.
Vallin, L., Nissling, A., 2000. Maternal effects on egg size and egg buoyancy of Baltic cod, *Gadus morhua* implications for stock structure effects on recruitment. Fish. Res. 49 (1), 21–37. https://doi.org/10.1016/S0165-7836(00)00194-6.
Westgård, T., 1989. Two models of the vertical distribution of pelagic fish eggs in the turbulent upper layer of the ocean. Rapp. P.-v. Reun. Cons. Int. Explor. Mer 191, 195–200.
Zuur, A., Ieno, E.N., Walker, N., Saveliev, A.A., Smith, G.M., 2009. Mixed Effects Models and Extensions in Ecology with R. Springer Science & Business Media.
Zuur, A.F., Ieno, E.N., Elphick, C.S., 2010. A protocol for data exploration to avoid common statistical problems. Methods Ecol. Evol. 1 (1), 3–14. https://doi.org/10.1111/j.2041-210X.2009.00001.x.

Supplementary graphs for the manuscript:

Egg size and density estimates for three gadoids in Icelandic waters and their implications for the vertical distribution of eggs along a stratified water column

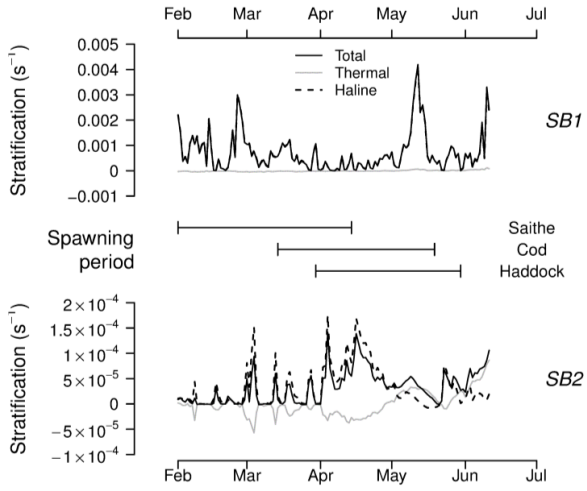

Figure S1: *Time series of stratification at each station in 2006. The water column's buoyancy frequency (N^2) from 0–40 m was used as a measure of stratification; this is decomposed into its thermal and haline components (total = thermal + haline). For details on this approach, see Li et al. (2015). The middle panel shows approximate spawning periods for each species.*

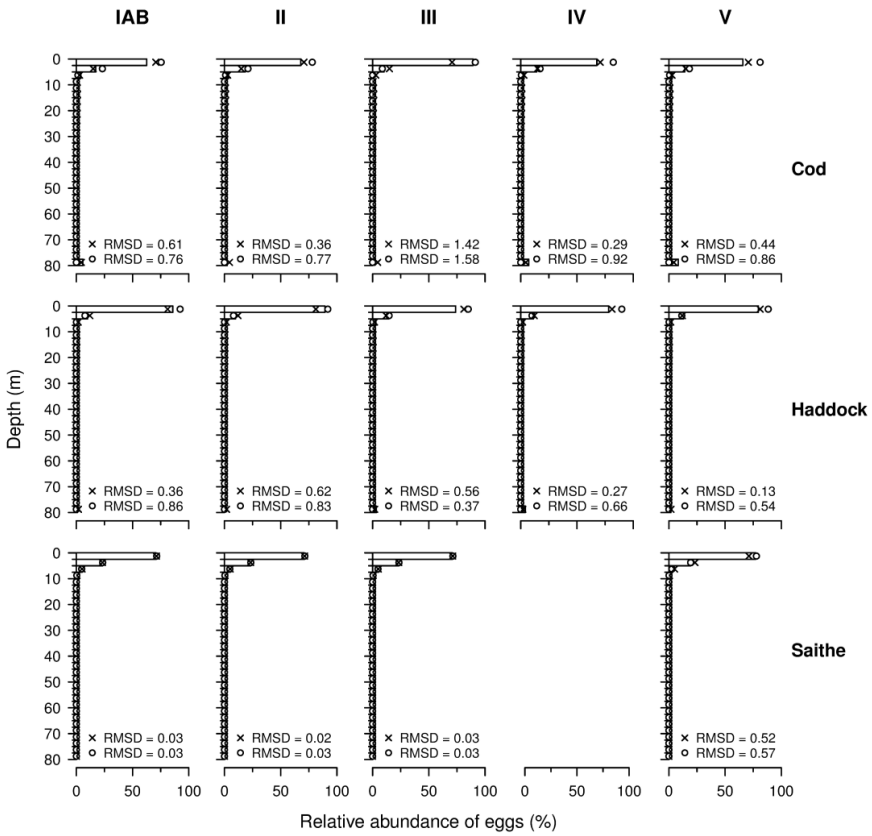

Figure S2: *Modelled relative abundance of eggs per grid cell at station SB2 for each species (different rows) at each ontogenetic stage (different columns). The bars indicate the relative abundance of eggs calculated using the stage-specific data for* ρ_{egg} *and D, i.e.,* $\varphi^{*}_{C_{IAB}}$ *in the top left panel. The circles show the equivalent distribution calculated without the MCMC procedure, i.e.,* $\varphi_{C_{IAB}}$ *in the top left panel. The crosses denote the baseline distribution, calculated from species-specific data pooled over ES (*φ^{*}_{C}*,* φ^{*}_{H} *and* φ^{*}_{S}*), these distributions do not change per stage. The RMSD values at the bottom of each panel show the difference in eggs per* m^3 *between stage-specific distributions (the bars) and both the other distributions. Results are presented for the environments that maximised the intraspecific differences for each species (18th April for cod and haddock, 9th April for saithe).*

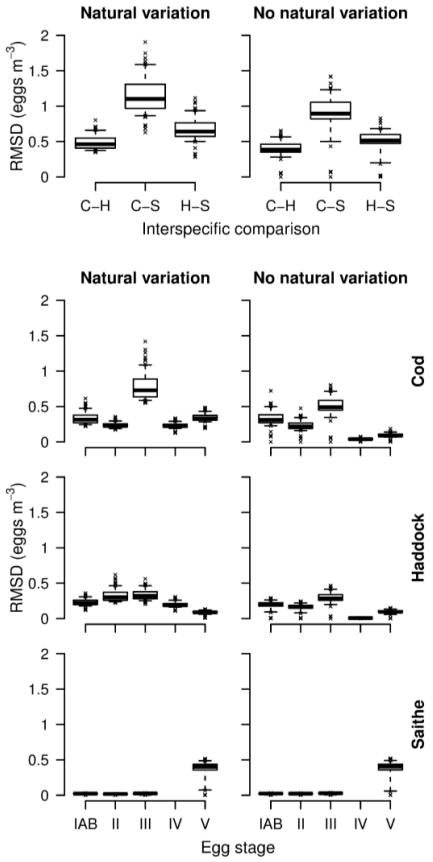

Figure S3: *Interspecific and ontogenetic differences at station SB2 are contrasted between the MCMC simulations that account for natural variation in ρ_{egg} (left column) and the analytical solution that assumes a single stage-specific density (right column). The top row shows the interspecific differences in egg distributions. The lower three rows show the ontogenetic comparisons between the baseline (pooled over ES) and the stage-specific vertical distributions for each species, i.e., for stage IAB cod eggs, the left panel shows $RMSD_{C^*C^*_{IAB}}$, whilst the right panel shows $RMSD_{CC_{IAB}}$. Note that the y-axis limits are substantially lower than Fig. 9 in the main article.*

Paper II

Paper II

Dispersal trajectories and connectivity matrices for larval cod spawned in southern Icelandic waters

William E. Butler, Kai Logemann, and Guðrún Marteinsdóttir.

Manuscript.

Author contributions: GM and WB conceived the study idea. GM supervised the project. KL developed the 3-d hydrodynamic model CODE. KL and WB developed the particle tracking model. WB carried out all simulations and analyses. WB prepared the initial manuscript. All authors contributed to revisions.

Dispersal trajectories and connectivity matrices for larval cod spawned in southern Icelandic waters

W.E. Butler[1,2], K. Logemann[3], G. Marteinsdóttir[1]

[1]MARICE, Faculty of Life and Environmental Sciences, University of Iceland, Askja, Sturlugata 7, 101 Reykjavik, Iceland.

[2]Marine and Freshwater Research Institute, Skúlagata 4, 101 Reykjavík, Iceland.

[3]Institute of Coastal Research, Helmholtz Centre Geesthacht, Max-Planck-Straße 1, 21502 Geesthacht, Germany.

Abstract

Particle tracking models are frequently used to estimate connectivity between spawning grounds and settlement areas for pelagic larvae. Connectivity can vary between and within years, with dispersal trajectories dependent upon regional oceanography and the displacement of particles through physical and/or behavioural mechanisms. Cod larvae spawned on the main spawning grounds off southwest Iceland typically drift clockwise to settlement areas in the north. To test the stability of this pattern, we developed a Lagrangian particle tracking model that simulated larval cod dispersal. Particles were released from 1998 to 2012 at inshore and offshore spawning grounds. Clockwise drift was stronger and more stable between and within years from the inshore spawning ground. From the offshore spawning ground, many eggs and larvae drifted anticlockwise to the southeast and in a neutral direction to the southwest, and the magnitude of dispersal in each direction fluctuated between years. Including vertical displacement of particles substantially altered connectivity patterns, highlighting the importance of including vertical migrations in drift models. The results improve our knowledge of the sub-stock structure of Icelandic cod by showing that variation in dispersal trajectories exists within the main spawning grounds and that proximity to shore is an explanation for this variation.

1. Introduction

Lagrangian particle tracking models that utilise flow fields from 3-d hydrodynamic models to advect particles through time and space are frequently used to understand the dispersal patterns of pelagic early life-stages. These models often incorporate an individual-based model (IBM) to capture biological and behavioural aspects of eggs/larvae that may, in turn, influence dispersal trajectories. For example, the vertical displacement of eggs through advection and diffusion, the cue-directed horizontal swimming of larvae, and the vertical movements of larvae via diel-vertical migrations (DVMs) have all been shown to produce spatiotemporal distributions that more closely reflect reality than simulating particles at fixed depths (North et al. 2008; Ospina-Álvarez et al. 2012; Staaterman et al. 2012). The end product (hereafter referred to as "biophysical IBM") consists of high resolution, realistic flow fields that simulate the physical transport of eggs/larvae, and an IBM that simulates key biological processes (e.g. growth, mortality, and behaviour) that both depend upon and influence the individual's environmental exposure.

Owing to the complexity of biophysical IBMs, they are typically rich in parameters and require extensive sensitivity analyses to understand how the assumptions of the model affect its emergent properties (e.g. Brickman et al. 2007a; Peck and Hufnagl 2012). For example, Kvile et al. (2018) found that interannual variation in circulation patterns had a larger impact on dispersal patterns than model resolution or DVM behaviour. Conversely, North et al. (2008) showed that implementing larval behaviours improved the spatial patterns of transport success over interannual variation in circulation patterns. These contradictory conclusions illustrate that dispersal patterns are system specific. From the regional hydrography to the density of an individual egg, biophysical IBMs need to be tailored to the study system to reflect its patterns and processes. Furthermore, dispersal patterns need to be understood in terms of the constraints imposed upon the model and the assumptions underlying its formulation.

In Icelandic waters, the main spawning grounds for Icelandic cod (Gadus morhua) are located south-west of Iceland (Jónsson 1982). In general, this area is a hotspot of productivity with the main spawning grounds for many species (e.g. capelin, haddock, and saithe) located in this area (Jónsson and Pálsson 2013). Larval and pelagic juvenile fish surveys and deployed drifters have shown that from these spawning grounds, the eggs/larvae drift clockwise around Iceland to the settlement areas in the north of Iceland (Valdimarsson and Malmberg 1999; Begg and Marteinsdottir 2000). This clockwise drift is driven by the Icelandic Coastal Current and the northward flowing Irminger Current – a continuation of the North Atlantic Drift. Both currents show variation between and within years (Jónsson and Valdimarsson 2012; Logemann et al. 2013) which is likely to be an important driver of the interannual spatial variation seen in the abundance and distribution of cod larvae (Begg and Marteinsdottir 2000). The coastal current is a freshwater induced narrow (~10 km alongshore) current that reaches from the surface to a depth between 10 and 30 m (Logemann et al. 2013). Several studies have highlighted the importance of this current for the clockwise transport of eggs/larvae spawned southwest (SW) of Iceland (Olafsson 1985; Begg and Marteinsdottir 2002; Jonasson et al. 2009).

Observations from 0-group survey data highlighted declining gradients in the age and length of larval cod from the north to the west of Iceland (Astthorsson et al. 1994; Begg and Marteinsdottir 2000). These negative spatial gradients were explained by age rather than growth, highlighting that females spawn progressively later in the season from the

west to the east coasts and that spawning grounds along the west, north and east coasts also contribute to the surviving 0-group population of larval cod (Begg and Marteinsdottir 2000; Marteinsdottir et al. 2000a). Furthermore, separate spawning components exist within the main spawning grounds. Spawning females within these sub-components differ in life-history characteristics (Marteinsdottir et al. 2000b) and have been distinguished via otolith chemistry, growth, and shape (Jónsdóttir et al. 2006a, b; Petursdottir et al. 2006). Although Brickman et al. (2007a) found little variation between SW spawning sub-components in drift trajectories, their offshore spawning sub-component comprised multiple potential spawning sub-components (Marteinsdottir et al. 2000b; Petursdottir et al. 2006) and further discretisation of the main spawning grounds is needed to fully evaluate whether drift trajectories vary between sub-components.

The overall aim of this study was to develop a biophysical IBM that can produce realistic predictions of larval dispersal in Icelandic waters. Simulations were carried out to examine dispersal trajectories and emergent connectivity matrices of larval cod from 1998 to 2012. Particles were released from two spawning grounds that reflected inshore and offshore spawning components. The following questions were addressed using a suite of simulations: (1) how stable is the clockwise drift of eggs/larvae between years; (2) how stable is the clockwise drift of eggs/larvae within years (i.e. throughout each spawning season); (3) how do these patterns vary between inshore and offshore spawning grounds. The results demonstrate how spatiotemporal variation in spawning activity affects the dispersal of pelagic larvae, thus improving the ability to model pelagic early life stages of fish.

2. Materials and Methods

2.1. Hydrodynamic model

The particle tracking model ran offline utilising output from the three-dimensional hydrodynamic model CODE (Cartesian coordinates Ocean model with three-Dimensional adaptive mesh refinement and primitive Equations [Logemann et al. 2013]). The model domain covered the entire North Atlantic including the Arctic Ocean. Starting with a baseline mesh resolution of 128 km horizontal and 160 m vertical, CODE utilised adaptive mesh refinement to resolve the mesh at a higher resolution in the waters surrounding Iceland and other areas of interest (e.g. Greenland-Iceland-Scotland ridge). The maximum resolution obtained was 1 km horizontal and 2.5 m vertical in coastal Iceland waters (Logemann et al. 2012). Freshwater runoff from 46 Icelandic watersheds, estimated by the hydrological model WaSiM (Schulla and Jasper 2007), formed boundary values to simulate the impact of river runoff on coastal circulation patterns. A total of 16,802 CTD profiles from the NISE and VEINS datasets were assimilated to minimise the deviation between observed and simulated temperature and salinity profiles. The model is fully documented in Logemann et al. (2012) and results from recent simulations are detailed in Logemann et al. (2013).

2.2. Particle tracking model

The particle tracking model operated at a timestep dt of 1200 s (20 minutes). Output from CODE was stored at 3-hour intervals, therefore a Euler discretisation routine was employed to obtain velocity fields and environmental variables at each grid cell at each timestep. Multivariate interpolation was then carried out to obtain precise estimates for each variable at each particle's spatiotemporal location.

Horizontal displacement was calculated using a naïve random displacement model (Visser 1997),

$$X_{t+1} = X_t + u \cdot dt + \sqrt{6A_H/dt} \cdot Q,$$

where X was the particles horizontal position, u was the velocity in direction X, A_H was the horizontal eddy diffusivity ($m^2\ s^{-1}$), and Q was a random variable with zero mean and unit variance. Turbulent exchange coefficients (e.g. A_H) were calculated by CODE and varied in both time and space. If particles crossed a horizontal ocean boundary, they were reflected along the angle of approach to the mean of its current and projected position. This was an iterative procedure that continued until a grid cell outside the boundary was found.

Icelandic cod eggs are pelagic and positively buoyant (Butler et al. 2020). Freshwater runoff and strong wind-driven turbulence may therefore lead to the vertical displacement of eggs which, in turn, may affect dispersal trajectories. To model the vertical displacement of eggs, we employed the first-order binned random walk developed by Thygesen and Ådlandsvik (2007). This is a finite-volume discretisation of the advection-diffusion equation which generates probabilities of transition to adjacent (in a 1-dimensional water column) grid cells based on an egg's terminal velocity (advection) and ambient vertical eddy diffusivity (diffusion). The model keeps track of the grid cell, rather than the specific vertical position, of each individual egg. A fixed grid cell height of 2.5 m (the maximum vertical resolution in CODE) was implemented with all variables of interest (see Thygesen and Ådlandsvik, 2007) linearly interpolated to the grid cell interfaces. An egg's terminal velocity—the velocity an egg ascends/descends when the buoyant forces balance the frictional drag—was calculated using the equations presented in Sundby (1983). The boundary conditions for the binned random walk were zero egg flux at the surface and seafloor. For both random walk models, an inner time loop was used to ensure the Courant-Friedrichs-Levy stability condition (eq. 17 in Thygesen and Ådlandsvik, 2007) was met at each timestep.

2.3. Individual-based model

Each individual particle i possessed a unique attribute vector $A_{i,t}$ (Chambers, 1993) which described the individual's spatiotemporal location and key biological attributes at each timestep:

$$A_{i,t} = \{x_{i,t}, y_{i,t}, z_{i,t}, a_{i,t}, S_{e,i}, D_{e,i}, w_{i,t}, DS_{i,t}\}.$$

The individual's horizontal location was described by x and y, and its depth by z (m). The age of an individual was stored in a (days). The parameters S_e and D_e were an egg's salinity of neutral buoyancy (PSU) and diameter (mm) respectively, these remained static for the duration of the egg stage. Whether or not an egg had hatched is stored in the binary factor DS. For the larval stage, w stored the individual's dry weight (mg).

Upon release, egg development proceeded at a temperature-dependent rate with hatch time H (d^{-1}) determined using the model developed by Pepin et al. (1997), $H = 46.1e^{-0.17T}$. When the cumulative sum of 1/H reached unity, the larva hatched with a dry weight of 0.059 mg (equivalent to 4.5 mm [Marteinsdottir and Steinarsson 1998]) and the binary factor DS was turned to a value of one, which activated the larval subroutines. The model provided a good approximation of hatching time when applied to a dataset of cod egg

measurements taken on discrete days (Butler et al. 2020). In 8 out of 10 samples, hatching was initialised at 13 days-post-fertilisation (DPF) and the model predicted 13.04 days. The remaining two samples had hatched prior to 13 DPF (Guðmundsdóttir 2013) and the model predicted 12.21 days which is entirely plausible given these two samples had the highest mean temperatures.

Upon hatching, larval growth proceeded at a size- and temperature-dependent rate SGR (% day^{-1}) using the model developed by Folkvord (2005) for Norwegian coastal cod:

$$SGR(T, w) = 1.2 + 1.8T = 0.078Tln(w) - 0.0946Tln(w)^2 + 0.0105Tln(w)^3.$$

In Iceland, this model provided a good fit for larvae originating from the southern spawning grounds, but potentially underestimated growth for larvae originating from the north (Folkvord 2005). The upper w limit of Folkvord's (2005) model was 600 mg, therefore the growth model of Björnsson et al. (2007) was used once individuals surpassed this limit. Weight to length L (mm) conversions were calculated using the second order polynomial used by Folkvord (2005).

2.4. Larval behaviour

Larvae were able to change their vertical position through DVM. The timing of the ascents and descents were determined by ambient light levels. To compute this, the surface irradiance E_0 (µmol photons m^{-2} s^{-1}) at the larva's horizontal position was computed at each timestep using the model by Skartveit and Olseth (1988). Subsequently, the ambient light level at the larva's depth was determined by the exponential decay of E_0 according to the Beer-Lambert law, $E_{i,t} = E_0 \mathrm{e}^{(-Kz_{i,t})}$. Here, K is the diffuse attenuation coefficient, assumed to take a value of 0.18 m^{-1} (Langangen et al. 2014). If $E_{i,t}$ was less than 1.0 µmol photons m^{-2} s^{-1}, low light conditions were set and vice versa.

To determine the vertical displacement in a timestep, the model of Opdal et al. (2011) was used:

$$\frac{dz}{dt} = C_l C_t(\alpha \cdot 0.33L \pm 0.1L).$$

The model split vertical movements between directional and random swimming components. For the former, the larvae swam at a speed of 0.1 body lengths (L) per second, whilst for the latter it swam at 0.33 body lengths per second. The random number α was a behavioural variable that modulated the random component and was drawn from a uniform distribution ranging from -1 to 1. The equation used the plus sign when low light conditions were set and the minus sign when high light conditions were set, corresponding to the ascent and descent of the individual respectively. The parameters C_l and C_t were conversion factors from mm to m and hours to seconds respectively (Langangen et al. 2014). Vertical boundaries that varied with light conditions and larval length, and constrained the larva's vertical displacement, were implemented in a similar fashion to Opdal et al. (2011).

2.5. Spawning grounds

Particles were released from two spawning grounds located in SW Iceland (Fig. 1B). The inshore spawning ground (SG) was adjacent to the coastline, with a maximum and mean depth of 100 m and 48 m respectively. The offshore SG was located ~61 km south of the coastline on the outskirts of the main spawning ground. All grid cells at the offshore SG had a depth of 240 m. Within each spawning ground, all unique surface grid cells in CODE were found and restricted to those with a depth range of 20 m – 240 m, which encompassed the depth range of spawning cod in Iceland (Jónsson and Pálsson 2013; Sólmundsson et al. 2017).

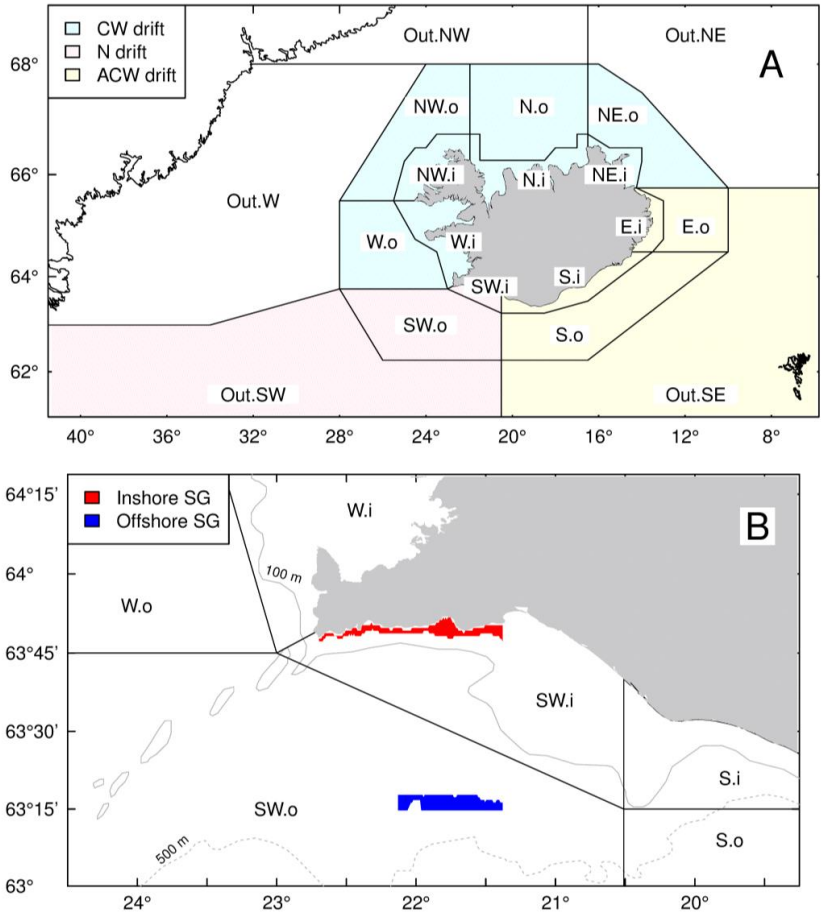

Figure 1*: Panel A shows the division of Icelandic and surrounding waters into distinct regions for analysing connectivity. The regions were divided into inshore and offshore components, identified by the "i" and "o" suffixes respectively. Regions located outside the regional grid have the prefix "Out". To analyse the direction of drifting particles, regions were grouped into clockwise (CW), neutral (N), and anticlockwise (ACW) components, indicated by the different shadings. Panel B shows the inshore and offshore spawning grounds utilized for the release of particles.*

2.6. Initialisation

Particles were released at 00:00 UTC. They were assigned a random latitude and longitude from within a spawning ground that corresponded to a surface grid cell in CODE's model domain. As Icelandic cod are known to rise a few meters from the seafloor when spawning (Grabowski et al. 2012), particles were then assigned a random initialisation depth within the deepest grid cell of CODE at x_i and y_i. Accounting for natural variation in S_e was shown to have a far larger impact on the vertical displacement of Icelandic cod eggs than natural variation in D_e (Butler et al. 2020). Therefore, for each simulation D_e was fixed at a value of 1.42 mm, whilst $S_{e,i}$ was randomly drawn from a gaussian distribution using summary statistics from Butler et al. (2020). Although ontogenetic changes in S_e have been recorded for Icelandic cod, the impact of these changes on vertical egg distributions was substantially reduced by accounting for natural variation in the overall S_e (Butler et al. 2020).

2.7. Simulations

Simulations were carried out from 1998 to 2012. For each year, one thousand eggs were released per day from mid-March to mid-May, the main spawning period for Icelandic cod (Marteinsdóttir and Björnsson 1999). The simulations stopped when the larvae were 120 days old. A suite of "number of particles" trials were performed to ensure this was an adequate number to generate high certainty in the spatiotemporal location of larvae at 120 days-post-release (see Brickman and Smith 2002). The reference simulation (RS) included the horizontal and vertical random walks, larval DVM behaviour, and bottom grid cell spawning. To gauge how dispersal trajectories and connectivity were affected by these formulations, we carried out several sensitivity analyses. Each sensitivity analysis involved turning off one subroutine and repeating the simulations in 2009 (a year with strong clockwise drift). These analyses included: (1) turning off the horizontal random walk, (2) turning off egg and larval vertical movements by maintaining a fixed depth throughout the simulation, and (3) turning off the spawning depth module at Off.SG. All simulations are summarised in Table 1.

Simulation	RW_H	RW_V	DVM	z_0	z_{fixed}	SG
Reference	✓	✓	✓	z_h	-	In, Off
Sim. 1	✓	-	-	5 m	✓	In, Off
Sim. 2	✓	-	-	15 m	✓	In, Off
Sim. 3	✓	-	-	30 m	✓	In, Off
Sim. 4	-	✓	✓	z_h	-	Off
Sim. 5	✓	✓	✓	20 m	-	In, Off

***Table 1**: Summary of simulations. RW_H = horizontal random walk; RW_V = vertical random walk; DVM = diel vertical migration; z_0 = initialisation depth; z_h = bottom grid cell; z_{fixed} = whether z remains static throughout the simulation; SG = spawning ground.*

2.8. Analyses

The statistical regions presented in Begg and Marteinsdottir (2000) were utilized to examine connectivity between spawning grounds and early life-stage spatiotemporal locations (Fig. 1A). These regions were derived from known spawning grounds, larval fish surveys (Marteinsdottir et al. 2000b) and bathymetry. Region 1 in Begg and Marteinsdottir

(2000) was divided into W and SW regions using the latitude at the tip of Reykjanes Peninsula as a dividing boundary. The two regions directly north of Iceland (regions 3b, 4b, 3a, 4a in Begg and Marteinsdottir [2000]) were pooled to form singular inshore and offshore northerly regions. Region 8 in Begg and Marteinsdottir (2000) was extended longitudinally to connect with the coast of Greenland. The resulting grid contained six regions surrounding Iceland, each of which was divided into inshore and offshore components (Fig. 1A). Furthermore, five outer regions were implemented to capture the drift of particles to Greenland (Out.W) and off the regional grid to the NE, NW, SE, and SW (Fig. 1A).

For each release date, larvae were assigned to a region based on their spatial location after 120 days of drift. This resulted in 67 connectivity matrices per year per spawning ground. For each matrix, the regions were ranked by the number of particles they contained, and the dominant region identified (rank = 1). To quantify the direction and magnitude of dispersal, the number of larvae that drifted clockwise, in a neutral direction SW of the spawning grounds, and anticlockwise along the south of Iceland were calculated (see the different shadings in Fig. 1A for how these directions were defined). Furthermore, the number of larvae that drifted to inshore endpoints in each direction was quantified. These procedures were replicated for different temporal and spatial regional configurations to understand how connectivity varies over- and between years.

To quantify differences between the connectivity matrices we calculated the fraction of unexplained variance ($FUV = 1 - r^2$), where r is the Pearson correlation coefficient of two connectivity matrices (see Simons et al. 2013).

2.9. Output

Output was stored at 10-day intervals. This included the individual's attribute vector and environmental exposure (temperature, salinity, ambient density, and freshwater thickness) averaged over the 10-day period.

3. Results

3.1. Overview

The model results highlighted strong clockwise drift of eggs/larvae from both SGs (Fig. 2). However, a greater proportion of larvae drifted clockwise from the inshore SG, whilst anticlockwise and neutral drift to the SE and SW of Iceland respectively was greater from the offshore SG (Fig. 3A). Furthermore, the magnitude of clockwise dispersal was greater from the inshore SG, highlighted by the higher proportions found in the north regions (Fig. 3B). Despite this difference, two trends in the magnitude of clockwise dispersal were evident from both SGs: (1) the proportion of larvae decreased as the distance from the SG increased (from W to NW to N); (2) a greater proportion of larvae drifted to inshore endpoints, a trend seen in the W, NW and N regions (Fig. 3B).

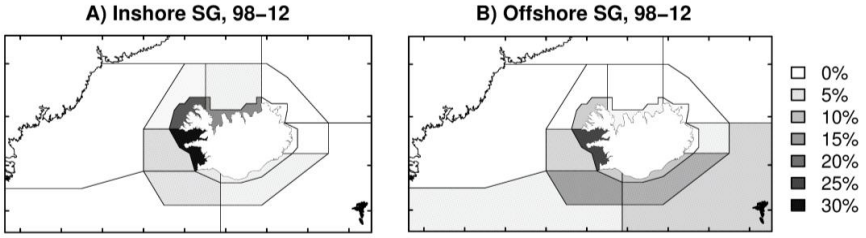

***Figure 2**: Connectivity between spawning grounds and drift endpoints for 120-day old larvae. The total percentage of larvae (i.e. pooled over years) which drifted to each region is shown for the inshore (A) and offshore (B) spawning grounds.*

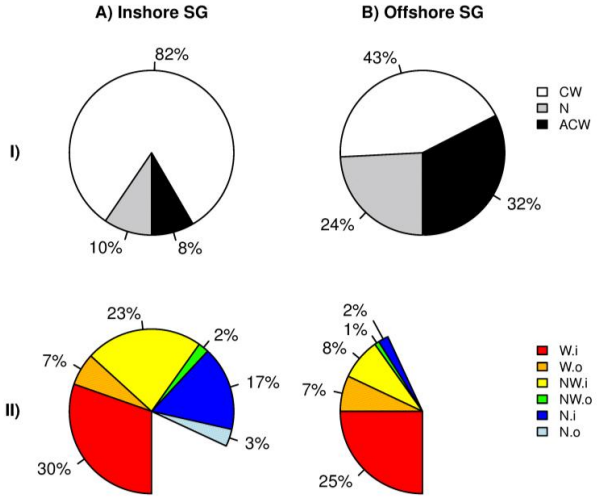

***Figure 3**: The proportion of larvae (pooled over years) that drifted to clockwise (CW), neutral (N), and anticlockwise (ACW) endpoints are shown in row I. The proportion of larvae that drifted to each region in the clockwise direction is shown in row II. Results are presented for the inshore (A) and offshore (B) spawning grounds. Less than 0.5% of larvae drifted to the NE regions from both spawning grounds, hence its omission from the graphs.*

3.2. Interannual variation in dispersal direction and magnitude

The direction of dispersal from the inshore SG was more stable across years than the offshore SG. Greater than 65% of larvae drifted to a clockwise endpoint in each year and less than 20% drifted anticlockwise to SE endpoints or in a neutral direction to SW endpoints (Fig. 4A). The exception was in 2010 when the clockwise drift was reduced (~14%) and ~60% of larvae drifted neutrally to a SW endpoint (Fig. 4A). From the offshore SG, the proportion of larvae that drifted in each direction varied considerably from year to year. Clockwise drift accounted for between 1% and 90% of larvae (the minimum was 20% when excluding 2010), whilst the proportions of larvae that drifted neutrally to SW endpoints and anticlockwise to SE endpoints ranged from 5% - 45% and 6% - 60% respectively.

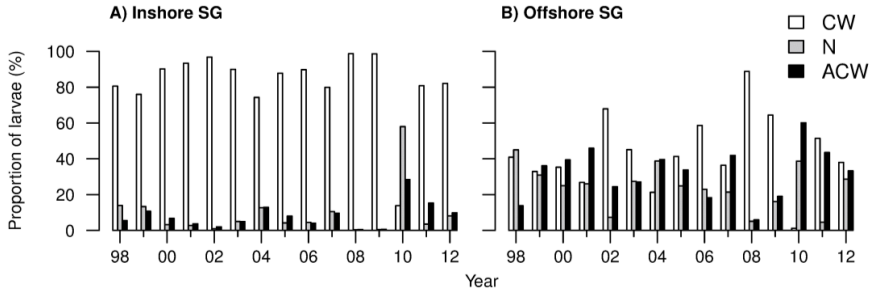

Figure 4*: Interannual variation in the direction of dispersal from the inshore (A) and offshore (B) spawning grounds. For each year, the proportion of larvae that drifted to clockwise (CW), neutral (N), and anticlockwise (ACW) endpoints are shown.*

The magnitude of clockwise dispersal from the inshore SG was consistently greater than from the offshore SG, whilst the magnitude of neutral (to the SW) and anticlockwise (to the SE) dispersal was consistently greater from the offshore SG (Fig. 5). The trend of decreasing proportions from the W to the N endpoints was reversed in three years (2002, 2008 and 2009) from the inshore SG (Fig. 5A), highlighting years when clockwise drift was particularly strong. This reversal was not seen in any years from the offshore SG (Fig. 5B). Of the larvae that drifted clockwise, the inshore endpoints contained greater proportions of larvae than the offshore endpoints, a trend seen across years from both SGs (Fig. 5). Of the larvae that drifted in a neutral direction to the SW, the offshore region was the most common endpoint in most years (Fig. 5B). In contrast, no trend was found in the interannual magnitude of anticlockwise dispersal to south-easterly endpoints, with the relative proportions of larvae in each endpoint varying from year to year.

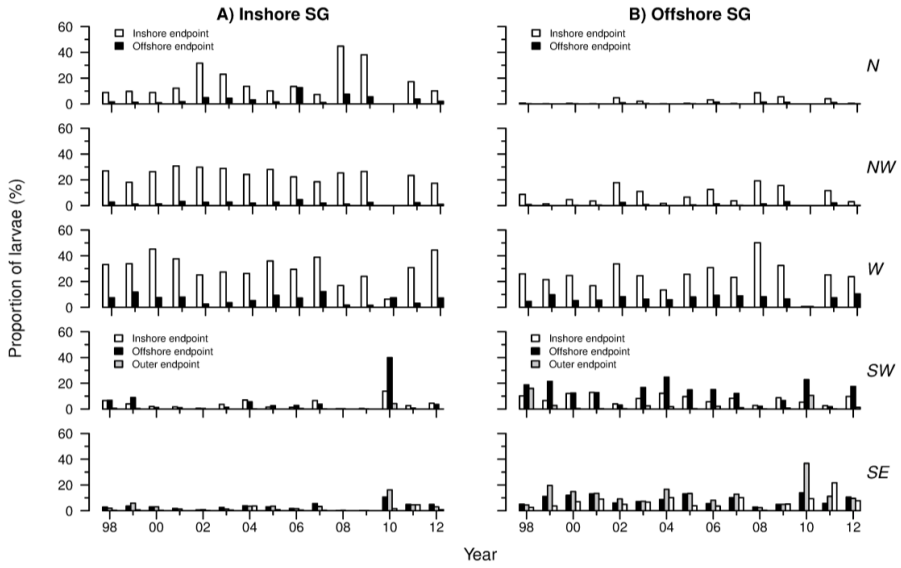

Figure 5*: Interannual variation in the magnitude of dispersal from the inshore (A) and offshore (B) spawning grounds. For five regions (different rows), the proportion of larvae that drifted to the region's inshore and offshore endpoints is shown per year. The outer SW and SE regions are shown together with the inshore and offshore SW and S regions respectively.*

The fraction of unexplained variance (FUV) between connectivity matrices was calculated for each possible yearly contrast (210 contrasts at each SG). The median FUV was 0.2 for the inshore SG and 0.4 for the offshore SG. This highlighted the greater stability in the direction and magnitude of dispersal across years from the inshore SG. To an extent this was because the offshore SG was ~62 km directly south of the inshore one. However, considering particles that drifted clockwise and correcting for this difference, the centres of gravity of both spawning grounds at 120-days differed from -11 km to 50 km per year with an average of 9.4 km. This provides further evidence that the magnitude of clockwise dispersal was greater from the inshore SG.

3.3. Seasonal variation in dispersal direction

Seasonal variation in the direction of dispersal was far greater from the offshore SG than the inshore SG. In 87% of the release dates, most larvae drifted to clockwise endpoints from the inshore SG (Fig. 6A). This value increased to 94% when omitting 2010, highlighting the low levels of drift to neutral and anticlockwise endpoints. Excluding 2010, the clockwise drift was dominant on > 70% of the release days within each year, whilst on < 20% of the release dates, drift to neutral or anticlockwise endpoints was dominant in each year (Fig. 6A). In contrast, the drift of larvae to clockwise endpoints was dominant in approximately half of the release dates from the offshore SG, with anticlockwise drift to SE endpoints contributing substantially more than neutral drift to SW endpoints (Fig. 6B). Between years, the proportion of days that each drift direction was dominant varied considerably more than from the inshore SG. Clockwise drift was dominant in 0% to 100% of the release dates (minimum of 24% when excluding 2010). The corresponding ranges for neutral and anticlockwise drift were 0% - 49% and 0% - 79% respectively.

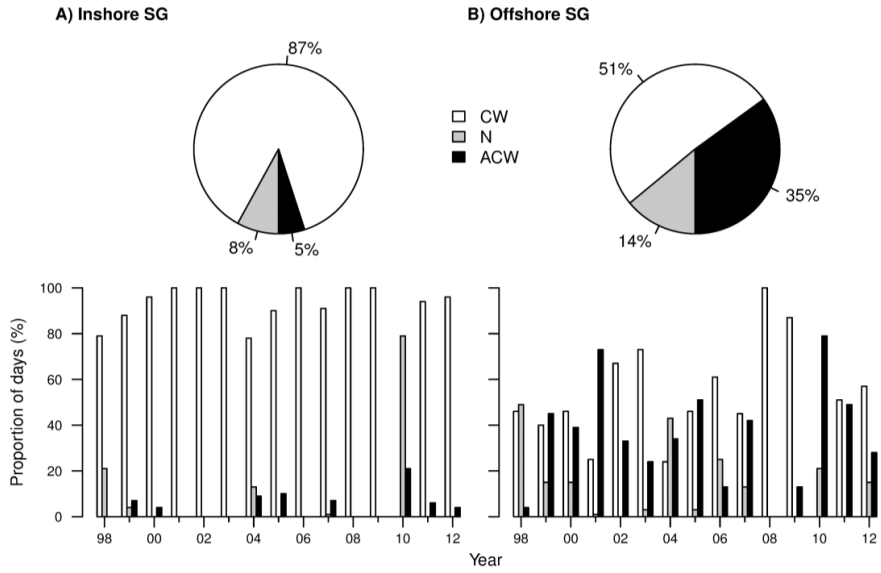

Figure 6*: Seasonal variation in the direction of dispersal. For each release date, the proportion of larvae that drifted to endpoints in the clockwise (CW), neutral (N), and anticlockwise (ACW) directions was calculated. Subsequently, the dominant drift direction – the direction that most larvae drifted -- was identified for each release date at both SGs. The pie charts show the total proportion of days that each drift direction was dominant. The bar charts show the proportion of days that each drift direction was dominant per year.*

Each spawning season could be broken down to clusters of dominant endpoints (or adjacent dominant endpoints) highlighting that changes in the direction of dispersal were driven by consistent (over multiple days) changes in circulation patterns. For instance, in 1998, strong clockwise drift was evident earlier in the season whilst strong neutral drift to the SW was evident later in the spawning season, a trend seen from both spawning sites (Fig. 7). These clusters of dominant regions were more frequent and extended over a longer time from the offshore SG (Fig. S2).

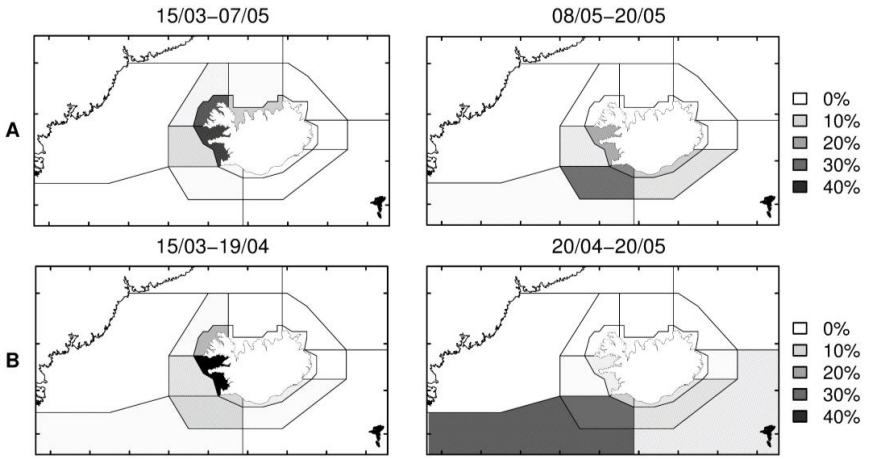

Figure 7*: Connectivity patterns for two adjacent time periods in 1998 from the inshore (A) and offshore (B) spawning grounds. The pooling dates are shown in the panel titles.*

A consistent seasonal pattern in clockwise drift across years was not evident from the offshore SG. However, a two-week period of stability in mid-April was evident from the inshore SG (Fig. S2). In this period, the drift of larvae to clockwise endpoints was consistently above 80% in all years. In general, there was little congruence in the seasonal patterns of clockwise drift between SGs. The number of days that the dominant drift direction matched between spawning grounds ranged from 16 to 67. Even in 2008, when clockwise drift was dominant on every release date at both SGs (Fig. 6B), the actual proportion of larvae that drifted clockwise varied between SGs (Fig. S2). The correlation between the proportions of larvae that drifted to clockwise endpoints from both SGs ranged from -0.6 to 0.2, illustrating the disparity in the seasonal direction of drift between SGs.

3.4. Sensitivity analyses

3.4.1. Fixed depth

The fixed depth simulations revealed strong stratification in the currents transporting the larvae to the north. Furthermore, pronounced differences in the connectivity matrices between the reference simulation and each of the fixed depth simulations highlighted the large impact that vertical movements of eggs/larvae had on the direction and magnitude of dispersal (Table 2; Fig. 8).

Sensitivity	**FUV**	
	Inshore SG	**Offshore SG**
z_{fixed} = 5 m	0.85, 0.90, 0.97	0.98, 0.99, 1.00
z_{fixed} = 15 m	0.09, 0.42, 0.67	0.06, 0.18, 0.34
z_{fixed} = 30 m	0.52, 0.88, 0.98	0.15, 0.33, 0.69
RW_H = F	0.03, 0.08, 0.18	0.10, 0.19, 0.31
z_0 = 20 m	-	0.02, 0.03, 0.08

***Table 2**: Shows the fraction of unexplained variance (FUV) between the connectivity matrices resulting from reference simulation and each the sensitivity analyses. The FUV was calculated for each release date in 2009 resulting in a distribution of FUVs for each SG (n = 67). The 25th percentile, the median, and the 75th percentile of the resulting distributions are shown (in that order). RW_H = horizontal random walk, z_{fixed} = fixed depth, z_0 = initialisation depth.*

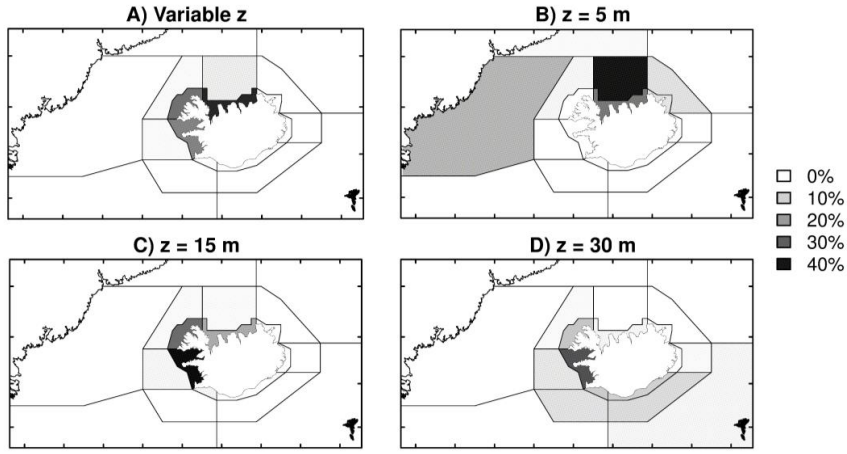

***Figure 8**: Annual connectivity matrices for the fixed depth simulations at the inshore SG in 2009. For comparison, panel A shows the reference connectivity matrix. Rows B, C and D show the connectivity matrices for the 5 m, 15 m, and 30 m fixed depth simulations respectively.*

At a fixed depth of 5 m, the proportion of larvae that drifted to clockwise endpoints was similar to the reference simulation. However, the magnitude of clockwise dispersal was far greater, illustrated by the greater proportion of larvae that drifted to the north region (Fig. 8B). Furthermore, a substantial proportion of larvae drifted towards Greenland which was not seen in the reference simulation (Fig. 8A). These dispersal patterns were seen from both SGs and highlighted a bifurcation in dispersal trajectories which was seen at the daily level (Fig. 9). For example, > 20% of larvae drifted east and west from the 120th day of the year from the inshore SG and periodically from the 112th day of the year from the offshore SG (Fig. S1).

The drift of larvae towards Greenland was highly dependent upon depth-selection. The reference simulation (which included larval DVM) and fixed depth simulations at 15 m and 30 m all produced negligible drift to Greenland. Furthermore, the reference simulation was run for an additional 30 days in 2009 but the proportion of larvae that drifted towards Greenland was still negligible. High proportions of larvae were found in the NW and N endpoints, demonstrating that the larvae drifted past the bifurcation point. The surface drift towards Greenland was also evident across years. For example, running the fixed depth = 5 m in 2011, 76% of larvae drifted to Greenland (with no bifurcation evident).

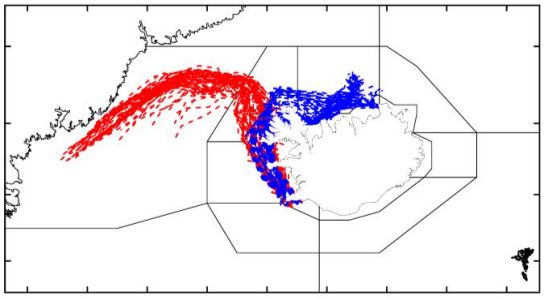

Figure 9*: Bifurcation of drift trajectories from the inshore SG in 2009. All particles were simulated at a fixed depth of 5 m. Each line corresponds to a single release date and connects the centres of gravity (n = 1000) at 10-day intervals until 120 days-post-release.*

Simulations with z fixed at 15 m and 30 m produced connectivity matrices that more closely resembled the reference simulation (Table 2). With z fixed at 15 m, the direction of drift from the inshore SG differed very little from the reference simulation; however, the magnitude of clockwise drift was reduced with the majority of larvae drifting to the inshore W endpoint as opposed to the inshore N endpoint (Fig. 8A, C). Neither the direction of drift nor the magnitude of clockwise drift differed substantially from the reference simulation for the offshore SG. The proportion of larvae that drifted to clockwise endpoints was substantially reduced (~40%) with z fixed at 30 m. Instead, more larvae drifted to endpoints in the neutral (SW) and anticlockwise (SE) directions (Fig. 8D). A similar pattern was seen from the offshore SG, although the reduction in the proportion of larvae that drifted to clockwise endpoints was smaller (~15%) than from the inshore SG.

3.4.2. Spawning depth

Spawning depth had a negligible impact on the connectivity matrices (Table 2). Eggs released in the deepest grid cells at the offshore SG took ~47 hours to reach surface waters (0 – 10 m). Furthermore, 99.2% of eggs reached the surface waters within 15 days, indicating that most eggs had reached neutral buoyancy prior to hatching. However, fixing the initialisation depth at 20 m resulted in endpoint proportions that differed by no more than 3% (mean = 0.4%) from the reference simulation. This result highlights that the ascent of eggs from deep SGs did not affect the overall direction or magnitude of dispersal seen at 120 days.

3.4.3. Random walk

Turning off the horizontal random walk had a larger impact on the connectivity matrices than the spawning depth simulation but a smaller one than the fixed depth simulations (Table 2). The direction of dispersal differed by no more than 7% from the reference simulation. On average, the endpoint proportions differed by 3% at the inshore SG and 2% at the offshore SG. The differences were explained predominantly by a reduction in the breath of dispersal. For example, the proportion of larvae that drifted clockwise to offshore endpoints was consistently reduced, highlighting the greater entrainment of larvae in inshore endpoints. This trend was seen from both spawning sites, and a similar trend of reduced dispersal breadth was seen in the larvae that drifted anticlockwise to SE endpoints from the offshore SG. However, the magnitude of differences that resulted from turning off the horizontal random walk were not substantial enough to generate different conclusions from the reference simulations.

4. Discussion

4.1. Drift trajectories vary between spawning components

The clockwise dispersal of larvae from the inshore SG was of a greater magnitude and more stable across years than from the offshore SG. The mechanism underlying these results lies in the situation of each spawning ground in relation to the regional hydrography. The inshore SG lies within the vicinity of the Icelandic Coastal Current which entrains eggs/larvae spawned within its path and transports them to the north. Jonasson et al. (2009) showed that abundance of cod larvae was inversely related to salinity, which together with other studies (e.g. Olafsson 1985; Begg and Marteinsdottir, 2002), have highlighted the importance of the Icelandic Coastal Current as a transport mechanism for larval cod. Conversely, Gislason et al. (2016) found a weak relationship between salinity and the spatiotemporal distribution of fish larvae sampled from SW Iceland. The model results showed that small portions of larvae from both spawning grounds are not entrained by the clockwise flowing currents and remain in the SW region. Furthermore, this observation may be explained by larvae originating from more easterly spawning grounds (see Brickman et al. 2007a).

The offshore SG is located outside the coastal current's path, trajectories are therefore dependent on the incoming Atlantic water. Dispersal trajectories of the larvae drifting clockwise showed a similar path to those from the inshore spawning ground, suggesting they are advected north and then entrained into the coastal current. However, the strong anticlockwise pulses to the SE are driven by larvae advected along the south coast with the South Icelandic Current (Logemann et al. 2013). Brickman et al. (2007a) released particles

from seven spawning grounds (including inshore and offshore components of the main SG) along the south coast but only found the clockwise/anticlockwise bifurcation in drift trajectories from SGs located east of the main SG. However, the equivalent offshore SG in that study (SG-1c) was directly adjacent to the inshore SG and situated further north than the offshore SG in this study. Furthermore, the offshore SG used by Brickman et al. (2007a) contained multiple potential spawning sub-components (Marteinsdottir et al. 2000b; Petursdottir et al. 2006). Simulations testing two SGs directly adjacent to the inshore SG (defined by depth intervals 75 m – 125 m and 125 m – 175 m) resulted in negligible differences in the connectivity matrices between simulations. These results highlight that differences in dispersal trajectories between sub-regions of the main spawning ground do exist and that distance-to-shore is a key SG descriptor when explaining these differences.

The existence of inshore and offshore intraspecific spawning components is a common feature of North Atlantic cod stocks. These components are often reproductively isolated (e.g. Beacham et al. 2002; Grabowski et al. 2011; Pampoulie et al. 2011) and characterised by differences in adult life-history and behavioural traits (e.g. Thorsteinsson et al. 2012). The differences in distance-to-shore between components naturally engenders variation in the environmental gradients experienced by the respective early life-stages. Inshore spawning grounds are typically situated in proximity to freshwater runoff, and in the path of nearshore circulation patterns that may differ substantially from offshore counterparts. For this reason, spawning site selection may be an important driver of sub-stock structure via the advection of eggs and larvae. This is particularly evident in fjords where eggs and larvae are retained through localised circulation patterns (e.g. Knutsen et al. 2007; Myksvoll et al. 2014). Our results suggest the larvae spawned at the offshore SG will mix with the inshore larvae in the northerly nursery grounds, and with the larvae spawned directly south of Iceland (SPG-13 [Kantur] in Brickman et al. 2007a) in the SE nursery grounds. The lack of a consistent seasonal signature in the direction of dispersal from the offshore SG suggests the degree of mixing in either direction will vary from year to year, and that dispersal trajectories alone do not contribute to the distinctions observed between these three regions (Jónsdottir et al. 2002, 2006; Marteinsdottir et al. 2000b; Petursdottir et al. 2006). However, the role of environmentally induced differences in growth and survival of the early life-stages cannot be ruled out.

4.2. Drift trajectories vary between and within years

The results highlight the importance of running biophysical IBM simulations over multiple years. Interannual variation in dispersal patterns was greater from the offshore spawning ground, suggesting that interannual variation in the abundance and distribution of cod larvae (Begg and Marteinsdottir 2000) may be better explained by variations in the inflow of Atlantic water (Valdimarsson and Malmberg 1999; Jónsson and Valdimarsson 2005) than variations in the coastal current, assuming that the offshore spawning ground contributes substantially to the surviving 0-group population. Several biophysical IBM studies have highlighted annual variations in circulation patterns as an important driver of variation in drift trajectories and connectivity matrices (e.g. Kvile et al. 2018; Thompson et al. 2018). In general, running biophysical IBMs over several years is required to capture interannual variation in circulation patterns and water mass characteristics (e.g. temperature) that shape the vital rates and connectivity patterns of marine early life-stages (Kristiansen et al. 2011; Romagnoni et al. 2020). For example, strong clockwise drift was evident in 2008 and 2009 from both SGs; however, in 2010, clockwise drift from both

spawning grounds was negligible. The reason(s) for this are not entirely clear. Gislason et al. (2016) found a very pronounced halocline at ~30 m which extended ~60 km offshore in late May 2010. This observation contrasted with the more well-mixed transects from 2011 and 2013 (Gislason et al. 2016) suggesting that the water mass southwest of Iceland in 2010 was more static and less mixed than other years.

The model also highlighted the importance of releasing particles daily throughout the spawning season. At lower temporal resolutions, an incomplete picture of dispersal patterns may emerge with clusters of dominant endpoints potentially missed. For species with protracted spawning periods, environments are characterised by seasonal gradients in variables (e.g. temperature, mixed-layer depth, primary production) that can directly or indirectly influence the survival of eggs and larvae. It is therefore important to release large quantities of particles at a high temporal resolution throughout the spawning season to obtain confidence in the realised dispersal kernel (Brickman and Smith 2002; Swearer et al. 2019). Seasonal changes in dispersal trajectories have been identified in other systems (e.g. Huret et al. 2010; Hinrichsen et al. 2012; Barbut et al. 2019). Whilst a clear seasonal signal was not seen in this study, the clockwise drift from the inshore SG appeared to stabilise above 80% across years in mid-April. Although the timing of spawning varies with the environment, stock structure, and individual traits (Marteinsdóttir and Björnsson 1999; Begg and Marteinsdottir 2000), this broadly coincides with the peak spawning for cod in SW Iceland and is therefore potentially an important mechanism for determining the spatiotemporal distribution of the 0-group pelagic population. As a similar signature was not seen from the offshore SG, this is likely to be due to an increase in the stability of the coastal current.

4.3. Comparing model output with observations and prior modelling studies

The model highlighted that more larvae drifted to inshore clockwise endpoints than the equivalent offshore endpoints. This pattern was consistent between years and spawning grounds. This result captures the general inshore-to-offshore abundance trend found in the 0-group pelagic surveys but not the observed large interannual variations in the abundance and distributions of larval cod in offshore waters (Begg and Marteinsdottir 2000; Sveinbjörnsson and Hjörleifsson 2003; Jónsdottir et al. 2019). A potential explanation for this discrepancy is that particles were aggregating in areas of low diffusivity, i.e., the model was underestimating dispersion. This is a known artifact of naïve random walks when the model includes spatial and/or temporal variability in turbulent exchange coefficients (e.g. Visser 1997). Comparisons between the current results and simulations that include a deterministic "drift correction" term (see Brickman and Smith 2002) would establish whether this was the cause for the under-dispersion. Another potential cause for the under-dispersion is the absence of horizontal swimming behaviour(s) in the model. Incorporating autocorrelated horizontal swimming has improved estimates of connectivity in coral reef populations (Staaterman et al. 2012; Berenshtein et al. 2018) and empirical evidence for orientation behaviour in North Sea larval haddock highlights that horizontal swimming may be an important mechanism for the transport of gadoid larvae (Cresci et al. 2019).

Considering clockwise dispersal, the majority of larvae drifted to inshore W, NW, and N endpoints from the inshore SG, whilst the majority of larvae from the offshore SG drifted to inshore W and NW endpoints. These results are broadly similar to the connectivity matrices from the main spawning grounds obtained by Brickman et al. (2007a). However, whilst the inshore W region was frequently the most dominant endpoint in the current

study, the NW region was in Brickman et al (2007a), suggesting that the present model was underestimating dispersal magnitude. A number of differences between the models may have caused this disagreement. Firstly, in Brickman et al. (2007a), interannual variation in the climatological flow-fields was not present. Furthermore, in 2002 and 2003—the years explicitly modelled in Brickman et al. (2007b)—the present study showed strong clockwise drift with the proportions of larvae drifting to NW and N endpoints greater than or equal to the W endpoint (Fig. 5) which is in better agreement with the results from Brickman et al. (2007a, b, c). Secondly, given the great sensitivity of dispersal patterns to particle depth (Fig. 8), differences in the connectivity matrices may have resulted from the different modes of vertical displacement utilised. In the present study, eggs were vertically displaced via an advection-diffusion model and larvae performed DVMs, whilst in Brickman et al. (2007a, b, c), eggs remained at a constant depth and larvae performed an ontogenetic vertical migration without a diel component.

The 0-group survey data also showed that the northwest and northern areas (areas 2, 3 and 4 in Begg and Marteinsdottir 2000; Jónsdottir et al. 2019) contained the greatest abundances of larvae consistently across years, and that the west area contained far smaller abundances. This may reflect under-dispersion in the model (discussed above), although a direct comparison with the survey data is not feasible because of the absence of simulations from spawning grounds (which contribute to the larval cod abundances north of Iceland) along the west and north-western coasts (Begg and Marteinsdottir 2000; Marteinsdottir et al. 2000a; Jonasson et al. 2009). The relative contribution of the main spawning grounds to the northern nursery grounds varies interannually (Jónsdottir et al. 2019). Begg and Marteinsdottir estimated that approximately ~90% and ~70% of larvae found in the NW and N regions respectively originated from the main spawning ground. Brickman et al. (2007a) estimated respective values of ~75% and ~80%. These studies highlight that additional spawning grounds along the west and northwest coasts, as well as additional sub-spawning components within the main spawning grounds, are required to validate the model output against the survey data.

4.4. Limited larval connectivity between Iceland and Greenland

Historically, there has been a high degree of mixing between the Icelandic and Greenlandic cod stocks (Schopka 1994; Bonanomi et al. 2016). This occurs through the drift of larvae from Iceland to Greenland (Begg and Marteinsdottir 2000; Brickman et al. 2007a, b), and the natal homing of adults from Greenland to Iceland (Storr-Paulsen et al. 2004; Bonanomi et al. 2016). Furthermore, this connectivity varies between Icelandic spawning components, with the offshore component having a stronger affinity with the Greenlandic subpopulations (Therkildsen et al. 2013; Bonanomi et al. 2016). Analysing 0-group survey data, Begg and Marteinsdottir (2000) found strong episodic pulses of larvae in the Greenland region. Furthermore, the age distribution of pelagic juveniles from this region was similar to those originating from the main spawning grounds in the SW, highlighting the strong likelihood of similar spawning origins. However, our results showed very small proportions of larvae drifting to Greenland and we found no evidence to suggest that larvae spawned in the offshore SG were more likely to drift towards Greenland. The most likely explanation for this result is that SGs outside of the two utilised in this study produce greater contributions to the 0-group abundance in Greenlandic waters. This is suggested by previous particle tracking exercises that found drift trajectories to Greenland arising predominantly from western SGs (Brickman et al.

2007a) and SGs located further to the SW than the two SGs used in this study (Ribergaard 2004).

The fixed depth simulations highlighted a transport bifurcation point northwest of the West Fjords where a portion of particles drifted west to Greenland and another portion east across the north of Iceland. This suggests that vertical current shear, potentially driven by wind stress and baroclinic eddies, are an important component of the transport of larvae from Iceland to Greenland. Furthermore, it entertains the possibility that transport to Greenland is to a degree behaviourally mediated. If this is the case, the vertical limits imposed on the vertical migrations in the reference simulation could have led to underestimates of larval drift to Greenland.

4.5. Vertical displacement of eggs and larvae substantially alters drift trajectories

The vertical positioning of eggs/larvae had a large impact on connectivity. This highlights the importance of including the vertical displacement of eggs and larvae through physical and behavioural mechanisms into spatially explicit biophysical IBMs. This was seen by vastly different connectivity matrices that emerged from the reference simulation and all fixed depth simulations. For instance, Valdimarsson and Malmberg (1999) estimated it took between 2 – 3 months for particles from the main spawning grounds to reach the north-western tip of Iceland (Hornbanki) based on deployed surface drifters. A similar pattern was seen with the fixed depth simulation at 5 m; however, this pattern was not reproduced (clockwise drift was slower) in the simulations with deeper fixed depths or when the DVM module was activated.

Vertical displacement occurred through a BRW for the egg stage and DVM for the larval stage. In the reference simulation, the emergent depths of neutral buoyancy for eggs ranged from 3 m to 10 m with a mean of 6 m. This is in agreement with previous empirical and theoretical work that has shown Icelandic cod eggs occupying a surface maximum (0 m – 5 m) in calm conditions (Fridgeirsson 1984) and a sub-surface, but still pelagic, distribution in well-mixed conditions (Butler et al. 2020). The depth of spawning had minimal impact on the connectivity matrices suggesting that the horizontal location of spawning is a more important determinant of dispersal patterns than the vertical position that the eggs are released.

Regarding cod larvae, Fridgeirsson (1984) observed small cod larvae exhibiting DVM behaviours, and Gislason et al. (2016) found fish larvae (predominantly gadoids) confined to the upper 50 m of the water column southwest of Iceland. These observations justify the use the DVM module; however, there was not sufficient data to parameterise the algorithm specifically for Icelandic larval cod. Given the great sensitivity of drift trajectories to DVM behaviour, further research to estimate parameters that describe the timing and amplitude of DVMs would provide a more robust parameterisation for larval cod DVMs, which could potentially lead to different dispersal and connectivity patterns at the population level.

4.6. Model assumptions and future perspectives

Our results highlighted that variation in dispersal patterns exists between inshore and offshore components of the main SGs. Underlying this result is the assumption that females are homogeneously distributed between the inshore and offshore components, they spawn at the same time, and produce equivalent numbers of eggs. However,

empirical work has shown that more females spawn closer to shore, they are larger and more fecund, and spawn over a longer period (Marteinsdóttir and Björnsson 1999; Marteinsdottir et al. 2000a, b; Marteinsdottir and Begg 2002). The dispersal trajectories identified in this study should serve as a useful baseline for particle tracking models that account for this variation via an egg production model (e.g. Scott et al. 2006). This would help to understand the relative contributions of inshore and offshore components to the surviving pelagic 0-group spatiotemporal distributions, and potentially the sub-stock structure of Icelandic cod.

We did not include mortality from predation or starvation in the model. Larval fish generally experience high levels of predation that decline through ontogeny (McGurk 1986; Houde 1997). Due to environmental differences between the two spawning grounds and throughout the protracted spawning period, inclusion of these components of mortality could substantially alter the connectivity matrices. This could take the form of a prescribed mortality rate (e.g. McGurk 1986) or through a risk-sensitive foraging module that would take a more mechanistic, evolutionary perspective that is more in tune with how individuals make behavioural decisions (see Fiksen et al. 2007; Kristiansen et al. 2009; Jørgensen et al. 2013). Such an approach could yield insights into variation in first year class strength due to the match-mismatch of larval cod with key prey items (see Thorisson 1989) at hatching and along drift trajectories.

Acknowledgements

This study is a product of the Nordic Centre for Research on Marine Ecosystems and Resources under climate Change (NorMER), which is funded by the Norden Top-Level Research Initiative sub-programme ‘Effect Studies and Adaptation to Climate Change’. We thank Professor Steven C. Campana for the detailed feedback he gave on two drafts of the manuscript.

References

Astthorsson, O.S., Gislason, A., Gudmundsdottir, A., 1994. Distribution, abundance, and length of pelagic juvenile cod in Icelandic waters in relation to environmental conditions. ICES Mar. Sci. Symp. 198, 529–541.

Barbut, L., Groot Crego, C., Delerue-Ricard, S., Vandamme, S., Volckaert, F.A.M., Lacroix, G., 2019. How larval traits of six flatfish species impact connectivity. Limnol. Oceanogr. 64, 1150–1171. https://doi.org/10.1002/lno.11104

Beacham, T.D., Brattey, J., Miller, K.M., Le, K.D., Withler, R.E., 2002. Multiple stock structure of Atlantic cod (Gadus morhua) off Newfoundland and Labrador determined from genetic variation. ICES J. Mar. Sci. 59, 650–665. https://doi.org/10.1006/jmsc.2002.1253

Begg, G.A., Marteinsdottir, G., 2002. Environmental and stock effects on spawning origins and recruitment of cod Gadus morhua. Mar. Ecol. Prog. Ser. 229, 263–277. https://doi.org/10.3354/meps229263

Begg, G.A., Marteinsdottir, G., 2000. Spawning origins of pelagic juvenile cod Gadus morhua inferred from spatially explicit age distributions: Potential influences on year-class strength and recruitment. Mar. Ecol. Prog. Ser. 202, 193–217. https://doi.org/10.3354/meps202193

Berenshtein, I., Paris, C.B., Gildor, H., Fredj, E., Amitai, Y., Lapidot, O., Kiflawi, M. 2018. Auto-correlated directional swimming can enhance settlement success and connectivity in fish larvae. J. Thor. Biol. 439, 76-85.

Björnsson, B., Steinarsson, A., Árnason, T., 2007. Growth model for Atlantic cod (Gadus morhua): Effects of temperature and body weight on growth rate. Aquaculture 271, 216–226. https://doi.org/10.1016/j.aquaculture.2007.06.026

Bonanomi, S., Overgaard Therkildsen, N., Retzel, A., Berg Hedeholm, R., Pedersen, M.W., Meldrup, D., Pampoulie, C., Hemmer-Hansen, J., Grønkjaer, P., Nielsen, E.E., 2016. Historical DNA documents long-distance natal homing in marine fish. Mol. Ecol. 25, 2727–2734. https://doi.org/10.1111/mec.13580

Brickman, D., Marteinsdottir, G., Logemann, K., Harms, I.H., 2007a. Drift probabilities for Icelandic cod larvae. ICES J. Mar. Sci. 64, 49–59. https://doi.org/10.1093/icesjms/fsl019

Brickman, D., Marteinsdottir, G., Taylor, L., 2007b. Formulation and application of an efficient optimized biophysical model. Mar. Ecol. Prog. Ser. 347, 275–284. https://doi.org/10.3354/meps06984

Brickman, D., Smith, P.C., 2002. Lagrangian stochastic modeling in coastal oceanography. J. Atmos. Ocean. Technol. 19, 83–99. https://doi.org/10.1175/1520-0426(2002)019<0083:LSMICO>2.0.CO;2

Brickman, D., Taylor, L., Gudmundsdóttir, Á., Marteinsdóttir, G., 2007c. Optimized biophysical model for Icelandic cod (Gadus morhua) larvae. Fish. Oceanogr. 16, 448–458. https://doi.org/10.1111/j.1365-2419.2007.00449.x

Butler, W.E., Guðmundsdóttir, L., Logemann, K., Langbehn, T.J., Marteinsdóttir, G., 2020. Egg size and density estimates for three gadoids in Icelandic waters and their implications for the vertical distribution of eggs along a stratified water column. J. Mar. Syst. 204, 103290. https://doi.org/10.1016/j.jmarsys.2019.103290

Chambers, R.C., 1993. Phenotypic Variability in Fish Populations and Its Representation in Individual-Based Models. Trans. Am. Fish. Soc. 122, 404–414. https://doi.org/10.1577/1548-8659(1993)122<0404:PVIFPA>2.3.CO;2

Cresci, A., Paris, C.B., Foretich, M.A., Durif, C.M., Shema, S.D., O'Brien, CJ.E., Vikebø, F.B., Skiftesvik, A.B., Browman., H.I. 2019. Atlantic Haddock (Melanogrammus aeglefinus) Larvae Have a Magnetic Compass that Guides Their Orientation. iScience 19, 1173-1178

Fiksen, Ø., Jørgensen, C., Kristiansen, T., Vikebø, F., Huse, G., 2007. Linking behavioural ecology and oceanography: Larval behaviour determines growth, mortality and dispersal. Mar. Ecol. Prog. Ser. 347, 195–205. https://doi.org/10.3354/meps06978

Folkvord, A., 2005. Comparison of size-at-age of larval Atlantic cod (Gadus morhua) from different populations based on size- and temperature-dependent growth models. Can. J. Fish. Aquat. Sci. 62, 1037–1052. https://doi.org/10.1139/f05-008

Fridgeirsson, E., 1984. Cod larvae sampling with a large pump off SW-Iceland, in: Dahl, E., Danielssen, D., Moksness, E., Solemdal, P. (Eds.), The Propagation of Cod Gadus Morhua L. Flødevigen rapportser, Reykjavik, pp. 317–333.

Gislason, A., Logemann, K., Marteinsdottir, G., 2016. The cross-shore distribution of

plankton and particles southwest of Iceland observed with a Video Plankton Recorder. Cont. Shelf Res. 123, 50–60. https://doi.org/10.1016/j.csr.2016.04.004

Grabowski, T.B., Boswell, K.M., McAdam, B.J., Wells, R.J.D., Marteinsdóttir, G., 2012. Characterization of Atlantic Cod Spawning Habitat and Behavior in Icelandic Coastal Waters. PLoS One 7. https://doi.org/10.1371/journal.pone.0051321

Grabowski, T.B., Thorsteinsson, V., McAdam, B.J., Marteinsdóttir, G., 2011. Evidence of segregated spawning in a single marine fish stock: Sympatric divergence of ecotypes in icelandic cod? PLoS One 6. https://doi.org/10.1371/journal.pone.0017528

Guðmundsdóttir, L.Ó., 2013. Intra-stock diversity in egg specific gravity of Atlantic cod in Icelandic waters. University of Iceland.

Hinrichsen, H.-H., Hüssy, K., Huwer, B., 2012. Spatio-temporal variability in western Baltic cod early life stage survival mediated by egg buoyancy, hydrography and hydrodynamics. ICES J. Mar. Sci. 69, 1744–1752.

Houde, E.D., 1997. Patterns and consequences of selective processes in teleost early life histories, in: Early Life History and Recruitment in Fish Populations. Springer, pp. 173–196.

Huret, M., Petitgas, P., Woillez, M., 2010. Dispersal kernels and their drivers captured with a hydrodynamic model and spatial indices: A case study on anchovy (Engraulis encrasicolus) early life stages in the Bay of Biscay. Prog. Oceanogr. 87, 6–17. https://doi.org/10.1016/j.pocean.2010.09.023

Jonasson, J.P., Gunnarsson, B., Marteinsdottir, G., 2009. Abundance and growth of larval and early juvenile cod (Gadus morhua) in relation to variable environmental conditions west of Iceland. Deep. Res. Part II Top. Stud. Oceanogr. 56, 1992–2000. https://doi.org/10.1016/j.dsr2.2008.11.010

Jónsdóttir, Ingibjörg G., Campana, S.E., Marteinsdottir, G., 2006. Otolith shape and temporal stability of spawning groups of Icelandic cod (Gadus morhua L.). ICES J. Mar. Sci. 63, 1501–1512. https://doi.org/10.1016/j.icesjms.2006.05.006

Jónsdóttir, I. G., Campana, S.E., Marteinsdottir, G., 2006. Stock structure of Icelandic cod Gadus morhua L. based on otolith chemistry. J. Fish Biol. 69, 136–150. https://doi.org/10.1111/j.1095-8649.2006.01271.x

Jónsdóttir, I.G., Woods, P., Jakobsdóttir, K.B., Jónasson, J.P., Elvarsson, B., Sólmundsson, J., 2019. Life history of juvenile Icelandic cod. Reykjavík.

Jónsdóttir, Ó.D.B., Imsland, A.K., Daníelsdóttir, A.K., Marteinsdóttir, G., 2002. Genetic heterogeneity and growth properties of different genotypes of atlantic cod (Gadus morhua L.) at two spawning sites off south Iceland. Fish. Res. 55, 37–47. https://doi.org/10.1016/S0165-7836(01)00296-X

Jónsson, E., 1982. A survey of spawning and reproduction of the Icelandic cod. Hafrannsóknastofnunin.

Jónsson, G., Pálsson, J., 2013. Íslenski fiskar (e. Icelandic fish). Mál og Menn. Reykjavik, Icel. 493.

Jónsson, S., Valdimarsson, H., 2012. Water mass transport variability to the North Icelandic shelf, 1994--2010. ICES J. Mar. Sci. 69, 809–815.

Jónsson, S., Valdimarsson, H., 2005. The flow of Atlantic water to the North Icelandic Shelf and its relation to the drift of cod larvae. ICES J. Mar. Sci. 62, 1350–1359. https://doi.org/10.1016/j.icesjms.2005.05.003

Jørgensen, C., Opdal, A.F., Fiksen, Ø., 2014. Can behavioural ecology unite hypotheses for fish recruitment? ICES J. Mar. Sci. 71, 909–917. https://doi.org/10.1093/icesjms/fst083

Knutsen, H., Olsen, E.M., Ciannelli, L., Espeland, S.H., Knutsen, J.A., Simonsen, J.H., Skreslet, S., Stenseth, N.C., 2007. Egg distribution, bottom topography and small-scale cod population structure in a coastal marine system. Mar. Ecol. Prog. Ser. 333, 249–255. https://doi.org/10.3354/meps333249

Kristiansen, T., Drinkwater, K.F., Lough, R.G., Sundby, S., 2011. Recruitment variability in North Atlantic cod and match-mismatch dynamics. PLoS One 6. https://doi.org/10.1371/journal.pone.0017456

Kristiansen, T., Jørgensen, C., Lough, R.G., Vikebø, F., Fiksen, Ø., 2009. Modeling rule-based behavior: Habitat selection and the growth-survival trade-off in larval cod. Behav. Ecol. 20, 490–500. https://doi.org/10.1093/beheco/arp023

Kvile, K.Ø., Romagnoni, G., Dagestad, K.F., Langangen, Ø., Kristiansen, T., 2018. Sensitivity of modelled North Sea cod larvae transport to vertical behaviour, ocean model resolution and interannual variation in ocean dynamics. ICES J. Mar. Sci. 75, 2413–2424. https://doi.org/10.1093/icesjms/fsy039

Langangen, Ø., Stige, L.C., Yaragina, N.A., Vikebø, F.B., Bogstad, B., Gusdal, Y., 2014. Egg mortality of northeast Arctic cod (Gadus morhua) and haddock (Melanogrammus aeglefinus). ICES J. Mar. Sci. 71, 1129–1136.

Logemann, K., Olafsson, J., Marteinsdóttir, G., 2012. Modelling the hydrography of Icelandic waters from 1992 to 2006. MARICE-E-Report MER-13-2012 221.

Logemann, K., Ólafsson, J., Snorrason, Á., Valdimarsson, H., Marteinsdóttir, G., 2013. The circulation of Icelandic waters - A modelling study. Ocean Sci. 9, 931–955. https://doi.org/10.5194/os-9-931-2013

Marteinsdottir, G., Gudmundsdottir, A., Thorsteinsson, V., Stefansson, G., 2000a. Spatial variation in abundance, size composition and viable egg production of spawning cod (Gadus morhua L.) in Icelandic waters. ICES J. Mar. Sci. 57, 824–830. https://doi.org/10.1006/jmsc.2000.0568

Marteinsdottir, G., Gunnarsson, B., Suthers, I.M., 2000b. Spatial variation in hatch date distributions and origin of pelagic juvenile cod in icelandic waters. ICES J. Mar. Sci. 57, 1182–1195. https://doi.org/10.1006/jmsc.2000.0880

Marteinsdøttir, G., Höskuldur, B., 1999. Time and Duration of Spawning of Cod in Icelandic Waters. ICES C. Y:34, 1–14.

Marteinsdottir, G., Steinarsson, A., 1998. Maternal influence on the size and viability of Iceland cod Gadus morhua eggs and larvae. J. Fish Biol. 52, 1241–1258. https://doi.org/10.1006/jfbi.1998.0670

McGurk, M.D., 1986. Natural mortality of marine pelagic fish eggs and larvae: role of spatial patchiness. Mar. Ecol. Prog. Ser. 34, 227–242.

Myksvoll, M.S., Jung, K.-M., Albretsen, J., Sundby, S., 2014. Modelling dispersal of eggs and quantifying connectivity among Norwegian coastal cod subpopulations. ICES J. Mar. Sci. 71, 957–969. https://doi.org/10.1093/icesjms/fst022 Contribution

North, E.W., Schlag, Z., Hood, R.R., Li, M., Zhong, L., Gross, T., Kennedy, V.S., 2008. Vertical swimming behavior influences the dispersal of simulated oyster larvae in a coupled particle-tracking and hydrodynamic model of Chesapeake Bay. Mar. Ecol. Prog. Ser. 359, 99–115. https://doi.org/10.3354/meps07317

Olafsson, J., 1985. Recruitment of Icelandic haddock and cod in relation to variability in the physical environment. ICES C. G:59, 10.

Opdal, A.F., Vikebø, F.B., Fiksen, Ø., 2011. Parental migration, climate and thermal exposure of larvae: Spawning in southern regions gives Northeast Arctic cod a warm start. Mar. Ecol. Prog. Ser. 439, 255–262. https://doi.org/10.3354/meps09335

Ospina-álvarez, A., Palomera, I., Parada, C., 2012. Changes in egg buoyancy during development and its effects on the vertical distribution of anchovy eggs. Fish. Res. 117–118, 86–95. https://doi.org/10.1016/j.fishres.2011.01.030

Pampoulie, C., Daníelsdóttir, A.K., Storr-Paulsen, M., Hovgård, H., Hjörleifsson, E., Steinarsson, B.A., 2011. Neutral and nonneutral genetic markers revealed the presence of inshore and offshore stock components of atlantic cod in Greenland waters. Trans. Am. Fish. Soc. 140, 307–319. https://doi.org/10.1080/00028487.2011.567850

Peck, M.A., Hufnagl, M., 2012. Can IBMs tell us why most larvae die in the sea? Model sensitivities and scenarios reveal research needs. J. Mar. Syst. 93, 77–93. https://doi.org/10.1016/j.jmarsys.2011.08.005

Pepin, P., Orr, D.C., Anderson, J.T., 1997. Time to hatch and larval size in relation to temperature and egg size in atlantic cod (Gadus morhua). Can. J. Fish. Aquat. Sci. 54, 2–10. https://doi.org/10.1139/cjfas-54-s1-2

Petursdottir, G., Begg, G.A., Marteinsdottir, G., 2006. Discrimination between Icelandic cod (Gadus morhua L.) populations from adjacent spawning areas based on otolith growth and shape. Fish. Res. 80, 182–189. https://doi.org/10.1016/j.fishres.2006.05.002

Ribergaard, M.H., 2004. On the coupling between hydrography and larval transport in Southwest Greenland waters. University of Copenhagen.

Romagnoni, G., Kvile, K.Ø., Dagestad, K.F., Eikeset, A.M., Kristiansen, T., Stenseth, N.C., Langangen, Ø., 2020. Influence of larval transport and temperature on recruitment dynamics of North Sea cod (Gadus morhua) across spatial scales of observation. Fish. Oceanogr. 29, 324–339. https://doi.org/10.1111/fog.12474

Schopka, S.A., 1994. Fluctuations in the cod stock off Iceland during the twentieth century in relation to changes in the fisheries and environment. ICES Mar. Sci. Symp. 198, 175–193.

Schulla, J., Jasper, K., 2007. Model description WASIM-ETH. Zürich.

Scott, B.E., Marteinsdottir, G., Begg, G.A., Wright, P.J., Kjesbu, O.S., 2006. Effects of population size/age structure, condition and temporal dynamics of spawning on reproductive output in Atlantic cod (Gadus morhua). Ecol. Modell. 191, 383–415.

https://doi.org/10.1016/j.ecolmodel.2005.05.015

Simons, R.D., Siegel, D.A., Brown, K.S., 2013. Model sensitivity and robustness in the estimation of larval transport: A study of particle tracking parameters. J. Mar. Syst. 119–120, 19–29. https://doi.org/10.1016/j.jmarsys.2013.03.004

Skartveit, A., Olseth, J.A., 1988. Some simple formulas for multiple Rayleigh scattered irradiance. Sol. Energy 41, 19–20.

Sólmundsson, J., Jónsdóttir, I.G., Ragnarsson, S.A., Björnsson, B., 2017. Connectivity among offshore feeding areas and nearshore spawning grounds; implications for management of migratory fish. ICES J. Mar. Sci. 75, 148–157. https://doi.org/10.1093/icesjms/fsx103

Staaterman, E., Paris, C.B., Helgers, J., 2012. Orientation behavior in fish larvae: A missing piece to Hjort's critical period hypothesis. J. Theor. Biol. 304, 188–196. https://doi.org/10.1016/j.jtbi.2012.03.016

Storr-Paulsen, M., Wieland, K., Hovgård, H., Rätz, H.J., 2004. Stock structure of Atlantic cod (Gadus morhua) in West Greenland waters: Implications of transport and migration. ICES J. Mar. Sci. 61, 972–982. https://doi.org/10.1016/j.icesjms.2004.07.021

Sundby, S., 1983. A one-dimensional model for the vertical distribution of pelagic fish eggs in the mixed layer. Deep Sea Res. Part A, Oceanogr. Res. Pap. 30, 645–661. https://doi.org/10.1016/0198-0149(83)90042-0

Sveinbjörnsson, Sveinn; Hjörleifsson, E., 2003. Report on the 0-group fish survey in Icelandic waters, August 2003. ICES ACFM, 1–16.

Swearer, S.E., Treml, E.A., Shima, J.S., 2019. A Review of Biophysical Models of Marine Larval Dispersal, in: Oceanography and Marine Biology. Taylor & Francis.

Therkildsen, N.O., Hemmer-Hansen, J., Hedeholm, R.B., Wisz, M.S., Pampoulie, C., Meldrup, D., Bonanomi, S., Retzel, A., Olsen, S.M., Nielsen, E.E., 2013. Spatiotemporal SNP analysis reveals pronounced biocomplexity at the northern range margin of Atlantic cod Gadus morhua. Evol. Appl. 6, 690–705. https://doi.org/10.1111/eva.12055

Thompson, D.M., Kleypas, J., Castruccio, F., Curchitser, E.N., Pinsky, M.L., Jönsson, B., Watson, J.R., 2018. Variability in oceanographic barriers to coral larval dispersal: Do currents shape biodiversity? Prog. Oceanogr. 165, 110–122. https://doi.org/10.1016/j.pocean.2018.05.007

Thorisson, K. (1989). The food of larvae and pelagic juveniles of cod (Gadus morhua L.) in the coastal waters west of Iceland. Rapports et Procés-Verbaux des Réunions du Conseil International pour l'Exploration de la Mer, 191:264–272.

Thorsteinsson, V., Pálsson, Ó.K., Tómasson, G.G., Jónsdóttir, I.G., Pampoulie, C., 2012. Consistency in the behaviour types of the Atlantic cod: Repeatability, timing of migration and geo-location. Mar. Ecol. Prog. Ser. 462, 251–260. https://doi.org/10.3354/meps09852

Thygesen, U.H., Ådlandsvik, B., 2007. Simulating vertical turbulent dispersal with finite volumes and binned random walks. Mar. Ecol. Prog. Ser. 347, 145–153. https://doi.org/10.3354/meps06975

Valdimarsson, H., Malmberg, S., 1999. Near-surface circulation in Icelandic waters derived from satellite tracked drifters. Rit Fiskid. 16, 23–39.

Visser, A.W., 1997. Using random walk models to simulate the vertical distribution of particles in a turbulent water column. Mar. Ecol. Prog. Ser. 158, 275–281. https://doi.org/10.3354/meps158275

Supplementary materials for:

Dispersal trajectories and connectivity matrices for larval cod spawned in southern Icelandic waters

W.E. Butler, K. Logemann, G. Marteinsdóttir

A1: Seasonality in the drift of larvae north of Iceland and towards Greenland

A2: Daily patterns in dispersal direction and magnitude

A1: Seasonality in the drift of larvae north of Iceland and towards Greenland

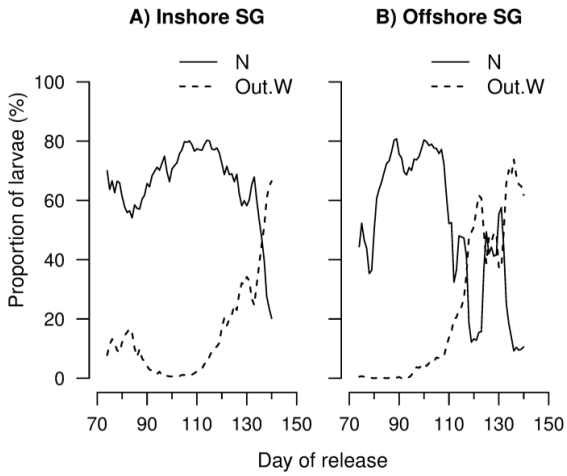

Figure A1*: The proportion of larvae that drifted to the northern region (N) and towards Greenland (the outer west region, Out.W) from the inshore (A) and offshore (B) spawning grounds in 2009. Particles were simulated using fixed depth of 5 m.*

A2: Daily patterns in dispersal direction and magnitude

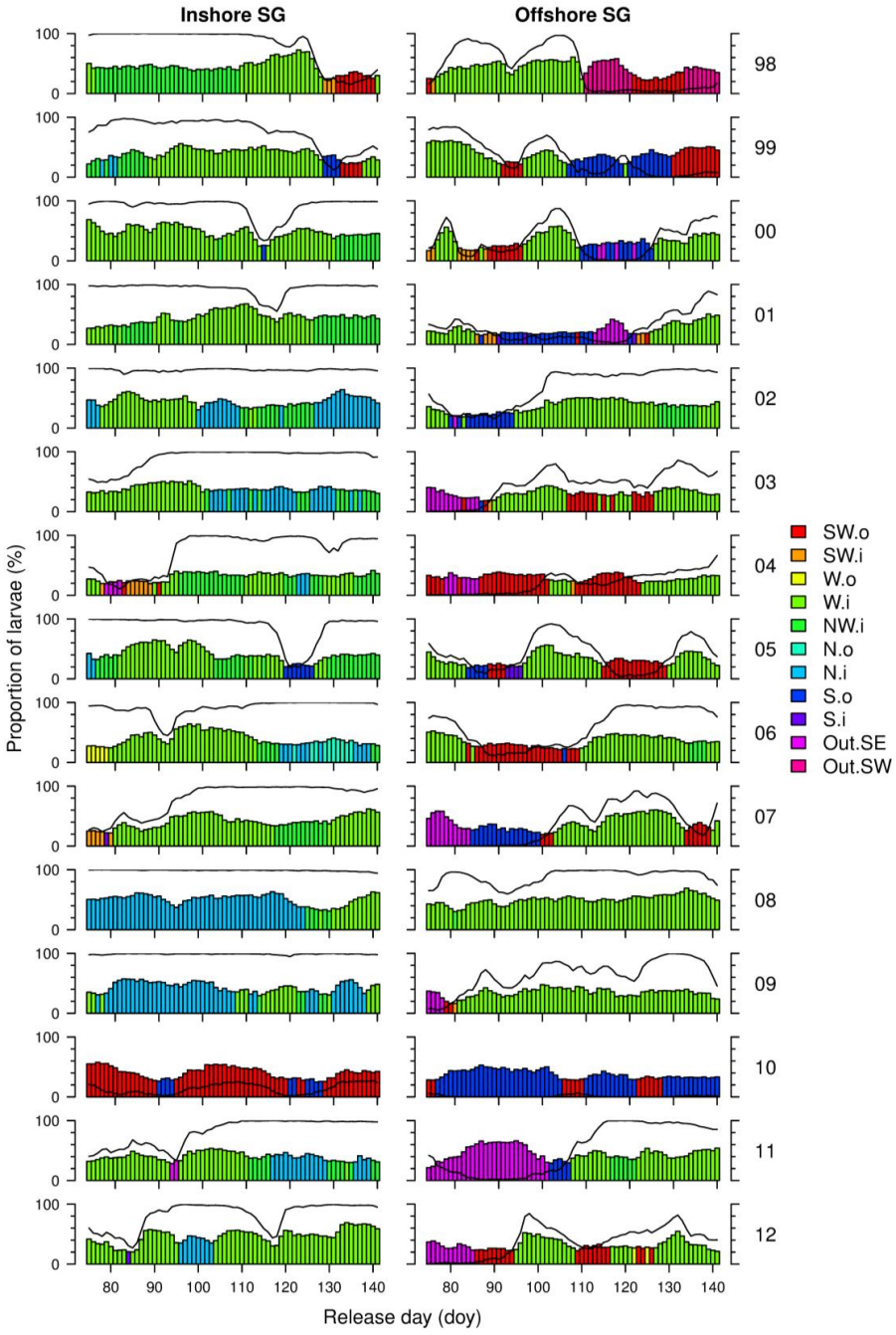

Figure A2: *The dominant endpoint – the region that contained the highest number of larvae at 120 days – for each spawning ground per release day per year. Drift regions that are not included in the legend did not contain the highest number of larvae on any release date. The overlaid black line shows the proportion of larvae that drifted clockwise.*

Paper III

Paper III

Can proximate cue-based rules produce optimal behavioural responses in a complex environment?

William E. Butler, Christian Jørgensen, Anders F. Opdal, Nadia Fouzai, Guðrún Marteinsdóttir, and Øyvind Fiksen.

Manuscript.

Author contributions: All authors conceived the study idea. GM and ØF supervised the project. WB developed the IBM, ran all simulations, and performed all analyses. AO, CJ, NF, and ØF developed the optimality model. WB prepared the initial manuscript. All authors contributed to revisions.

Can proximate cue-based rules produce optimal behavioural responses in a complex environment?

W.E. Butler[1,2], C. Jørgensen[3], A.F. Opdal[3], N. Fouzai[3], G. Marteinsdottir[1], Ø. Fiksen[3]

[1]MARICE, Faculty of Life and Environmental Sciences, University of Iceland, Askja, Sturlugata 7, 101 Reykjavik, Iceland.

[2]Marine and Freshwater Research Institute, Skúlagata 4, 101 Reykjavík, Iceland.

[3]Department of Biology, University of Bergen, Thormøhlensgt 53, 5020 Bergen, Norway and the Hjort Centre for Marine Ecosystem Dynamics, Bergen, Norway.

Abstract

The success of organisms and the functioning of ecosystems depend much on the behaviour of individuals. To include adaptive behaviour into ecological models, a set of rules specifying individual responses to available information is required. How this is formulated can have major implications for the emergent system properties. Ideally, such rules would be evolutionarily consistent, reflecting the flexible nature of behaviours and preferably their dependence on individual state. They should be constrained by the individual's limited ability to sense and predict whilst containing enough information to perform well in a dynamic environment. Using optimal behaviour as a benchmark, we examined a variety of proximate rules that determine the risk-sensitive foraging behaviour of a fish in a spatially and temporally variable environment. We show that the rule is improved by sequentially incorporating multiple behavioural traits, proximate cues, and size-dependence. Whilst optimal behaviour was never fully achieved, with each step, key facets of the optimal strategy were approximated. By combining the interplay between proximate cues and ontogeny into a fitness-seeking objective, the rule serves as a useful template for models that include adaptive foraging in complex spatial gradients. This will make predictions from ecological models more reliable by integrating plastic responses into models of population dynamics, environmental change, and spatial distribution.

1. Introduction

Adaptive foraging is a prominent behavioural trait of many organisms. Such individual traits are drivers of higher levels of biological organisation, and important for community and ecosystem structure and functioning (Schmitz et al. 2008; Beckerman et al. 2010; Schmitz and Trussell 2016). To predict higher-level patterns from individual traits we need to understand how traits depend on individual condition and the environment (Heithaus et al. 2009; Rosenblatt and Schmitz 2014; Schmitz and Trussell 2016). From a modelling perspective, this requires explicit representation of the dynamic landscapes in which organisms reside, and how, at any given time and place, individuals utilise the information available to them as they make foraging decisions. Organisms experience multitudinous data streams simultaneously and may possess sophisticated cue integration methods that utilise subsets of this information to generate specific behaviours (Munoz and Blumstein 2012). Yet, to gain insights into potential behavioural responses to future (and potentially novel) environments, we need to understand how this wealth of information translate into behavioural responses via the cue-response system (Sih 2013; Robertson and Chalfoun 2016; Ehlman et al. 2019).

Individual- or agent-based models (hereafter referred to as IBMs) are well equipped to tackle this task (Grimm and Railsback 2005). They explicitly represent the individual, the level of organisation at which interactions occur (Huston et al. 1988) and the phenotype becomes visible to selective pressures. From detailed depictions of an individual's physiology and environmental heterogeneity, their respective constraints on behaviour can be accounted for. IBMs can handle both the ultimate fitness-perspective of optimised behaviours and the proximate mechanisms on which natural selection has operated (Grimm and Railsback 2005; Giske et al. 2013; Budaev et al. 2019). The decisions individuals make will not necessarily be optimal, but given a history of natural selection in similar environments, they should perform well (Todd and Gigerenzer 2007; McNamara and Houston 2009; Fawcett et al. 2013). Therefore, the challenge is to formulate rules in IBMs that distil an individual's local environment and internal state down to a few key components that reflect real organism's sensory and cognitive abilities, and to distinguish which strategies generate plasticity corresponding to that seen in nature.

Dynamic state-variable models (Mangel and Clark 1988; Houston and McNamara 1999) are frequently used in behavioural ecology to find an organism's optimal strategy — the strategy that maximises fitness in a stable environment. To achieve this, it is assumed the individual has foresight of future events and is free from phenotypic constraints other than those specifically imposed on the model (McNamara and Houston 2009). Given that environments are characterised by spatiotemporal gradients in variables directly and indirectly related to fitness (e.g. Staaterman et al. 2014; Gallagher et al. 2017; Kohl et al. 2018), these assumptions are unlikely to be met in nature. IBMs tackle adaptive behaviour from a different perspective; rather than finding the strategy that maximises fitness using dynamic programming, strategies can be implemented explicitly by a set of rules or found via a search heuristic that optimises a set of life-history and/or behavioural strategies (e.g. Huse et al. 1999). These approaches allow individuals to make decisions in dynamic landscapes where future conditions are uncertain because the proximate causes of behaviours are acknowledged. However, because expression of behaviours are constrained by the information incorporated (directly or indirectly) in the decision making module, its formulation can have drastic effects on a system's emergent properties (e.g. Railsback and Harvey 2002; Kristiansen et al. 2009; Kulakowska et al. 2009; Watkins and Rose 2013).

One way forward is to compare optimal and proximate strategies to reveal deficiencies in proximate, rule-based formulations and then improve the rules against a known, optimal benchmark strategy (Hutchinson and Gigerenzer 2005).

Here, we ask two questions: (1) How do simple rule-based algorithms for behaviour compare with evolutionary optimal strategies in environments with a diel cycle and a spatial gradient? (2) How can behavioural rules be formulated so that they retain simplicity and still capture adaptive phenotypic plasticity? To address these questions, we developed an IBM to simulate the early life-history of cod (*Gadus morhua*). The model serves as a counterpart to an existing state-dependent optimality model (Fiksen and Jørgensen 2011; Fouzai et al. 2019) with identical functions, sub-models, parameterisation, and environmental gradients. Differences arise in how behavioural responses and patterns are found: the IBM simulates phenotypically plastic behaviour using a myopic proximate rule that evaluates the trade-off between growth and mortality, whereas the optimal equivalent is determined using dynamic programming with no constraints on information, cognition, or rule complexity. Optimised behaviour therefore acts as an unattainable benchmark for a suite of simple, proximate rules (e.g. Sainmont et al. 2015). We incorporate multiple cues (from internal and external sources) into a single rule, allowing us to examine their relative importance through ontogeny. The resulting rule offers a general template of behavioural rules that capture adaptive foraging in complex environments.

2. Methods

The model description follows the ODD (Overview, Design concepts, Details) protocol (Grimm et al. 2006; Grimm et al. 2010). The model includes mechanistic subroutines for ingestion, growth, physiology, and predation which are detailed in previous publications (Fouzai et al. 2019 and references within). A brief overview of these subroutines is provided to illustrate the trade-offs associated with risk-sensitive foraging. A full description of each subroutine can be found in the online appendix B.

2.1. Purpose

Our objective with the IBM is to evaluate how various myopic proximate rules for risk-sensitive foraging behaviour compare to optimal behaviour in environmental gradients. We assess how adaptive phenotypic plasticity can be built into an IBM through foraging traits responding to internal and external foraging cues, including length-dependence in the cue-response system.

2.2. Entities, state variables, and scales

2.2.1. Individuals

The model simulates the early life-history of a larval cod from 5 mm to 15 mm. The individual is characterised by the following numerical attributes: body length L (mm), stomach fullness S (proportion), depth position z (m), hour of day h, hour of day at initialization h_0 (for statistical purposes), accrued probability of survival P, and accrued probability of survival per mm length interval P_L. In addition, each larva has a behavioural strategy vector consisting of four parameters which can be fixed or variable throughout ontogeny ($\beta_1 - \beta_4$). The complete attribute vector $A_{i,t}$ for an individual is:

$$A_{i,t} = \{L_{i,t}, S_{i,t}, z_{i,t}, P_{i,t}, P_{L,i,t}, h_i, h_{0,i}, \beta_{1,i,L}, \beta_{2,i,L}, \beta_{3,i,L}, \beta_{4,i,L}\}. \quad (1)$$

2.2.2. Environment

The individual resides in a 1-dimensional vertically stratified water column specified for a fixed day of the year at an hourly timestep. Gradients in temperature, prey, chlorophyll *a*, and optical attenuation coefficients are dependent on the mixed layer depth (30 m) and remain fixed in time (Fig. 1A). Hourly ambient light levels at each grid cell are computed from the exponential decay of surface irradiance with depth (and chlorophyll *a*) according to Beer's law (Fig. 1B). Predators are homogeneously distributed throughout the water column; however, the risk of predation varies with ambient light levels and larval state. This captures some of the key features of temperate marine ecosystems that are known to influence a larval fish's growth and mortality, such as the thermocline and spatiotemporal gradients in ambient light.

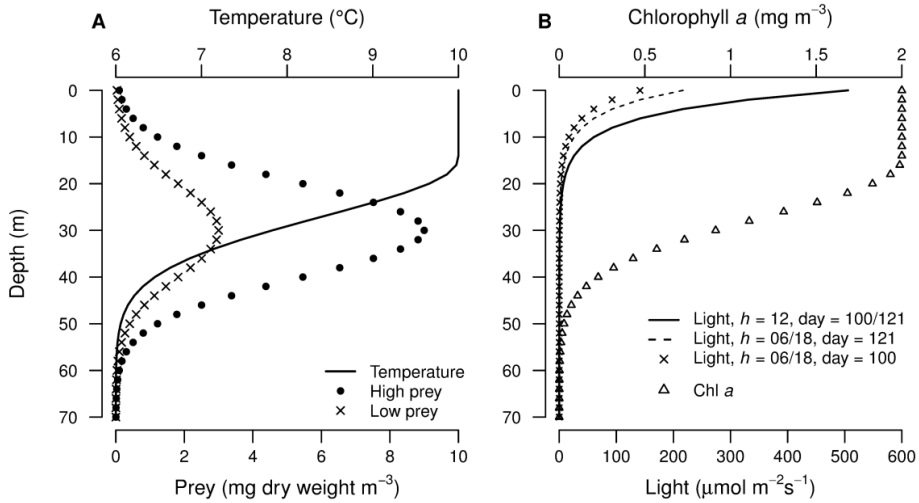

Figure 1*: Key environmental gradients for the model. Panel A shows the vertical gradients in temperature and prey density, including two scenarios for prey density. Panel B shows the vertical gradients in ambient light at midday (1200) and dawn/dusk (0600/1800) for two scenarios: an early date (day 100) and a late date (day 121), note that the vertical gradient in ambient light at midday is the same for both scenarios. The vertical gradient in chlorophyll a is also shown in panel B, this determines how light is attenuated down the water column.*

2.3. Process overview and scheduling

Upon setting the environment, individuals are released and required to make two decisions at each timestep: where to move and how actively to forage. To make these choices, ingestion and predation are computed for each potential combination of habitat and foraging activity. The individual subsequently determines the best behavioural choice using a myopic proximate rule, it executes the decision, the attribute vector is updated, and time moves forward one hour. The simulation continues until the larva reaches 15 mm, the simulation time exceeds 99 days, or the individual's weight drops below 0.003 mg (the larva dies in the two latter instances).

2.4. Design concepts

2.4.1. Basic principles

Adaptive foragers evaluate trade-offs between energetic gain and risk of dying before acting. Trade-off is a central concept in behavioural ecology (Houston et al. 1993; Werner and Anholt 1993; Railsback and Harvey 2013). For example, some diel vertical migrations (DVM) appear because periods around dusk and dawn provide an opportunity for individuals to both fulfil their energetic requirements and minimise their visibility to visual predators (Clark and Levy 1988). Maximizing the ratio between growth and mortality (or its alternative formulations) is an intuitive rule that has explained adaptive habitat selection in several contexts (e.g. Gilliam and Fraser 1987; Turner and Mittelbach 1990; Dahlgren and Eggleston 2000). However, as a decision-making rule in IBMs, the assumptions on which it was founded may be frequently violated, leading to irrational decision-making and emergent properties with little validity (Railsback et al. 1999).

The behavioural rules developed in this paper retain the intuitive, fitness-seeking appeal of Gilliam's rule but circumvents many of the problems associated with this rule outlined by Railsback et al. (1999). Firstly, we utilise the difference rather than the ratio ensuring that rational decisions are made when growth is negative or ingestion equals zero. Secondly, linearization of the trade-off allows incorporation of multiple proximate cues that collectively determine the marginal substitution rate of mortality for growth. This allows the individual to make foraging decisions based on local information from external and internal sources. We utilised cues from the individual's internal state and changes in light intensity, both of which are important cues for larval fish foraging behaviours (Munk 1995; Hurst et al. 2009; Vollset et al. 2013) and zooplankton in general (reviewed in Pearre 2003; Cohen and Forward 2009). By incorporating proximate cues into a fitness-seeking objective, the rule captures the essence of how organisms make foraging decisions in the wild (Nathan et al. 2008; Mueller and Fagan 2008; Munoz and Blumstein 2012). In doing so, it allows a quantitative appraisal (from an evolutionary standpoint) of how a diverse suite of proximate cues drive foraging behaviour, examination of how the cue-response system changes through ontogeny, and how individual differences in behavioural strategies shape emergent properties like growth and survival.

2.4.2. Sensing

The larva has a sensory zone within which it has complete knowledge of predation risk and foraging potential. The vertical range of this zone includes every grid cell within the larva's swimming range per timestep. This is defined using a maximum swimming speed of one body length (bl) per second, thus an individual's sensory range expands through ontogeny (from ± 18 m at 5 mm to ± 54 m at 15 mm). It is also assumed the individual is fully aware of its internal state and can perceive changes in light intensity.

2.4.3. Adaptive behavioural traits

The larva possesses two adaptive traits: habitat selection and foraging activity. The larva is a visual predator and is predated upon by larger visually hunting fish. Ambient light levels, which vary with hour of day and depth (Fig. 1B), therefore play a critical role in shaping the trade-off between ingestion and mortality. By changing depth, the larva can utilise the spatiotemporal light gradients to seek food (Fig. 2A) and hide from visual predators (Fig. 2B). As the larva grows, it is more easily detected by visual predators (Fig.

2B), its visual range increases (Aksnes and Utne 1997), and its sensory zone expands. This means it can scan a larger volume of water for prey within a timestep (Fig. 2A) and utilise a greater extent of habitat for foraging and refuge.

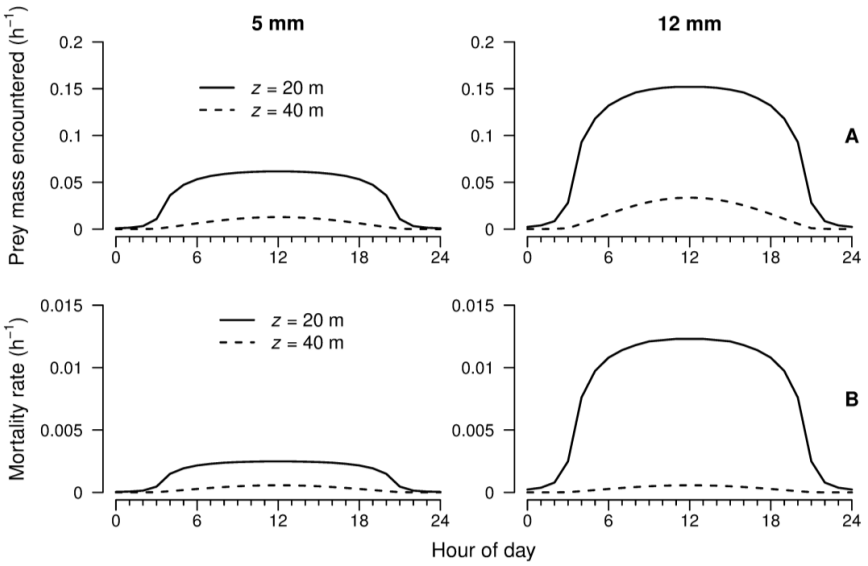

Figure 2*: The benefits and costs associated with the habitat selection behavioural trait. Row A shows the prey mass encountered (standardised by larval weight) at two depths (z) throughout the diel cycle. Row B shows the mortality rate from piscivores at two depths throughout the diel cycle. Both rates are presented for a small (5 mm) and a large larva (12 mm).*

The activity trait determines the individual's foraging speed a (bl s^{-1}) which has six possible values evenly distributed between zero and one. By increasing its foraging speed, the larva scans a larger volume of water and encounters both more prey items (Fig. 3A) and more invertebrate ambush predators (Fig. 3B; Bailey and Houde 1989, Fouzai et al 2019). As the larva grows, it can scan a larger volume of water for prey (Fig. 3A) and it develops improved escape abilities (Fuiman 1994) leading to a general decline in predation from invertebrate predators (Fig 3B; McGurk 1986; Bailey and Houde 1989). To allow the larva to forage whilst migrating or to forage at its current depth, overall activity levels take the maximum of foraging speed and migration velocity u (bl s^{-1}). The migration velocity takes values between zero and one, and is calculated with the following equation:

$$u = \frac{|z_{t+1} - z_t|}{1000L \cdot dt} \quad (2)$$

Here, the numerator is the distance displaced within a timestep and the denominator is the maximum distance that could be displaced within a timestep.

The individual can also optimise its bioenergetics (e.g. Sims et al. 2006) in two ways: (1) by migrating above and below the thermocline (Fig. 1A) to determine the temperature at which growth rates and routine metabolic costs are calculated, and (2) by controlling its overall activity level which contribute proportionally to metabolic costs.

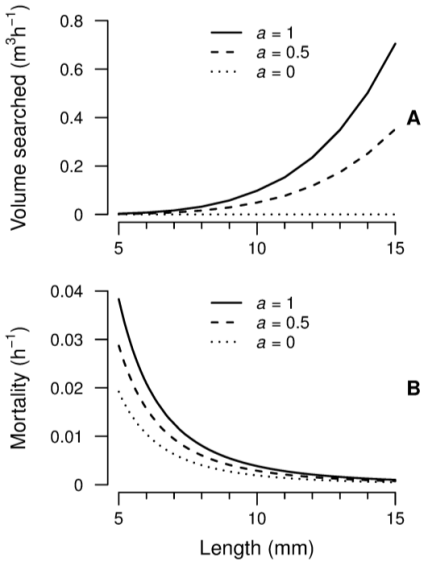

Figure 3*: The benefits and costs associated with the foraging activity behavioural trait. Responses throughout ontogeny are shown for three different activity levels (a) ranging from 0-1 bl per second. Panel A shows the volume of water scanned for prey items per timestep (z = 20 m and h = 12). Panel B shows the mortality rate from invertebrates per timestep (this does not vary with depth or hour).*

In summary, ingestion and mortality rates depend on the larva's behavioural choices at each timestep. Ingestion is a function of overall activity levels, depth, hour, and length. Note that the prey's energetic value is standardised across the larva's size range (see Fiksen and Jørgensen 2011). Total instantaneous mortality m (h^{-1}) is the sum of mortality from invertebrates m_i (s^{-1}) and visual feeding fish m_f (h^{-1}), and is a function of length, hour, overall activity levels and depth:

$$m(L,h,a,u,z) = m_f(L,h,z) + m_i(L,a,u). \quad (3)$$

2.4.4. Behavioural rules

As a baseline rule, we start with an individual that remains at a fixed depth throughout ontogeny but can adapt its foraging activity as a function of local ingestion and mortality rates:

$$a_i^* = max_a\left[F_{a,z^*} - m_{a,z^*}\right]. \quad (4)$$

Here, a is foraging activity (bl s^{-1}), F is weight-specific ingestion (h^{-1}) constrained by gut fullness (so if $S = 1$, $F = 0$ h^{-1}), m is total mortality rate (h^{-1}) and z is the fixed depth (m). In this rule, the individual i evaluates the trade-off for all potential activity levels at each timestep, and executes a decision based on the activity level a_i^* that maximises the trade-off. The fixed depth was determined by running the model at each grid cell and selecting the depth (z^*) that maximised fitness.

To improve upon this rule, we added a trait for habitat selection:

$$z_i^* = max_z\left[F_{z,a^*} - m_{z,a^*}\right]. \quad (5)$$

This allows the larva to seek food and safety by altering its vertical position in tandem with its activity level (Fig. 3). Starting at the shallowest depth, the model loops over all grid cells within the larva's sensory zone. An inner loop then evaluates the rule for all potential activity levels at each grid cell. This provides an approximation of fitness for each potential combination of *z* and *a*, and the larva selects the habitat z_i^* and activity level a_i^* that maximises the approximation of fitness.

Three proximate cues were added to equation 5 to examine how local information (from internal and external sources) may influence foraging behaviour. Collectively, these cues determine the marginal substitution rate of mortality for growth (θ) at each timestep (see Houston and McNamara 1999; Skalski and Gilliam 2002):

$$z_i^* = max_z\left[\theta_{i,L}F_{z,a^*} - m_{z,a^*}\right]. \quad (6)$$

This rule operates similarly to the previous rule (5) except the foraging rate is weighted by stimulation from cues (θ). The importance of ingestion may therefore increase or decrease depending on the forager's internal state and external environment. The cues are implemented in an additive manner and are described by four parameters:

$$\theta_{i,L} = \beta_{1,i,L} + \beta_{2,i,L}l + \beta_{3,i,L}(1 - S)^{\beta_{4,i,L}}. \quad (7)$$

Here, β_1 is a fixed value where stimulation equals the parameter's value (Fig. 4A). Independent of both physical state and the external environment, this term reflects the individual's inclination to accept risk. The parameter β_2 determines the strength of stimulation from the rate of change in light intensity l,

$$l = ln\left(\frac{E_{b_{t+1}}}{E_{b_{t-1}}}\right) \quad (8)$$

where E_b is the surface irradiance. In the model's light regime, maximum stimulation occurs at 03:00 and 21:00, whilst stimulation approaches zero at midday and midnight (Fig. 4B). Parameters β_3 and β_4 determine the strength of stimulation from the individual's stomach fullness (Fig. 4C). The slope of the exponential curve is determined by β_4, which increases from zero stimulation when the stomach is full to maximum stimulation when empty. With decreasing values of β_4, ingestion is stimulated at higher values of stomach fullness, and vice versa (see Kristiansen et al. 2009). A multiplier describing the importance of stimulation from the stomach is provided by β_3. With increasing values, stimulation from the stomach becomes more important, i.e., if β_3 is equal to two and the stomach is completely empty, stimulation arising from the stomach will equal two.

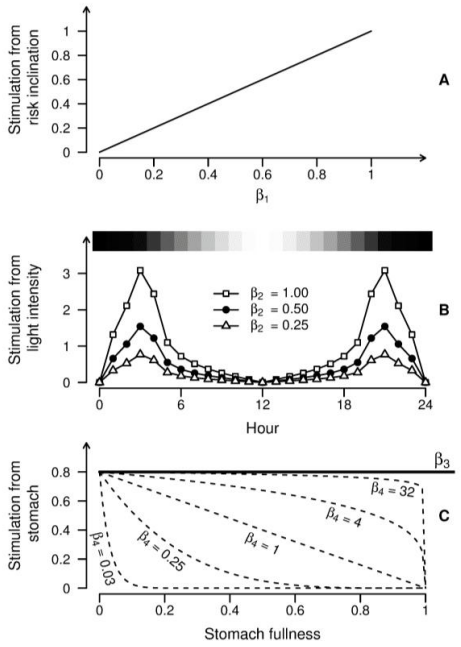

Figure 4*: The functional forms of the four parameters and how they contribute to the weighting of sources of information within the rule. The top panel (A) refers to stimulation from the larva's inclination to take risk (β_1). The middle panel (B) shows stimulation from the rate of change in light intensity and how this is modulated by β_2. The shaded bar at the top of the graph shows hourly surface irradiance, this ranges from approximately 0–500 µmol $m^{-2}s^{-1}$ at midnight and midday respectively. The bottom panel (C) shows stimulation derived from stomach fullness (β_3 and β_4). The slope of the stomach term is determined by β_4. If this equals 1, stimulation increases linearly as stomach fullness decreases; as β_4 increases, stimulation is achieved at progressively lower values of stomach fullness, and vice versa. A threshold determining the importance of stimulation from the stomach is supplied by β_3. In this example, if the stomach is completely empty, the maximum possible stimulation from the stomach will be attained (0.8).*

Taken together, this formulation combines a suite of proximate sensory information associated with DVM into an ultimate fitness-seeking objective. The individual finds the best possible behaviours solely using information that is presently available. Behavioural responses are innate (Mery and Burns 2010), guided by four traits (β_1–β_4) that determine how each cue is translated into a stimulus for spatial movement and activity. In this manner, the rule can be viewed as a lightweight version of the hedonic tones and neuronal responses used by Giske et al. (2003, 2013) and Andersen et al. (2016); whilst the multi-layered proximate architecture (Budaev et al. 2019) is not fully implemented, the basic essence of the information appraisal and response phases are captured.

2.4.5. State-dependent optimality model

A state-dependent optimality model (Fouzai et al. 2019) was run in identical environments to the rule-based IBMs. This model used dynamic programming to find the optimal depth z^* and activity a^* for each combination of the following state variables: stomach fullness (S, 11 states), body size (L, 10 states), hour of day (h, 24 hours) and vertical position (z, 35 grid cells). Once matrices of optimal depth and activity were obtained, the model simulated an individual larva from 5 mm to 15 mm, which gave a maximum baseline survival through the larval period for comparison with each proximate rule. The optimal larva was subjected to the same swimming constraints as the IBM larva (see sensing section).

2.4.6. Initialisation

For all models, individuals were initialised at 5 mm with a half-full stomach to provide adequate energy reserves for initial growth. Release depth was set to 10 m, and both survival measures were set to a value of one. A total of twenty-four larvae were released, one at each hour of the day to even out day-night cycles, particularly the bias in early-stage survival caused by the time of day at initialization (h_0).

2.4.7. Survival and fitness measures

Both survival measures (P and P_L) decreased exponentially according to the total mortality rate ($P_{t+1} = P_t \cdot e^{-m}$). An individual's fitness was defined as its survival at 15 mm.

2.4.8. Simulations

An extensive parameter search was conducted by releasing larvae with all possible permutations of strategies (each one fixed throughout the simulation) at the resolution defined in Table C1. If an individual died before reaching the target length (15 mm), survival (P and P_L) was set to zero for the current length interval and the larva was re-initialized at the next mm length interval using the following attributes: hour of day = h_0, z = 10 m, S = 0.5, P = 0 and P_L = 1. This approach allowed evaluation of all potential strategies throughout ontogeny (i.e. a strategy that performed very badly at 5 mm is still evaluated for subsequent length intervals). For each unique strategy vector, all emergent properties were averaged across the twenty-four larvae for each mm length interval.

2.4.9. Strategy evaluation

The parameter search enabled us to find the fitness-seeking parameters for rules containing any permutation of stimuli (from one to all three). For each rule, we considered two different larval behavioural resolutions: (1) with a fixed proximate (FP) strategy throughout ontogeny; (2) with a length-dependent proximate strategy (LdP) where parameter values can vary per mm length interval (Table 1). The best fixed strategy maximised fitness with a single parameter set. The best length-dependent strategy maximised fitness by maximizing P_L for each mm length interval. To evaluate the rules, the performance of each proximate strategy was defined by its survival per mm and fitness relative to the optimal behaviour's equivalent values.

Rule	Acronym	Equation	Trait	Strategy vector
Baseline	BL	$max_a[F_{a,z^*} - m_{a,z^*}].$	*a*	-
Ingestion - mortality	F-m	$max_z[F_{z,a^*} - m_{z,a^*}].$	*a*, *z*	-
Fixed proximate strategy	FP	$max_z[\theta_i F_{z,a^*} - m_{z,a^*}].$	*a*, *z*	$\{\beta_{1,i}, \beta_{2,i}, \beta_{3,i}, \beta_{4,i}\}.$
Length-dependent proximate strategy	LdP	$max_z[\theta_{i,L} F_{z,a^*} - m_{z,a^*}].$	*a*, *z*	$\{\beta_{1,i,L}, \beta_{2,i,L}, \beta_{3,i,L}, \beta_{4,i,L}\}$.

Table 1*: Description of the behavioural rules evaluated; a = activity levels, z = habitat selection, m = total mortality. In the equations, a star superscript denotes the optimum value for that trait.*

2.4.10. Sensitivity analysis

To test the robustness of strategies to environmental variation, we carried out a sensitivity analysis where the parameter search was conducted in different environmental contexts. The reference environment was simulated using high prey (HP) concentrations (9 mg dry weight m^{-3}) at a late date (LD, Day 121), hereafter referred to as the HP-LD scenario. Additional runs were performed using low prey (LP) concentrations (3 mg dry weight m^{-3}) at a late date (LP-LD), high prey concentrations at an earlier date (ED, Day 100) with a shorter day length and thus less time for foraging (HP-ED), and low prey concentrations at an early date (LP-ED). These environments provide harsher conditions that may require different behavioural strategies to perform well.

To identify whether environmental gradients constrained the ability of the IBM to capture optimal behaviour, we also tested three scenarios that simplified a single aspect of the reference scenario (Fig. 1): (1) a fixed temperature through depth; (2) a fixed prey concentration through depth; (3) a fixed background mortality from invertebrates through ontogeny. A detailed description of these tests and their results are presented in appendix A1.

3. Results

3.1. Adaptive phenotypic plasticity increases with rule complexity

The IBMs ability to produce emergent properties that resembled the optimal equivalents was greatly improved by including multiple foraging traits, proximate cues that stimulated foraging behaviours, and length-dependence in the cue-response system.

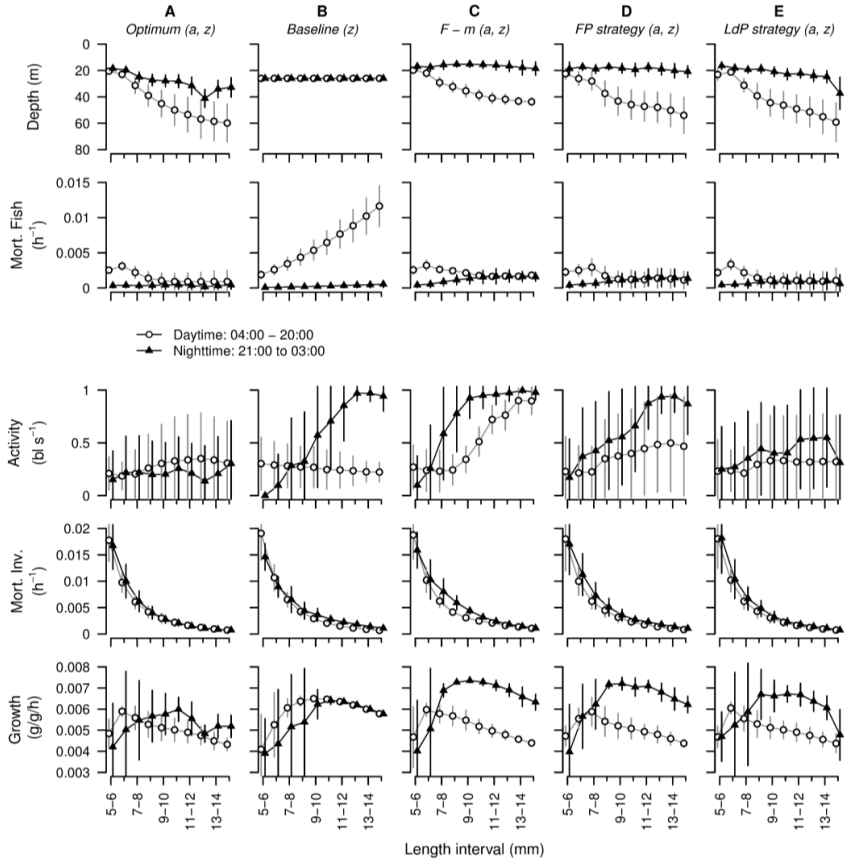

Figure 5*: Emergent properties for five behavioural strategies. Panel A shows the properties that resulted from the state-dependent optimality model, whilst panels B-E shows the properties that emerged from four proximate strategies that sequentially increase in complexity (from B to E): the baseline strategy that possesses a single trait for foraging activity (B); the F – m strategy that has a traits for foraging activity and habitat selection (C); the best fixed proximate (FP) strategy where stimulation from proximate cues is determined by a parameter set that remains fixed throughout ontogeny (D); the best length-dependent proximate (LdP) strategy where the parameter set can vary per mm length interval (E). Mean and standard deviations per mm (n = 24) were calculated for two time periods: daytime (04:00 to 20:00) and nighttime (21:00 to 03:00).*

The optimal behaviour consisted of a DVM and an ontogenetic vertical migration (OVM) with the larvae seeking progressively deeper habitat through ontogeny from 20 – 40 m in nighttime and 20 – 60 m in daytime (Fig. 5A). During daytime, the ability of the proximate strategies to capture optimal behaviour increased with increasing strategy

complexity (Table 2). The baseline larvae, which remained at 20 m through time, suffered an ontogenetic increase in visual predation because it formed a larger visual target as it grew but was unable to seek refuge at depth (Fig. 5B). The three strategies that contained a habitat selection trait substantially reduced the visual mortality rates by DVM and OVM. Despite this, the $F - m$ strategy selected depths consistently higher than optimal levels resulting in higher visual mortality rates throughout ontogeny (Fig. 5C). Introducing proximate cues led to depth profiles similar to optimal behaviour; however, the length-dependent strategy was closer to optimal behaviour earlier in ontogeny, notably by triggering deeper depth (and thus lower visual mortality rate) at 7 – 8 mm (Fig. 5D and Fig. 5E). Counterintuitively, the baseline strategy was most effective at capturing the optimal depth and visual predation rates at nighttime (Table 2). This was because it best approximated the mean optimal depth. The length-dependent strategy captured the gradual decline in depth through ontogeny, but its depth values were consistently higher (except for 14 – 15 mm) than optimal behaviour leading to consistently higher visual predation rates (Fig. 5B and 5E).

Variable	**Time**	**Proximate strategy**			
		Baseline	F – m	FP	LdP
z	D	22.57	10.72	5.20	2.91
m_f		6.09	0.76	0.42	0.16
z	N	6.94	13.64	11.58	8.23
m_f		0.19	1.01	0.82	0.45
a	D	0.09	0.32	0.10	0.03
m_i		0.53	0.44	0.17	0.18
a	N	0.50	0.62	0.49	0.23
m_i		0.95	1.17	0.81	0.62
g	D	1.22	0.20	0.16	0.08
g	N	0.68	1.37	1.24	0.86

***Table 2**: Root mean square deviation (RMSD) between the emergent properties of the optimal strategy and four proximate strategies that increase in complexity (from the baseline to the LdP strategy). The RMSD units are the same as the respective variables, although the values for mortality and growth rates were multiplied by 1000 for clarity. F = ingestion; m = mortality; FP = fixed proximate; LdP = length-dependent proximate; D = daytime, N = nighttime, z = depth, m_f = mortality from fish, m_i = mortality from invertebrates; a = activity levels, g = growth.*

Mean activity levels for the optimal larvae were consistently below 0.5 bl s^{-1} in both time periods (Fig. 5A). The length-dependent strategy produced the mean activity levels and invertebrate mortality rates that best resembled the optimal equivalents in both periods (Table 2). In daytime, the baseline, fixed and length-dependent strategies all produced fairly stable activity levels through ontogeny (Fig. 5B, 5D and 5E), although the baseline larvae's high activity levels at 5 – 6 mm led to higher invertebrate mortality rates (Fig. 5B). During nighttime, the baseline, $F - m$ and fixed strategies all produced large ontogenetic increases in activity levels (Fig. 5B, 5C and 5D) with larvae effectively foraging continuously at full speed when larger (shown by the smaller standard deviations). The length-dependent proximate strategy was the only one which produced a similar pattern to optimal behaviour, with mean activity levels (and thus invertebrate mortality rates) slightly higher than the optimum.

The length-dependent strategy most closely approximates the optimal mean growth in daytime, although all strategies with the habitat selection trait have similar growth patterns (Table 2 and Fig. 5A, 5C, 5D and 5E). This is due to lower temperatures at depth which the baseline larvae were not subjected too, thus maintaining higher growth rates from 7 mm onwards.

3.2. Ontogenetic decline in mortality constrains adaptive phenotypic plasticity

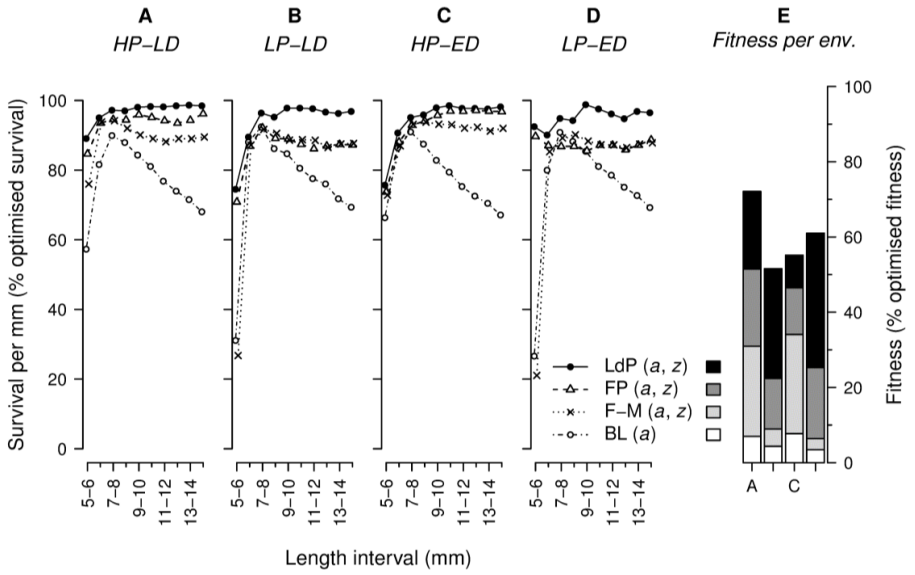

***Figure 6**: Mean survival per mm (n = 24) and fitness relative to optimised behaviour for various proximate strategies. Panel A shows results from the reference environment with high prey (HP) concentrations at a late date (LD). Results are also shown for the low prey – late date (column B), high prey – early date (column C), and low prey – early date (column D) environments. Column E shows fitness (survival at 15 mm) relative to optimised fitness for each environment. The following rules are shown: the baseline (BL), the ingestion – mortality (F – m), the fixed proximate (FP), and the length-dependent proximate (LdP) strategies (see Table 1).*

In the reference environment, the length-dependent strategy reached 72% of optimised fitness (Fig. 6A). All length intervals obtained > 95% with the exception of 5 – 6 mm which had a value of 89% (Fig. 6A). The trend for the length-dependent strategy to obtain relatively less fitness earlier in ontogeny was seen across environments (although to a lesser extent in the LP-ED environment, Fig. 6D). In each case this was due to the larvae foraging more actively than optimal which led to greater predation from invertebrates. So, despite maintaining higher-than-optimal growth rates from 5 – 7 mm, the costs of additional foraging activity always outweighed the benefits. This was clearly a constraint on the IBM's ability to capture optimal behaviour because in the fixed prey and fixed invertebrate mortality scenarios (where foraging is easier and less costly, respectively), values > 95% were seen in all environments from 5 – 7 mm (Fig. B1C and B1D) and resultant fitness was always higher than the reference scenario (Fig. B1E). In general, simplifying one of the environmental gradients always improved the ability of the L-D, fixed and F – m strategies to capture optimal behaviour (Fig. B1E). Of the three tested, the fixed temperature gradient did not appear to be as large a constraint to achieving optimal behaviour as the other gradients (see Appendix B1).

3.3. Developmental shifts in foraging behaviour from risk-prone to risk-averse

Incorporating length-dependence into the cue-response system substantially improved the performance of the proximate strategies (Fig. 6). An ontogenetic shift in the behaviour of individuals was seen with small larvae foraging continually in the surface waters and large larvae undertaking large vertical migrations and foraging more sporadically. Underlying this shift in foraging behaviour was a shift in the proximate cues that stimulated foraging. For small larvae, foraging was stimulated continually by the risk inclination trait and small drops in stomach fullness, whilst for large larvae, foraging was stimulated by changes in light intensity and a near empty stomach (Fig. B2).

A single shift from risk-prone to risk-averse behaviour was far more important than any of the pre- or proceeding changes in the parameter set per mm length interval. We found the best length-dependent strategy that only changed the parameter set ($\beta_1 - \beta_4$) once through ontogeny. This contrasted with the fully length-dependent strategy that changed its parameter set at each mm length interval (9 times). The best single shift in strategy occurred at either 7 mm or 8 mm and captured between 44% and 71% of the optimised fitness difference between the fixed proximate and fully length-dependent strategies (Table 3). In each environment, the shift was characterised by a substantial reduction in the risk inclination trait (from 0.8 – 1.6 pre-shift to 0.0 – 0.1 post-shift).

Environment	LdP strategy	pLdP strategy	FP strategy	Length of OS (mm)
HP-LD	72	66	51	7
LP-LD	51	36	21	7
HP-ED	55	51	46	7
LP-ED	61	41	25	8

***Table 3**: Fitness relative to optimised behaviour (%) of different proximate strategies. Results are shown for the fully length-dependent strategy (LdP) that could change its strategy vector at each mm length interval; the partially length-dependent strategy (pLdP) that could change its strategy vector once through ontogeny; the fixed proximate strategy (FP) that could not change its strategy vector. The final column shows the length at which the ontogenetic shift in strategy occurred for the partially length-dependent strategy, OS = ontogenetic shift, HP = high prey, LD = late date, LP = low prey, ED = early date.*

3.4. Stomach fullness is the most important proximate cue

The best proximate strategy in each environment contained stimulation from all cues; however, the cues varied in their relative importance (Fig. 7). In a strategy based on a single cue, stimulation from the stomach was clearly the most important. On average, this strategy performed approximately 13% and 18% better than the single risk inclination and light intensity strategies respectively. Furthermore, in all environments it captured a greater percent of optimised fitness than the strategy containing both risk inclination and light (Fig. 7). Complementing stomach fullness with light intensity gave the best strategy based on two cues. This was 5% below the full strategy in the LP-ED environment and within 1% in all other environments. These patterns were broadly consistent across all the scenarios tested. In only one scenario (Fixed prey, HP-ED) was stomach fullness not the most important stimuli (light intensity was) whereas stomach fullness + light intensity was always the best two-cue strategy.

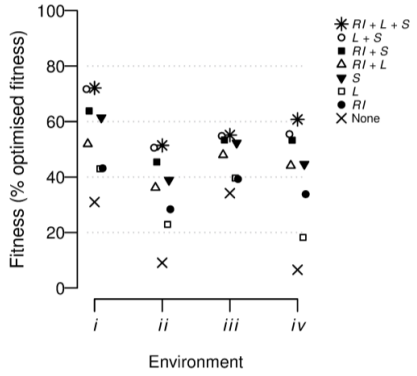

Figure 7*: Fitness (relative to optimised behaviour) for length-dependent proximate strategies that represent each possible combination of foraging cues. Results are presented for the high prey – late date (i), low prey – late date (ii), high prey – early date (iii) and low prey – early date (iv) environments.*

4. Discussion

4.1. How well do proximate rules capture optimal behaviour?

The best proximate rule was successful in capturing the general behavioural patterns of the optimality model. However, small-scale differences in emergent behaviours throughout ontogeny led to fitness values < 82% of optimised fitness. In all the environments tested, the largest contribution to this deficit was earlier in ontogeny (5 – 7 mm) when the individuals were unable to modulate activity levels to the same degree as the optimal larva. The high mortality rates early in ontogeny are a strong selective pressure to grow fast in order to reap the benefits of reduced mortality at larger sizes (Werner and Gilliam 1984; Biro et al. 2005; Jørgensen et al. 2013). The optimal larvae knew this by looking into the future and achieved it by foraging in short, punctuated bursts. The IBM larvae did not have any foresight and tried to grow too fast by foraged continuously which led to elevated mortality from invertebrates. The low performance early in ontogeny may indicate missing proximate information in the rule or simply that the optimality assumption is too optimistic. The sensitivity analyses showed that the decline in mortality with size was a major constraint on the rule's ability to mimic optimal behaviour earlier in ontogeny (Appendix B1). Assuming a constant background mortality rate produced similar deviations in activity levels from the optimal benchmark; however, these deviations were penalised far less meaning it captured a greater portion of optimised fitness.

Gilliam's rule works well in constant environments but are less reliable rules of life in variable or seasonal settings (Sainmont et al. 2015). No environments are constant, and even the day-night cycling seems to reduce its fitness relative to the optimal strategy. There are many ways to trade growth and mortality in an equation, and we explored variants of Gilliam's rule and found that the F – m formulation is most effective in terms of fitness (Appendix A1). With weight-specific ingestion (F) as a trade-off component the larva fills its stomach before dawn (Kristiansen et al. 2009). The downside of using F is that the individual ignores both metabolic costs and temperature from the decision-making process. To incorporate these elements, the individual requires predictive abilities or a rule that includes additional cues (e.g., Goss-Custard and Stillman 2008; Kulakowska et al. 2013). For the G – m strategy to avoid negative growth rates (or to growth optimally), growth rates would need to be calculated over the entire period that feeding is food limited. Railsback et al. (2005) circumvented this problem by utilizing memory of the last diel-cycle's attribute vector as a basis for predicting the attribute vector in the forthcoming diel cycles.

Is there a robust behavioural rule that performs well under variable environmental conditions? The assumption of a priori knowledge required for dynamic optimisation models is incompatible with many ecological questions in dynamic spatially explicit environments. For instance, IBMs of larval fish and plankton are often embedded in large-scale ocean circulation models, with a need to define behavioural traits and responses. For an individual to succeed in such environments, the rule needs to include the mechanisms that have evolved across the range of environments experienced by its ancestors. Without these attributes, the rule will not reflect the behavioural plasticities seen in nature (Topping et al. 2015). Our sensitivity analysis included plausible conditions a larva would experience rather than entirely novel ones. However, transplanting the best length-dependent strategy from a specific environment to a new one (e.g. simulating the best high

prey – late date strategy in the low prey – late date environment) led to a substantial reduction in its capacity to capture the new environment's optimal behaviour (Fig. A2). This suggests that the length-dependent strategies were overfitting their respective environments. We found the proximate strategy that performed best across all environments. This was the second-best performing strategy in each environment and probably a better reflection of a strategy that could evolve in variable environments through natural selection.

4.2. How can adaptive phenotypic plasticity be specified whilst retaining simplicity?

There are many ways to build proximate cues for animal behaviour into IBMs. For instance, using a series of sequential boolean rules, where thresholds on causal factors determine the appropriate action(s) to be taken (e.g. Rinke and Petzoldt 2008; Semeniuk et al. 2012) or by evolving reaction norms that define the behavioural action in response to stimuli (e.g., Quinones et al. 2016). The rules developed in this study lie somewhere between these two approaches; they have a mechanistic and evolutionary side due to the parameter optimisation (fitness-seeking) module, but the rules are predefined instead of evolving through simulations. An individual's strategy specifies exactly how each cue modulates the ultimate goals of energetic gain and survival, and its performance is evaluated in terms of a fitness proxy. This avoids any arbitrariness in setting thresholds on stimuli or the use of any top-down behavioural controls. By incorporating the proximate cues directly into the fitness-seeking objective, the system's emergent properties can be understood in terms of how individuals respond to a variety of sensory information. Thus, rules constructed in this manner can facilitate dialogue with empirical studies by testing and generating hypotheses regarding the composition and relative strength of cues for behavioural plasticity in complex environments (Miner et al. 2005).

Many IBMs use genetic algorithms to search for optimal solutions. These can train artificial neural networks (e.g. Huse et al. 1999; Strand et al. 2002; Morales et al. 2005), or evolve norms of reaction (e.g., Giske et al. 2013; Quinones et al. 2016) or strategy vectors that provides life history and behavioural strategies (e.g. Huse et al. 2018). One of the primary reasons for the use of artificial life techniques in IBMs is that simple "rules of thumb" may exclude the mechanisms underlying observed behaviours (Seth et al. 2007; Mueller et al. 2011). A genetic algorithm could be used to evolve strategies that contain discrete norms of reaction for each proximate cue (e.g., one for food, light, gut content, and predators). Rules would then emerge from the (fitness maximizing) interactions between individual's and the environment (Morales et al. 2005; Mueller et al. 2011). This approach may provide a more thorough exploration of the parameter space, potentially highlighting stimuli interactions that were not possible due to the explicit rule's formulation. However, as the larva evaluates multiple grid cells within a timestep, the norms of reaction need a link between the stimuli and the habitat grid cell. This may involve a utility measure (e.g. Bandara et al. 2019) or an evolvable parameter that describes, for instance, the amplitude of migration (e.g. Huse et al. 2018). This eliminates optimisation, but not a relationship between the stimuli and vertical movement. The optimisation module used in this paper provides a simple, computationally efficient method of implementing adaptive behaviour into complex ecosystem models. However, prior to this step, validation against empirical data is required to ensure the formulation is representative of behaviours in the nature.

Although the IBM is designed to capture the early life-history of a temperate larval fish, the behavioural rule itself can easily be tailored to specific systems (Grimm 1999). Stimulation from cues is captured in the variable θ, which can comprise any number of cues (irrespective of sensory mode) from both internal and external sources. Ultimately, the composition of cues should be knowledge-based, guided by the empirical sciences (Singer et al. 2016). For example, turbulence or ultraviolet radiation, as opposed to light intensity, may be the dominant cue for DVM (Miller and Morgan 2013; Fischer et al. 2015). Furthermore, multiple cues may operate in an additive (e.g. Amo et al. 2004) or synergistic (e.g. Schmidt and Persson 2006) fashion. The former mode will not reproduce realistic behaviours if non-linearities are involved (Soluk 1993) but does serve as an essential null model against which alternative cue integration methods should be tested (Soluk 1993; Schmidt and Persson 2006).

4.3. Which cues contain information that improves fitness the most?

Basing decisions solely on perceived predation risk and ingestion potential (the $F - m$ rule) was insufficient to achieve optimal behaviour. The rule led to a progressive increase in foraging activity through ontogeny. This was because the predation cost of activity declined with size, but ingestion potential remained constant. Thus, the difference between trade-off components increased through ontogeny and more active foraging was favoured. Essentially the costs of activity were valued less as the larvae grew (see also Railsback et al. 1999), but this makes little sense from an evolutionary perspective. Taking foraging risks is adaptive when mortality rates are high (small larvae), whilst when mortality rates are low (large larvae), foraging more cautiously is adaptive (Werner and Gilliam 1984; Biro et al. 2005; Jørgensen et al. 2013). The problem originates from the lack of information about ontogeny and timing. For instance, if a large larva's stomach is partially full at midday, the $F - m$ rule may lead to risky behaviour just because the individual can potentially ingest more food. In contrast, the optimal decision in such circumstances tend to minimise the risk of dying at the expense of gut content. This disparity arises because the optimal larva knows the fitness consequences of each alternative foraging option (Houston and McNamara 1999), but the larva obeying the $F - m$ rule can only approximate these consequences. Introducing additional proximate cues provided the missing information so that the individual was able to make decisions more similar to the optimal one (i.e. sacrificing state for safety). Technically, this was achieved when F was scaled to a value close to or equal to zero by stimulation from light intensity and/or gut fullness. In this manner, the proximate cues serve to reduce uncertainty in future conditions by telling the larva to forage only when famished or environmental conditions are favourable, which is more consistent with how individuals move and forage in the real world (Mueller and Fagan 2008; Nathan et al. 2008; Schmidt et al. 2010; Munoz and Blumstein 2012).

In this study, the individual's gut content and risk inclination encapsulate its internal state. The former component was the most important cue, confirming that condition, whether gut content or a more holistic measure including the costs associated with metabolic expenditure, is an essential consideration for foragers (Mangel and Clark 1986; Higginson et al. 2018). The importance of gut fullness as a foraging cue for larval fish has been demonstrated in numerous empirical studies (e.g. Munk 1995; Vollset et al. 2013). The risk inclination trait could be removed from the rule without any substantial drop in performance across environments (Fig. 7). However, it is also a cue that requires little sensing and information processing such that it could easily evolve through natural

selection to control the response to different environments, as suggested by the best length-dependent strategies.

Light is an important structuring force in marine ecosystems (Aksnes et al. 2017) and for larval fish assemblages (Lough and Potter 1993). The prevalence of foraging schedules across natural environments that are in some way synchronised with, or entrained to, optical gradients makes changes in light intensity or spectral composition (e.g. Walmsley et al. 2015) obvious candidates for indirect foraging cues. These cues provide reliable information to the individual that enables it to approximate the 'antipredation windows' (Ferrari et al. 2008) that the optimal strategies would 'know' through the benefit of foresight (Clark and Levy 1988; Fiksen and Jørgensen 2011). We used the rate of change in light intensity which is widely regarded as a key cue for DVM in invertebrates and fish (Cohen and Forward 2009; Ringelberg 2010; Mehner 2012). However, different hypotheses exist regarding the functional form of light as a cue for DVMs (reviewed in Cohen and Forward 2009), and these different functional forms may serve different ultimate goals (Ringelberg and Van Gool 2003). Simulating alternative formulations of the light cue would provide useful predictions regarding the initiation, amplitude, and cessation of DVMs that could be tested with empirical data from the field or controlled laboratory experiments.

4.4. Which traits should a rule specify?

By letting the decision-making process specify two traits, the individual has a more diverse set of alternative actions from which to choose. Accounting for such interactions, as demonstrated in this study, can lead to vastly different estimates of emergent properties. We also simulated the optimal and length-dependent strategies without the activity trait, meaning the individuals had to migrate to forage. Without the activity trait, the length-dependent strategy captured a smaller percent of optimised fitness (Fig. A3), suggesting that the number of adaptive traits is not a constraint on the IBMs ability to capture optimal behaviour. Adaptive phenotypic plasticity will often involve the expression of multiple traits and the resulting phenotypes may be contingent upon one another or highly correlated (Ghalambor et al. 2007; David et al. 2014). For example, opportunities to feed and to shelter rarely overlap; a change of habitat is often required to carry out one action or the other (Railsback et al. 2005).

Ontogeny is important in models of the cue-response system. For many organisms, rapid morphological and physiological development occurs through ontogeny which can generate gradients in foraging abilities, metabolic demands, and vulnerability to stressors (both abiotic and biotic). Assuming these constraints and pressures have honed behavioural strategies that best balance the conflicting demands of growth and survival along these gradients (Werner and Gilliam 1984), an explicit behavioural rule ought to reflect such strategies to capture the ontogeny of behaviours seen in nature (Skalski and Gilliam 2002; Kristiansen et al. 2009). For larval fish, the development of notochord flexion can lead to shifts in vertical movement from little to no movement in the preflexion stage to regular DVMs in the postflexion stage (Hurst et al. 2009; Hernandez et al. 2009; Smart et al. 2013).

We accounted for length-dependence by allowing an individual's strategy vector to vary in a discreet manner (per mm length interval). Whilst this approach does not allow plasticity in the timing of behavioural shift's (i.e. it is hardcoded into the strategy vector), it does provide a tractable explanation for such shifts in terms of the cue-response system (Fig.

B2). In this case, the shifts in the strategy vector allowed the larva to forage in a continual manner when constrained to the surface and a vigilant manner when it could make use of depth as a refuge by sacrificing state and using light as a cue for emergence/sheltering. The results are consistent with the risk-allocation hypothesis (Lima and Bednekoff 1999; Ferrari et al. 2008, 2009): as the temporal variation in risk increases with body size (due to higher visibility), a vigilant strategy is favoured at a particular length and is exercised by selectively sacrificing state when risk is highest (e.g. Houston et al. 1993; Kotler et al. 2010) and foraging only when risk is low or state is precariously low. The timing of the shift in the cue-response system was context-dependent (Table 3), so another approach would be to incorporate trait(s) that describe when shifts in response to various cues are made. Viewing ontogenetic shifts as an adaptive trait is likely to be an important feature of multitrophic models where the shifts' timing may depend on, for example, the prevailing predation regime (Urban 2007).

5. Conclusion

In this study, we presented behavioural rules that captures the interplay between proximate cues and ontogeny in a single fitness-seeking objective. In doing so, the rule offers a simple template for any model seeking to capture adaptive foraging in complex spatial gradients (McNamara and Houston 2009). The myopic nature of the rule means it is computationally efficient and thus easily embedded within, or coupled to, complex spatiotemporal models to examine trait-mediated interactions. The rule's formulation retains the intuitive appeal of Gilliam's rule (Gilliam and Fraser 1987) but circumvents problems identified with this rule by allowing the organism to use local information from both internal and external sources to modulate the trade-off between growth and mortality. The flexibility of the rule's construction allows multiple cues from multiple sources (both internal and external, direct and indirect) to be integrated in a manner that can capture the complexities involved in individual foraging (or moving) decisions (Nathan et al. 2008; Mueller and Fagan 2008; Munoz and Blumstein 2012).

Acknowledgements

This study is a product of the Nordic Centre for Research on Marine Ecosystems and Resources under Climate Change (NorMER), which is funded by the Norden Top-Level Research Initiative sub-programme 'Effect Studies and Adaptation to Climate Change'.

References

Aksnes, D.L., Røstad, A., Kaartvedt, S., Martinez, U., Duarte, C.M., Irigoien, X., 2017. Light penetration structures the deep acoustic scattering layers in the global ocean. Sci. Adv. 3, 1–6. https://doi.org/10.1126/sciadv.1602468

Aksnes, D.L., Utne, A.C.W., 1997. A revised model of visual range in fish. Sarsia 82, 137–147. https://doi.org/10.1080/00364827.1997.10413647

Amo, L., López, P., Martín, J., 2004. Wall lizards combine chemical and visual cues of ambush snake predators to avoid overestimating risk inside refuges. Anim. Behav. 67, 647–653. https://doi.org/10.1016/j.anbehav.2003.08.005

Andersen, B.S., Jørgensen, C., Eliassen, S., Giske, J., 2016. The proximate architecture for decision-making in fish. Fish Fish. 17, 680–695. https://doi.org/10.1111/faf.12139

Bailey, K.M., Houde, E.D., 1989. Predation on eggs and larvae of marine fishes and the recruitment problem, in: Advances in Marine Biology. Elsevier, pp. 1–83.

Bandara, K., Varpe, Ø., Ji, R., Eiane, K., 2019. Artificial evolution of behavioral and life history strategies of high-latitude copepods in response to bottom-up and top-down selection pressures. Prog. Oceanogr. 173, 134–164. https://doi.org/10.1016/j.pocean.2019.02.006

Beckerman, A., Petchey, O.L., Morin, P.J., 2010. Adaptive foragers and community ecology: Linking individuals to communities and ecosystems. Funct. Ecol. 24, 1–6. https://doi.org/10.1111/j.1365-2435.2009.01673.x

Biro, P.A., Post, J.R., Abrahams, M. V., 2005. Ontogeny of energy allocation reveals selective pressure promoting risk-taking behaviour in young fish cohorts. Proc. R. Soc. B Biol. Sci. 272, 1443–1448. https://doi.org/10.1098/rspb.2005.3096

Budaev, S., Jørgensen, C., Mangel, M., Eliassen, S., Giske, J., 2019. Decision-Making From the Animal Perspective: Bridging Ecology and Subjective Cognition. Front. Ecol. Evol. 7, 1–14. https://doi.org/10.3389/fevo.2019.00164

Clark, C.W., Levy, D.A., 1988. Diel Vertical Migrations by Juvenile Sockeye Salmon and the Antipredation Window. Am. Nat. 131, 271–290. https://doi.org/10.1126/science.26.678.918

Cohen, J.H., Forward Jr, R.B., 2009. Zooplankton diel vertical migration: a review of proximate control. Oceanogr. Mar. Biol. An Annu. Rev. 47.

Dahlgren, C.P., Eggleston, D.B., 2000. Ecological Processes Underlying Ontogenetic Habitat Shifts in a Coral Reef. Ecology 81, 2227–2240.

David, M., Salignon, M., Perrot-Minnot, M.J., 2014. Shaping the antipredator strategy: Flexibility, consistency, and behavioral correlations under varying predation threat. Behav. Ecol. 25, 1148–1156. https://doi.org/10.1093/beheco/aru101

Ehlman, S.M., Trimmer, P.C., Sih, A., 2019. Prey responses to exotic predators: Effects of old risks and new cues. Am. Nat. 193, 575–587. https://doi.org/10.1086/702252

Fawcett, T.W., Hamblin, S., Giraldeau, L.A., 2013. Exposing the behavioral gambit: The evolution of learning and decision rules. Behav. Ecol. 24, 2–11. https://doi.org/10.1093/beheco/ars085

Ferrari, M.C.O., Rive, A.C., MacNaughton, C.J., Brown, G.E., Chivers, D.P., 2008. Fixed vs. random temporal predictability of predation risk: An extension of the risk allocation hypothesis. Ethology 114, 238–244. https://doi.org/10.1111/j.1439-0310.2007.01468.x

Ferrari, M.C.O., Sih, A., Chivers, D.P., 2009. The paradox of risk allocation: a review and prospectus. Anim. Behav. 78, 579–585. https://doi.org/10.1016/j.anbehav.2009.05.034

Fiksen, Ø., Jørgensen, C., 2011. Model of optimal behaviour in fish larvae predicts that food availability determines survival, but not growth. Mar. Ecol. Prog. Ser. 432, 207–219. https://doi.org/10.3354/meps09148

Fischer, J.M., Olson, M.H., Theodore, N., Williamson, C.E., Rose, K.C., Hwang, J., 2015. Diel vertical migration of copepods in mountain lakes: The changing role of

ultraviolet radiation across a transparency gradient. Limnol. Oceanogr. 60, 252–262. https://doi.org/10.1002/lno.10019

Fouzai, N., Opdal, A.F., Jørgensen, C., Fiksen, Ø., 2019. Dying from the lesser of three evils: facilitation and non-consumptive effects emerge in a model with multiple predators. Oikos 128, 1307–1317. https://doi.org/10.1111/oik.05631

Fuiman, L.A., 1994. The interplay of ontogeny and scaling in the interactions of fish larvae and their predators. J. Fish Biol. 45, 55–79.

Gallagher, A.J., Creel, S., Wilson, R.P., Cooke, S.J., 2017. Energy Landscapes and the Landscape of Fear. Trends Ecol. Evol. 32, 88–96. https://doi.org/10.1016/j.tree.2016.10.010

Ghalambor, C.K., McKay, J.K., Carroll, S.P., Reznick, D.N., 2007. Adaptive versus non-adaptive phenotypic plasticity and the potential for contemporary adaptation in new environments. Funct. Ecol. 21, 394–407. https://doi.org/10.1111/j.1365-2435.2007.01283.x

Gilliam, J.F., Fraser, D.F., 1987. Habitat selection under predation hazard: test of a model with foraging minnows. Ecology 68, 1856–1862.

Giske, J., Eliassen, S., Fiksen, Ø., Jakobsen, P.J., Aksnes, D.L., Jørgensen, C., Mangel, M., 2013. Effects of the emotion system on adaptive behavior. Am. Nat. 182, 689–703. https://doi.org/10.1086/673533

Giske, J., Mangel, M., Jakobsen, P., Huse, G., Wilcox, C., Strand, E., 2003. Explicit trade-off rules in proximate adaptive agents. Evol. Ecol. Res. 5, 835–865.

GOSS-CUSTARD, J.D., Stillman, R.A., 2008. Individual-based models and the management of shorebird populations. Nat. Resour. Model. 21, 3–71.

Grimm, V., 1999. Ten years of individual-based modelling in ecology: What have we learned and what could we learn in the future? Ecol. Modell. 115, 129–148. https://doi.org/10.1016/S0304-3800(98)00188-4

Grimm, V., Berger, U., Bastiansen, F., Eliassen, S., Ginot, V., Giske, J., Goss-Custard, J., Grand, T., Heinz, S.K., Huse, G., Huth, A., Jepsen, J.U., Jørgensen, C., Mooij, W.M., Müller, B., Pe'er, G., Piou, C., Railsback, S.F., Robbins, A.M., Robbins, M.M., Rossmanith, E., Rüger, N., Strand, E., Souissi, S., Stillman, R.A., Vabø, R., Visser, U., DeAngelis, D.L., 2006. A standard protocol for describing individual-based and agent-based models. Ecol. Modell. 198, 115–126. https://doi.org/10.1016/j.ecolmodel.2006.04.023

Grimm, V., Berger, U., DeAngelis, D.L., Polhill, J.G., Giske, J., Railsback, S.F., 2010. The ODD protocol: A review and first update. Ecol. Modell. 221, 2760–2768. https://doi.org/10.1016/j.ecolmodel.2010.08.019

Grimm, V., Railsback, S.F., 2005. Individual-based modeling and ecology. Princeton university press.

Heithaus, M.R., Wirsing, A.J., Burkholder, D., Thomson, J., Dill, L.M., 2009. Towards a predictive framework for predator risk effects: The interaction of landscape features and prey escape tactics. J. Anim. Ecol. 78, 556–562. https://doi.org/10.1111/j.1365-2656.2008.01512.x

Hernandez, F.J., Hare, J.A., Fey, D.P., 2009. Evaluating diel, ontogenetic and environmental effects on larval fish vertical distribution using generalized additive models for location, scale and shape. Fish. Oceanogr. 18, 224–236. https://doi.org/10.1111/j.1365-2419.2009.00508.x

Higginson, A.D., Fawcett, T.W., Houston, A.I., McNamara, J.M., 2018. Trust your gut: Using physiological states as a source of information is almost as effective as optimal bayesian learning. Proc. R. Soc. B Biol. Sci. 285. https://doi.org/10.1098/rspb.2017.2411

Houston, A.I., McNamara, J.M., Hutchinson, J.M.C., 1993. General results concerning the trade-off between gaining energy and avoiding predation. Philos. Trans. R. Soc. B Biol. Sci. 341, 375–397.

Houston, A.I., McNamara, J.M., others, 1999. Models of adaptive behaviour: an approach based on state. Cambridge University Press.

Hurst, T.P., Cooper, D.W., Scheingross, J.S., Seale, E.M., Laurel, B.J., Spencer, M.L., 2009. Effects of ontogeny, temperature, and light on vertical movements of larval pacific cod (Gadus macrocephalus). Fish. Oceanogr. 18, 301–311. https://doi.org/10.1111/j.1365-2419.2009.00512.x

Huse, G., Melle, W., Skogen, M.D., Hjøllo, S.S., Svendsen, E., Budgell, W.P., 2018. Modeling emergent life histories of copepods. Front. Ecol. Evol. 6, 23.

Huse, G., Strand, E., Giske, J., 1999. Implementing behaviour in individual-based models using neural networks and genetic algorithms. Evol. Ecol. 13, 469–483. https://doi.org/10.1023/A:1006746727151

Huston, M., DeAngelis, D., Post, W., 1988. New computer models unify ecological theory. Bioscience 38, 682–691.

Hutchinson, J.M.C., Gigerenzer, G., 2005. Simple heuristics and rules of thumb: Where psychologists and behavioural biologists might meet. Behav. Processes 69, 97–124. https://doi.org/10.1016/j.beproc.2005.02.019

Jørgensen, C., Opdal, A.F., Fiksen, Ø., 2014. Can behavioural ecology unite hypotheses for fish recruitment? ICES J. Mar. Sci. 71, 909–917. https://doi.org/10.1093/icesjms/fst083

Kohl, M.T., Stahler, D.R., Metz, M.C., Forester, J.D., Kauffman, M.J., Varley, N., White, P.J., Smith, D.W., MacNulty, D.R., 2018. Diel predator activity drives a dynamic landscape of fear. Ecol. Monogr. 88, 638–652. https://doi.org/10.1002/ecm.1313

Kotler, B.P., Brown, J., Mukherjee, S., Berger-Tal, O., Bouskila, A., 2010. Moonlight avoidance in gerbils reveals a sophisticated interplay among time allocation, vigilance and state-dependent foraging. Proc. R. Soc. B Biol. Sci. 277, 1469–1474. https://doi.org/10.1098/rspb.2009.2036

Kristiansen, T., Jørgensen, C., Lough, R.G., Vikebø, F., Fiksen, Ø., 2009. Modeling rule-based behavior: Habitat selection and the growth-survival trade-off in larval cod. Behav. Ecol. 20, 490–500. https://doi.org/10.1093/beheco/arp023

Kułakowska, K.A., Kułakowski, T.M., Inglis, I.R., Smith, G.C., Haynes, P.J., Prosser, P., Thorbek, P., Sibly, R.M., 2014. Using an individual-based model to select among alternative foraging strategies of woodpigeons: Data support a memory-based model

with a flocking mechanism. Ecol. Modell. 280, 89–101. https://doi.org/10.1016/j.ecolmodel.2013.09.019

Lima, S.L., Bednekoff, P.A., 1999. Temporal variation in danger drives antipredator behavior: The predation risk allocation hypothesis. Am. Nat. 153, 649–659. https://doi.org/10.1086/303202

Lough, R.G., Potter, D.C., 1993. Vertical distribution patterns and diel migrations of larval and juvenile haddock Melanogrammus aeglefinus and Atlantic cod Gadus morhua on Georges Bank. Fish. Bull. 91, 281–303.

Mangel, M., Clark, C.W., others, 1988. Dynamic modeling in behavioral ecology. Princeton University Press.

McGurk, M.D., 1986. Natural mortality of marine pelagic fish eggs and larvae: role of spatial patchiness. Mar. Ecol. Prog. Ser. 34, 227–242.

McNamara, J.M., Houston, A.I., 2009. Integrating function and mechanism. Trends Ecol. Evol. 24, 670–675. https://doi.org/10.1016/j.tree.2009.05.011

Mehner, T., 2012. Diel vertical migration of freshwater fishes - proximate triggers, ultimate causes and research perspectives. Freshw. Biol. 57, 1342–1359. https://doi.org/10.1111/j.1365-2427.2012.02811.x

Mery, F., Burns, J.G., 2010. Behavioural plasticity: An interaction between evolution and experience. Evol. Ecol. 24, 571–583. https://doi.org/10.1007/s10682-009-9336-y

Miller, S.H., Morgan, S.G., 2013. Interspecific differences in depth preference: Regulation of larval transport in an upwelling system. Mar. Ecol. Prog. Ser. 476, 301–306. https://doi.org/10.3354/meps10150

Miner, B.G., Sultan, S.E., Morgan, S.G., Padilla, D.K., Relyea, R.A., 2005. Ecological consequences of phenotypic plasticity. Trends Ecol. Evol. 20, 685–692. https://doi.org/10.1016/j.tree.2005.08.002

Morales, J.M., Fortin, D., Frair, J.L., Merrill, E.H., 2005. Adaptive models for large herbivore movements in heterogeneous landscapes. Landsc. Ecol. 20, 301–316. https://doi.org/10.1007/s10980-005-0061-9

Mueller, T., Fagan, W.F., 2008. Search and navigation in dynamic environments behaviors to population distributions - from individual behaviors to population distributions. Oikos 117, 654–664. https://doi.org/10.1111/j.2008.0030-1299.16291.x

Mueller, T., Fagan, W.F., Grimm, V., 2011. Integrating individual search and navigation behaviors in mechanistic movement models. Theor. Ecol. 4, 341–355. https://doi.org/10.1007/s12080-010-0081-1

Munk, P., 1995. Foraging behaviour of larval cod (Gadus morhua) influenced by prey density and hunger. Mar. Biol. 122, 205–212.

Munoz, N.E., Blumstein, D.T., 2012. Multisensory perception in uncertain environments. Behav. Ecol. 23, 457–462. https://doi.org/10.1093/beheco/arr220

Nathan, R., Getz, W.M., Revilla, E., Holyoak, M., Kadmon, R., Saltz, D., Smouse, P.E., 2008. A movement ecology paradigm for unifying organismal movement research. Proc. Natl. Acad. Sci. U. S. A. 105, 19052–19059.

Pearre, S., 2003. Eat and run? The hunger/satiation hypothesis in vertical migration: History, evidence and consequences. Biol. Rev. 78, 1–79. https://doi.org/10.1017/S146479310200595X

Quiñones, A.E., van Doorn, G.S., Pen, I., Weissing, F.J., Taborsky, M., 2016. Negotiation and appeasement can be more effective drivers of sociality than kin selection. Philos. Trans. R. Soc. B Biol. Sci. 371, 20150089.

Railsback, S.F., Harvey, B.C., 2013. Trait-mediated trophic interactions: Is foraging theory keeping up? Trends Ecol. Evol. 28, 119–125. https://doi.org/10.1016/j.tree.2012.08.023

Railsback, S.F., Harvey, B.C., 2002. Analysis of habitat-selection rules using an individual-based model. Ecology 83, 1817–1830. https://doi.org/10.1890/0012-9658(2002)083[1817:aohsru]2.0.co;2

Railsback, S.F., Harvey, B.C., Hayse, J.W., LaGory, K.E., 2005. Tests of theory for diel variation in salmonid feeding activity and habitat use. Ecology 86, 947–959. https://doi.org/10.1890/04-1178

Railsback, S.F., Lamberson, R.H., Harvey, B.C., Duffy, W.E., 1999. Movement rules for individual-based models of stream fish. Ecol. Modell. 123, 73–89. https://doi.org/10.1016/S0304-3800(99)00124-6

Ringelberg, J., 2010. Diel Vertical Migration in Lakes, in: Diel Vertical Migration of Zooplankton in Lakes and Oceans. Springer, pp. 171–215.

Ringelberg, J., Van Gool, E., 2003. On the combined analysis of proximate and ultimate aspects in diel vertical migration (DVM) research. Hydrobiologia 491, 85–90. https://doi.org/10.1023/A:1024407021957

Rinke, K., Petzoldt, T., 2008. Individual-based simulation of diel vertical migration of Daphnia: A synthesis of proximate and ultimate factors. Limnologica 38, 269–285. https://doi.org/10.1016/j.limno.2008.05.006

Robertson, B.A., Chalfoun, A.D., 2016. Evolutionary traps as keys to understanding behavioral maladapation. Curr. Opin. Behav. Sci. 12, 12–17. https://doi.org/10.1016/j.cobeha.2016.08.007

Rosenblatt, A.E., Schmitz, O.J., 2014. Interactive effects of multiple climate change variables on trophic interactions: a meta-analysis. Clim. Chang. Responses 1, 1–10. https://doi.org/10.1186/s40665-014-0008-y

Sainmont, J., Andersen, K.H., Thygesen, U.H., Fiksen, Ø., Visser, A.W., 2015. An effective algorithm for approximating adaptive behavior in seasonal environments. Ecol. Modell. 311, 20–30. https://doi.org/10.1016/j.ecolmodel.2015.04.016

Schmidt, K.A., Persson, L., 2006. Non-Additivity among Multiple Cues of Predation Risk: A Behaviorally-Driven Trophic Cascade between Owls and Songbirds. Oikos 113, 82–90.

Schmitz, O.J., Grabowski, J.H., Peckarsky, B.L., Preisser, E.L., Trussell, G.C., Vonesh, J.R., 2008. From Individuals to Ecosystem Function: Toward an Integration of Evolutionary and Ecosystem Ecology. Ecology 89, 2436–2445.

Schmitz, O.J., Trussell, G.C., 2016. Multiple stressors, state-dependence and predation

risk — foraging trade-offs: toward a modern concept of trait-mediated indirect effects in communities and ecosystems. Curr. Opin. Behav. Sci. 12, 6–11. https://doi.org/10.1016/j.cobeha.2016.08.003

Semeniuk, C.A.D., Musiani, M., Hebblewhite, M., Grindal, S., Marceau, D.J., 2012. Incorporating behavioral-ecological strategies in pattern-oriented modeling of caribou habitat use in a highly industrialized landscape. Ecol. Modell. 243, 18–32. https://doi.org/10.1016/j.ecolmodel.2012.06.004

Seth, A.K., 2007. The ecology of action selection: Insights from artificial life. Philos. Trans. R. Soc. B Biol. Sci. 362, 1545–1558. https://doi.org/10.1098/rstb.2007.2052

Sih, A., 2013. Understanding variation in behavioural responses to human-induced rapid environmental change: A conceptual overview. Anim. Behav. 85, 1077–1088. https://doi.org/10.1016/j.anbehav.2013.02.017

Sims, D.W., Wearmouth, V.J., Southall, E.J., Hill, J.M., Moore, P., Rawlinson, K., Hutchinson, N., Budd, G.C., Righton, D., Metcalfe, J.D., Nash, J.P., Morritt, D., 2006. Hunt warm, rest cool: Bioenergetic strategy underlying diel vertical migration of a benthic shark. J. Anim. Ecol. 75, 176–190. https://doi.org/10.1111/j.1365-2656.2005.01033.x

Singer, A., Johst, K., Banitz, T., Fowler, M.S., Groeneveld, J., Gutiérrez, A.G., Hartig, F., Krug, R.M., Liess, M., Matlack, G., Meyer, K.M., Pe'er, G., Radchuk, V., Voinopol-Sassu, A.J., Travis, J.M.J., 2016. Community dynamics under environmental change: How can next generation mechanistic models improve projections of species distributions? Ecol. Modell. 326, 63–74. https://doi.org/10.1016/j.ecolmodel.2015.11.007

Skalski, G.T., Gilliam, J.F., 2002. Feeding under predation hazard: Testing models of adaptive behavior with stream fish. Am. Nat. 160, 158–172. https://doi.org/10.1086/341012

Smart, T.I., Siddon, E.C., Duffy-Anderson, J.T., 2013. Vertical distributions of the early life stages of walleye pollock (Theragra chalcogramma) in the Southeastern Bering Sea. Deep. Res. Part II Top. Stud. Oceanogr. 94, 201–210. https://doi.org/10.1016/j.dsr2.2013.03.030

Soluk, D.A., 1993. Multiple Predator Effects: Predicting Combined Functional Response of Stream Fish and Invertebrate Predators. Ecology 74.

Staaterman, E., Paris, C.B., DeFerrari, H.A., Mann, D.A., Rice, A.N., D'Alessandro, E.K., 2014. Celestial patterns in marine soundscapes. Mar. Ecol. Prog. Ser. 508, 17–32. https://doi.org/10.3354/meps10911

Strand, E., Huse, G., Giske, J., 2002. Artificial evolution of life history and behavior. Am. Nat. 159, 624–644. https://doi.org/10.1086/339997

Todd, P.M., Gigerenzer, G., 2007. Environments that make us smart: Ecological rationality. Curr. Dir. Psychol. Sci. 16, 167–171. https://doi.org/10.1111/j.1467-8721.2007.00497.x

Topping, C.J., Alrøe, H.F., Farrell, K.N., Grimm, V., 2015. Per aspera ad astra: Through complex population modeling to predictive theory. Am. Nat. 186, 669–674. https://doi.org/10.1086/683181

Turner, A.M., Mittelbach, G.G., 1990. Predator Avoidance and Community Structure : Interactions among Piscivores. Ecology 71, 2241–2254.

Urban, M.C., 2007. The Growth-Predation Risk Trade-Off under a Growing Gape-Limited Predation Threat. Ecology 88, 2587–2597.

Vollset, K.W., Catalán, I.A., Fiksen, Ø., Folkvord, A., 2013. Effect of food deprivation on distribution of larval and early juvenile cod in experimental vertical temperature and light gradients. Mar. Ecol. Prog. Ser. 475, 191–201. https://doi.org/10.3354/meps10129

Walmsley, L., Hanna, L., Mouland, J., Martial, F., West, A., Smedley, A.R., Bechtold, D.A., Webb, A.R., Lucas, R.J., Brown, T.M., 2015. Colour As a Signal for Entraining the Mammalian Circadian Clock. PLoS Biol. 13, 1–20. https://doi.org/10.1371/journal.pbio.1002127

Watkins, K.S., Rose, K.A., 2013. Evaluating the performance of individual-based animal movement models in novel environments. Ecol. Modell. 250, 214–234. https://doi.org/10.1016/j.ecolmodel.2012.11.011

Werner, E.E., Anholt, B.R., 1993. Ecological consequences of the trade-off between growth and mortality rates mediated by foraging activity. Am. Nat. 142, 242–272.

Werner, E.E., Gilliam, J.F., 1984. The ontogenetic niche and species interaction in size-structured populations. Annu. Rev. Ecol. Syst. 15, 393–425.

Supplementary materials for:

Can proximate cue-based rules produce optimal behavioural responses in a complex environment?

W.E. Butler, C. Jørgensen, A.F. Opdal, N. Fouzai, G. Marteinsdottir, Ø. Fiksen

Appendix A: Additional analyses

- A1: The difference between ingestion and mortality performs better than the ratio
- A2: How well do the best proximate rules perform in different environments?
- A3: Including multiple traits improves the performance of proximate rules

Appendix B: Supplementary analyses and graphs

- B1: Proximate rules and environmental complexity
- B2: Which proximate cues underly the ontogenetic shift in behaviour? (Graph only).

Appendix C: Description of model subroutines

Appendix A: Additional analyses

A1: The difference between ingestion and mortality performs better than the ratio

There are lots of ways to balance growth (G) and mortality (m) in a fitness-seeking rule. We contrasted four rules, two that used growth as the benefit and two that used weight-specific ingestion (F) as the benefit. For each benefit, we simulated a rule that maximised the difference against mortality (e.g. F – m) and a rule that maximised the ratio (e.g. F/m).

The F – m rule consistently performed better across environments (Fig. A1E). In two environments, the F/m performed better later in ontogeny; however, differences between the two rules were negligible (Fig. A1A, A1B). The main difference between the F – m and F/m rules was in the activity levels at night-time. In all environments, the F/m foraged at full speed (1.00 bl s^{-1}) throughout ontogeny leading to high mortality rates from invertebrates. The F – m produced negligible activity levels (similar to optimal behaviour) early in ontogeny but foraged at full speed later in ontogeny (unlike optimal behaviour). This demonstrates that when F approaches zero, utilising the difference produces emergent properties that more closely resemble the optimal, but only earlier in ontogeny.

The motivation for using weight-specific ingestion as a trade-off component was to encourage the larva to fill its stomach prior to the period when feeding becomes light limited. This was illustrated by comparing the G – m and F – m rules. Firstly, the F – m rule captured a larger portion of optimised survival per mm and fitness across environments (Fig. A1). Secondly, this was because the F – m larvae had consistently positive growth rates at night-time (mean = 0.003 g/g/h), whilst the G – m larvae had consistently negative growth rates (mean = -0.002 g/g/h). Thus, maximising immediate growth did not necessarily lead to a full stomach at dusk, whereas maximising ingestion did. This was the main difference between the two strategies and was a trend seen across all environments, only in the low prey – late date scenario from 10 –15 mm did the G – m rule produce positive growth rates.

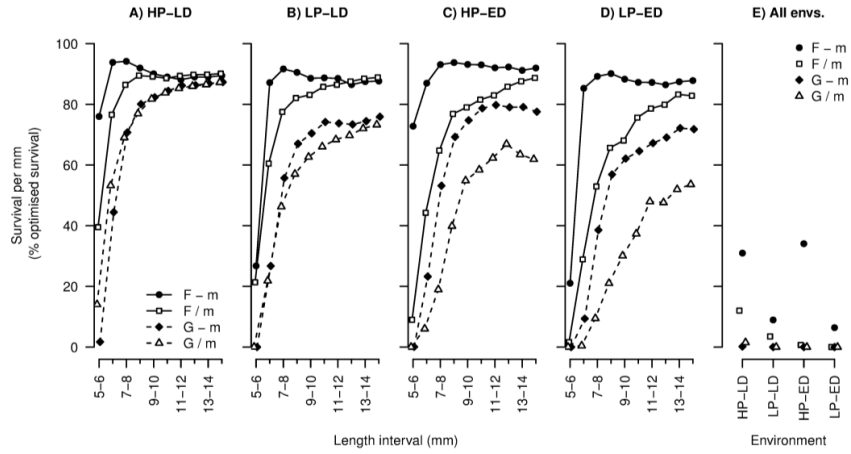

Figure A1*: Mean survival per mm (n = 24) relative to optimised behaviour for various formulations of the trade-off between growth and mortality. Each rule selects the behavioural decision(s) that maximises either the difference or the ratio between the benefit (growth [G] or weight-specific ingestion [F]) and the cost (mortality [m]). Results are presented for four environments (panels A-D) that contain either high prey (HP) or low prey (LP) concentrations and*

occur on an early date (ED) or a late date (LD). Column E shows fitness (survival at 15 mm) relative to optimised fitness.

A2: How well do the best proximate rules perform in different environments?

Dynamic optimisation models require static environments and presume organisms can foresee future events. These assumptions are incompatible with many ecological questions in dynamic spatially explicit environments. We performed a virtual transplant experiment to see how the best length-dependent strategies in each environment performed in different conditions. Four environments were considered: high prey – late date (HP-LD), low prey – late date (LP-LD), high prey – early date (HP-ED), and low prey – early date (LP-ED). We found the single strategy that performed best across all environments, referred to as the best generic strategy. To find this strategy we ranked all potential strategy vectors by their fitness in each specific environment, summed the ranks across environments for each unique strategy vector, and found the strategy that maximised the summed rank.

The best generic strategy was the second-best performing strategy in each environment, capturing between 10% (LP-LD) and 17% (HP-LD) less optimised fitness than the best environment-specific strategies (Fig. A2). This confirms that a general strategy that performs well across environments can be attained, but the sensitivity analysis also emphasises the need for careful consideration of environmental context when deriving such a strategy. The scenarios tested all represented plausible conditions a larva likely would experience as opposed to entirely novel ones, so adaptive rather than maladaptive phenotypic plasticity would be expected. Yet, neither of the HP strategies performed well in the LP environments, capturing < 10% optimised fitness (Fig. A2). This was because stimulation to forage from strategies evolved at high prey conditions was insufficient to maintain positive growth in LP conditions. Conversely, the high stimulation arising from the LP strategies led to increased mortality (from overzealous activity levels) but not reduced growth in the HP scenarios. These results highlight that the best proximate strategies were overfitting their respective environments, the inevitable result of which is a loss of predictive power in new environments.

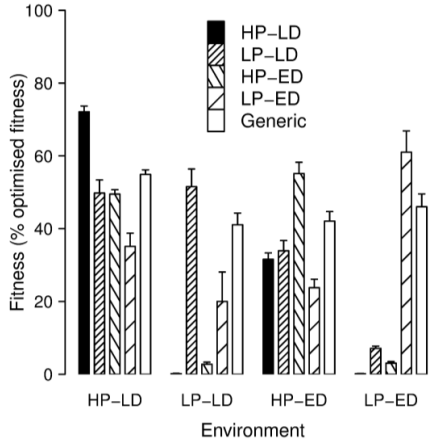

Figure A2*: Fitness (relative to optimised behaviour) of the best length-dependent proximate strategy from each environment when they are run in the alternative environments. The x-axis represents the environment (HP = high prey; LP = low prey; LD = late date; ED = early date) and each shaded bar represents the environment-specific strategy. For example, the black bar is*

the best length-dependent strategy in the HP-LD environment (i.e., it has the highest fitness). The generic strategy (white bar) represents the length-dependent strategy that performed best across all environments.

A3: Including multiple traits improves the performance of proximate rules

The number of foraging traits included in the proximate rule did not constrain its ability to capture optimal behaviour. To gauge the importance of the activity trait, we tested a variety of rules that included either both traits (habitat selection and foraging activity) or just habitat selection. When the activity trait was dropped, it meant that the larvae could only forage by migrating. Dropping the activity trait led to a decrease in the percent of optimised fitness captured by 5% – 13% in all environments (Fig. A3, black vs grey bars). This highlights the importance of allowing the larva to de-couple foraging activity and habitat selection. The improvements seen by using both traits were perhaps a foregone conclusion given that the state-dependent model optimised both these traits. However, dropping the activity trait from the optimal model did not make it any easier for the equivalent length-dependent proximate strategy to capture optimal fitness (Fig. A3, white bar). In 3 out of 4 environments, optimal behaviour was better captured when it emerged from both traits (Fig. A3).

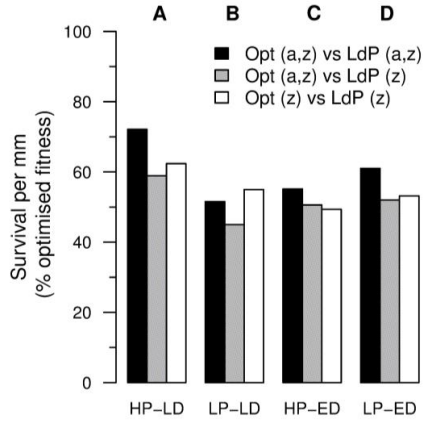

Figure A3*: Fitness (relative to optimised behaviour) for different combinations of adaptive traits in the optimal (Opt) and length-dependent proximate strategies (LdP), the traits that are present are shown in the brackets (a = activity levels, z = habitat selection). Results are shown for the following environments: high prey – late date (A), low prey – late date (B), high prey – early date (C), and low prey – early date (D).*

Appendix B: Supplementary analyses and graphs

B1: Proximate rules and environmental complexity

In each environment, we tested three scenarios, each of which simplified one aspect of the reference scenario (Fig. 1 in main article). The aim was to identify whether environmental gradients constrained the IBM's ability to capture optimal behaviour. In the first scenario, the temperature gradient was fixed through depth at 8°C – the temperature at the mixed layer. In the second scenario, the prey concentration was fixed through depth at the prey maximum (3 or 9 mg d-w m^{-3} depending on whether the environment was high or low prey). In the third scenario, the background decline in morality through ontogeny (from invertebrates) was held constant in time at 0.01 h^{-1}.

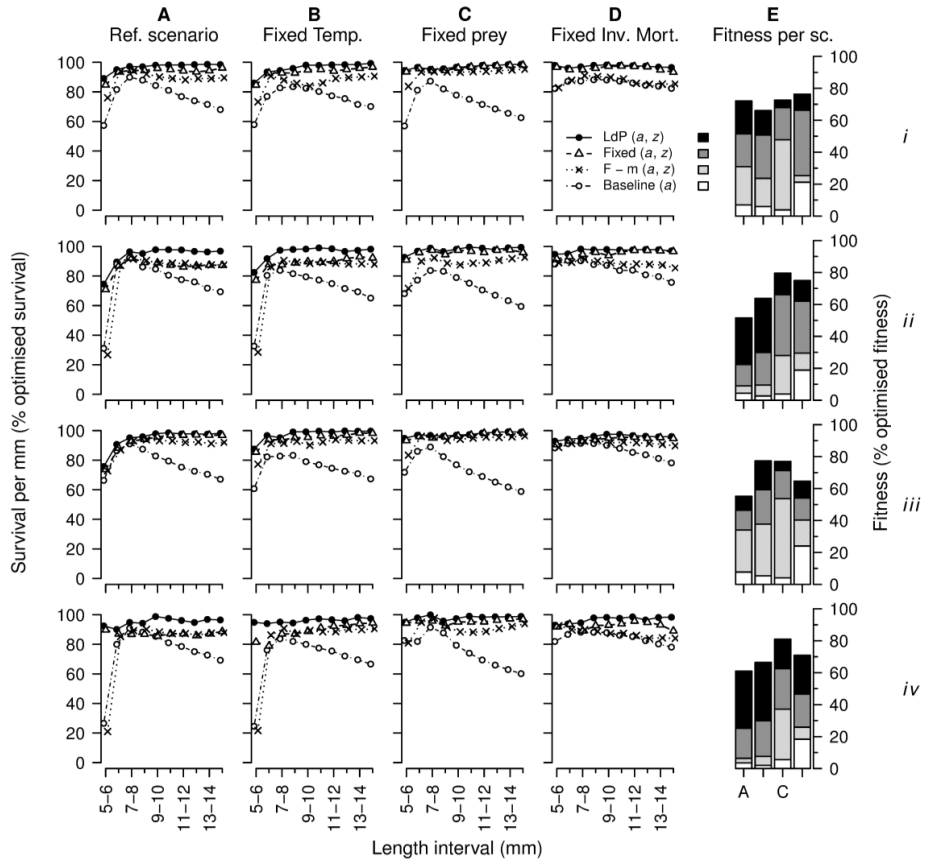

Figure B1: *Mean survival per mm (n = 24) and fitness relative to optimized behaviour for various proximate strategies. Panel A shows results from the reference scenario with vertical gradients in temperature and prey, and a size-dependent decline in invertebrate mortality. Additional scenarios which simplified the following gradients to a constant value are shown: temperature (B), prey (C), and invertebrate mortality rate (D). Column E shows fitness (survival at 15 mm) relative to optimized fitness for each scenario. The following rules are shown: the baseline (BL), the F – m, the fixed proximate (FP), and the length-dependent proximate (LdP) strategies. Results are shown for the high prey-late date (i), low prey-late date (ii), high prey-early date (iii), and low prey-early date (iv) environments.*

In general, simplifying one of the environmental gradients always improved the ability of the length-dependent, fixed and F – m proximate strategies to capture optimal behaviour (Fig. B1E). Although fitness improved in 3 out of 4 environments, the temperature gradient did not appear to be as large a constraint to achieving optimal behaviour as the other gradients (when considering the best proximate rule). For instance, the trend of lower survival earlier in ontogeny was still visible in all environments except the LP-ED one (Fig. 6Biv). The lesser importance of the temperature gradient is also exemplified by the baseline and F – m strategies at 5 – 6 mm in the LP environments (Fig. B1Bii and B1Biv). The percent of optimised survival is < 40% in the reference and fixed temperature scenarios, but substantially improved in the fixed prey and fixed invertebrate mortality scenarios (Fig. B1C and B1D). Removing the size-dependent costs of activity and the depth-dependent prey concentrations considerably improved the IBM's ability to capture optimised survival per mm, particularly in the 5 – 7 mm length interval (Fig. B1C, B1D).

B2: Which proximate cues underly the ontogenetic shift in behaviour?

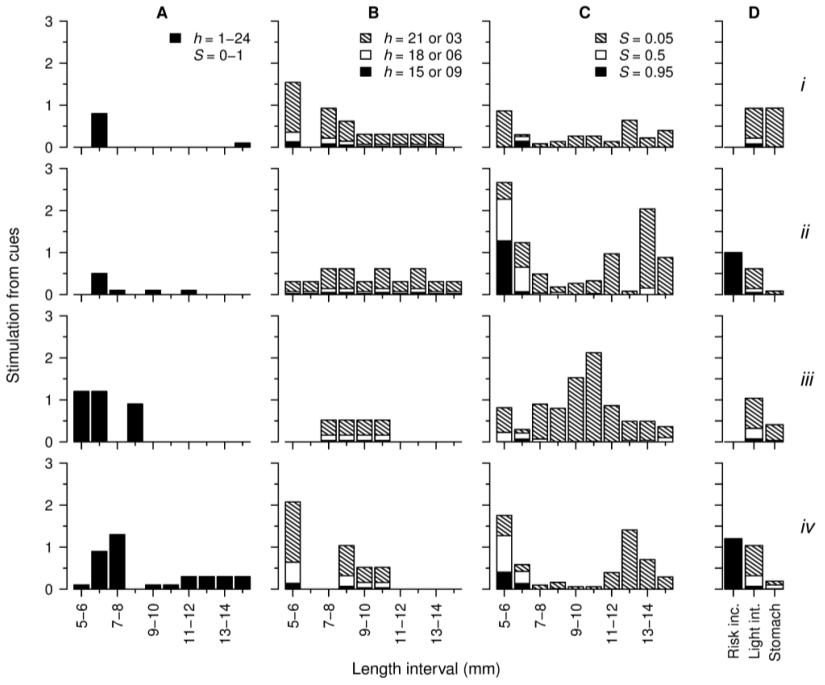

Figure B2*: How the three proximate cues modulate the trade-off between ingestion and mortality. The best length-dependent strategies are shown in columns A-C. Column A shows stimulation from the risk inclination trait ("Rick inc."), column B shows stimulation from the light intensity trait ("Light Int."), column C shows stimulation from stomach fullness. Stimulation from all three cues is shown for the best ontogenetically fixed strategy in column D. For each strategy, bars are stacked in a way to show how each cue contributes to overall stimulation at particular hours of the day h and states of stomach fullness S. Results are shown for the high prey-late date (i), low prey-late date (ii), high prey-early date (iii), and low prey-early date (iv) environments.*

Appendix C: Model subroutines

Light

Hourly surface irradiance E_s is computed using the model by Skartveit and Olseth (1988). Subsequently, the ambient level of light at each grid cell E_b at each hour is determined by the exponential decay of E_s according to the Beer-Lambert law:

$$E_b = E_s \mathrm{e}^{(-Kz)} \tag{C1}$$

where K is the diffuse attenuation coefficient derived from Wozniak et al. (2003) for wavelengths equal to 550 nm:

$$K = 0.0567 + \mathrm{chla}(0.0506 \exp(-0.606\mathrm{chla}) + 0.0285) + 0.068. \tag{C2}$$

The beam attenuation coefficient c is a function of chlorophyll (chla) concentration and is calculated with the following equation (Voss 1992; Mobley et al. 1994):

$$c = 0.0657 + (0.39\mathrm{Chla}^{0.57})(1.563 - 0.001149 \cdot 550). \tag{C3}$$

Ingestion

The larva is assumed to be a cruising predator whose ability to capture and ingest prey depends on its visual faculties and the properties of light in the water column. Firstly, the larva's visual range R_l (m) is estimated using the model by Aknes and Utne (1997):

$$R_l^2 = k_l A_l e^{-cR_l} \frac{E_b(z,h)}{K_e + E_b(z,h)}. \tag{C4}$$

Prey items are assumed to be cylindrical with an area A_l (mm^2) 0.05 times the predator's length and with a uniform inherent contrast against the background. The product of this contrast and the larva's visual capacity (its ability to process radiance) is denoted by k_l, which is calculated assuming the larva's visual range R_l is always 1 body length for a 0.015 mm^2 naupilar prey image area under non-limiting light conditions (Fiksen and MacKenzie 2002; Fiksen and Jørgensen 2011). The saturation parameter K_e (µmol m^2 s^{-1}) accounts for adaptational processes and the conversion of photons entering the retina to neural activity (Aknes and Utne 1997; Fiksen and MacKenzie 2002).

The visual range is subsequently used to estimate the clearance rate δ ($m^3 s^{-1}$):

$$\delta(L, z, a, u, h) = 0.5\pi R_l^2(\mathrm{L, z, h})\max(a, u). \tag{C5}$$

This characterises the volume of water scanned for prey per unit time. For this, it is assumed the larva has a 90° field of vision extending upwards and sideways, hence the scaling value of 0.5 (Fiksen and Jørgensen 2011). The volume of water scanned is also dependent on the velocity at which the larva is traveling. Therefore, to allow the larva to feed whilst migrating, its foraging velocity (m s^{-1}) is defined as the maximum of foraging activity a and migration velocity u, the latter of which is calculated from the migration distance, $u = |z' - z\,|/3600$ (Fiksen and Jørgensen 2011). As the larva's swimming abilities improve with size, its clearance rate is a therefore a function of body length, depth, hour of day, foraging and migration activity.

The clearance rate is then used as an input to a type II Holling disk foraging equation to estimate the prey mass encountered i (mg s^{-1}). Here, $n(z)$ is the concentration of prey at depth z (prey m^{-3}), γ is the handling time (s $prey^{-1}$) and c_p the probability of capture.

$$i(L,z,a,u,h) = \frac{c_p \delta(L,z,a,u,h) \cdot n(z)}{1+\gamma \cdot \delta(L,z,a,u,h) \cdot n(z)} \quad \text{(C6)}$$

Predation

Predation pressure is exerted from invertebrates and piscivores. The invertebrate component is split between ambush and tactile predators and centred around the size-dependent mortality term kl^b from McGurk (1986). Mortality from ambush predators increases with foraging velocity, whereas predation from tactile invertebrates is solely dependent on body size. The fraction of predation from both sources is determined by the parameter f_a:

$$m_i(L,a,u) = kl^b \left\{ \left[\frac{\max(a,u)}{L} \right] \cdot f_a + (1 - f_a) \right\}. \quad \text{(C7)}$$

Piscivores are assumed to be visual feeders, homogeneously distributed throughout the water column at density d_f, who forage at a fixed velocity v_f with 100% capture success. The piscivores visual range R_f is modelled in the same manner as the larva (equation C4), but with A_l and k_l taking values specific for piscivores (A_f and k_f). These assume a length-to-width ratio of 0.2 for the larva, a contrast against the background of 0.3, and an eye sensitivity of the predator of 5 x 10^3 (Fiksen and Jørgensen 2011).

$$m_f(L,z,h) = 0.5\pi R_f(L,z,h)^2 v_f d_f \quad \text{(C8)}$$

Growth

Growth proceeds at a specific temperature-dependent growth rate SGR (% day^{-1}) unless the stomach cannot provide enough mass, in which case food limitation occurs. The size- and temperature-dependent growth model developed by Folkvold (2005) provides estimates of instantaneous growth potential (equation C9), this is expressed as an instantaneous rate of mass increase g (g/g/s) below (equation C10):

$$\mathrm{SGR}(T,w) = 1.2 + 1.8T - 0.078T\ln(w) - 0.0946T\ln(w)^2 + 0.0105T\ln(w)^3 \quad \text{(C9)}$$

$$g = \ln\left[\left((\mathrm{SGR}/100) + 1\right)/\mathrm{dt}\right] \quad \text{(C10)}$$

To proceed at this rate, the stomach needs to supply enough mass D to account for g, routine respiration R (g dw h^{-1}) and energy losses from the conversion of stomach content to body mass (e.g. faeces) which is captured in the assimilation efficiency parameter A:

$$D = \mathrm{dt}(gw + R)/A. \quad \text{(C11)}$$

If there is insufficient mass in the stomach at time t (S_t) to meet these requirements, growth becomes food-limited, whereby all stomach content is assimilated, and respiration costs subtracted leading to negative growth:

$$w_{t+1} = \begin{cases} w_t(\exp(\mathrm{dt} \cdot g) - 1) & if\ D < S_t \\ w_t + S_t A - \mathrm{dt}R & if\ D > S_t \end{cases}. \quad \text{(C12)}$$

Routine respiration is a function of body mass and temperature and is taken from Finn et al. (2002) who estimated *R* in light and dark conditions, the average of which is used in this study, as in Kristansen et al. (2007).

$$R(T, w_t) = 2.38 \cdot 10^{-7} w^{0.9} \exp(0.088T) \quad \text{(C13)}$$

As the larva migrates and forages there are additional metabolic costs to consider. To capture these, *R* (at 7°C) is scaled by the foraging velocity giving a potential maximum and minimum metabolic costs of 2*R* and *R* respectively.

$$R_{active} = \max(a, u) R(7, w_t) \quad \text{(C14)}$$

State updates

Weight at the subsequent timestep is a function of current weight, food-limited or temperature-dependent growth and additional metabolic costs (equation C15). The stomach mass is bounded by zero and weight-dependent stomach size, assumed to be $0.06w_t$ (Kristiansen et al. 2007). Within these bounds, its content is dependent on growth costs (*D*) and the amount of ingested material *i* (equation A16). Length at t+1 is calculated using a model derived from laboratory experiments by Otterlei et al (1999; equation C17).

$$w_{t+1} = w_{t+1} - R_{active} \quad \text{(C15)}$$

$$S_{t+1} = S_t - D + i \quad \text{(C16)}$$

$$L_{t+1} = \exp\left(\frac{((\ln(w_{t+1}) + 9.2)}{3.9}\right) \quad \text{(C17)}$$

When an individual's length entered a new mm interval during a timestep, survival per mm (P_L) was initially reset to a value of one. To obtain precise estimates, the difference in length between t and $t + 1$ was linearly interpolated to find the portion of time spent in the old and the new length states. This was then used to scale the resultant P_L at t and the initial P_L at $t + 1$.

Literature only cited in appendices A, B, and C

Fiksen, Ø., MacKenzie, B.R., 2002. Process-based models of feeding and prey selection in larval fish. Mar. Ecol. Prog. Ser. 243, 151–164. https://doi.org/10.3354/meps243151

Finn, R.N., Rønnestad, I., Van der Meeren, T., Fyhn, H.J., 2002. Fuel and metabolic scaling during the early life stages of Atlantic cod Gadus morhua. Mar. Ecol. Prog. Ser. 243, 217–234. https://doi.org/10.3354/meps243217

Mobley, C.D., 1994. Light and water: radiative transfer in natural waters. Academic press, New York.

Otterlei, E., Nyhammer, G., Folkvord, A., Stefansson, S.O., 1999. Temperature- and size-dependent growth of larval and early juvenile Atlantic cod (Gadus morhua): a comparative study of Norwegian coastal cod and northeast Arctic cod. Can. J. Fish. Aquat. Sci. 56, 2099–2111. https://doi.org/10.1139/cjfas-56-11-2099

Skartveit, A., Olseth, J.A., 1988. Varighetstabellar for timevis belysning mot 5 flater pa 16 norske statsjonar. Geofys. Inst., Avd. for Meteorologi.

Voss, K.J., 1992. A spectral model of the beam attenuation coefficient in the ocean and coastal areas. Limnol. Oceanogr. 37, 501–509. https://doi.org/10.4319/lo.1992.37.3.0501

Woźniak, B., Dera, J., Ficek, D., Majchrowski, R., Ostrowska, M., Kaczmarek, S., 2003. Modelling light and photosynthesis in the marine environment. Oceanologia 45, 171–245. https://doi.org/10.1119/1.1970309

Paper IV

Paper IV

When is a fish stock collapsed?

Johanna Yletyinen* and William E. Butler*, Geir Ottersen, Ken H. Andersen, Sara Bonanomi, Florian K. Diekert, Carl Folke, Martin Lindegren, Marie C. Nordström, Andries Richter, Lauren Rogers, Giovanni Romagnoni, Benjamin Weigel, Jason D. Whittington, Thorsten Blenckner and Nils Christian Stenseth.

*These authors contributed equally.

Manuscript.

Author contributions: JY and WEB jointly conceived the study idea. TB and NCS supervised the project. JY, WEB, SB, GR, BW, AR and JDW contributed to the literature review. JY, WEB, KHA, SB, ML, MCN, LR, GR, BW, JDW, GO, AR and NCS contributed to stock selection and data collection. WEB programmed the definitions and performed all analyses. JY, WEB, GO, TB and NCS interpreted the results and discussed the implications with assistance from all authors. JY, WEB, GO, TB and NCS prepared the initial manuscript and all authors contributed to the revisions.

When is a fish stock collapsed?

J. Yletyinen[1,2] and W.E. Butler[3,4], G. Ottersen[5,6], K.H. Andersen[7], S. Bonanomi[8], F.K. Diekert[6,9], C. Folke[2,10], M. Lindegren[7], M.C. Nordström[11], A. Richter[6,12], L. Rogers[6], G. Romagnoni[6], B. Weigel[11,13], J.D. Whittington[6], T. Blenckner[1] and N.C. Stenseth[6, 14]

[1] Stockholm Resilience Centre, Stockholm University, Kräftriket 2B, SE-10691 Stockholm, Sweden

[2] Manaaki Whenua Landcare Research, PO Box 69040, Lincoln 7640, New Zealand

[3] MARICE, Faculty of Life and Environmental Sciences, University of Iceland, 101 Reykjavik, Iceland

[4] Marine and Freshwater Research Institute, Skúlagata 4, 101 Reykjavík, Iceland.

[5] Institute of Marine Research, P.O. Box 1870 Nordnes, N-5817 Bergen, Norway

[6] Centre for Ecological and Evolutionary Synthesis (CEES), Department of Biosciences, University of Oslo, P.O. Box 1066 Blindern, N-0316 Oslo, Norway

[7] Centre for Ocean Life, c/o National Institute of Aquatic Resources, Technical University of Denmark, Bygning 202, 2800 Kgs. Lyngby, Denmark

[8] Italian National Research Council (CNR), Institute of Marine Sciences (ISMAR), Largo Fiera della Pesca 1, 60125, Ancona, Italy

[9] Department of Economics, Heidelberg University, Bergheimer Str 20, 69115 Heidelberg, Germany

[10] Beijer Institute, Royal Swedish Academy of Sciences, P.O. Box 50005, SE-10405 Sweden, Stockholm, Sweden

[11] Environmental and Marine Biology, Faculty of Science and Engineering, Åbo Akademi University, Artillerigatan 6, FI-20520 Åbo, Finland

[12] Environmental Economics and Natural Resources Group, Sub-Department of Economics, Wageningen University, 6700 EW Wageningen, The Netherlands

[13] Research Centre for Ecological Change, Organismal and Evolutionary Biology Research Programme, University of Helsinki, Helsinki, Finland

[14] The Centre for Coastal Research, University of Agder, NO-4604 Kristiansand, Norway.

Abstract

Assessment reports on the state of natural resources are of high interest as the dialogue on sustainable resource use is escalating in politics and the public. Due to the severe impacts on ecosystem resilience, food security and livelihoods of millions of people, marine fish stock collapses are among the most concerning resource depletions globally. However, the occurrence rate of fish stock collapses remains unclear despite a long debate on the topic. We hypothesise that the lack of a unified definition has contributed to contrasting perceptions of the state of fish stocks. To test this hypothesis, we applied 20 existing and 270 simulated collapse definitions to 44 diverse stocks to test the common practice of performing multi-stock collapse analyses with a single definition. Our results show that individual definitions are unreliable for summarising the state of multiple fish stocks. Classifications are highly sensitive to a definition's parameters and its overall formulation due to the inability of single definitions to capture complex population dynamics and diverse fisheries management strategies. We suggest a new practice of utilising multiple definitions for assessing collapse status to increase our understanding of the context dependencies of fish stock collapses and to improve fisheries status worldwide.

1. Introduction

Anthropogenic activities are challenging the sustainability of marine ecosystems (Cheung et al. 2018), it is therefore of high importance to improve knowledge on methods that in a robust way inform about the current status of marine ecosystems. Management is an essential tool for rebuilding overexploited fish stocks (Hilborn et al. 2020); however, reliable information regarding fish stock health is required to elicit effective management responses. The persistence of overfished stocks is an area of great concern for both food security and ecosystem health (FAO 2020). Despite recent progress towards sustainable fishing in several regions (Fernandes and Cook 2013; FAO 2020; Hilborn et al. 2020), the effects of overfishing have expanded from a predominantly local to global scale in the past century (Worm et al. 2009; Costello et al. 2012). Fish stock collapses have been reported in many parts of the world (e.g. Toresen and Østvedt 2000; Bonanomi et al. 2015; Buren et al. 2019) and are of specific interest to scientists and the general public due to the high associated risks for livelihoods, ecosystem resilience, food security and cultural meaning (Jackson et al. 2001; Worm et al. 2009; Hammerschlag et al. 2019).

Resource assessments covering multiple stocks and resource locations are a prerequisite for monitoring global trends in resource abundance and for transitioning to sustainable resource management. The challenge of assessing the status of multiple fish stock is well illustrated in scientific reports: during the past 15-20 years, it has been reported that fisheries have caused a general decline in fish stocks worldwide (e.g. Myers and Worm 2003; Pauly et al. 2005; Worm et al. 2006, 2009; Costello et al. 2012; Froese et al. 2012), but numerous replies contested the extent of some of these claims (Hilborn 2007; Branch et al. 2008, 2011; Cook 2013). In particular, the projection of a universal fish stock collapse by 2048 (Worm et al. 2006) heated the scientific debate concerning data preferences and assessment methods, and triggered considerable media attention to the reportedly disastrous state of the world's fish stocks (Stokstad 2009).

A precise and robust assessment approach is importance to improve knowledge on the current status of fish stocks. Assessing the "big picture" by classifying multiple fish stocks is particularly important for data-limited stocks and those that do not have effective management frameworks (Hilborn et al. 2020). Such "state of the resource" classifications may trigger political responses with potentially far-reaching biological, social, and economic consequences. While overly pessimistic interpretations of fish stock health may produce alarmist narratives, excessively optimistic views can allow continued fishing pressure even when stocks are at persistently low levels. Such overly optimistic views likely increased the severity of major stock crashes, for example the Canadian Northern cod (*Gadus morhua*) around 1990 (Myers et al. 1997) and the Norwegian spring spawning herring (*Clupea harengus*) in the late 1960s (Toresen and Østvedt 2000). Moreover, prolonged heavy fishing of over-exploited stocks is likely to delay rebuilding (Pinsky and Byler 2015).

In this study, we question the common practice of performing multi-stock analyses with a single "fish stock collapse" definition without evaluating or reporting the fit of the definition to the assessed stocks. We hypothesise that the difficulty of summarising the collapsed state of fish stocks is caused by 1) having numerous collapse definitions in use in scientific literature, which has led to contrasting collapse classifications and added noise and disagreement to scientific debate, and 2) attempts to capture diverse, complex collapse

events with simple rules. To overcome these obstacles, we propose the use of multiple collapse criteria with the aim to report their confidence and the overall risk of collapse.

To test our hypothesis, we first explored the range of existing fish stock collapse definitions by reviewing the scientific literature. Based on the existing quantitative and verbal definitions of "collapse", we developed a conceptual framework for simple fish stock collapse definition. This framework is used to propose a new quantitative definition that can be applied across multiple stocks in a consistent manner. We then applied each definition to 44 diverse fish stocks and evaluated each classified time-series against a benchmark definition obtained from stock-specific management thresholds. To strengthen our hypothesis testing, we repeated this multi-stock assessment with 270 simulated definitions to identify the specific components of collapse definitions that perform best on each stock.

2. Materials and Methods

2.1. Literature review

We reviewed scientific literature from 1984 to 2015 in ecology, fisheries science, and economics. Comparable to snowball sampling, we started with the most well-established collapse articles and expanded the article selection to collapse papers cited by or citing these articles. The review was conducted with the purpose of finding the range of how a fish population/stock collapse is defined, not to collect all existing collapse definitions. Hence, when we had acquired approximately 20 definitions from 82 references, we considered the sample adequate and finished the review. We included social science articles in the review, but no explicit fish stock collapse definitions were found in that field.

2.2. Collapse definition framework and terminology

"*Fish stock collapse: the reduction of a fish stock by fishing or other causes to levels at which the production is only a negligible proportion of its former levels. The word is normally used when the process is sudden compared with the likely time scale of recovery, if any, but is sometimes used melodramatically for any case of overfishing*" – Cooke (1984).

The theory behind stock collapses was outlined by Cook et al. (1997). When the slope of the replacement line (y recruits required to replace x biomass) exceeds the slope of the stock-recruitment relationship, a stock spirals towards the origin as there is no non-zero equilibrium (Cook et al. 1997). Estimating the slope of the stock-recruitment curve close to zero is often not possible due to a lack of observations. Furthermore, several of the world's fish stocks are data limited and do not have established management reference points. These are among the motives for the use of "simpler" definitions of collapse.

All quantitative time-series based definitions of a population or stock collapse contain one essential element: that a collapse occurs if abundance drops below a certain threshold. The threshold determines the level at which production is impaired—a defining feature of a "collapse" (Cooke 1984)—and is typically defined by a percentage decline from a reference biomass. The reference biomass may be a theoretical, for example, a stock's virgin biomass (e.g. Worm et al. 2009), or it may be a direct function of the biomass time-series. Examples include the historical maximum biomass, the maximum biomass within *n*

preceding generations (hereafter referred to as the "recent maximum"), or the mean biomass. The specific relationship between the reference biomass and the threshold has important implications for how definitions operate and thus status categorisations across stocks. For instance, using the recent maximum as a reference biomass indicates that a collapse must occur within a population's recent past (hereafter referred to as "abrupt decline"). These definitions are based on the IUCN's extinction-risk criteria (Mace et al. 2008) and focus on the rate of decline rather than the magnitude of decline. "Abruptness" is implicitly implied in biological and non-biological definitions of collapse (Cooke et al. 1984; Cumming and Petersen 2017), but does this mean that the stock is not collapsed if the decline takes place over n+1 generations? Negative associations between decline and recovery rates suggest that filtering out depletions from collapses is important for the allocation of resources to rebuild stocks. Similarly, definitions should be able to filter out natural fluctuations from collapses. This can only be done by specifying a criterion that ensures biomass remains below the threshold for a period of time. We refer to this component as "prolonged depletion".

2.3. Proposed fish stock collapse definition

The definition we propose views a collapse as an abrupt change to an undesired state. It consists of two interlinked criteria that capture the collapse process: an abrupt decline, and an ensuing period of prolonged depletion. Indicative of impaired production, prolonged depletion is an undesired state for a fish stock. Each criterion is defined as follows:

1) *Abrupt decline*: a stock's adult biomass declines by 70% within a maximum of three generations or 10 years.

2) *Prolonged depletion*: the stock's mean adult biomass over a succeeding generation remains below the 70% abrupt decline threshold.

Applying our definition to a time-series of adult biomass (spawning stock biomass, SSB), a stock had collapsed if an abrupt decline (criteria 1) is immediately followed by a prolonged depletion (criteria 2). For any year i, the mean biomass over a succeeding generation ($\overline{B_i}$) is simply a left-aligned average with an averaging window of one generation (n),

$$\overline{B_i} = \frac{1}{n}\sum_{j=i}^{i+n-1} B_j. \quad (1)$$

If both criteria are met, a threshold T_B is set at 70% of the reference biomass (B_{ref})—the stock's biomass at the beginning of the abrupt decline (Fig. 1C). Subsequently, all years following the abrupt decline are evaluated for prolonged depletion (criterion 2). If a year's mean adult biomass over a succeeding generation is below or equal to the threshold ($\overline{B_i} \leq T_B$), the stock remains in a collapsed state, whereas if it is above the threshold ($\overline{B_i} > T_B$), the stock is exhibits potential recovery from the collapsed state (Fig. 1C). Once a threshold is set, it remains static unless a stock fully recovers (i.e. $B_i > B_{ref}$).

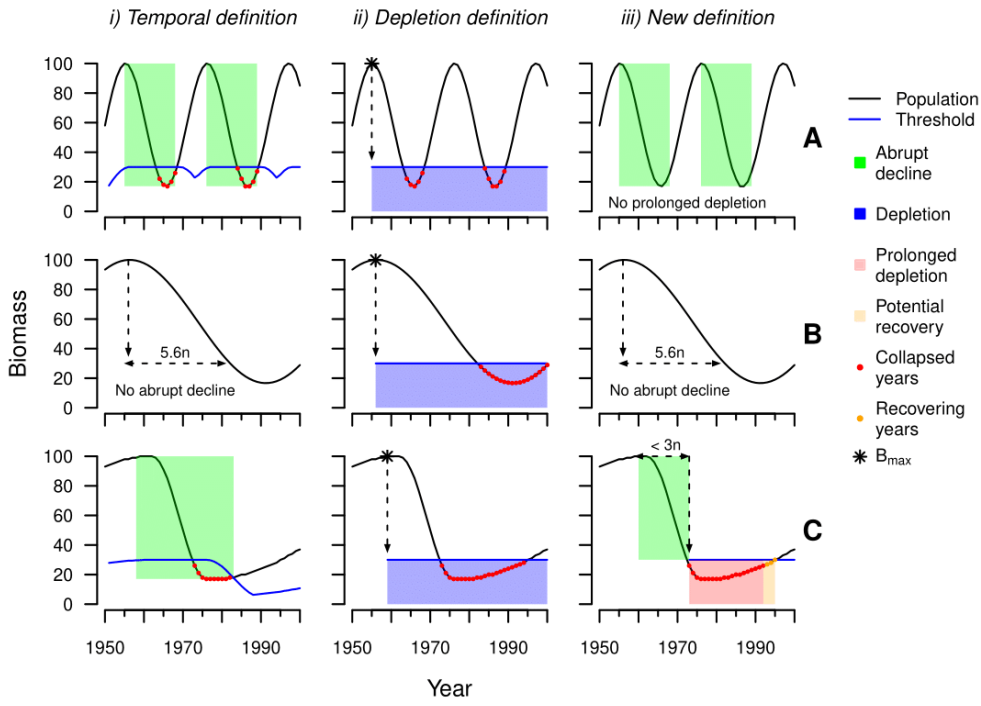

***Figure 1**: Three different collapse criteria (columns i, ii and iii) are applied to three hypothetical stocks (rows A, B and C) to demonstrate how the formulation of a collapse criteria can result in misleading classifications of a stock's state. Stock A fluctuates in a cyclic manner, stock B gradually depletes over a long period of time, stock C rapidly declines and exhibits prolonged depletion following the decline. The first definition (i) classifies a year as collapsed if a 70% decline occurs within three generations (i.e., it captures an abrupt decline). This can misclassify stocks with cyclic dynamics (i, A) because there is no consideration of prolonged depletion. The second definition (ii) classifies a year as collapsed if the stock's biomass falls below 30% of the historical maximum (B_{max}). This definition misclassifies a stock that gradually depletes (B, ii) because the rate of decline is not considered, and it misclassifies a stock with cyclic dynamics (A, ii) because it does not consider prolonged depletion. The proposed definition (iii) classifies a stock as collapsed if a decline of 70% within 3 generations is immediately followed by a period of prolonged depletion where biomass remains below the threshold for a generation. By considering the abrupt decline and prolonged depletion as an interlinked process, the proposed definition can filter out natural fluctuations (A, iii) and gradual depletions (B, iii) from more drastic collapses (C, iii).*

If an abrupt decline was not immediately followed by a prolonged depletion, we classified the event as a "temporary fluctuation" instead of a collapse (Fig. 1A) because the decline was temporary suggesting that production was not impaired. If the timespan for a 70% decline was greater than a maximum of three generations or 10 years, the event was classified as a "gradual depletion" because the decline is not abrupt (Fig 1B). Specifying a threshold and a temporal window within which the decline must occur ensured the decline was both large and abrupt. Importantly, the temporal window negated the shifting baseline syndrome (Pauly 1995) because the reference biomass was not specified in advance (e.g. maximum historical biomass can be significantly affected by the length of the time series).

The exclusion of gradually depleting stocks may seem too cautionary, but the abrupt decline draws from the IUCN criteria that are developed through wide consultation (IUCN 2012). Previous studies (Hutchings 2000; Hutchings and Reynolds 2004) have highlighted that IUCN's decline-rate thresholds can contribute to the detection of fish stocks most in need of restoration measures due to negative associations between decline- and recovery-rates, and through the inclusion of intrinsic life-history traits (Reynolds et al. 2005). We focus on the 70% threshold, but tested all three IUCN threshold values (70%, 80%, and 90%) in our analyses. The proposed definition is thus based on conservation thresholds, while consideration for recovery potential allows recognition of successful fisheries management. This aspect aims to unify the views of conservation and fisheries science (Salomon et al 2011).

2.4. Stock data

We extracted time-series data for 44 North Atlantic fish stocks from the ICES stock assessment database (ICES 2019). Starting with the complete database, we identified all stocks that had collapsed according to the SSB < B_{lim} definition (Lindegren et al. 2009). Subsequently, we filtered out stocks that had not declined to B_{lim} (i.e. SSB was below B_{lim} at the beginning of the time-series) or did not meet the data requirements for the analyses. The resulting selection of fish stocks represented a diverse array of population dynamic trends and life-histories (Table A1). Many of the selected stocks have been classified as collapsed according to other definitions, whilst others displayed trends that would intuitively suggest that a collapse has occurred, making for a suitable database to explore the consequences of various collapse definitions. For each stock, maturity ogives (*M*), numbers-at-age (*N*) and weights-at-age (*W*) were extracted from the respective stock annexes and expert reports. These were used to estimate the mean age ($\bar{A}$) of the mature stock. Used as a proxy for generation time, $\bar{A}$ was defined as the spawner biomass-weighted average across all mature age classes:

$$\bar{A}_i = \frac{\sum_{a=a_{min}}^{a=a_{max}} aM_{a,i}N_{a,i}W_{a,i}}{\sum_{a=a_{min}}^{a=a_{max}} M_{a,i}N_{a,i}W_{a,i}} \quad (2)$$

where a_{min} and a_{max} are the youngest and oldest spawners in year *i* respectively. This provided a time-series of $\bar{A}$ for each stock that enabled estimates of generation length (*n*) pre- and post-collapse, the former being a requirement for the IUCN extinction-based criteria (Mace et al. 2008). The one exception was Barents Sea capelin for which the estimate of *n* was taken from Dodson et al. (2007).

Stock assessments by ICES do not estimate the spawning stock biomass that can sustain maximum sustainable yield (SSB_{msy}), therefore we used $SSB_{MSY} = 2 \cdot MSY\ B_{trigger}$ as a proxy (ICES 2018). For stocks that did not have estimates of MSY $B_{trigger}$ available (11 stocks), we assumed $SSB_{MSY} = 2 \cdot B_{pa}$, a rule that was found to provide reasonable estimates by Froese et al. (2016). Estimates of SSB_{msy} were not possible for two stocks and catch-based classifications were not possible on seven stocks due to limited data.

2.5. Application of definitions

Each definition was coded in the R programming language and applied to each of the stocks resulting in 1186 classified time-series. Each classified time-series described whether a stock was in a "collapsed" or a "not collapsed" state for each year of the time-series that could be evaluated. In addition, information describing each collapse event was stored (reference biomass, threshold value, and the magnitude and rate of decline) together with a number of collapse metrics. These included the number of years in a collapsed or a non-collapsed state, the duration of the collapsed state(s), and the stock's present status. Taken together, the output gave a broad overview of how each definition operates across multiple, diverse fish stocks.

Data type	**Ref. Biomass**	**% Decline**	**PD (*n*)**
SSB	Hist. Max	[10, 90, 10]	[0, 2, 0.5]
Catches	Recent Max (within 3*n*)		
	Pop. Mean		

***Table 1**: Parameters and their resolutions used in the simulation experiment where n describes a stocks generation time and PD stands for prolonged depletion. The "% Decline" and "PD (n)" parameters are described in the format [min, max, increment].*

We also carried out a simulation experiment to find which components of collapse definitions perform best for each stock. We built definitions using four parameters (Table 1) which describe the type of data, how the reference biomass is calculated, the magnitude of decline (from the reference biomass), and duration of prolonged depletion (how many generations biomass must remain below the threshold to be collapsed). For the reference biomass "Recent Max within 3*n*", we applied the definition proposed in this paper rather than the IUCN definition. The difference being that once a stock has collapsed in the proposed definition a threshold is set for the remaining years (it may increase but not decrease), whereas the IUCN definition generates a threshold that fluctuates on an annual basis dependent upon the previous 3 generation's biomass. We applied all possible permutations of these parameters to each stock.

2.6. Definition evaluation

To evaluate the performance of each definition, we compared each stock's classification time-series against the equivalent time-series that resulted from the $SSB < B_{lim}$ definition (Lindegren et al. 2009). The reference point B_{lim} is a key parameter in the precautionary approach to fisheries management adopted by ICES. Defined as "a deterministic biomass limit below which a stock is considered to have reduced reproductive capacity" (ICES 2017), it captures the essence of a collapsed state and is thus a suitable benchmark against which to test the literature and simulated definitions. For each comparison we calculated the F_1 score which is a measure of a test's accuracy in binary classification. Defined as the harmonic mean of precision and recall, where precision is the proportion of predicted "collapsed" years that were correct, and recall is the proportion of actual "collapsed" years that were predicted correctly. A value of 1 indicated perfect precision and recall, whilst a value of 0 indicated that a definition's precision and/or recall completely failed.

3. Results

3.1. Literature review of collapse definitions

Twenty different time-series-based stock level definitions were found (Table A2). Most definitions captured a state of depletion by setting a threshold below which the stock is classified as "collapsed". From these twenty time-series-based stock level definitions, we identified four weaknesses: 1) the definitions often lacked temporal context, which can lead to classifying stocks that naturally fluctuate or gradually decline as collapsed (Figure 1A, 1B); 2) the justification for setting thresholds was often unclear or missing, and there was little numerical consistency between definitions (e.g. the percent decline from maximum historical biomass required to set a threshold varied from 1% to 25% [Table A2]); 3) definitions were related to study-specific reference values (e.g. maximum historical biomass), yet the arbitrary historical condition used as a reference point is often subject to data availability and what individual scientists perceived to be healthy fish stocks (Pauly 1995); 4) few definitions account for prolonged depletion, and only one definition frames this criterion in life-history terms which is an essential consideration for comparing status across diverse fish stocks.

3.2. Performance of collapse definitions

The definitions found in the literature review comprised a wide variety of formulations and parameter values. Consequently, their ability to reproduce the classifications of the benchmark definition ($SSB < B_{lim}$) was limited, suggesting that attempts to fit a rich variety of stock data into one collapse pattern to summarise the state of fish stocks may be too simplistic. An F_1 score of one meant a definition captured the classifications of the benchmark definition with complete success, whilst an F_1 score of zero meant a definition completely failed to capture the benchmark definition's classifications. Out of the 23 definitions tested, only five (three when excluding the proposed definitions) produced an F_1 score greater than zero in 50% of the stocks (Fig. 2B). Each definition tested produced a score of zero in at least one stock, whilst only six definitions produced at least a single score of one. For instance, the best performing definition overall—"25% Hist. Max. SSB"—resulted in three scores of one and nine scores of zero. From these results it can be concluded that the literature and proposed definitions captured a "high risk of collapse" in particular stocks but were unable to perform consistently across stocks. In general, the literature and proposed definitions set thresholds lower than B_{lim} that resulted in large numbers of false negatives at the expense of true positives, i.e. years classified as "not collapsed" when the benchmark definition classified them as "collapsed" (Fig. 2A). A scenario which leads to an overly optimistic view of fish stock state.

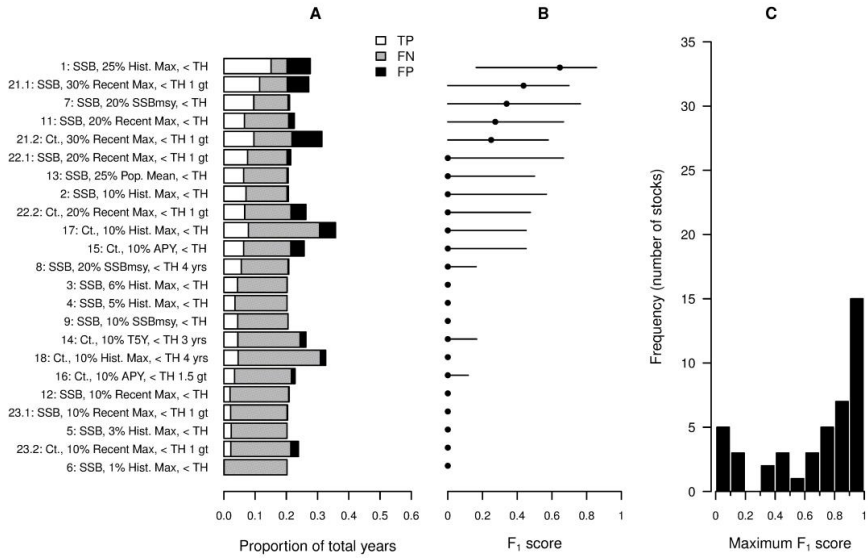

Figure 2*: Classification success of the literature and proposed collapse definitions. Panel A shows the composition of true positives (TP), false negatives (FN), and false positives (FP) for each definition (pooled over stocks). True positives occur when the test and benchmark (SSB < B_{lim}) definitions both classify a year as collapsed; false negatives occur when the benchmark definition classifies a year as collapsed but the test definition does not, and vice versa for false positives. Panel B shows the median and interquartile range of F_1 scores from across all stocks. Panel C shows the distribution of "best" F_1 scores (one value per stock, irrespective of definition).*

3.3. Performance of simulated collapse definitions

The results from the simulated experiment reinforced the conclusion from the literature definitions: that particular definitions can perform well on particular stocks but not consistently across stocks. A selection of simulated definitions performed better and more consistently across stocks than the literature definitions (Fig. 3B). Out of 270 definitions tested, 202 produced an F_1 score greater than zero in 50% of the stocks. However, only six definitions improved upon the best literature definition (Fig. 3B). The best performing simulated definition—"< 40% Pop. Mean"—produced F_1 scores of one and zero in six and 11 stocks respectively (median = 0.74), highlighting that a single definition that performed consistently well across stocks was not found (within the parameter space tested). The best simulated definitions captured more true positives at the expense of false positives (Fig. 3A). This highlights that the thresholds were higher than B_{lim} which, in direct contrast to the literature definitions, leads to an overly pessimistic view of fish stock state compared to the benchmark definition (i.e. more years classified as collapsed). We re-ran the analyses using $F_{0.5}$ as a performance measure which gave twice the weight to precision (thus penalising false positives more); however, this had a minimal impact on the results and did not alter the conclusions.

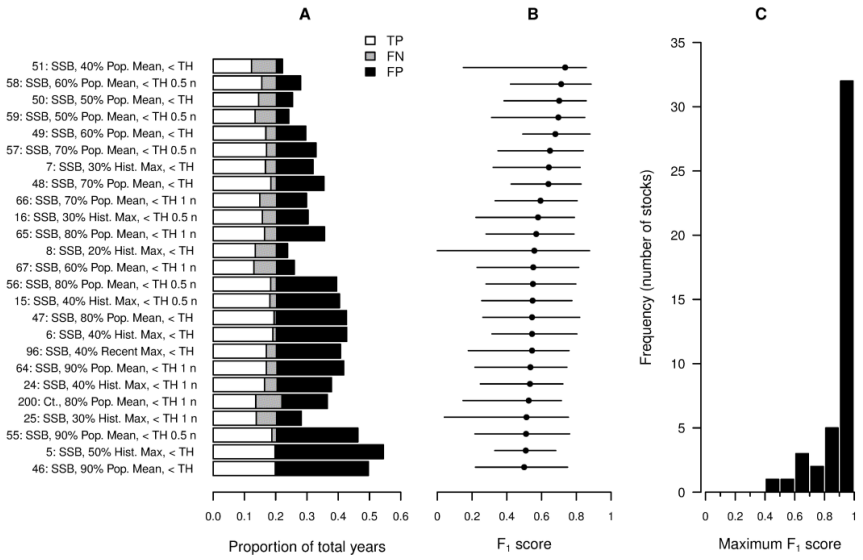

***Figure 3**: Classification success of the top 25 simulated definitions. Panel A shows the composition of true positives (TP), false negatives (FN), and false positives (FP) for each definition (pooled over stocks). True positives occur when the test and benchmark (SSB < B_{lim}) definitions both classify a year as collapsed; false negatives occur when the benchmark definition classifies a year as collapsed but the test definition does not, and vice versa for false positives. Panel B shows the median and interquartile range of F_1 scores from across all stocks. Panel C shows the distribution of "best" F_1 scores (one value per stock, irrespective of definition).*

Utilising the population mean as a reference biomass was a consistent feature among the best simulated definitions (Fig. 3A). However, variation among the population mean deciles (see Table 1) was considerably smaller than the historical maximum deciles and thus more likely to approximate B_{lim} successfully. This is because the population mean is (in most cases) less than the historical maximum. An exception can occur if SSB increases over time, then the population mean can be greater than the historical maximum earlier in the time-series, but only if a running historical maximum is used to generate the threshold (i.e. historical maximum from any previous year, rather than the whole time-series).

3.4. The formulation of collapse definitions

Developing single collapse definitions involves definition-dependent trade-offs on what a "collapse" as a concept entails (Fig. 1). Characterising the collapses to B_{lim} utilising potential "collapse" components clarified why a single definition did not perform well across stocks. The magnitude of decline varied from 25% to 98% for the historical and recent maximum reference biomasses respectively, and from -16% to 95% for the population mean reference biomass (negative numbers meaning the population mean was below B_{lim}; Fig. 4A). The speed of the decline from the historical maximum varied from 0.5 to 8.1 generations and in 21 stocks it was below 3 generations (in which case the historical maximum and abrupt decline definitions are equivalent [Fig. 4B]). In 34 stocks, prolonged depletion was less than one generation highlighting that the decline below B_{lim} was temporary for the majority of stocks (3.6 years on average; Fig 4C). The longest period of depletion was the Irish Sea whiting which has remained below B_{lim} since 1993.

The second largest was the North Sea sprat stock which collapsed below B_{lim} in 1982 and remained in a collapsed state for 6 generations. Due to its short generation time, this equates to 9 years; in contrast, the East/Southwest Greenland cod stock was collapsed below B_{lim} for 11 years but only 1.4 generations.

The variation in these collapse components illustrated why no single definition is capable of performing well across stocks. For example, a 90% decline from the historical and recent maximum reference biomasses resulted in 15 and 9 stocks classified as "collapsed" respectively (at some point in the time-series; Table 2). Changing the threshold to a 70% decline increased the number of collapsed stocks to 38 and 32 respectively (Table 2), an alarming increase if reporting the collapsed state of stocks. Including a requirement for the stock to remain below the threshold for one generation (prolonged depletion) in the 70% definitions led to 4 and 3 less stocks classified as "collapsed" for the historical and recent maximum reference biomasses respectively. These results illustrated the great sensitivity of collapse classifications to both small changes in parameter values and to the definition's overall formulation.

Threshold	**HM**	**AD**	**AD + PD**
70%	38 (0.28)	32 (0.25)	29 (0.18)
80%	31 (0.17)	25 (0.14)	22 (0.09)
90%	15 (0.08)	9 (0.04)	7 (0.02)

***Table 2**: The number of stocks (total = 44) and the proportion of years (across all stocks) classified as "collapsed" according the historical maximum (HM), abrupt decline (AD), and AD + PD (prolonged depletion) definitions with three different thresholds (rows).*

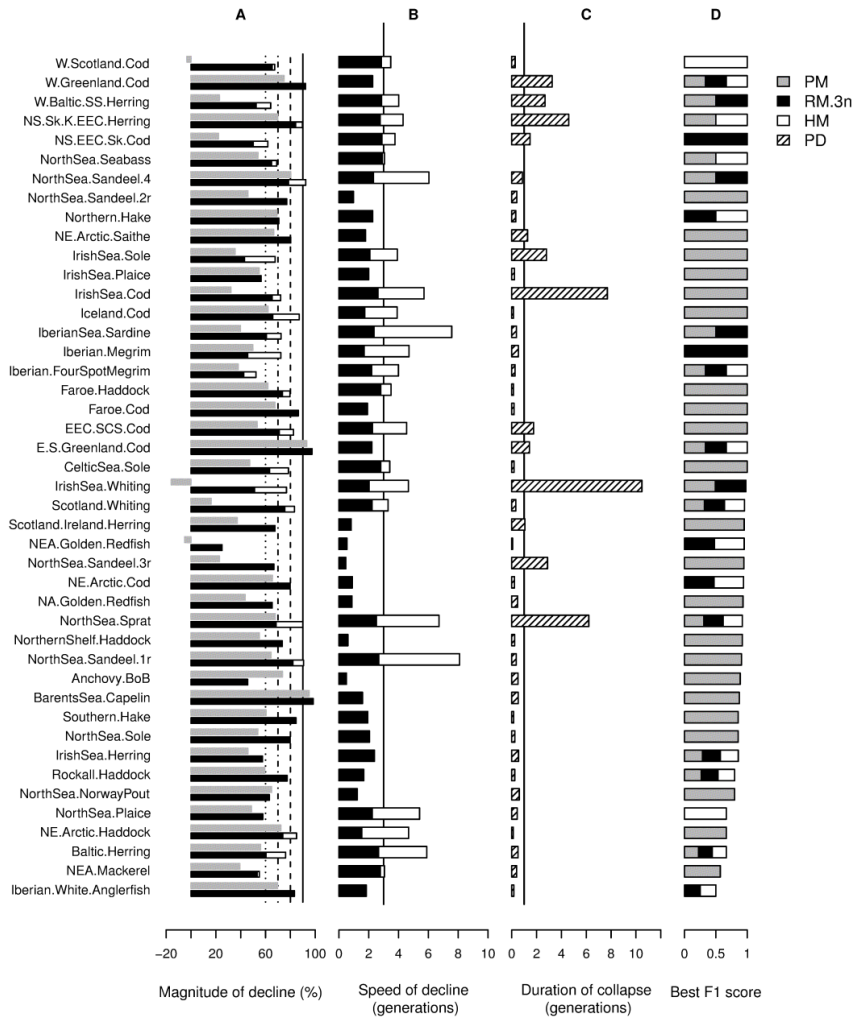

Figure 4*: Characterising the stock collapses below B_{lim} for each fish stock. Panel A shows the magnitude of decline from each reference biomass to the first collapsed year (Y_C). Three reference biomasses were identified prior to Y_C according to the definition SSB < B_{lim}: (1) the maximum historical biomass (HM), (2) the recent maximum biomass within 3 generations (RM.3n; an abrupt decline), and (3) the population mean (PM). The second panel shows the time in generations from the reference biomass to Y_C (this excludes PM definitions). The third panel shows the duration of the collapse (expressed in generations), calculated from the number of consecutive years below B_{lim}. The fourth panel shows the best F_1 score achieved in the simulation experiment, the colour(s) of each bar shows the reference biomass that defines the best definition(s), e.g. a white and black bar means the historical and recent maximum reference biomasses both performed best. In each panel the vertical lines indicate parameter values that are used in a variety of definitions.*

3.5. Performance of the proposed collapse definition

The authors' collapse criterion, which was aimed to perform well in multi-stock analyses, was the second-best performing collapse definition in the literature definitions (70% threshold; Fig. 2A). However, in the simulated definitions it did not perform as well. The results showed that our definition would perform better if the decline in biomass was calculated from the historical maximum instead of the recent maximum, i.e., the magnitude of decline was a better description of the collapses to B_{lim} than the rate of decline. This suggests that including a criterion that specifies a number of years within which a collapse must occur can lead to the unwanted situation of classifying collapsed stocks as "not collapsed" because the drivers of the "collapse" event are not captured within the specified temporal window.

The motivation for the definition's construction was to distinguish collapses from gradual depletions and natural fluctuations. Table 2 highlights how the definition distinguished these states across stocks. The proposed definition classified less stocks as collapsed, and seeing as all stocks collapsed according to the benchmark definition, this partly explains its lower F_1 scores (higher number of false negatives). At each threshold level, six stocks show "gradual" rather than "abrupt" declines. Whilst comparing the AD and "AD + PD" definitions, three (70% and 80%) and two stocks (90%) would be classified as "natural fluctuations" (the composition of stocks varied depending on the threshold). There are some instances where classifications from the proposed definition were likely to be erroneous. For example, the Irish sea cod and sole experienced large declines to below B_{lim} in the 90s with signs of recovery only occurring in the last few years of the time-series (Fig. C1). These trends are highly suggestive of a collapse; however, the historical maximum definitions were far more effective at capturing the benchmark's classification patterns. In this case, the "decline within 3 generations" criterion constrained the proposed definition's ability to detect the collapse. In contrast, Barents Sea capelin (*Mallotus villosus*) (Fig. C1) is a naturally fluctuating stock frequently classified as collapsed according to many definitions, whereas our definition identified collapse for only a small number of these years. For the 70%, 80% and 90% thresholds, our definition categorises 26%, 13% and 11% of years as collapsed respectively, as opposed to the equivalent IUCN definitions which categorise 43%, 35% and 33% of years as collapsed. However, the results do suggest that whilst incorporating a parameter for prolonged depletion can filter out dips below thresholds, it can also lead to overly optimistic classifications based on minor rises above the threshold.

4. Discussion

The number of collapse definitions found in our literature review indicates that there is no consensus regarding the choice of analytical approach used to reliably classify the status of a fish stock as collapsed. Our analysis shows that collapse classifications are highly sensitive to small changes in a definition's parameters and its overall formulation. A result of this sensitivity is that simple collapse definitions can perform well on individual stocks but not across multiple stocks. Such inconsistency in stock classification that is driven by the choice of collapse definition offers a plausible explanation for disagreement among scientists on the general state of the global fish stocks.

Our results highlight that careful evaluation of collapse definitions against individual stocks is required to reduce uncertainty in the collapsed state classifications. Rather than argue that faulty collapse definitions are in use, this conclusion is based on the insight that

different collapse criteria focus on different aspects of the stock dynamics. Therefore, trusting the results of a multi-stock analysis performed with a single collapse definition requires knowledge regarding the mechanisms driving stock-specific population dynamics. For example, Petitgas et al. (2010) defined a depletion as a loss of biomass, and a collapse as a depletion that is accompanied by a breakdown in its contingent (migrant vs resident) structure and habitat-use patterns (spawning and feeding). Approaches that look beyond changes in biomass are likely to uncover the mechanisms underlying collapses and offer more robust classifications (see also Buren et al. 2019). In general, the inclusion of life-history traits is essential to understanding collapses and recoveries (Kindsvater et al. 2016; Hutchings and Kuparinen 2017). For instance, species with "fast" life-histories (e.g. they mature young and have short life-spans) tend to have better recovery potential than those with "long" life-histories due to the positive association between "fast" life-history traits and population growth rates. However, the recovery potential of such species may be greatly reduced (and the potential to collapse greatly increased) by unfavourable environmental conditions (Kindsvater et al. 2016) or within-population temporal changes in life-history traits that reduce productivity, e.g., reduced length-at-maturity due to exploitation (Hutchings and Kuparinen 2017). Furthermore, the inclusion of ecosystem-level signals could reveal additional important aspects of collapse and recovery dynamics (Pikitch et al. 2004; Pedersen et al. 2017; Cook 2019), but this approach requires greater data, that will not be available for many stocks that are not rigorously assessed.

Our analyses assumed that the benchmark definition "SSB < B_{lim}" accurately captures the collapsed state across stocks. Due to its precautionary nature, this definition identifies stocks that are at a high risk of collapse as opposed to actually collapsed. For stocks with established stock-recruitment relationships, B_{lim} is the change-point in a segmented regression (see O'Brian 2003). If SSB falls below B_{lim}, recruitment declines with biomass; if SSB is above B_{lim}, recruitment is constant. For stocks that are data limited or that have weak or non-existent stock-recruitment relationships, alternative approaches are used to estimate B_{lim}, for instance, the lowest SSB that has produced a good year class. These approaches are potentially more ad hoc, and concerns have been raised over precautionary values derived from B_{lim} reference points (Froese et al. 2016). However, the general improvement in European fish stocks with defined management reference points (Fernandes and Cook 2013, Table A2) does suggest that B_{lim} is a suitable benchmark for identifying collapsed stocks. Furthermore, because B_{lim} is determined through dedicated expert groups under standardised guidance outlined by the "precautionary approach to fisheries management" (ICES 2003; Rindorf et al. 2016), evaluating definitions against B_{lim} provides a useful baseline for the future application of definitions to data-limited stocks or those without equivalent management reference points.

Another caveat of our analyses regards the inclusion of the prolonged depletion parameter. The inclusion of this parameter is important to distinguish between short-term fluctuations and long-term depletions or collapses. Prolonged depletion is of great significance because it can indicate an insufficient management response, decreased population/ecosystem resilience, depensation, or that the causes that lead to the low recruitment persist (Hutchings and Reynolds 2004; Worm et al. 2006; Lotze et al. 2011; Neubauer et al. 2013; Pinsky and Byler 2015; Hutchings and Kuparinen 2017). However, due to the technicalities of the analyses, its inclusion in a collapse definition can lead to misclassifications when compared to B_{lim}. For instance, a decline of 70% from a reference biomass may generate a threshold equal to B_{lim}. If the definition also includes a prolonged depletion criterion, it will generate a number of false negatives because years that are

below B_{lim} for less than a generation will be classified as "not collapsed" (assuming that n > 1 year). Under the framework we employed, this would make sense because the stock would either be recovering or bouncing back from a natural fluctuation. However, it would also lead to a lower F-score—the metric we used to evaluate the performance of collapse definitions. Conversely if a definition sets a threshold above B_{lim}, its performance may improve by including prolonged depletion because it would reduce the number of false positives. An effective management response is required regardless of the duration of depletion, therefore this would not be a useful parameter for real-time management; however, we recommend its inclusion in retrospective analyses because it is indicative of impaired production—a central tenet of collapses (Cooke 1984)—and if used in conjunction with fisheries pressure information, it can help to disentangle natural fluctuations from successful management scenarios.

In light of our results, we propose two methods to improve multi-stock collapse analyses. Firstly, definitions could be implemented within a Bayesian framework to account for uncertainties in biomass estimates by generating distributional thresholds. A common limitation of fish stock collapse definitions is that the generation of collapse thresholds may be sensitive to interannual fluctuations in abundance due to environmental stochasticity and/or uncertainty in the estimates of abundance (Aagaard et al. 2016). For instance, spikes in biomass due to large recruitment events. Although time series smoothing would help to remove fluctuations, a Bayesian approach would be more appropriate as it takes into account uncertainty in abundance estimates (Aagaard et al. 2016).

Secondly, we suggest estimating the collapse status of fish stocks using multiple definitions. Including several definitions in stock status analyses and reporting (dis-)agreement among these definitions provides a more robust approach to status categorisations than single collapse definition assessments. A critical benefit of the multi-definition approach is that using a suite of collapse criteria allows reporting uncertainty in the collapse status categorisation of fish stocks. In doing so, such approaches will enhance our ability to interpret seemingly biased (overly optimistic or pessimistic) research results and reduce controversy. Transparency in the uncertainty of definitions used contributes to the stringent communication of science and the state of natural resources to the public and policy-makers, aiding in the allocation of limited management resources to the most severe cases. In doing so, it can reduce both alarmist and overly optimistic collapse reporting to those cases where fish stock declines actually imply severe risks for fish production and ecosystem functioning. Furthermore, multi-definition collapse assessments can support policy-making fisheries management by acknowledging diversity in fish stock dynamics instead of practicing "one size fits all" approaches.

5. Conclusions

The past two decades have witnessed considerable scientific debate regarding the state of the world's fish stocks and the occurrence rate of collapses. The importance of reliable statistics and status assessments of the world's fisheries is increasingly acknowledged as the fraction of sustainable fished fish stocks in the world has decreased concomitant with increase in per capita fish consumption (FAO 2020). Our work shows that multi-stock analyses using single criteria are unreliable and contribute to diverging views on the collapse state of fish stocks. We suggest that to obtain a more robust view of the global collapsed state, multiple collapse definitions should be applied in multi-stock assessments.

This approach would generate greater certainty in collapse classifications which is required for sustainable fisheries management.

Data availability

Data sources for the time series analysis and collapse definitions are listed in the Supplementary Materials.

Acknowledgements

This paper is a result of two workshops organised within the Nordic Centre of Excellence NorMER programme. We thank the Nordic Centre of Excellence NorMER programme early career scientists for their great contribution towards the literature review and collapse discussions. We would like to thank Jeff Hutchings and Keith Brander for valuable comments on the "collapse" problematics.

Funding

This paper is a deliverable of the Nordic Centre for Research on Marine Ecosystems and Resources under Climate Change (NorMER), which is funded by the Norden Top-level Research Initiative sub-programme 'Effect Studies and Adaptation to Climate Change'. In addition, GO was supported by the Research Council of Norway through the projects CoDINA, grant no. 255460/E40 and ADMAR, grant no. 200497/130, ML and KHA were funded by the Centre for Ocean Life, a VKR Centre of Excellence supported by the Villum foundation was supported by the Åbo Akademi University Foundation.

References

Aagaard, K., Lockwood, J.L., Green, E.J., 2016. A Bayesian approach for characterizing uncertainty in declaring a population collapse. Ecol. Modell. 328, 78–84. https://doi.org/10.1016/j.ecolmodel.2016.02.014

Bonanomi, S., Pellissier, L., Therkildsen, N.O., Hedeholm, R.B., Retzel, A., Meldrup, D., Olsen, S.M., Nielsen, A., Pampoulie, C., Hemmer-Hansen, J., Wisz, M.S., Grønkjær, P., Nielsen, E.E., 2015. Archived DNA reveals fisheries and climate induced collapse of a major fishery. Sci. Rep. 5, 1–8. https://doi.org/10.1038/srep15395

Branch, T.A., 2008. Not all fisheries will be collapsed in 2048. Mar. Policy 32, 38–39. https://doi.org/10.1016/j.marpol.2007.04.001

Branch, T.A., Jensen, O.P., Ricard, D., Ye, Y., Hilborn, R., 2011. Contrasting Global Trends in Marine Fishery Status Obtained from Catches and from Stock Assessments. Conserv. Biol. 25, 777–786. https://doi.org/10.1111/j.1523-1739.2011.01687.x

Buren, A.D., Murphy, H.M., Adamack, A.T., Davoren, G.K., Koen-Alonso, M., Montevecchi, W.A., Mowbray, F.K., Pepin, P., Regular, P.M., Robert, D., Rose, G.A., Stenson, G.B., Varkey, D., 2019. The collapse and continued low productivity of a keystone forage fish species. Mar. Ecol. Prog. Ser. 616, 155–170. https://doi.org/10.3354/meps12924

Cook, R.M., 2019. Stock collapse or stock recovery? Contrasting perceptions of a depleted cod stock. ICES J. Mar. Sci. 76, 787–793. https://doi.org/10.1093/icesjms/fsy190

Cook, R.M., 2013. A comment on "What catch data can tell us about the status of global fisheries" (Froese et al. 2012). Mar. Biol. 160, 1761–1763. https://doi.org/10.1007/s00227-013-2183-y

Cook, R.M., Sinclair, A., Stefánsson, G., 1997. Potential collapse of North Sea cod stocks. Nature. https://doi.org/10.1038/385521a0

Cooke, J.G., 1984. Glossary of technical terms. Exploit. Mar. Communities 341.

Costello, C., Ovando, D., Hilborn, R., Gaines, S.D., Deschenes, O., Lester, S.E., 2012. Status and solutions for the world's unassessed fisheries. Science (80-.). 338, 517–520. https://doi.org/10.1126/science.1223389

Cumming, G.S., Peterson, G.D., 2017. Unifying Research on Social–Ecological Resilience and Collapse. Trends Ecol. Evol. 32, 695–713. https://doi.org/10.1016/j.tree.2017.06.014

Dodson, J.J., Tremblay, S., Colombani, F., Carscadden, J.E., Lecomte, F., 2007. Trans-Arctic dispersals and the evolution of a circumpolar marine fish species complex, the capelin (Mallotus villosus). Mol. Ecol. 16, 5030–5043. https://doi.org/10.1111/j.1365-294X.2007.03559.x

Essington, T.E., Moriarty, P.E., Froehlich, H.E., Hodgson, E.E., Koehn, L.E., Oken, K.L., Siple, M.C., Stawitz, C.C., 2015. Fishing amplifies forage fish population collapses. Proc. Natl. Acad. Sci. U. S. A. 112, 6648–6652. https://doi.org/10.1073/pnas.1422020112

FAO, 2020. The State of World Fisheries and Aquaculture 2020. Sustainability in action. Rome.

Fernandes, P.G., Cook, R.M., 2013. Reversal of fish stock decline in the northeast atlantic. Curr. Biol. 23, 1432–1437. https://doi.org/10.1016/j.cub.2013.06.016

Froese, R., Coro, G., Kleisner, K., Demirel, N., 2016. Revisiting safe biological limits in fisheries. Fish Fish. 17, 193–209. https://doi.org/10.1111/faf.12102

Froese, R., Zeller, D., Kleisner, K., Pauly, D., 2012. What catch data can tell us about the status of global fisheries. Mar. Biol. 159, 1283–1292. https://doi.org/10.1007/s00227-012-1909-6

Hammerschlag, N., Schmitz, O.J., Flecker, A.S., Lafferty, K.D., Sih, A., Atwood, T.B., Gallagher, A.J., Irschick, D.J., Skubel, R., Cooke, S.J., 2019. Ecosystem Function and Services of Aquatic Predators in the Anthropocene. Trends Ecol. Evol. 34, 369–383. https://doi.org/10.1016/j.tree.2019.01.005

Hilborn, R., 2007. Reinterpreting the state of fisheries and their management. Ecosystems 10, 1362–1369. https://doi.org/10.1007/s10021-007-9100-5

Hilborn, R., Amoroso, R.O., Anderson, C.M., Baum, J.K., Branch, T.A., Costello, C., De Moor, C.L., Faraj, A., Hively, D., Jensen, O.P., Kurota, H., Little, L.R., Mace, P., McClanahan, T., Melnychuk, M.C., Minto, C., Osio, G.C., Parma, A.M., Pons, M., Segurado, S., Szuwalski, C.S., Wilson, J.R., Ye, Y., 2020. Effective fisheries management instrumental in improving fish stock status. Proc. Natl. Acad. Sci. U. S.

A. 117, 2218–2224. https://doi.org/10.1073/pnas.1909726116

Hutchings, J.A., 2000. Collapse and recovery of marine fishes. Nature 406, 882–885.

Hutchings, J.A., Kuparinen, A., 2017. Empirical links between natural mortality and recovery in marine fishes. Proc. R. Soc. B Biol. Sci. 284. https://doi.org/10.1098/rspb.2017.0693

Hutchings, J.A., Reynolds, J.D., 2004. Marine fish population collapses: Consequences for recovery and extinction risk. Bioscience 54, 297–309. https://doi.org/10.1641/0006-3568(2004)054[0297:MFPCCF]2.0.CO;2

ICES, 2019. ICES Stock Assessment Database [accessed 1st January 2019].

ICES, 2018. ICES reference points for stocks in categories 3 and 4, in: ICES Technical Guidelines. Copenhagen, Denmark, p. 50. https://doi.org/10.17895/ices.pub.4128

ICES, 2017. ICES fisheries management reference points for category 1 and 2 stocks, in: ICES Advice Technical Guidelines. Copenhagen, Denmark, p. 19. https://doi.org/10.17895/ices.pub.3036

ICES, 2003. Report of the Study Group on the Further Development of the Precautionary Approach to Fishery Management, in: ICES Document CM 2003/ ACFM: 15. Copenhagen, p. 144.

IUCN, 2012. IUCN Red List Categories and Criteria: Version 3.1, 2nd ed. Gland, Switzerland and Cambridge, UK: IUCN.

Jackson, J.B.C., Kirby, M.X., Berger, W.H., Bjorndal, K.A., Botsford, L.W., Bourque, B.J., Bradbury, R.H., Cooke, R., Erlandson, J., Estes, J.A., Hughes, T.P., Kidwell, S., Lange, C.B., Lenihan, H.S., Pandolfi, J.M., Peterson, C.H., Steneck, R.S., Tegner, M.J., Warner, R.R., 2001. Historical overfishing and the recent collapse of coastal ecosystems. Science (80-.). 293, 629–637. https://doi.org/10.1126/science.1059199

Kindsvater, H.K., Mangel, M., Reynolds, J.D., Dulvy, N.K., 2016. Ten principles from evolutionary ecology essential for effective marine conservation. Ecol. Evol. 6, 2125–2138. https://doi.org/10.1002/ece3.2012

Lindegren, M., Möllmann, C., Nielsen, A., Stenseth, N.C., 2009. Preventing the collapse of the Baltic cod stock through an ecosystem-based management approach. Proc. Natl. Acad. Sci. U. S. A. 106, 14722–14727. https://doi.org/10.1073/pnas.0906620106

Lotze, H.K., Coll, M., Magera, A.M., Ward-Paige, C., Airoldi, L., 2011. Recovery of marine animal populations and ecosystems. Trends Ecol. Evol. 26, 595–605. https://doi.org/10.1016/j.tree.2011.07.008

Mace, G.M., Collar, N.J., Gaston, K.J., Hilton-Taylor, C., Akçakaya, H.R., Leader-Williams, N., Milner-Gulland, E.J., Stuart, S.N., 2008. Quantification of extinction risk: IUCN's system for classifying threatened species. Conserv. Biol. 22, 1424–1442. https://doi.org/10.1111/j.1523-1739.2008.01044.x

Myers, R.A., Hutchings, J.A., Barrowman, N.J., 1997. Why do fish stocks collapse? The example of cod in Atlantic Canada. Ecol. Appl. 7, 91–106. https://doi.org/10.1890/1051-0761(1997)007[0091:WDFSCT]2.0.CO;2

Myers, R.A., Worm, B., 2003. Rapid worldwide depletion of predatory fish communities. Nature 423, 280–283.

Neubauer, P., Jensen, O.P., Hutchings, J.A., Baum, J.K., 2013. Resilience and recovery of overexploited marine populations. Science (80-.). 340, 347–349. https://doi.org/10.1126/science.1230441

Pauly, D., 1995. Anecdotes and the shifting baseline syndrome of fisheries. Trends Ecol. Evol. 10, 430. https://doi.org/10.1016/S0169-5347(00)89171-5

Pauly, D., Watson, R., Alder, J., 2005. Global trends in world fisheries: impacts on marine ecosystems and food security. Philos. Trans. R. Soc. B Biol. Sci. 360, 5–12.

Pedersen, E.J., Thompson, P.L., Ball, R.A., Fortin, M.J., Gouhier, T.C., Link, H., Moritz, C., Nenzen, H., Stanley, R.R.E., Taranu, Z.E., Gonzalez, A., Guichard, F., Pepin, P., 2017. Signatures of the collapse and incipient recovery of an overexploited marine ecosystem. R. Soc. Open Sci. 4. https://doi.org/10.1098/rsos.170215

Petitgas, P., Secor, D.H., McQuinn, I., Huse, G., Lo, N., 2010. Stock collapses and their recovery: Mechanisms that establish and maintain life-cycle closure in space and time. ICES J. Mar. Sci. 67, 1841–1848. https://doi.org/10.1093/icesjms/fsq082

Pikitch, E.K., Santora, C., Babcock, E.A., Bakun, A., Bonfil, R., Conover, D.O., Dayton, P., Doukakis, P., Fluharty, D., Heneman, B., Houde, E.D., Link, J., Livingston, P.A., M, M., McAllister, M.K., Pope, J., Sainsbury, K.J., 2004. Ecosystem-Based Fishery Management. Science (80-.). 305, 346–348.

Pinsky, M.L., Byler, D., 2015. Fishing, fast growth and climate variability increase the risk of collapse. Proc. R. Soc. B Biol. Sci. 282, 1–9. https://doi.org/10.1098/rspb.2015.1053

Reynolds, J.D., Dulvy, N.K., Goodwin, N.B., Hutchings, J.A., 2005. Biology of extinction risk in marine fishes. Proc. R. Soc. B Biol. Sci. 272, 2337–2344. https://doi.org/10.1098/rspb.2005.3281

Rindorf, A., Cardinale, M., Shephard, S., De Oliveira, J.A.A., Hjorleifsson, E., Kempf, A., Luzenczyk, A., Millar, C., Miller, D.C.M., Needle, C.L., Simmonds, J., Vinther, M., 2017. Fishing for MSY: Using “pretty good yield” ranges without impairing recruitment. ICES J. Mar. Sci. 74, 525–534. https://doi.org/10.1093/icesjms/fsw111

Salomon, A.K., Gaichas, S.K., Jensen, O.P., Agostini, V.N., Sloan, N.A., Rice, J., McClanahan, T.R., Ruckelshaus, M.H., Levin, P.S., Dulvy, N.K., Babcock, E.A., 2011. Bridging the divide between fisheries and marine conservation science. Bull. Mar. Sci. 87, 251–274. https://doi.org/10.5343/bms.2010.1089

Stokstad, E., 2009. Global fisheries: Détente in the fisheries war. Science (80-.). 324, 170–171. https://doi.org/10.1126/science.324.5924.170

Toresen, R., Østvedt, O.J., 2008. Variation in abundance of Norwegian spring-spawning herring (Clupea harengus, Clupeidae) throughout the 20th century and the influence of climatic fluctuations. Fish Fish. 1, 231–256. https://doi.org/10.1111/j.1467-2979.2000.00022.x

Worm, B., Barbier, E.B., Beaumont, N., Duffy, J.E., Folke, C., Halpern, B.S., Jackson, J.B.C., Lotze, H.K., Micheli, F., Palumbi, S.R., Sala, E., Selkoe, J.J.S., Watson, R., 2006. Impacts of Biodiversity Loss on Ocean Ecosystem Services. Science (80-.).

314, 787–791. https://doi.org/10.1126/science.1132294

Worm, B., Hilborn, R., Baum, J.K., Branch, T.A., Collie, J.S., Costello, C., Fogarty, M.J., Fulton, E.A., Hutchings, J.A., Jennings, S., Jensen, O.P., Lotze, H.K., Mace, P.M., McClanahan, T.R., Minto, C., Palumbi, S.R., Parma, A.M., Ricard, D., Rosenberg, A.A., Watson, R., Zeller, D., 2009. Rebuilding Global Fisheries. Science (80-.). 325, 578–585. https://doi.org/10.1126/science.1173146

Supplementary materials for:

When is a fish stock collapsed?

J. Yletyinen and W.E. Butler, G. Ottersen, K.H. Andersen, S. Bonanomi, F.K. Diekert, C. Folke, M. Lindegren, M.C. Nordström, A. Richter, L. Rogers, G. Romagnoni, B. Weigel, J.D. Whittington, T. Blenckner and N.C. Stenseth

Appendix A: Tables

- A1: Fish stock collapse definitions found in the literature review.
- A2: ICES fish stocks used in the analyses.
- A3: Region codes used for stock identification.

Appendix B: Supplementary graphs

- B1: Individual multi-definition graphs for each stock

***Table A1**: The collapse definitions found in the literature search that are applied in the analyses. Columns show the indicator of stock size used (SSB = spawning stock biomass; TB = total biomass), the actual definition and its source(s), and to which specific components of our collapse framework the definition relates (see Fig. 1 in the main article).*

ID	Indicator	Collapsed definition	Definition type	Source
1	TB	< 20% TB_{MSY} (equivalent to < 10% virgin biomass under Schaefer model)	Depletion	Branch et al. 2011, Costello et al. 2012, Pinsky et al. 2011, Thorson et al. 2012; Pinsky and Byler 2015; Worm et al. 2009
2		< 20% TB_{MSY} for 4 consecutive years	Prolonged depletion	Pinsky and Byler 2015
3	SSB	< 25% maximum historical value	Depletion	Frank et al. 2005, Myers et al. 1997, Fricke 2015
4		< 10% maximum historical value		
5		< 6% maximum historical value		
6		< 5% maximum historical value		
7		< 3% maximum historical value		
8		< 1% maximum historical value		
9		< 20% SSB_{MSY}		Branch et al. 2011, Costello et al. 2012, Thorson et al. 2012
10		< 10% SSB_{MSY}		Froese et al. 2012
11		< Bpa		Lindegren et al. 2009 (collapsed below ecologically safe levels)
12		< Blim		

13		80% decline in the maximum of 10 years or 3 generations	Rate of decline	Post et al. 2002
14		90% decline in the maximum of 10 years or 3 generations		MacKenzie et al. 2009
15.1 15.2	TB SSB	< 25% of mean TB/SSB	Depletion	Essington et al. 2015
16	Catches	< 10% of maximum recorded catch	Depletion	Branch et al. 2011; Costello et al. 2008; Froese & Kesner-Reyes 2002; Froese et al. 2012; Grainger & Costello 2014; Worm et al. 2006
17		≤ 10% of any previous annual catch		Mutsert et al. 2008
18		< 20% of MSY		Froese et al. 2012
19		< 10% of maximum recorded catch for 4 consecutive years	Prolonged depletion	Mullon et al. 2005
20		≤ 10% of any previous annual catch for 1.5 generations		Mutsert et al. 2008
21.1 21.2 21.3	TB SSB Catches	70% decline within the maximum of three generations or 10 years & the subsequent biomass remains below the threshold for 1 generation	Rate of decline & Prolonged depletion	Collapse definition proposed in this paper
22.1	TB	80% decline within the maximum of		

22.2 22.3	SSB Catches	three generations or 10 years & the subsequent biomass remains below the threshold for 1 generation		
23.1 23.2 23.3	TB SSB Catches	90% decline within the maximum of three generations or 10 years & the subsequent biomass remains below the threshold for 1 generation		

***Table A2**: Description of stocks utilised in the analyses. Stock ID refers to the ICES codes. The time-series span begins in the 1900's and ends in the 2000's for all stocks. All stocks had collapsed at some point in the past according to the < B_{lim} definition, the year that each stock first collapsed (YOC) and its present status (PS), i.e., status in the last year evaluated, are shown according to this definition. In the PS column, "C" and "NC" denote collapsed and not collapsed states respectively.*

Stock ID	Stock	Species	T-S	YOC	PS
ane.27.8	Anchovy (BoB)	*Engraulis encrasicolus*	87-18	1989	NC
bss.27.4bc7ad-h	Seabass (cNS.IS.EC.BC.CS)	*Dicentrarchus labrax*	85-18	2016	C
cap.27.1-2	Capelin (BS)	*Mallotus villosus*	72-18	1986	NC
cod.21.1	Cod (WG)	*Gadus morhua*	76-18	1992	NC
cod.2127.1f14	Cod (EG.SG)	*Gadus morhua*	73-18	1993	NC
cod.27.1-2	Cod (NEA)	*Gadus morhua*	46-18	1957	NC
cod.27.47d20	Cod (NS.EEC.Sk)	*Gadus morhua*	63-18	1989	NC
cod.27.5a	Cod (IG)	*Gadus morhua*	55-18	1993	NC
cod.27.5b1	Cod (FP)	*Gadus morhua*	59-18	1992	NC
cod.27.6a	Cod (WS)	*Gadus morhua*	81-17	1992	C
cod.27.7a	Cod (IS)	*Gadus morhua*	68-18	1993	NC
cod.27.7e-k	Cod (EEC.SCS)	*Gadus morhua*	71-18	2004	C
had.27.1-2	Haddock (NEA)	*Melanogrammus aeglefinus*	50-18	1985	NC
had.27.46a20	Haddock (NS.WS.Sk)	*Melanogrammus aeglefinus*	72-18	1979	NC
had.27.5b	Haddock (FG)	*Melanogrammus aeglefinus*	57-18	1994	NC
had.27.6b	Haddock (R)	*Melanogrammus aeglefinus*	91-18	2001	NC
her.27.20-24	Herring (Sk.KT.WB)	*Clupea harengus*	91-18	2007	C
her.27.25-2932	Herring (CBS)	*Clupea harengus*	74-18	2001	NC
her.27.3a47d	Herring (NS.Sk.Kt.EEC)	*Clupea harengus*	47-18	1968	NC
her.27.6a7bc	Herring (wS.wI)	*Clupea harengus*	57-18	1976	C
her.27.nirs	Herring (IS)	*Clupea harengus*	80-18	1996	NC
hke.27.3a46-	Hake (GNS.nBoB)	*Merluccius merluccius*	78-18	1994	NC
hke.27.8c9a	Hake (CtS.AIW)	*Merluccius*	82-18	1995	NC
ldb.27.8c9a	Four-spot megrim	*Lepidorhombus boscii*	86-17	2001	NC
mac.27.nea	Mackerel (NEAaw)	*Scomber scombrus*	80-18	2002	NC
meg.27.8c9a	Megrim (CtS.AIW)	*L. whiffiagonis*	86-18	2008	NC
mon.27.8c9a	White anglerfish	*Lophius piscatorius*	80-18	1993	NC
nop.27.3a4	Norway pout (NS.Sk.Kt)	*Trisopterus esmarkii*	84-18	1986	NC
pil.27.8c9a	Sardine (CtS.AIW)	*Sardina pilchardus*	78-18	2000	C
ple.27.420	Plaice (NS.Sk)	*Pleuronectes platessa*	57-18	1996	NC
ple.27.7a	Plaice (IS)	*Pleuronectes platessa*	81-18	1995	NC
pok.27.1-2	Saithe (NEA)	*Pollachius virens*	60-18	1985	NC
reg.27.1-2	Golden redfish (NEA)	*Sebastes norvegicus*	90-17	2008	C
reg.27.561214	Golden redfish	*Sebastes norvegicus*	71-18	1993	NC
san.sa.1r	Sandeel (csNS.DB)	*Ammodytes*	83-18	2004	NC
san.sa.2r	Sandeel (Sk.csNS)	*Ammodytes*	83-18	1989	NC
san.sa.3r	Sandeel (Sk.ncNS)	*Ammodytes*	86-18	1986	NC
san.sa.4	Sandeel (ncNS)	*Ammodytes*	93-18	2008	NC
sol.27.4	Sole (NS)	*Solea solea*	57-18	1998	NC
sol.27.7a	Sole (IS)	*Solea solea*	70-18	2004	C
sol.27.7fg	Sole (BC.CS)	*Solea solea*	71-18	1998	NC
spr.27.4	Sprat (NS)	*Sprattus sprattus*	74-18	1982	NC
whg.27.6a	Whiting (WS)	*Merlangius merlangus*	81-18	1989	C
whg.27.7a	Whiting (IS)	*Merlangius merlangus*	80-17	1993	C

***Table A3**: Region codes for stock identification.*

Region code	Region
AIW	Atlantic Iberian Waters
BC	Bristol Channel
BoB	Bay of Biscay
BS	Barents Sea
CBS	Central Baltic Sea
cNS	Central and Southern North Sea
CS	Celtic Sea
csNS	Central and Southern North Sea
CtS	Cantabrian Sea
DB	Dogger Bank
eAIW	East Atlantic Iberian Waters
EC	English Channel
EEC	East English Channel
EG	East Greenland
FG	Faroes Grounds
FP	Faroes Plateau
GNS	Greater North Sea
IG	Iceland Grounds
IS	Irish Sea
Kt	Kattegat
NA	North of Azores
nBoB	Northern Bay of Biscay
ncNS	Northern and Central North Sea
NEA	Northeast Arctic
NEAaw	Northeast Atlantic and Adjacent Waters
NS	North Sea
R	Rockall
sBoB	Southern Bay of Biscay
SCS	Southern Celtic Sea
SG	South Greenland
Sk	Skagerrak
WB	Western Baltic
WG	West Greenland
WI	West of Ireland
WS	West of Scotland

References not included in the main article:

Costello, C., Gaines, S.D., Lynham, J., 2008. Can Catch Shares Prevent Fisheries Collapse? Science (80-.). 321, 1678–1681. https://doi.org/10.5040/9780755621101.0007

De Mutsert, K., Cowan, J.H., Essington, T.E., Hilborn, R., 2008. Reanalyses of Gulf of Mexico fisheries data: Landings can be misleading in assessments of fisheries and fisheries ecosystems. Proc. Natl. Acad. Sci. U. S. A. 105, 2740–2744. https://doi.org/10.1073/pnas.0704354105

Frank, K.T., Petrie, B., Choi, J.S., Leggett, W.C., 2005. Ecology: Trophic cascades in a formerly cod-dominated ecosystem. Science (80-.). 308, 1621–1623. https://doi.org/10.1126/science.1113075

Fricke, L., 2015. The economics of regime shifts in marine ecosystems. University of Kiel.

Froese, R., Kesner-Reyes, K., 2002. Impact of fishing on the abundance of marine species. ICES C. L, 12.

Grainger, C.A., Costello, C.J., 2014. Capitalizing property rights insecurity in natural resource assets. J. Environ. Econ. Manage. 67, 224–240. https://doi.org/10.1016/j.jeem.2013.12.005

MacKenzie, B.R., Mosegaard, H., Rosenberg, A.A., 2009. Impending collapse of bluefin tuna in the northeast Atlantic and Mediterranean. Conserv. Lett. 2, 26–35. https://doi.org/10.1111/j.1755-263x.2008.00039.x

Mullon, C., Fréon, P., Cury, P., 2005. The dynamics of collapse in world fisheries. Fish Fish. 6, 111–120. https://doi.org/10.1111/j.1467-2979.2005.00181.x

Pinsky, M.L., Jensen, O.P., Ricard, D., Palumbi, S.R., 2011. Unexpected patterns of fisheries collapse in the world's oceans. Proc. Natl. Acad. Sci. U. S. A. 108, 8317–8322. https://doi.org/10.1073/pnas.1015313108

Post, J.R., Sullivan, M., Cox, S., Lester, N.P., Walters, C.J., Eric, A., Paul, A.J., Jackson, L., Shuter, B.J., 2002. Canada's Recreational Fisheries: The Invisible Collapse? Fisheries 27, 6–17. https://doi.org/10.1577/1548-8446(2002)027<0006

Thorson, J.T., Branch, T.A., Jensen, O.P., 2012. Using model-based inference to evaluate global fisheries status from landings, location, and life history data. Can. J. Fish. Aquat. Sci. 69, 645–655. https://doi.org/10.1139/F2012-016

Appendix B: Individual multi-definition graphs for each stock

Figure caption:

Figure B1*: Stock summaries for the literature/proposed definitions (panels A, B, C) and the simulated definitions (panels (D, E, F). Panels A and D show the proportions of true positive (TP), false negative (FN), and false positive (FP) classifications for each definition. Panes B and E show the* F_1 *score for each definition. Panels C shows time-series classifications for the top 3 literature (including proposed) definitions. Panel F shows the top simulated definition for three reference biomasses: the population mean (PM), the historical maximum (H. max) and the recent maximum (R. Max), i.e. the maximum within 3 generations (n). The time-series classification from the benchmark definition (SSB <* B_{lim}*) is shown at the top of each page.*

Anchovy (BoB) − ane.27.8

Abbreviations

TP = True positive
FN = False negative
FP = False positive
HM = Historic maximum
RM.3n = Recent maximum (within 3 n)
PM = Population mean
n = Generation length
B_{ref} = Reference biomass
TH = Threshold
t = tonne

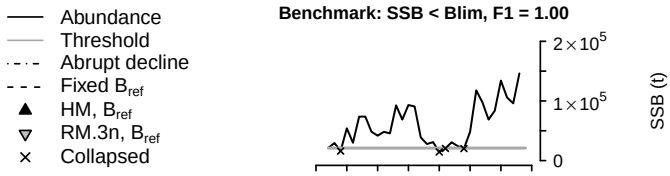

Literature and proposed definitions

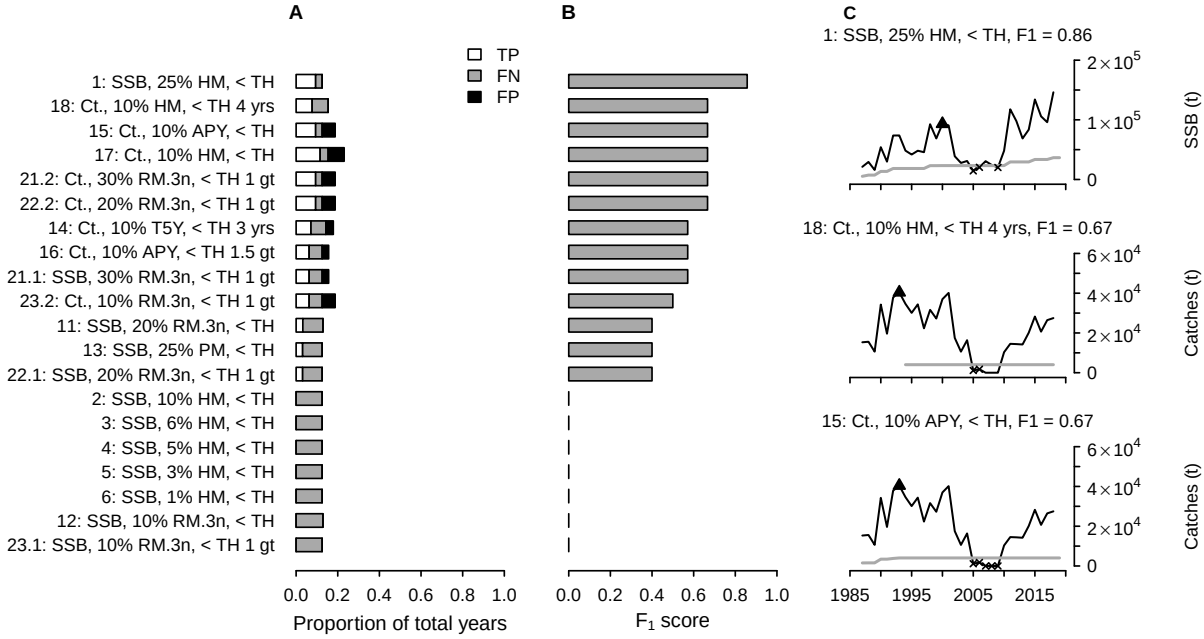

Simulated definitions

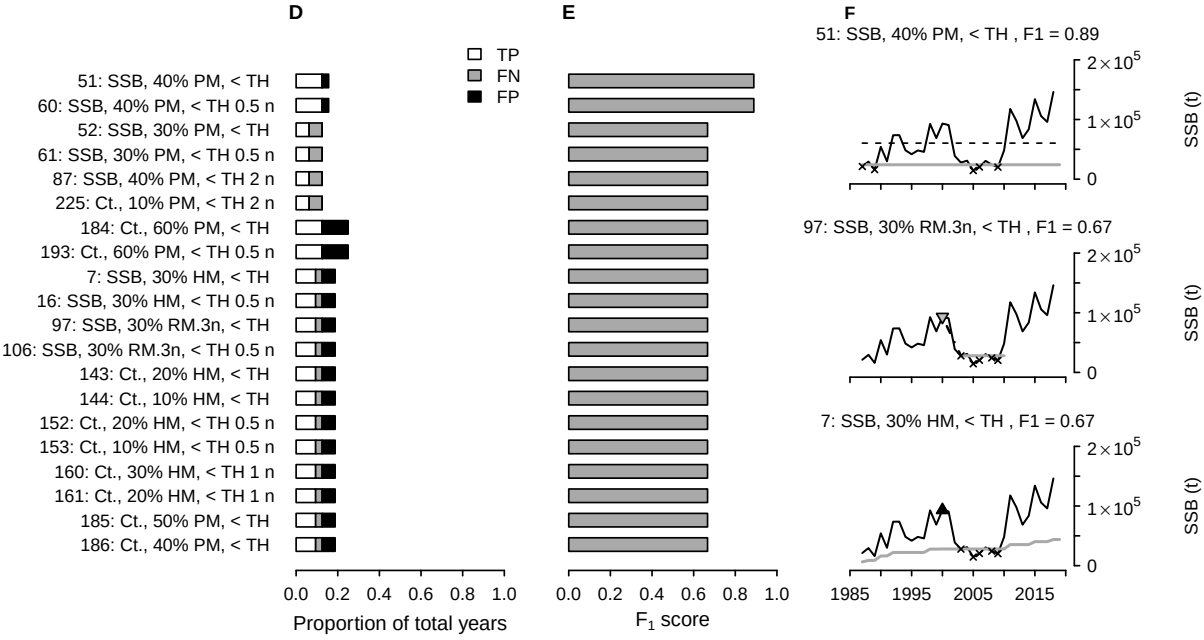

Seabass (csNS.IS.EC.BC.CS) − bss.27.4bc7ad−h

Abbreviations

TP = True positive
FN = False negative
FP = False positive
HM = Historic maximum
RM.3n = Recent maximum (within 3 n)
PM = Population mean
n = Generation length
B_{ref} = Reference biomass
TH = Threshold
t = tonne

Abundance
Threshold
Abrupt decline
Fixed B_{ref}
HM, B_{ref}
RM.3n, B_{ref}
Collapsed

Benchmark: SSB < Blim, F1 = 1.00

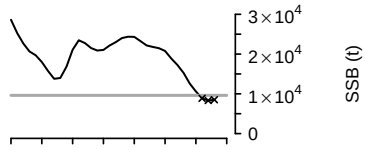

Literature and proposed definitions

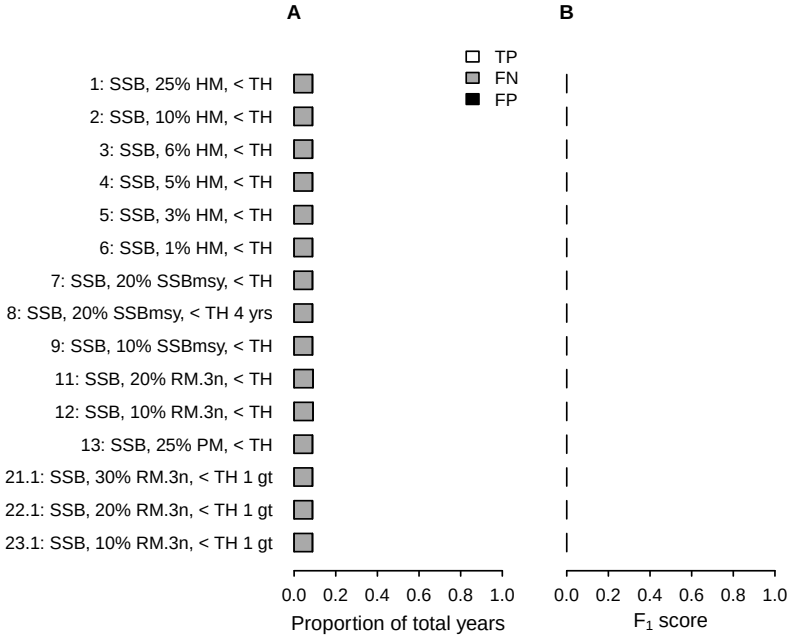

Simulated definitions

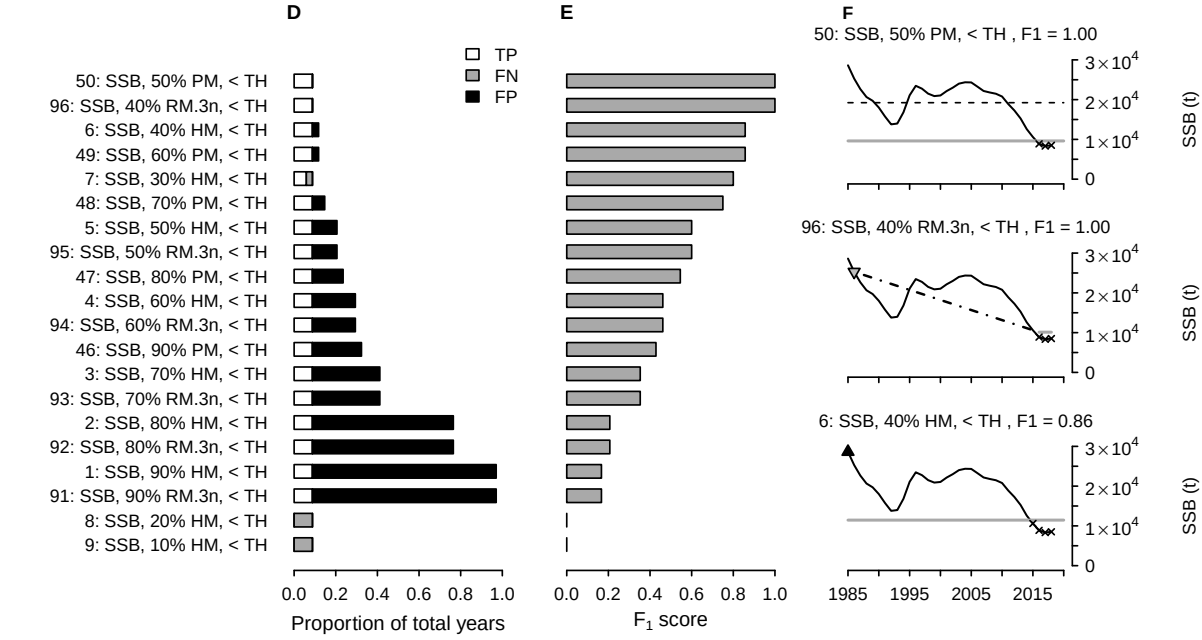

Capelin (BS) − cap.27.1−2

Abbreviations

TP = True positive
FN = False negative
FP = False positive
HM = Historic maximum
RM.3n = Recent maximum (within 3 n)
PM = Population mean
n = Generation length
B_{ref} = Reference biomass
TH = Threshold
t = tonne

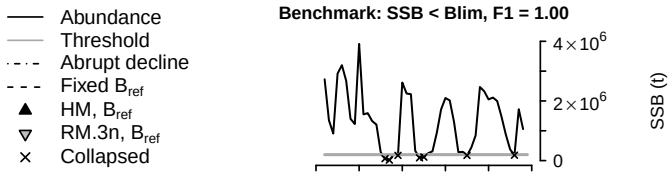

Literature and proposed definitions

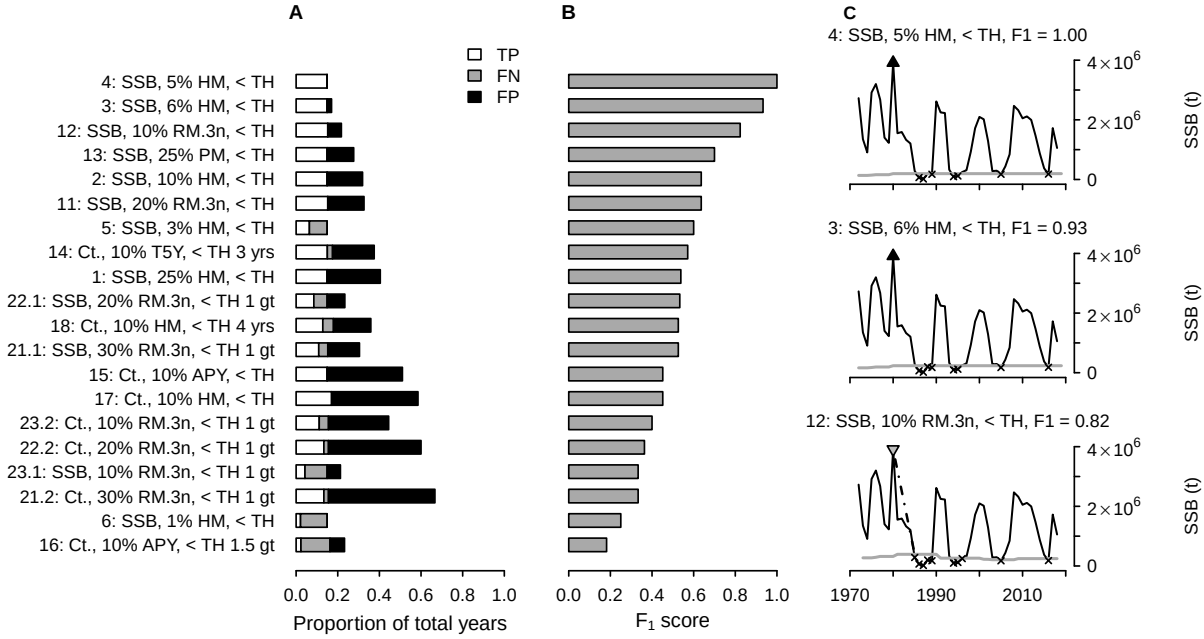

Simulated definitions

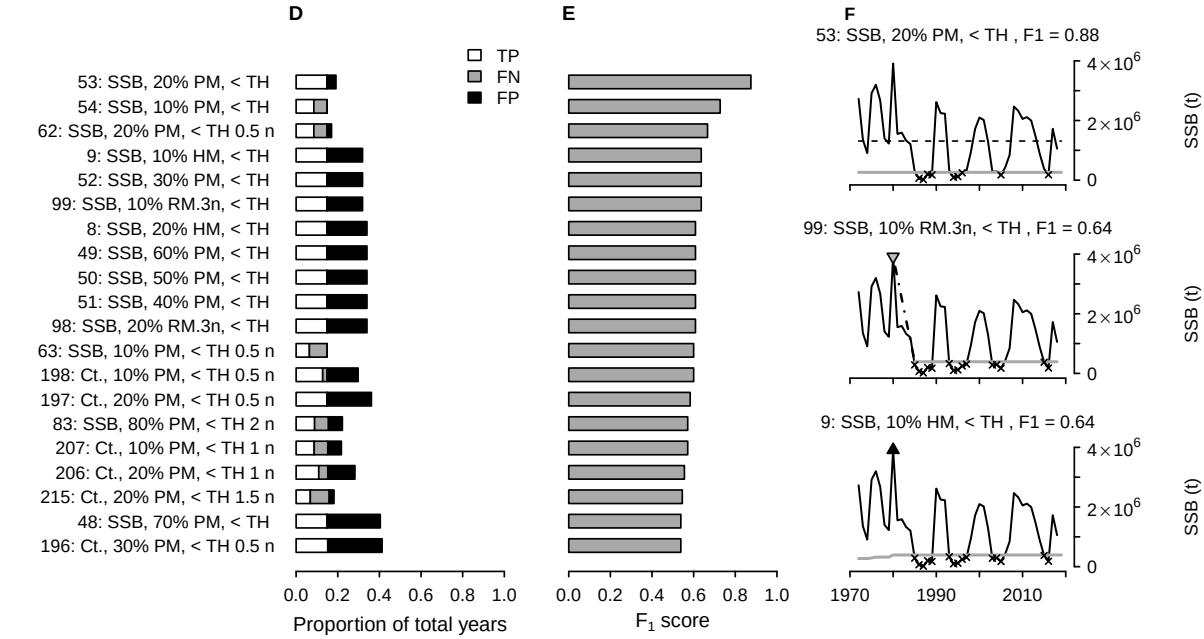

Cod (WG) − cod.21.1

Abbreviations

TP = True positive
FN = False negative
FP = False positive
HM = Historic maximum
RM.3n = Recent maximum (within 3 n)
PM = Population mean
n = Generation length
B_{ref} = Reference biomass
TH = Threshold
t = tonne

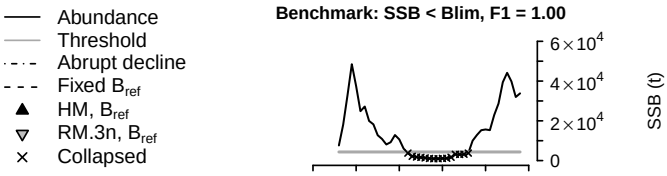

Literature and proposed definitions

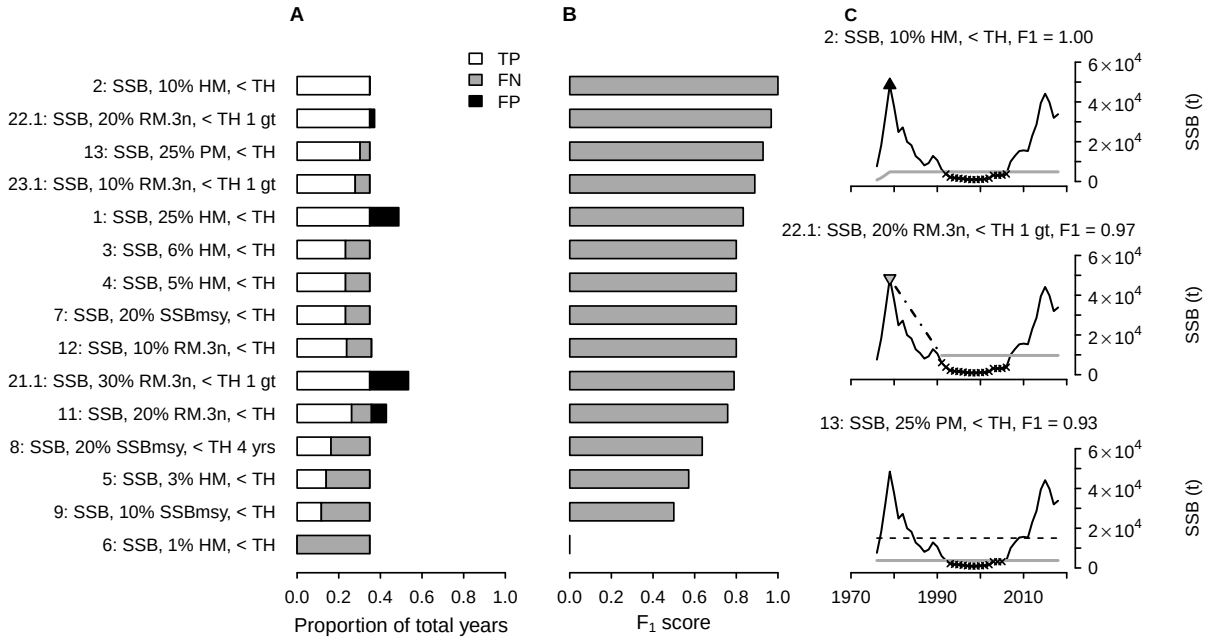

Simulated definitions

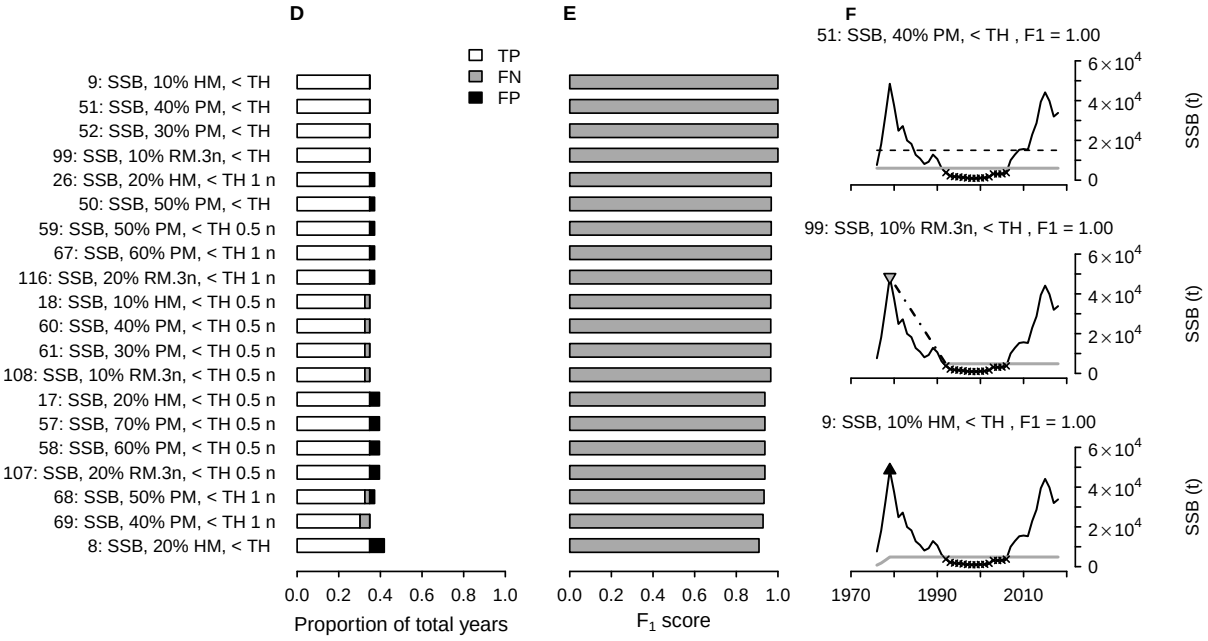

Cod (EG.SG) − cod.2127.1f14

Abbreviations

TP = True positive
FN = False negative
FP = False positive
HM = Historic maximum
RM.3n = Recent maximum (within 3 n)
PM = Population mean
n = Generation length
B_{ref} = Reference biomass
TH = Threshold
t = tonne

Abundance
Threshold
Abrupt decline
Fixed B_{ref}
HM, B_{ref}
RM.3n, B_{ref}
Collapsed

Benchmark: SSB < Blim, F1 = 1.00

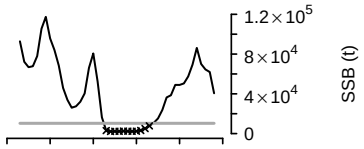

Literature and proposed definitions

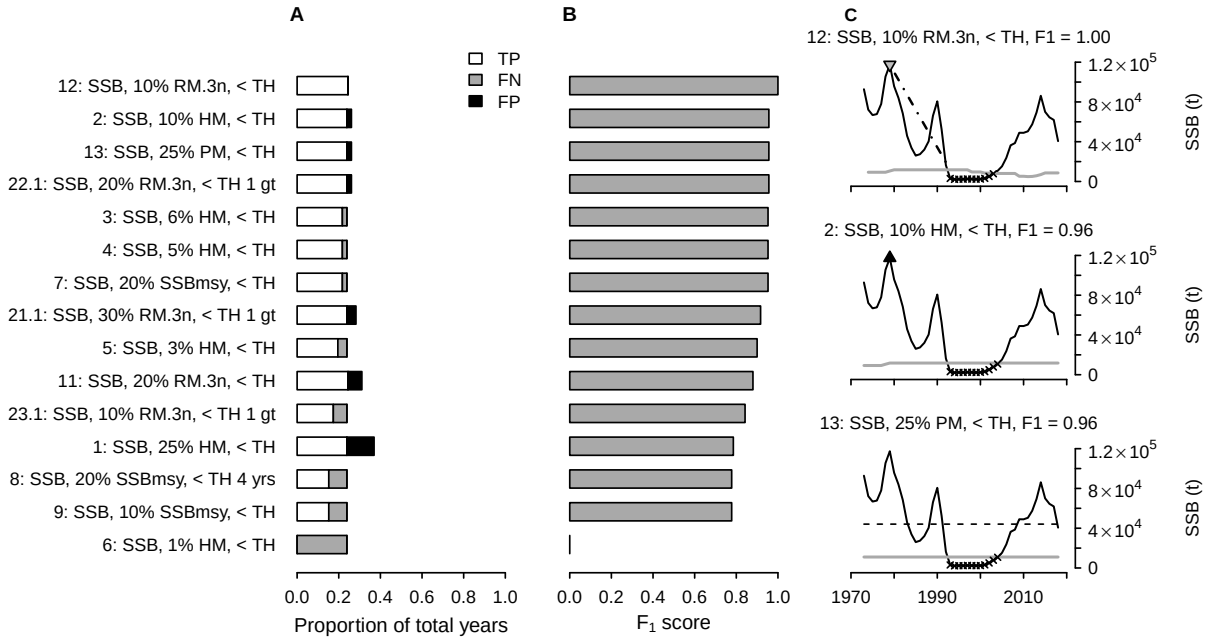

Simulated definitions

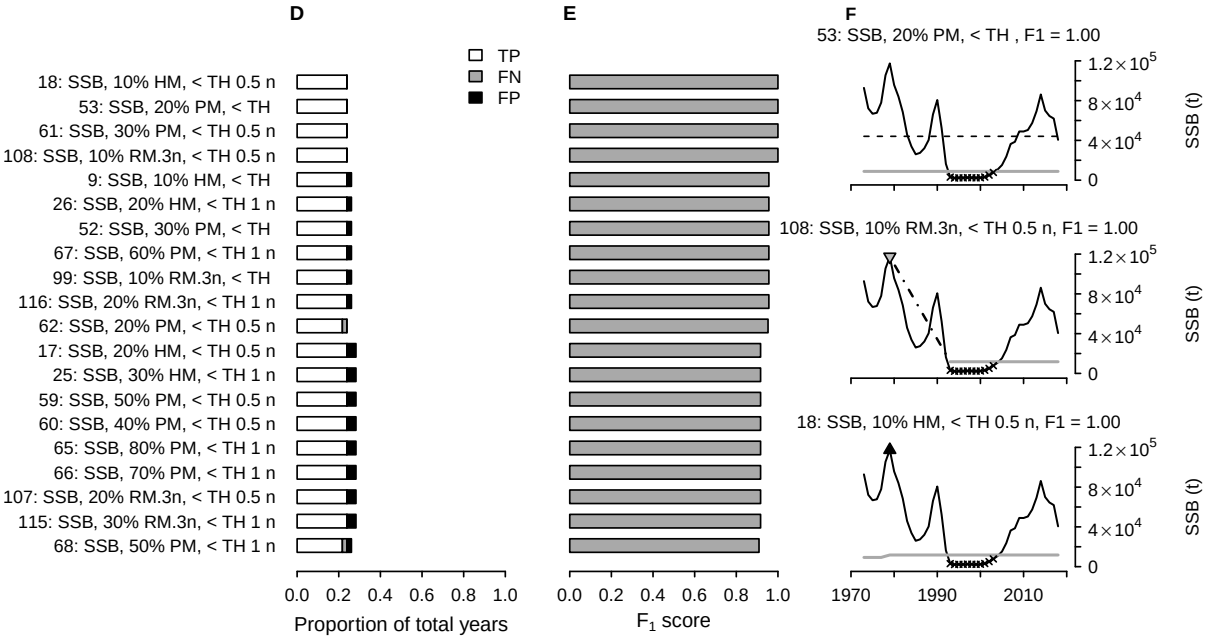

Cod (NEA) − cod.27.1−2

Abbreviations

TP = True positive
FN = False negative
FP = False positive
HM = Historic maximum
RM.3n = Recent maximum (within 3 n)
PM = Population mean
n = Generation length
B_{ref} = Reference biomass
TH = Threshold
t = tonne

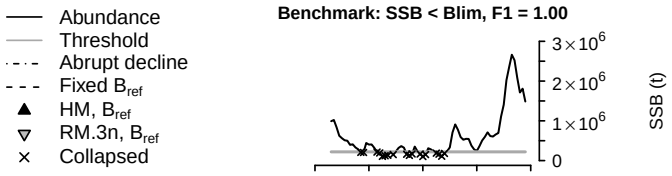

Literature and proposed definitions

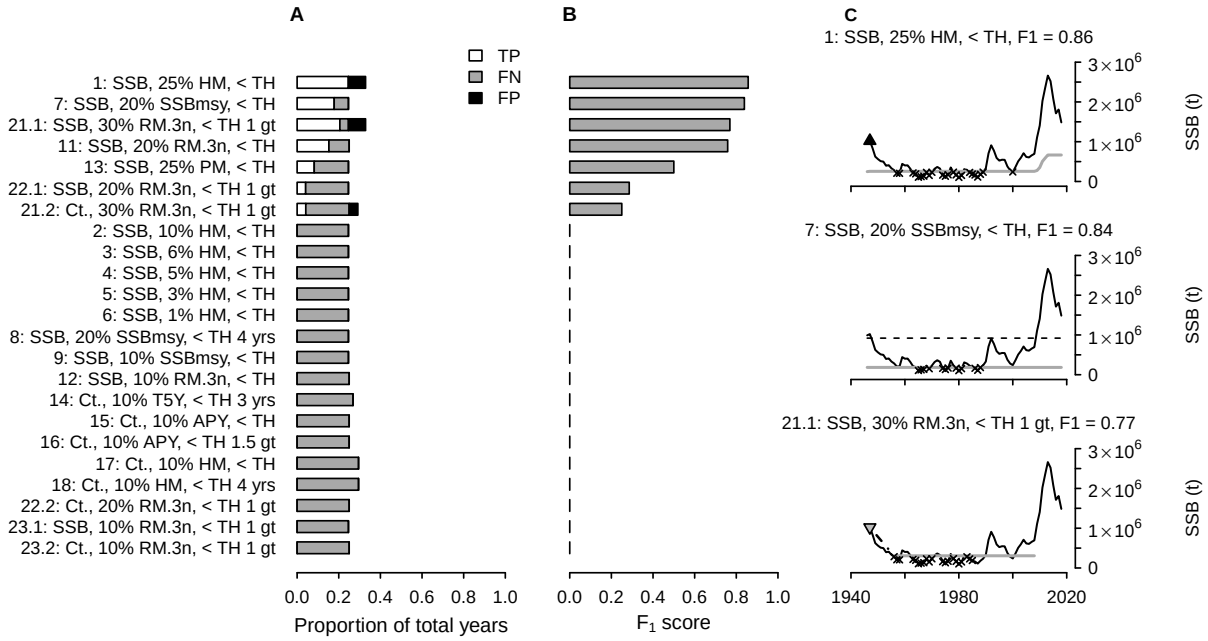

Simulated definitions

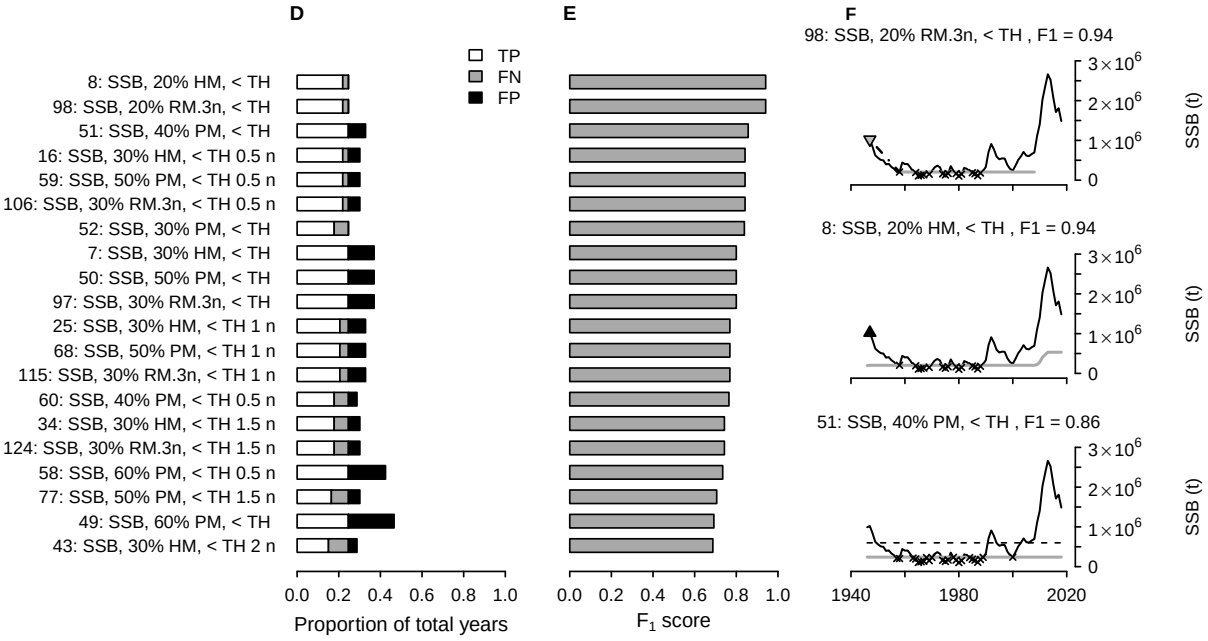

Cod (NS.EEC.Sk) − cod.27.47d20

Abbreviations

TP = True positive
FN = False negative
FP = False positive
HM = Historic maximum
RM.3n = Recent maximum (within 3 n)
PM = Population mean
n = Generation length
B_{ref} = Reference biomass
TH = Threshold
t = tonne

Abundance
Threshold
Abrupt decline
Fixed B_{ref}
HM, B_{ref}
RM.3n, B_{ref}
Collapsed

Benchmark: SSB < Blim, F1 = 1.00

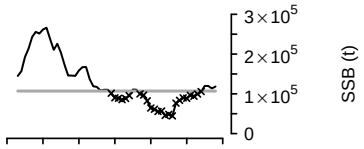

Literature and proposed definitions

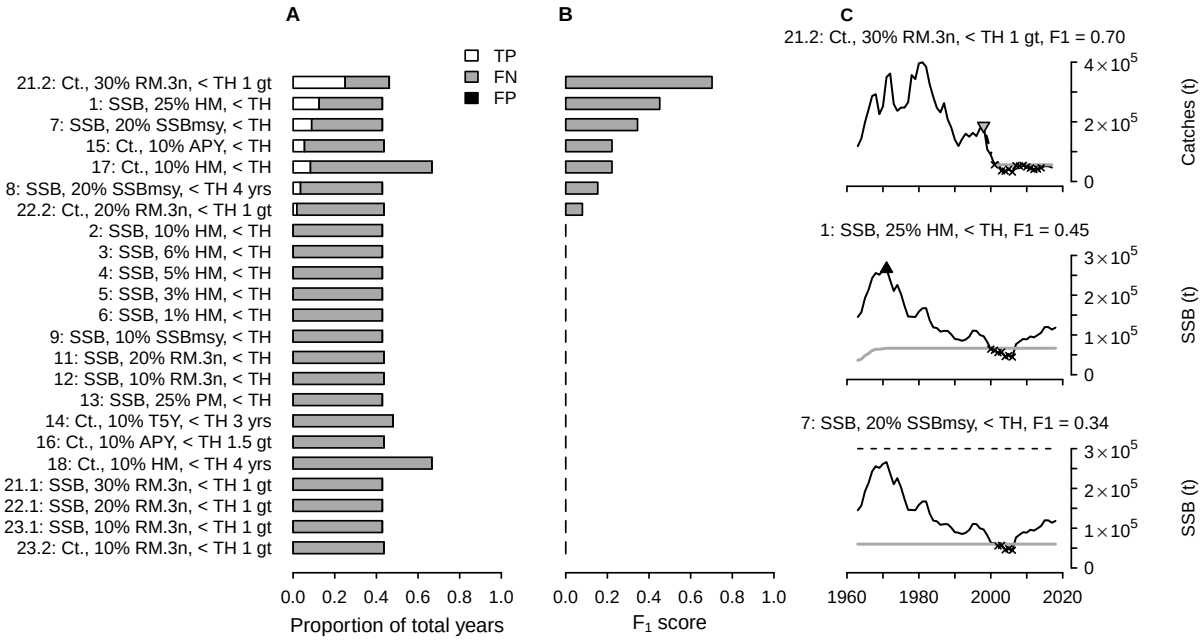

Simulated definitions

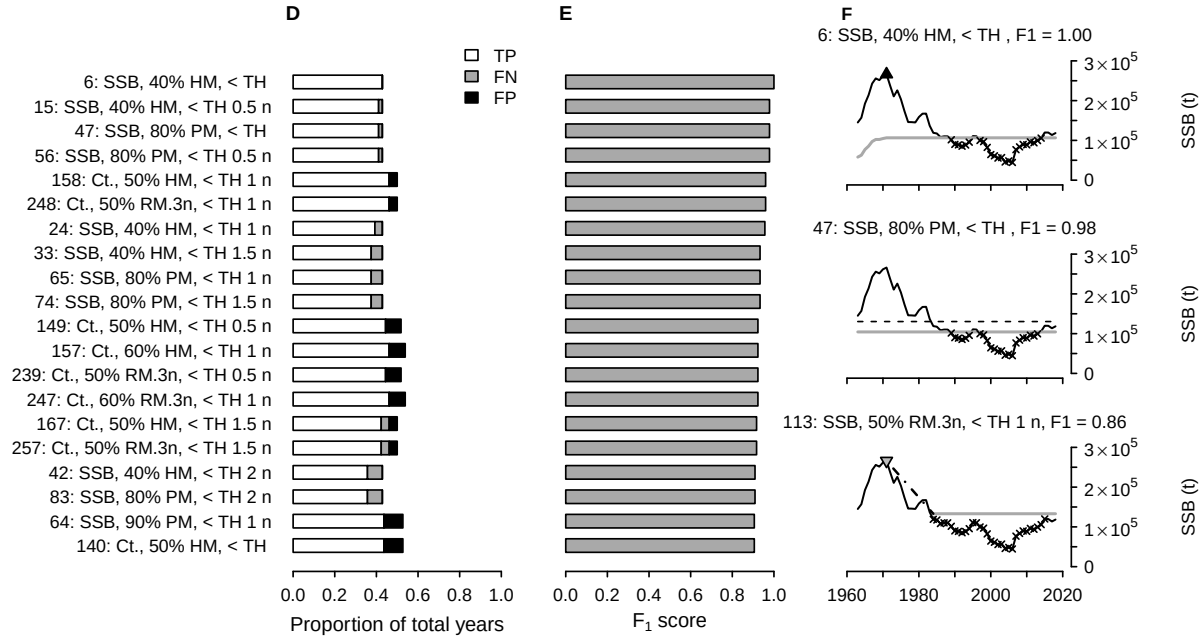

Cod (IG) − cod.27.5a

Abbreviations

TP = True positive
FN = False negative
FP = False positive
HM = Historic maximum
RM.3n = Recent maximum (within 3 n)
PM = Population mean
n = Generation length
B_{ref} = Reference biomass
TH = Threshold
t = tonne

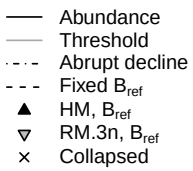

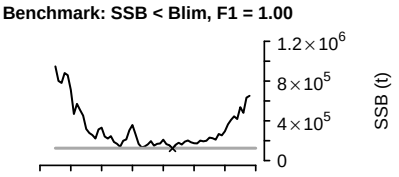

Literature and proposed definitions

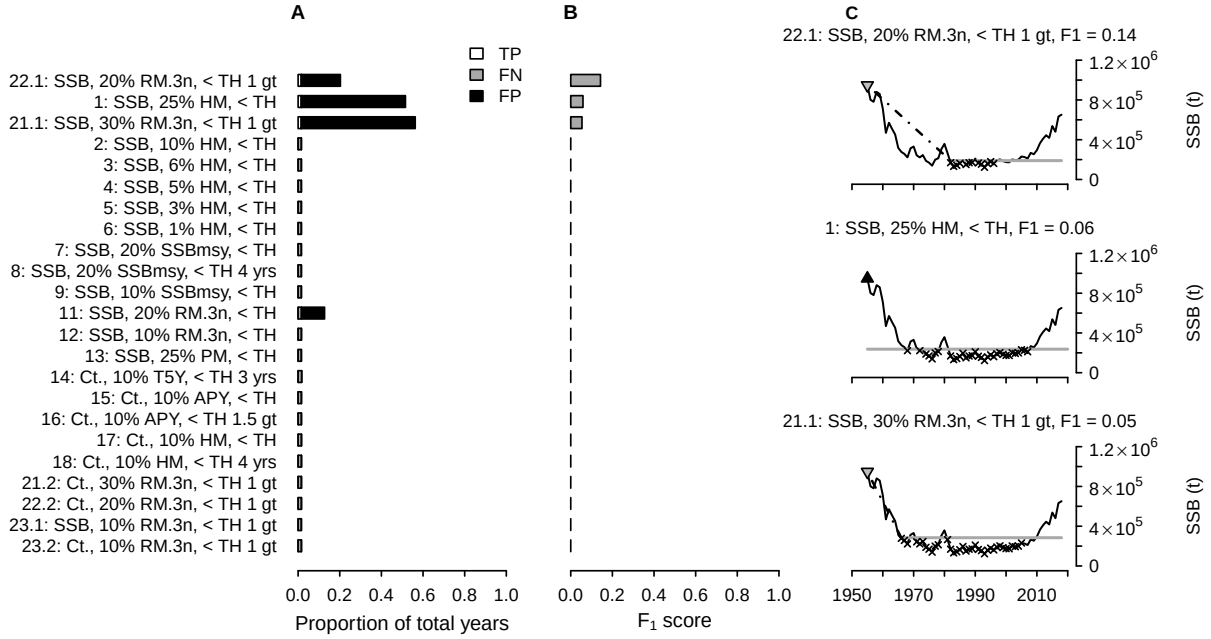

Simulated definitions

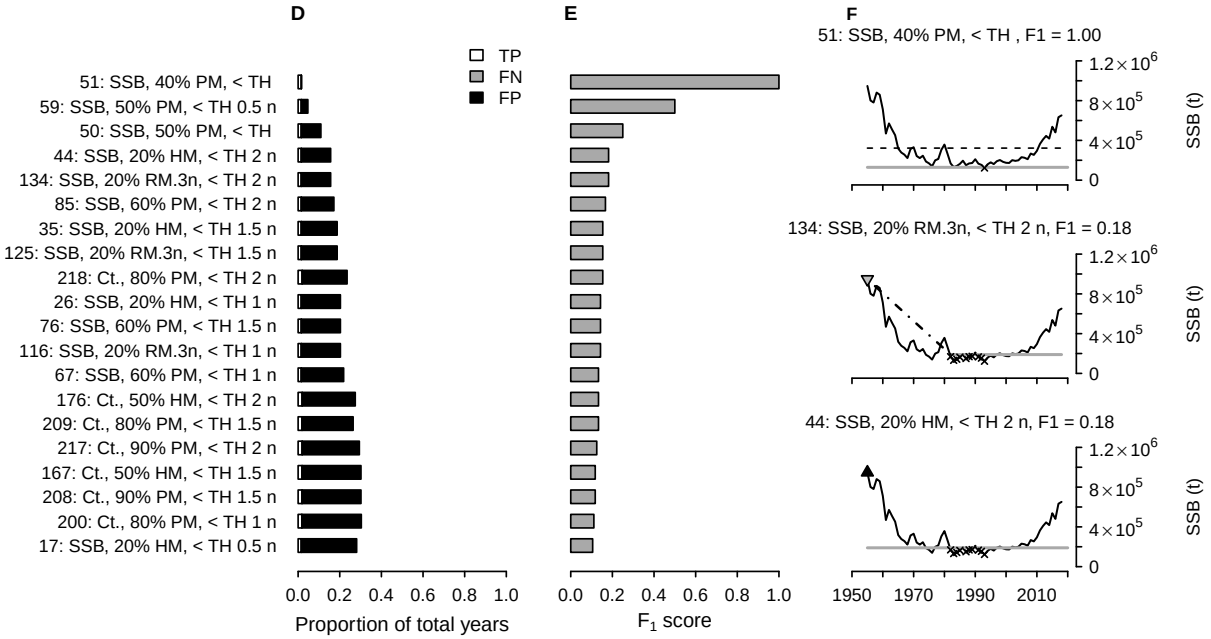

Cod (FP) − cod.27.5b1

Abbreviations

TP = True positive
FN = False negative
FP = False positive
HM = Historic maximum
RM.3n = Recent maximum (within 3 n)
PM = Population mean
n = Generation length
B_{ref} = Reference biomass
TH = Threshold
t = tonne

Abundance
Threshold
Abrupt decline
Fixed B_{ref}
HM, B_{ref}
RM.3n, B_{ref}
Collapsed

Benchmark: SSB < Blim, F1 = 1.00

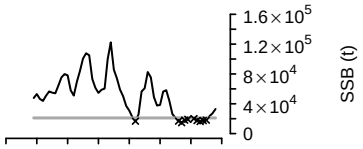

Literature and proposed definitions

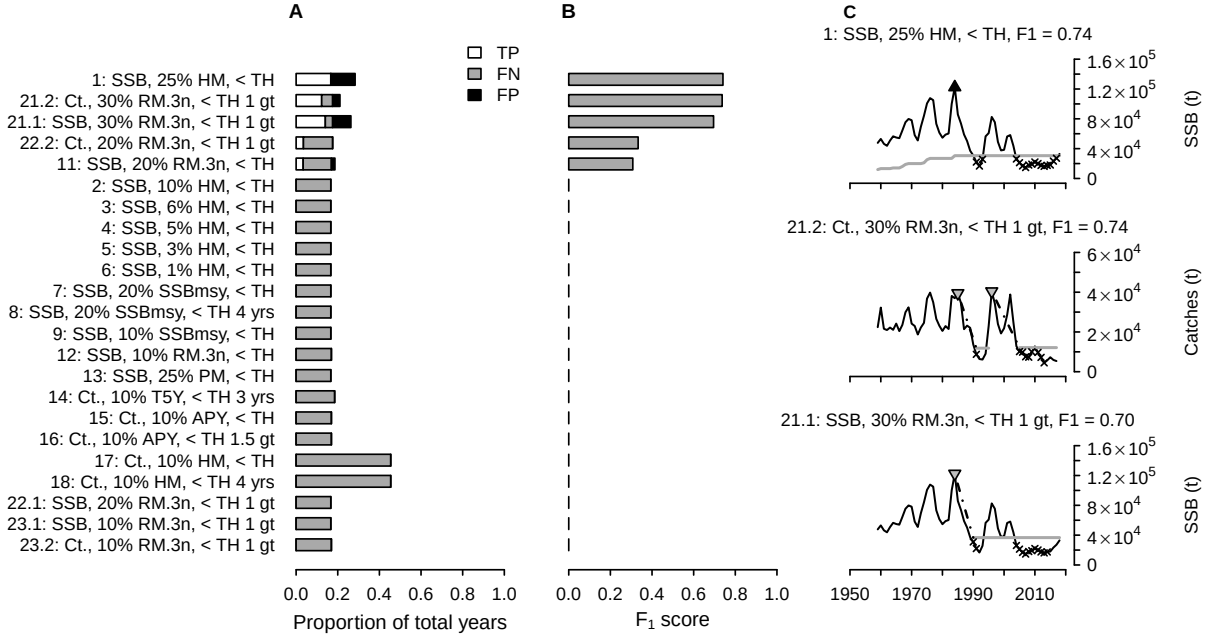

Simulated definitions

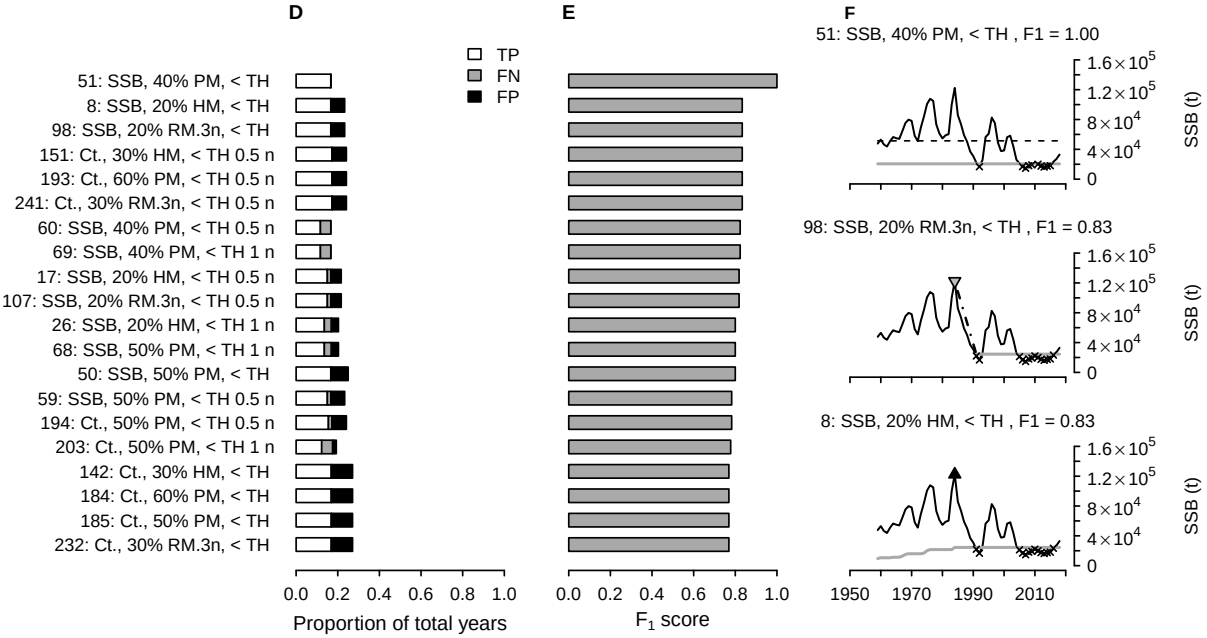

Cod (WS) − cod.27.6a

Abbreviations

TP = True positive
FN = False negative
FP = False positive
HM = Historic maximum
RM.3n = Recent maximum (within 3 n)
PM = Population mean
n = Generation length
B_{ref} = Reference biomass
TH = Threshold
t = tonne

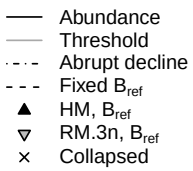

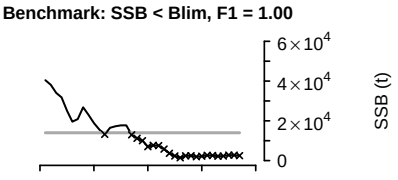

Literature and proposed definitions

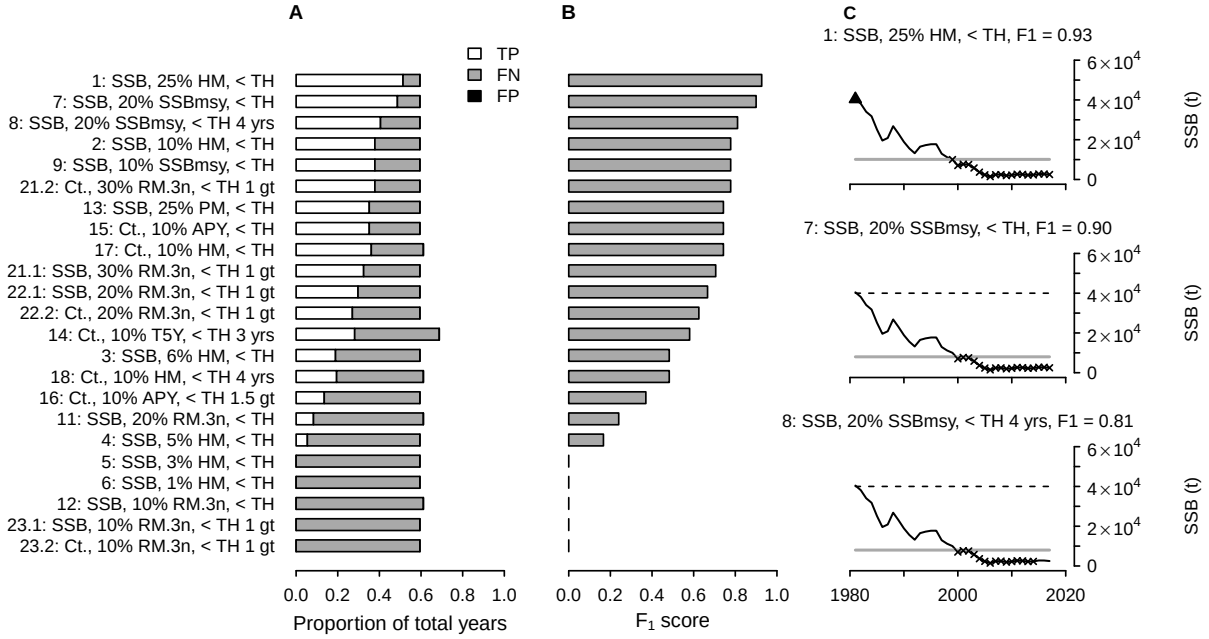

Simulated definitions

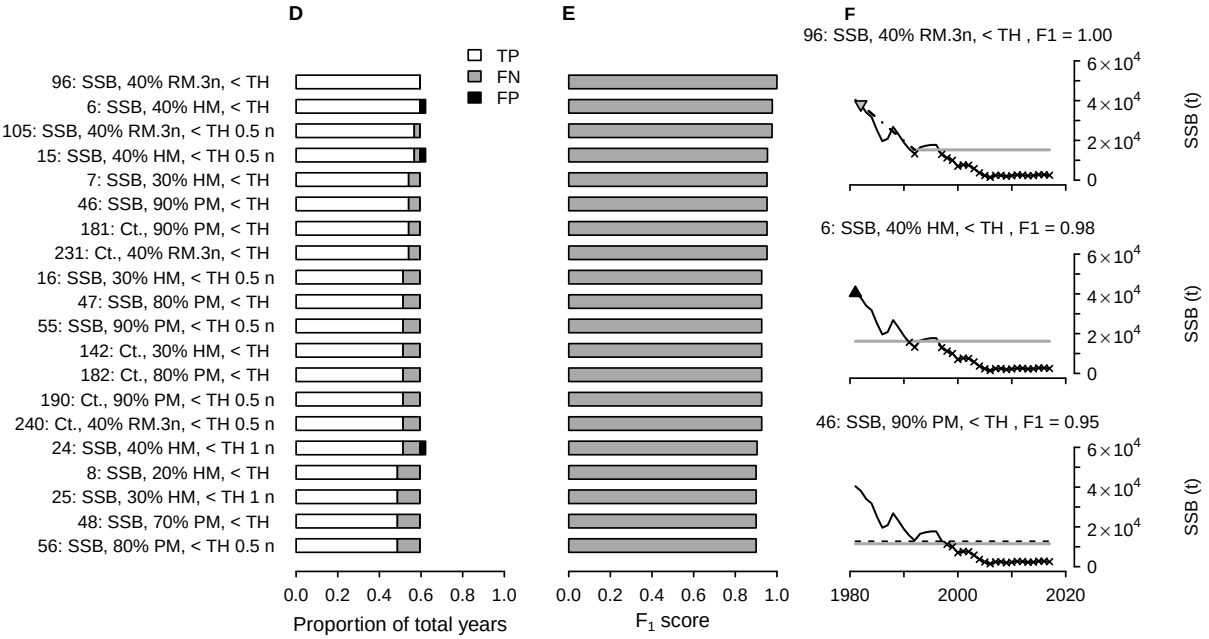

Cod (IS) − cod.27.7a

Abbreviations

TP = True positive
FN = False negative
FP = False positive
HM = Historic maximum
RM.3n = Recent maximum (within 3 n)
PM = Population mean
n = Generation length
B_{ref} = Reference biomass
TH = Threshold
t = tonne

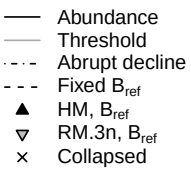

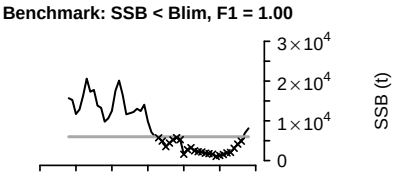

Literature and proposed definitions

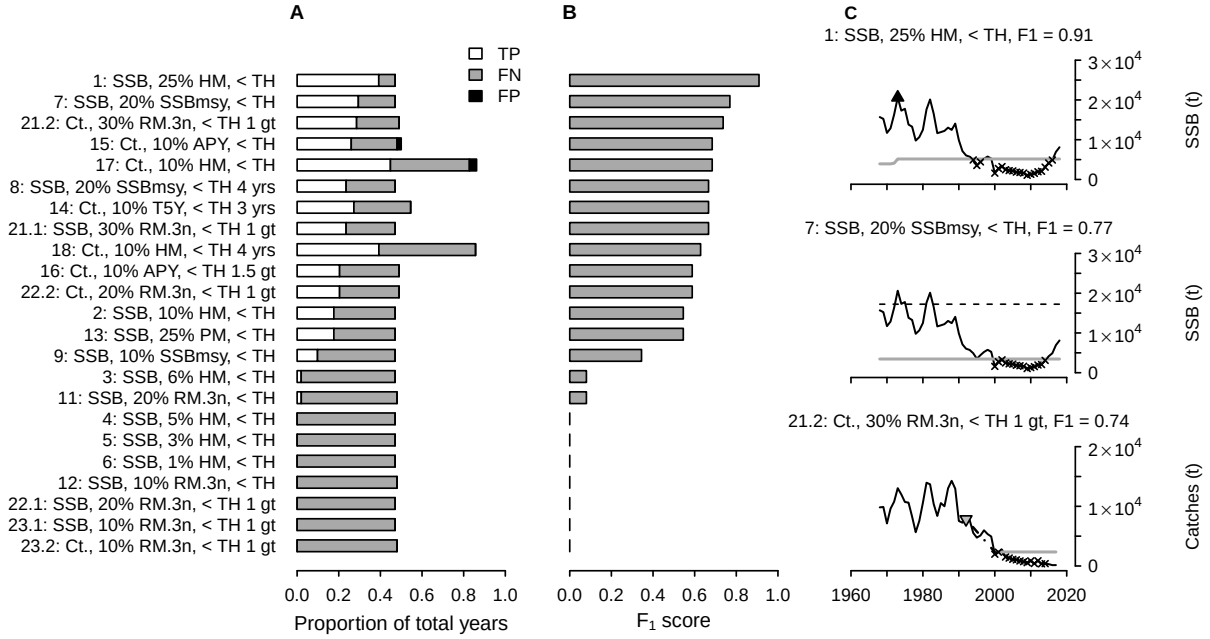

Simulated definitions

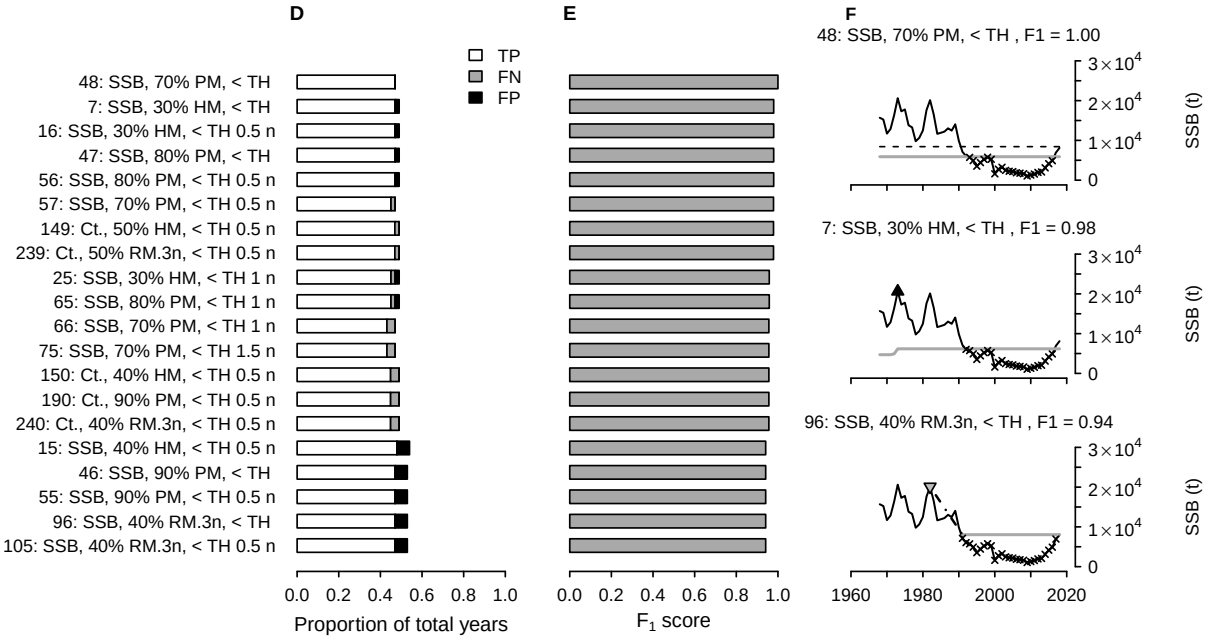

Cod (EEC.SCS) − cod.27.7e−k

Abbreviations

TP = True positive
FN = False negative
FP = False positive
HM = Historic maximum
RM.3n = Recent maximum (within 3 n)
PM = Population mean
n = Generation length
B_{ref} = Reference biomass
TH = Threshold
t = tonne

Abundance
Threshold
Abrupt decline
Fixed B_{ref}
HM, B_{ref}
RM.3n, B_{ref}
Collapsed

Benchmark: SSB < Blim, F1 = 1.00

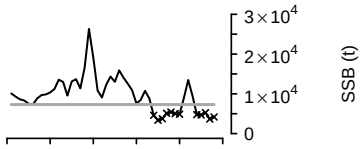

Literature and proposed definitions

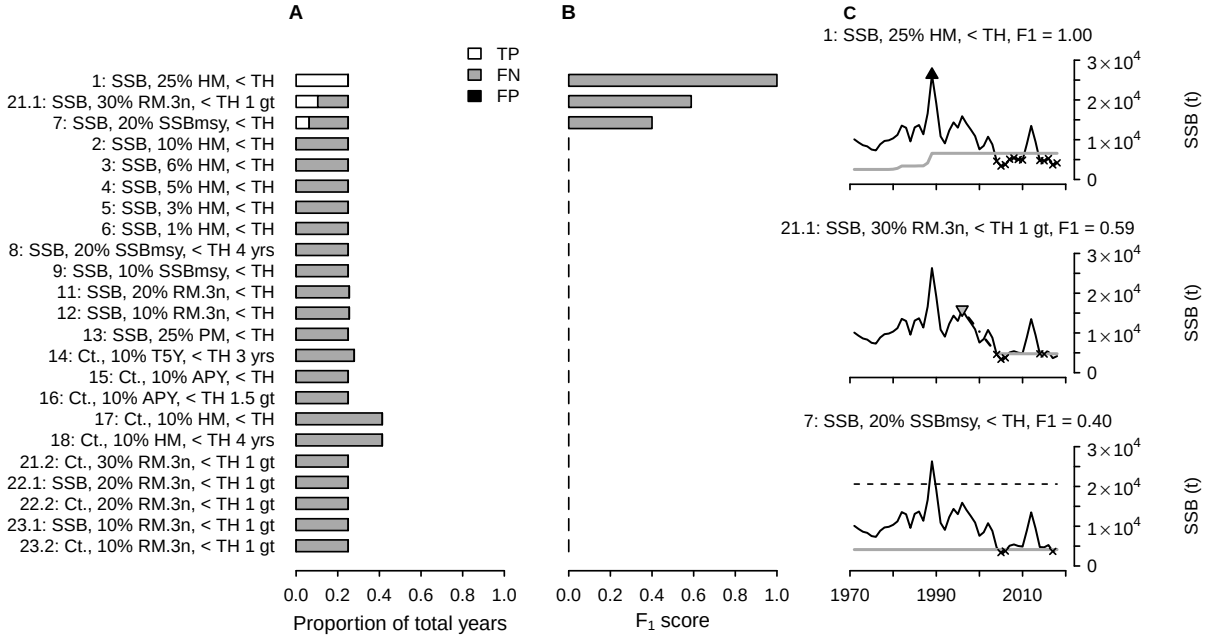

Simulated definitions

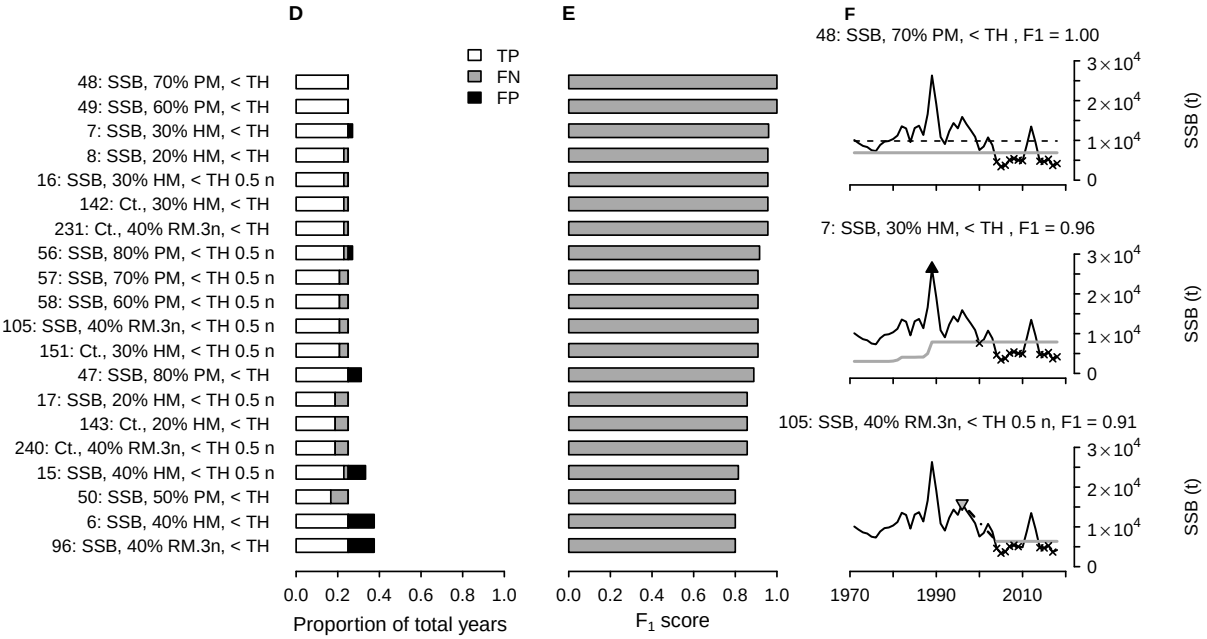

Haddock (NEA) − had.27.1−2

Abbreviations

TP = True positive
FN = False negative
FP = False positive
HM = Historic maximum
RM.3n = Recent maximum (within 3 n)
PM = Population mean
n = Generation length
B_{ref} = Reference biomass
TH = Threshold
t = tonne

Abundance
Threshold
Abrupt decline
Fixed B_{ref}
HM, B_{ref}
RM.3n, B_{ref}
Collapsed

Benchmark: SSB < Blim, F1 = 1.00

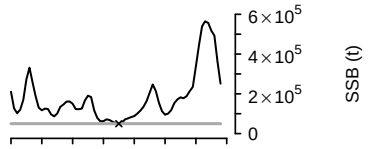

Literature and proposed definitions

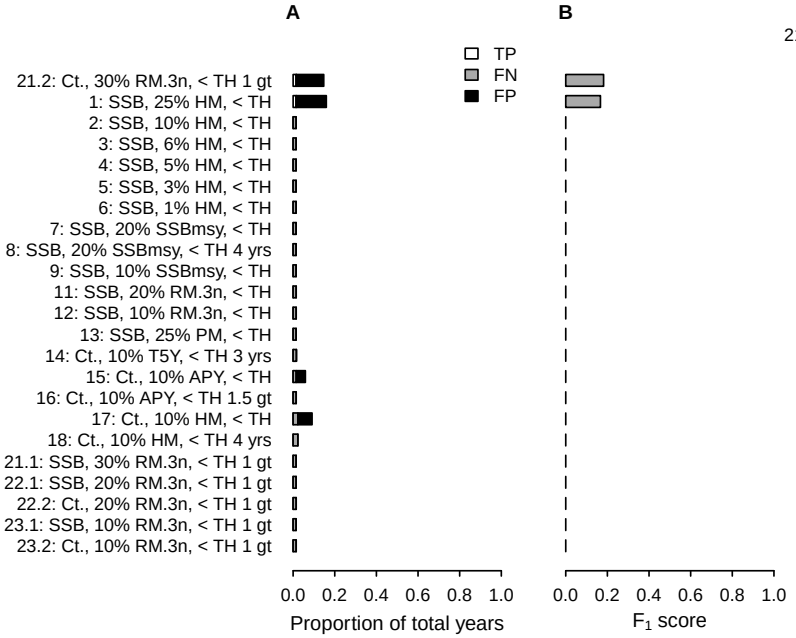

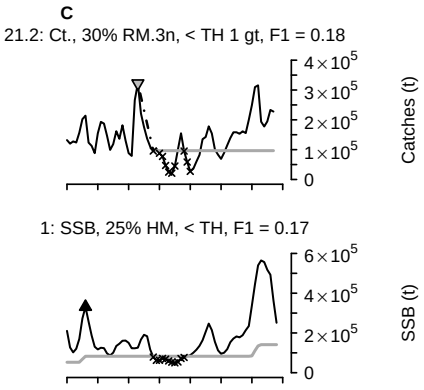

Simulated definitions

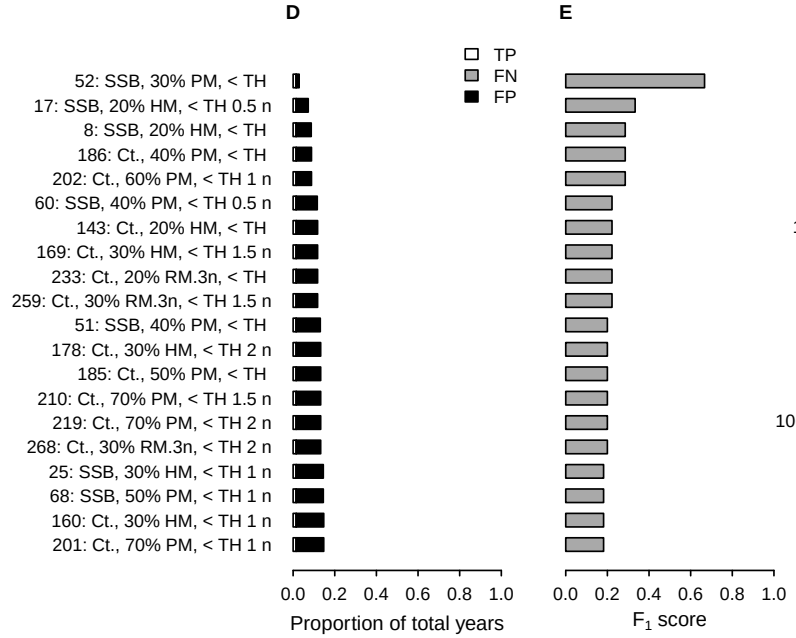

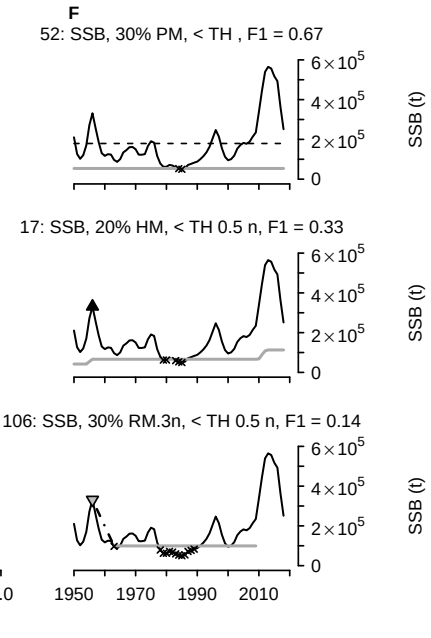

Haddock (NS.WS.Sk) − had.27.46a20

Abbreviations

TP = True positive
FN = False negative
FP = False positive
HM = Historic maximum
RM.3n = Recent maximum (within 3 n)
PM = Population mean
n = Generation length
B_{ref} = Reference biomass
TH = Threshold
t = tonne

Abundance
Threshold
Abrupt decline
Fixed B_{ref}
HM, B_{ref}
RM.3n, B_{ref}
Collapsed

Benchmark: SSB < Blim, F1 = 1.00

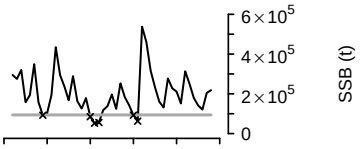

Literature and proposed definitions

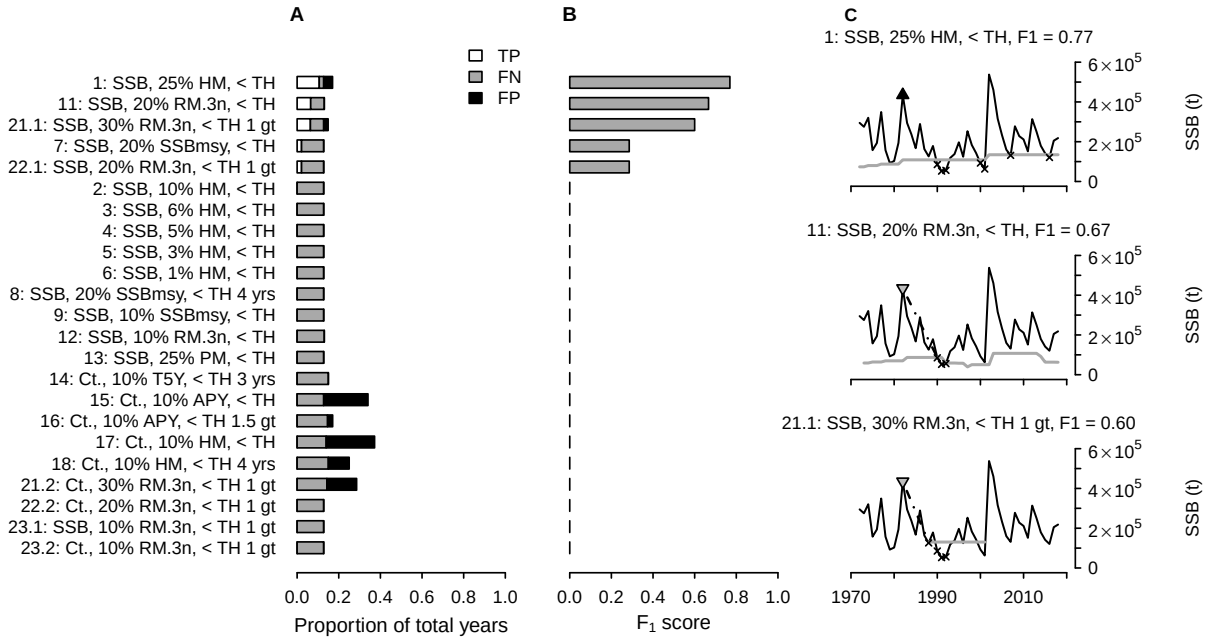

Simulated definitions

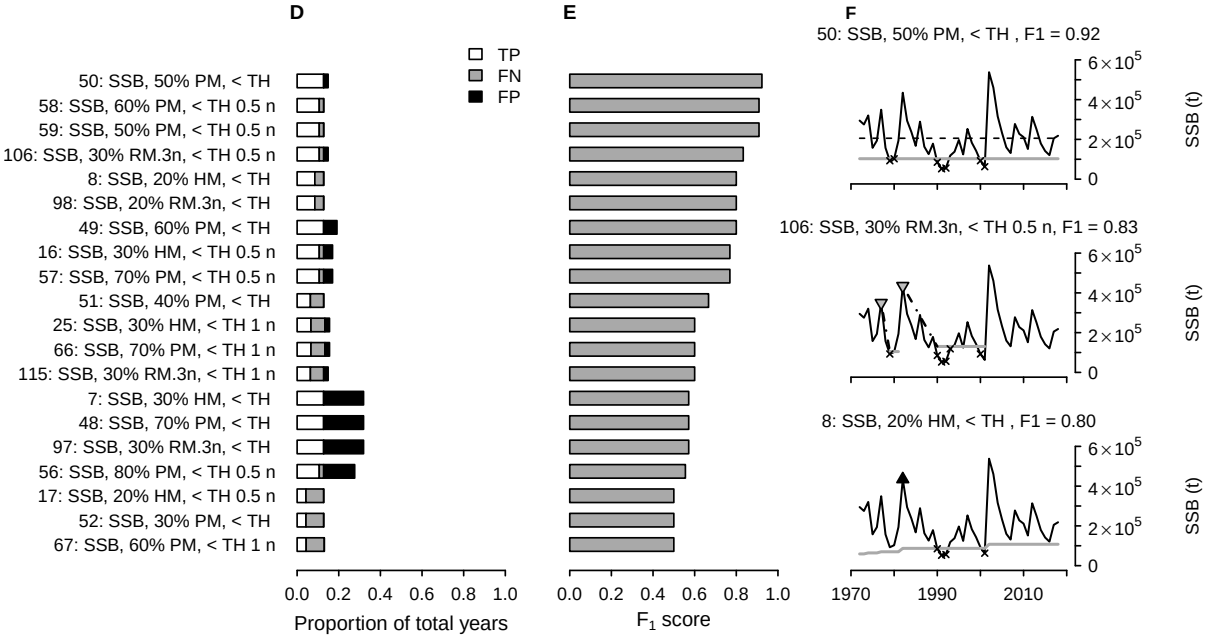

Haddock (FG) − had.27.5b

Abbreviations

TP = True positive
FN = False negative
FP = False positive
HM = Historic maximum
RM.3n = Recent maximum (within 3 n)
PM = Population mean
n = Generation length
B_{ref} = Reference biomass
TH = Threshold
t = tonne

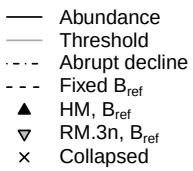

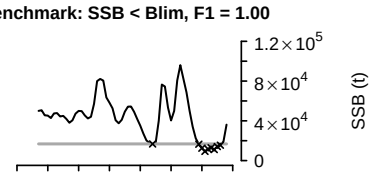

Literature and proposed definitions

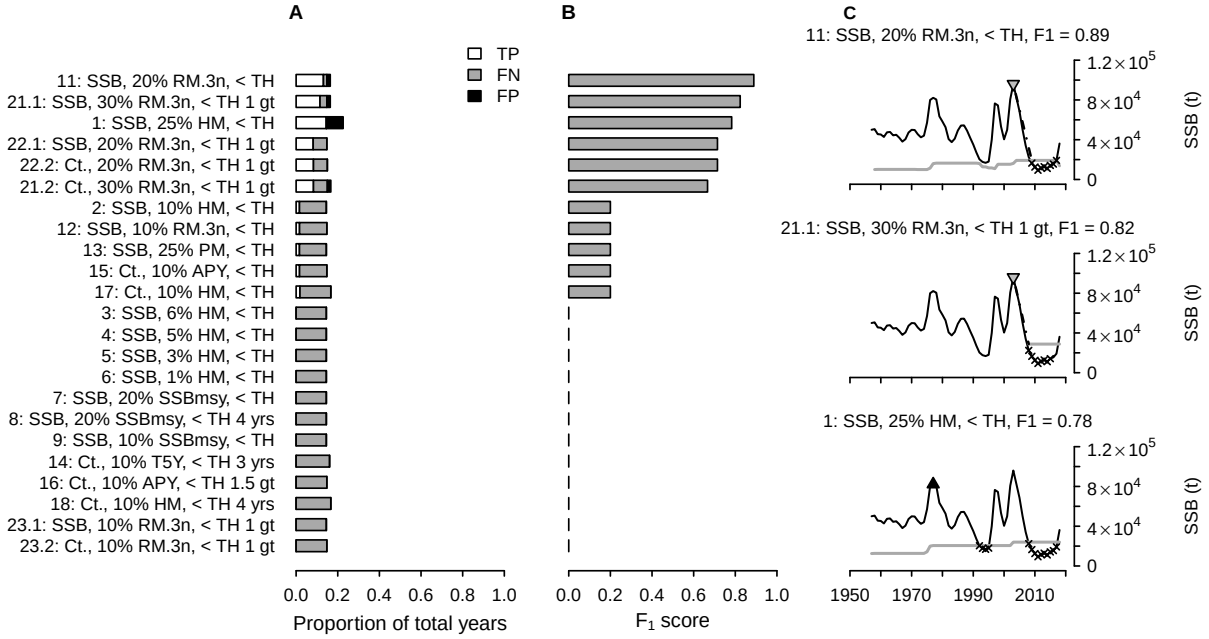

Simulated definitions

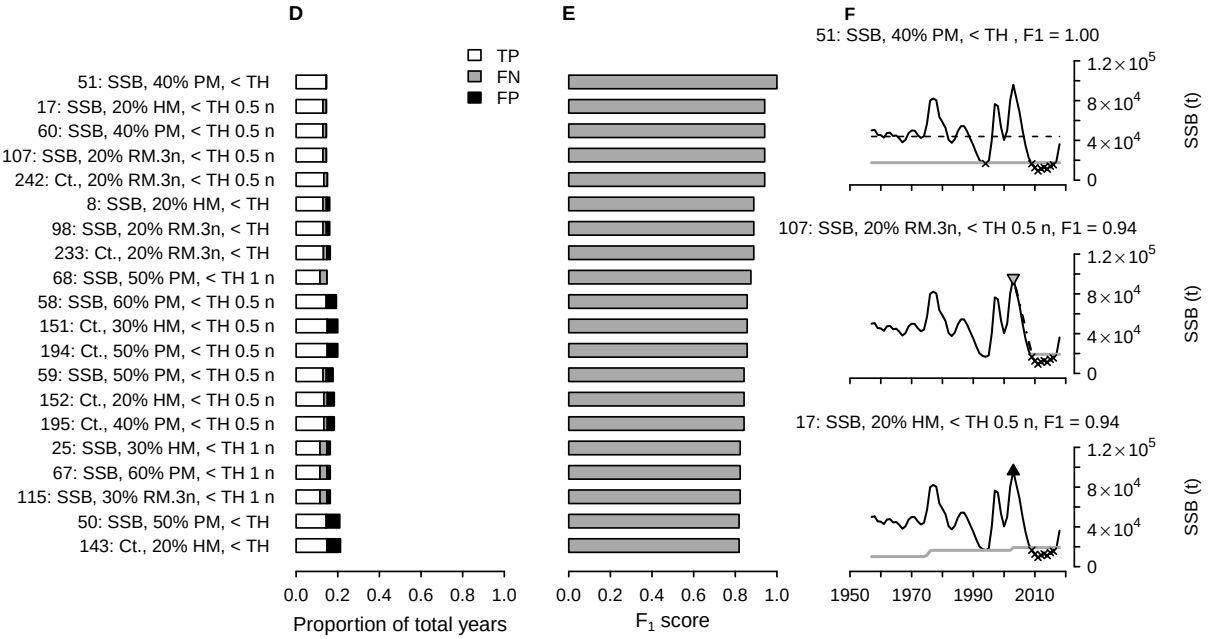

Haddock (R) − had.27.6b

Abbreviations

TP = True positive
FN = False negative
FP = False positive
HM = Historic maximum
RM.3n = Recent maximum (within 3 n)
PM = Population mean
n = Generation length
B_{ref} = Reference biomass
TH = Threshold
t = tonne

Abundance
Threshold
Abrupt decline
Fixed B_{ref}
HM, B_{ref}
RM.3n, B_{ref}
Collapsed

Benchmark: SSB < Blim, F1 = 1.00

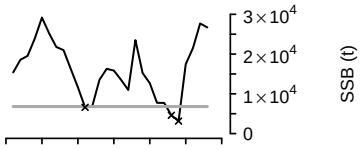

Literature and proposed definitions

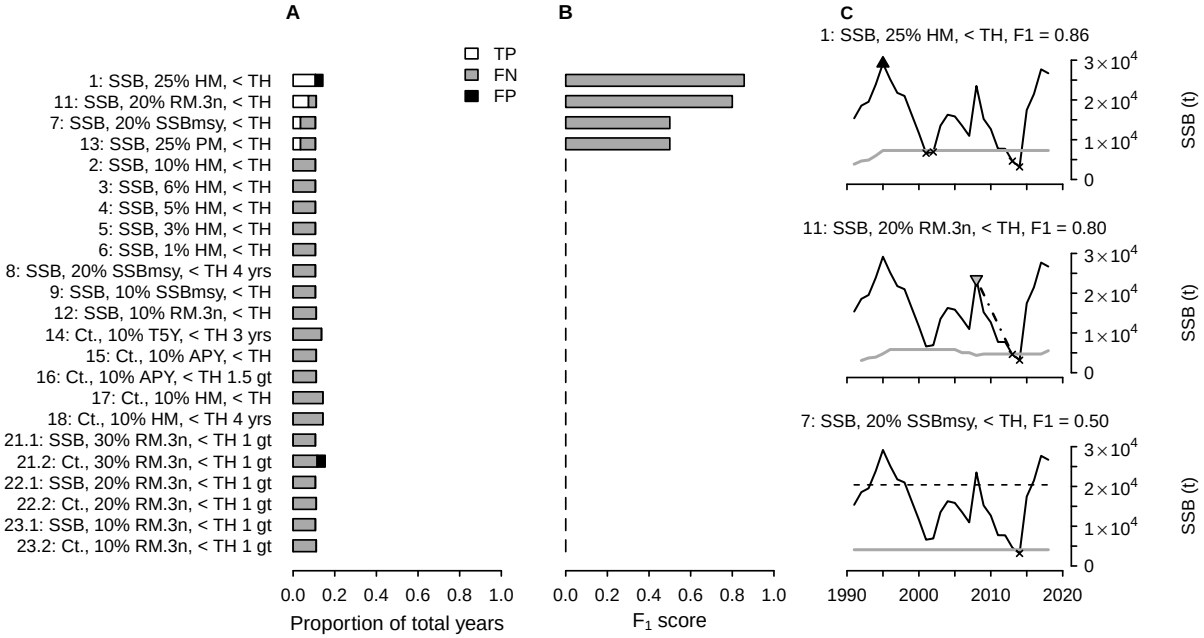

Simulated definitions

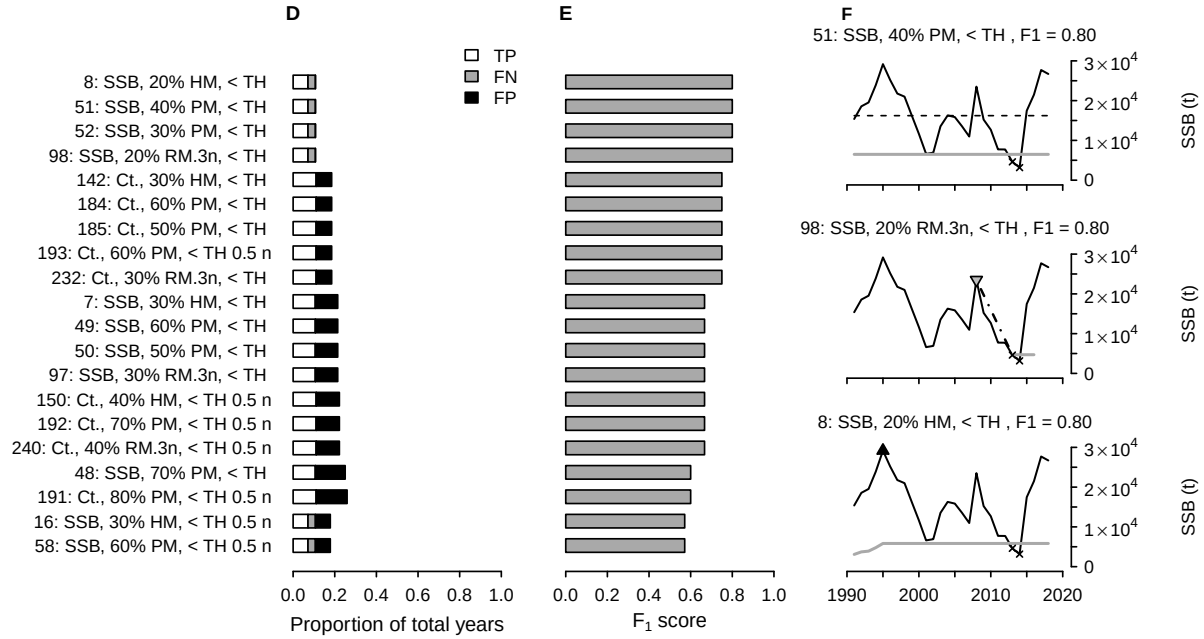

Herring (Sk.KT.WB) − her.27.20−24

Abbreviations

TP = True positive
FN = False negative
FP = False positive
HM = Historic maximum
RM.3n = Recent maximum (within 3 n)
PM = Population mean
n = Generation length
B_{ref} = Reference biomass
TH = Threshold
t = tonne

Abundance
Threshold
Abrupt decline
Fixed B_{ref}
HM, B_{ref}
RM.3n, B_{ref}
Collapsed

Benchmark: SSB < Blim, F1 = 1.00

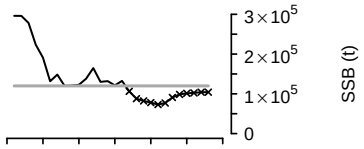

Literature and proposed definitions

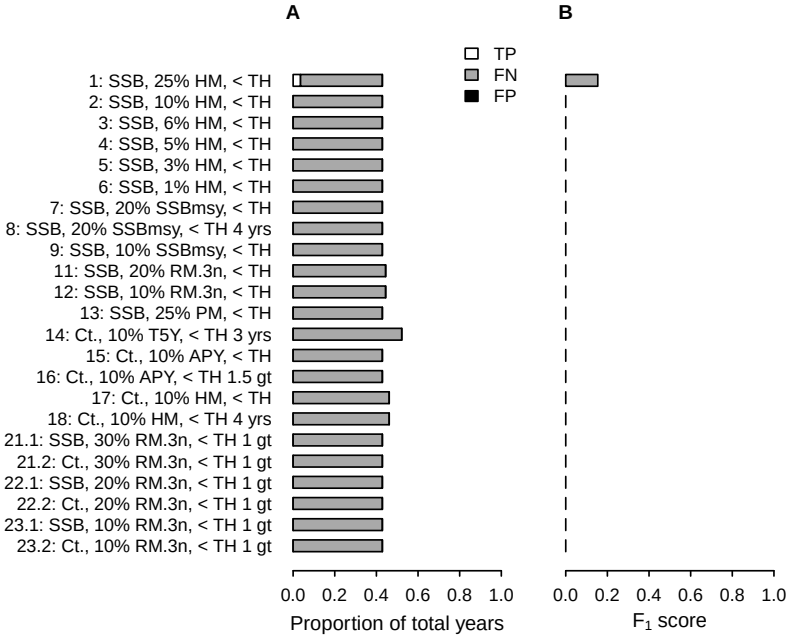

C

1: SSB, 25% HM, < TH, F1 = 0.15

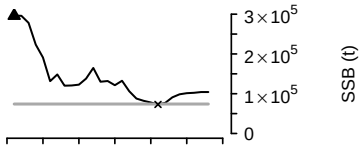

Simulated definitions

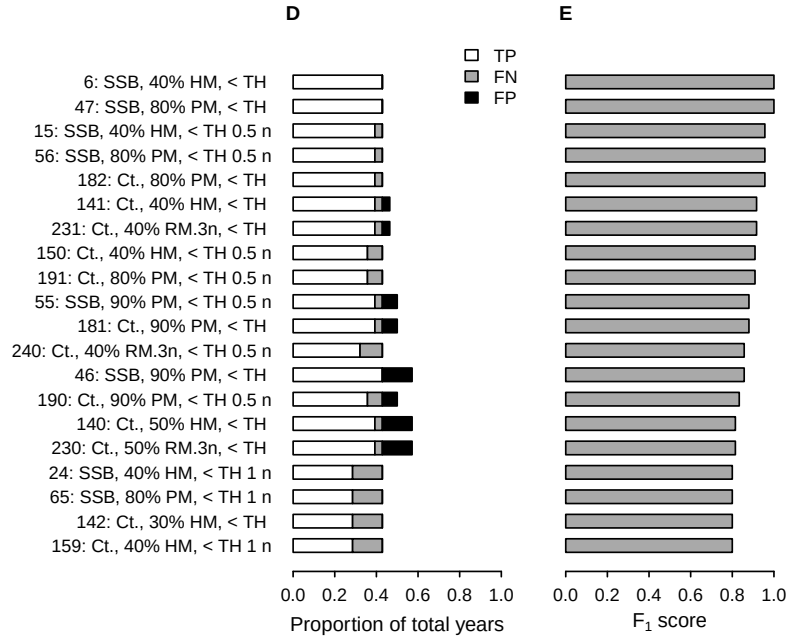

F

47: SSB, 80% PM, < TH , F1 = 1.00

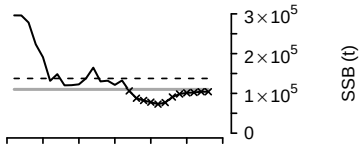

6: SSB, 40% HM, < TH , F1 = 1.00

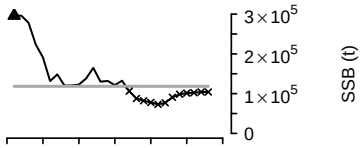

95: SSB, 50% RM.3n, < TH , F1 = 0.73

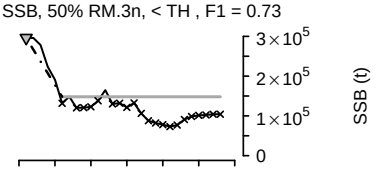

Herring (CBS) − her.27.25−2932

Abbreviations

TP = True positive
FN = False negative
FP = False positive
HM = Historic maximum
RM.3n = Recent maximum (within 3 n)
PM = Population mean
n = Generation length
B_{ref} = Reference biomass
TH = Threshold
t = tonne

Abundance
Threshold
Abrupt decline
Fixed B_{ref}
HM, B_{ref}
RM.3n, B_{ref}
Collapsed

Benchmark: SSB < Blim, F1 = 1.00

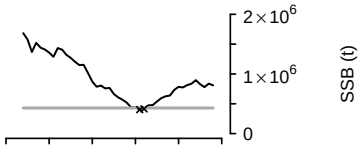

Literature and proposed definitions

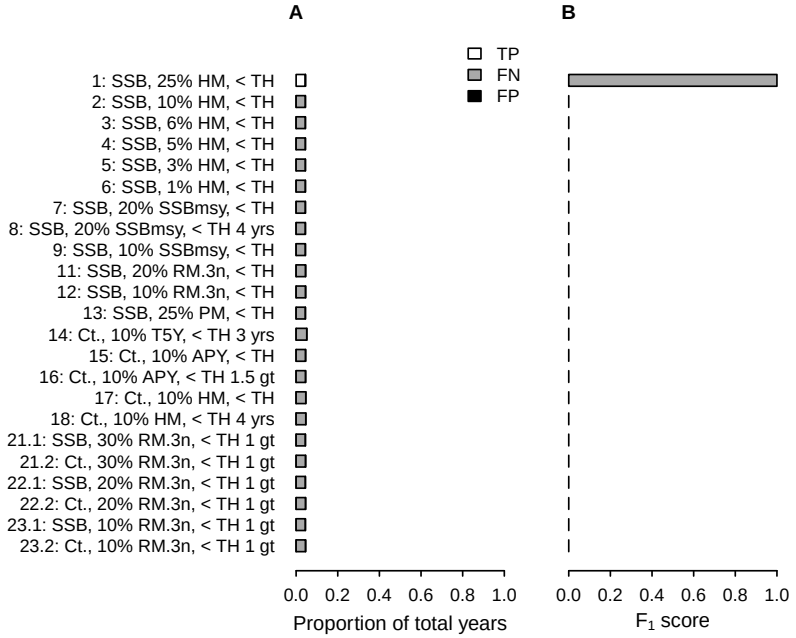

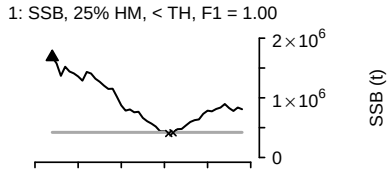

Simulated definitions

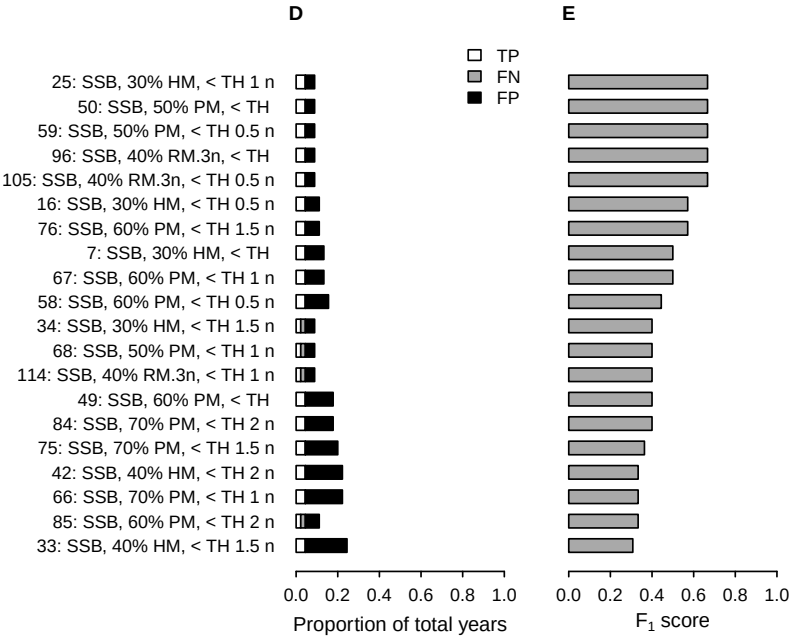

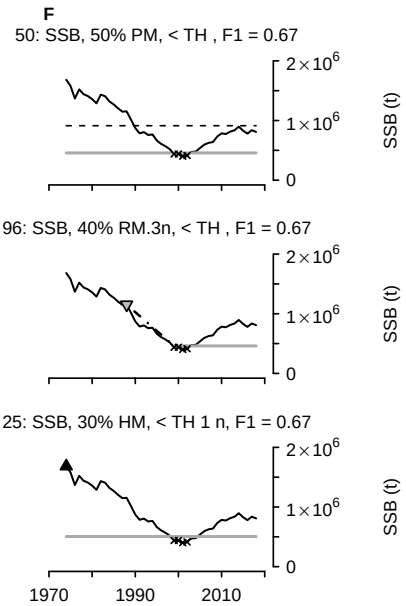

Herring (NS.Sk.Kt.EEC) − her.27.3a47d

Abbreviations

TP = True positive
FN = False negative
FP = False positive
HM = Historic maximum
RM.3n = Recent maximum (within 3 n)
PM = Population mean
n = Generation length
B_{ref} = Reference biomass
TH = Threshold
t = tonne

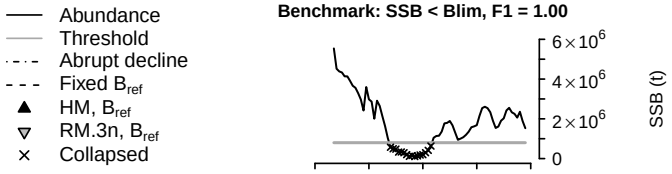

Literature and proposed definitions

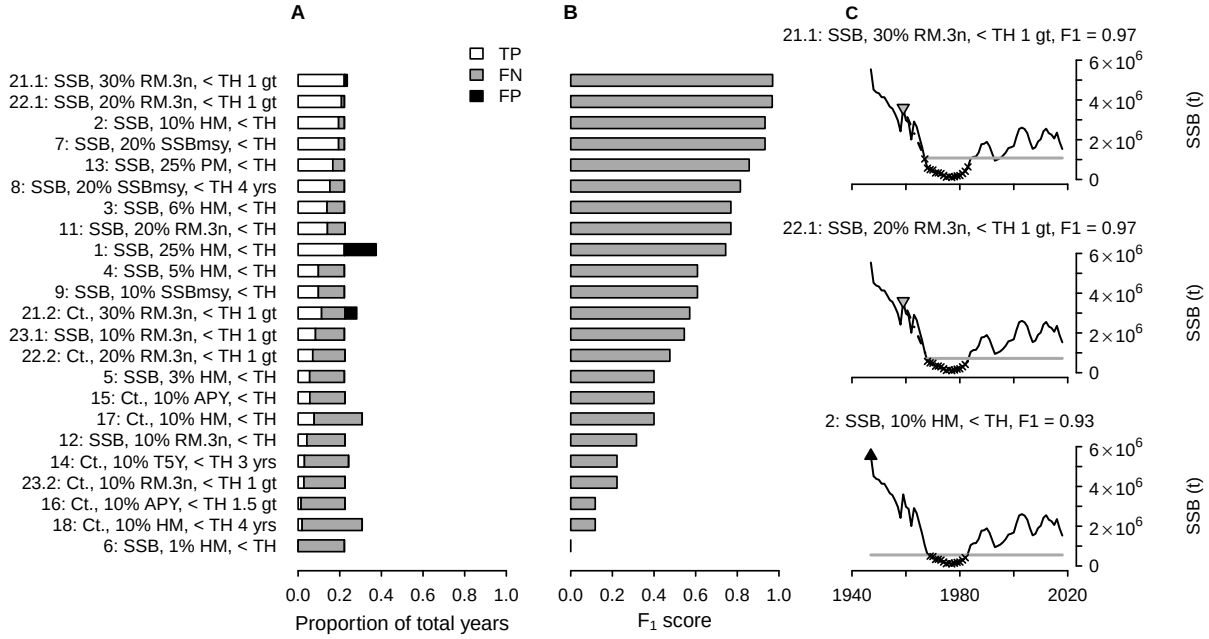

Simulated definitions

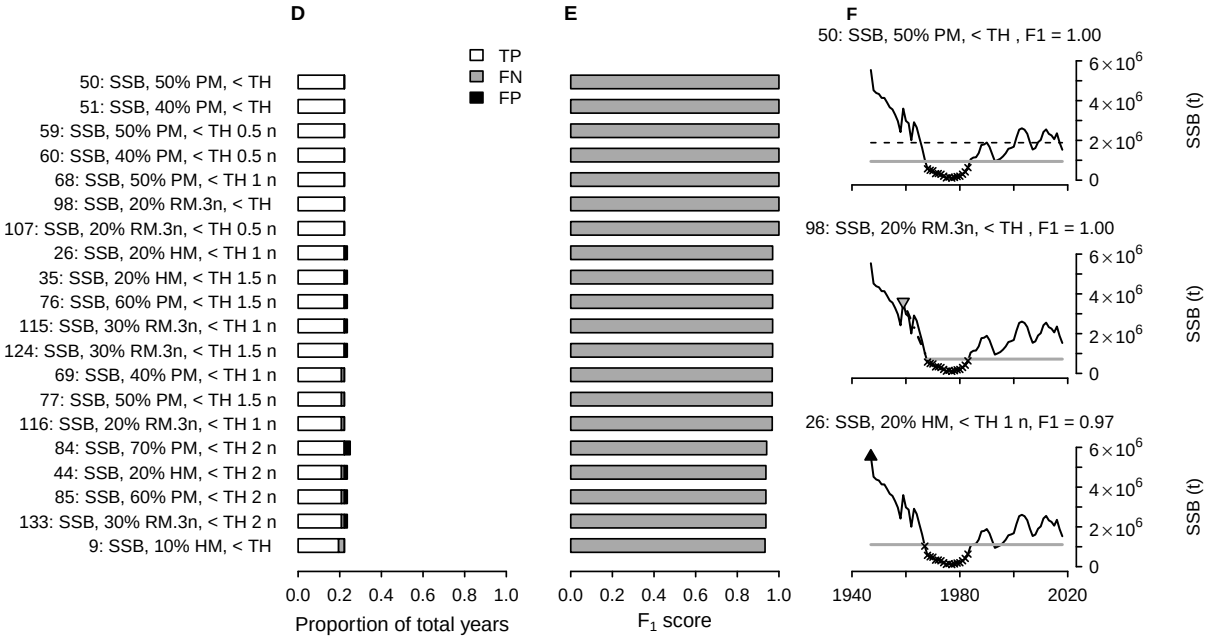

Herring (wS.wI) − her.27.6a7bc

Abbreviations

TP = True positive
FN = False negative
FP = False positive
HM = Historic maximum
RM.3n = Recent maximum (within 3 n)
PM = Population mean
n = Generation length
B_{ref} = Reference biomass
TH = Threshold
t = tonne

Abundance
Threshold
Abrupt decline
Fixed B_{ref}
HM, B_{ref}
RM.3n, B_{ref}
Collapsed

Benchmark: SSB < Blim, F1 = 1.00

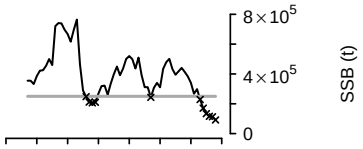

Literature and proposed definitions

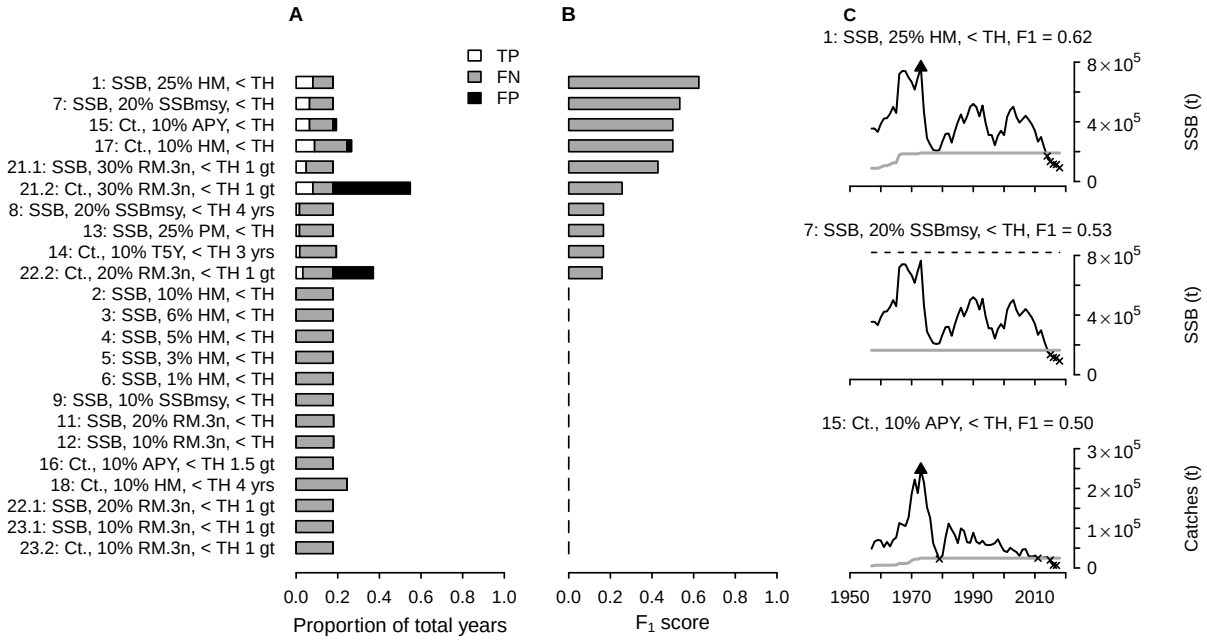

Simulated definitions

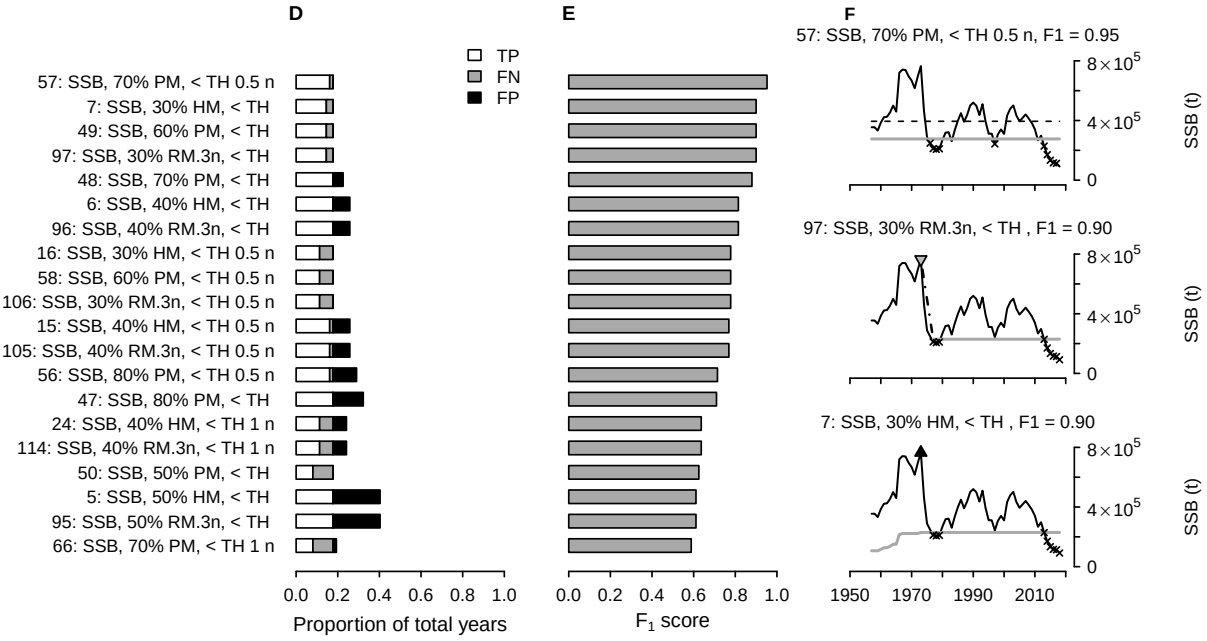

Herring (IS) − her.27.nirs

Abbreviations

TP = True positive
FN = False negative
FP = False positive
HM = Historic maximum
RM.3n = Recent maximum (within 3 n)
PM = Population mean
n = Generation length
B_{ref} = Reference biomass
TH = Threshold
t = tonne

Abundance
Threshold
Abrupt decline
Fixed B_{ref}
HM, B_{ref}
RM.3n, B_{ref}
Collapsed

Benchmark: SSB < Blim, F1 = 1.00

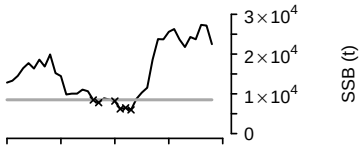

Literature and proposed definitions

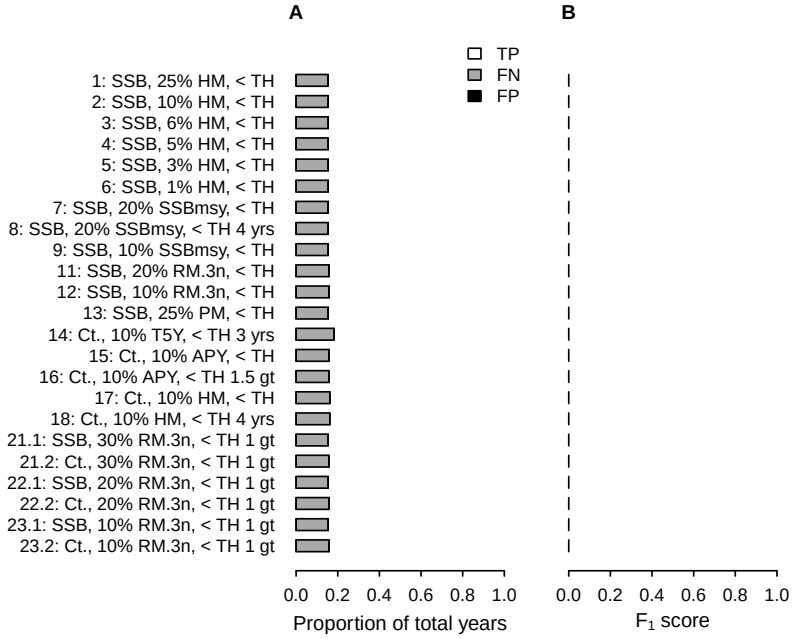

Simulated definitions

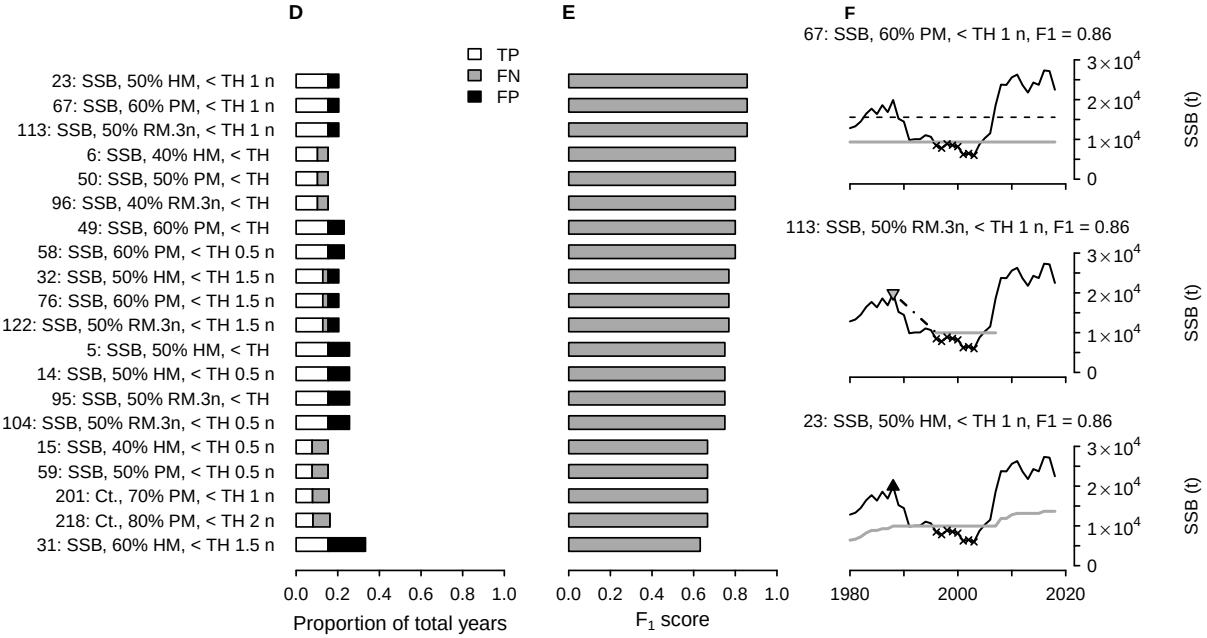

Hake (GNS.nBoB) − hke.27.3a46−8abd

Abbreviations

TP = True positive
FN = False negative
FP = False positive
HM = Historic maximum
RM.3n = Recent maximum (within 3 n)
PM = Population mean
n = Generation length
B_{ref} = Reference biomass
TH = Threshold
t = tonne

Abundance
Threshold
Abrupt decline
Fixed B_{ref}
HM, B_{ref}
RM.3n, B_{ref}
Collapsed

Benchmark: SSB < Blim, F1 = 1.00

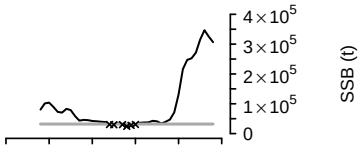

Literature and proposed definitions

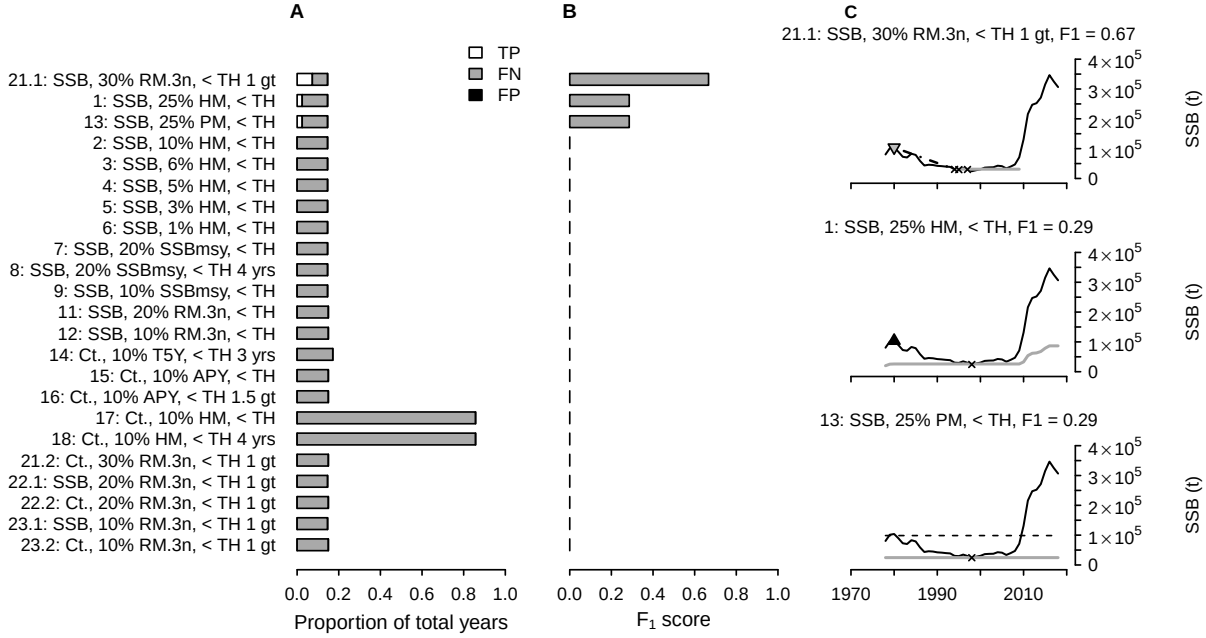

Simulated definitions

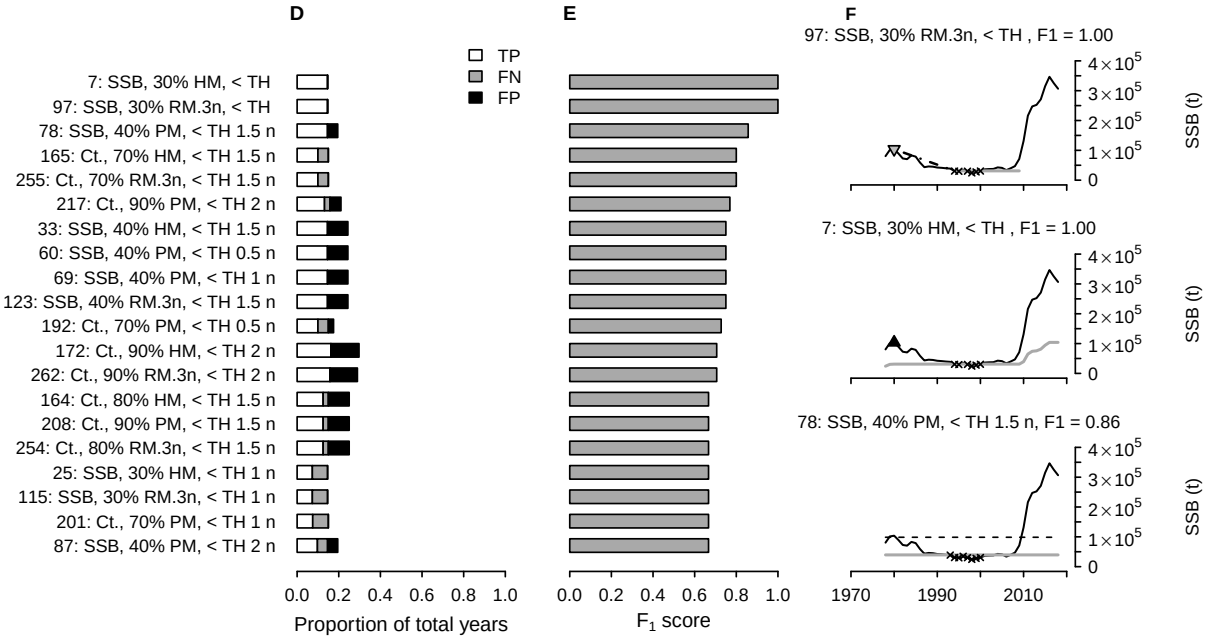

Hake (CtS.AIW) − hke.27.8c9a

Abbreviations

TP = True positive
FN = False negative
FP = False positive
HM = Historic maximum
RM.3n = Recent maximum (within 3 n)
PM = Population mean
n = Generation length
B_{ref} = Reference biomass
TH = Threshold
t = tonne

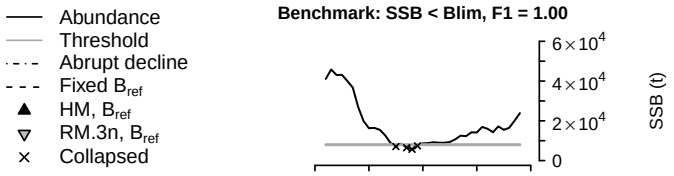

Literature and proposed definitions

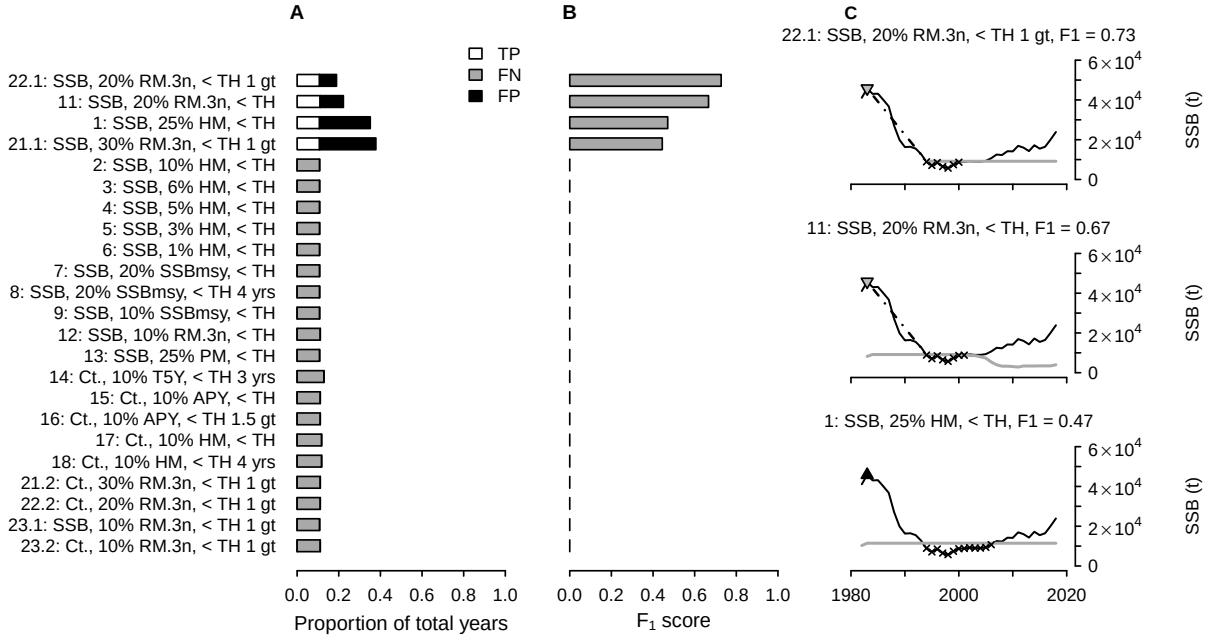

Simulated definitions

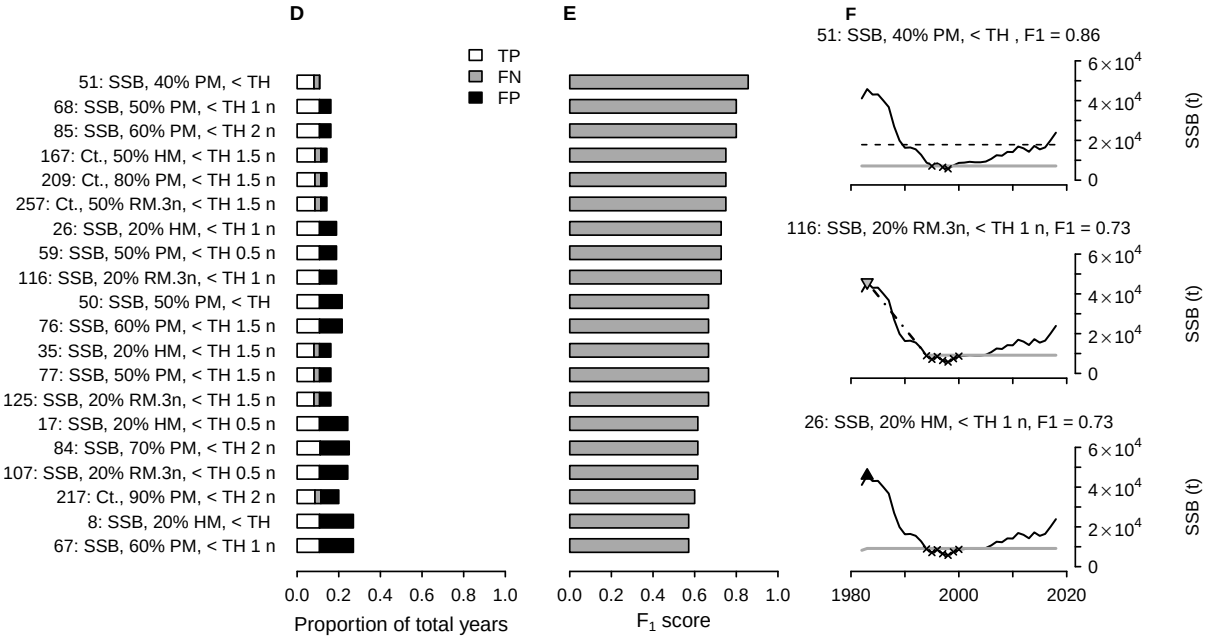

Four−spot megrim (sBoB.eAIW) − ldb.27.8c9a

Abbreviations

TP = True positive
FN = False negative
FP = False positive
HM = Historic maximum
RM.3n = Recent maximum (within 3 n)
PM = Population mean
n = Generation length
B_{ref} = Reference biomass
TH = Threshold
t = tonne

Abundance
Threshold
Abrupt decline
Fixed B_{ref}
HM, B_{ref}
RM.3n, B_{ref}
Collapsed

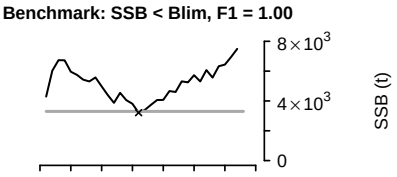

Literature and proposed definitions

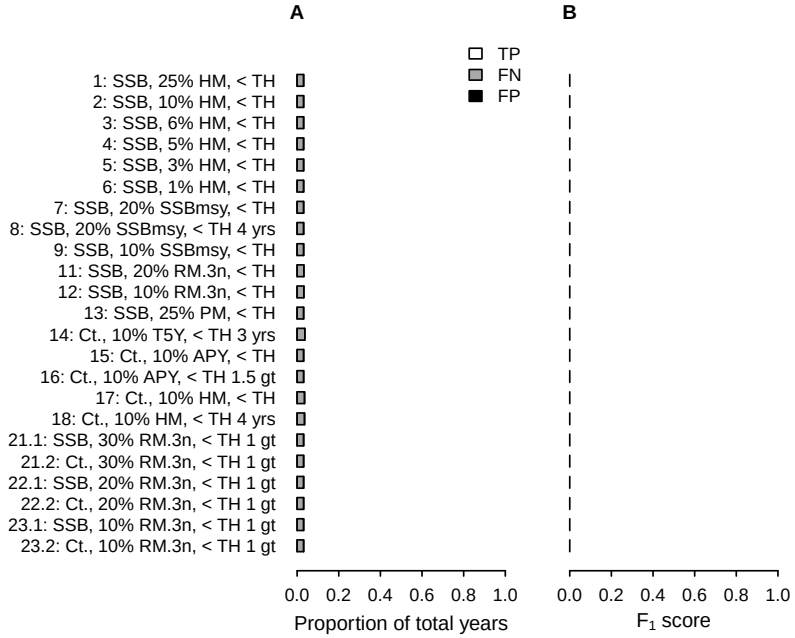

Simulated definitions

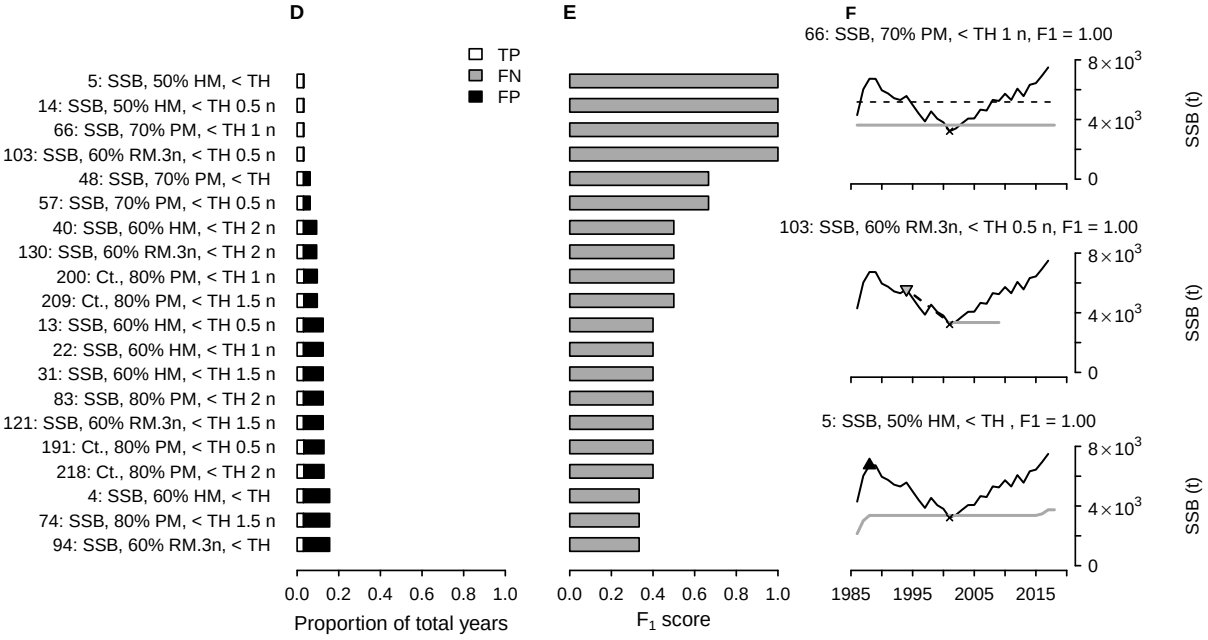

Mackerel (NEAaw) − mac.27.nea

Abbreviations

TP = True positive
FN = False negative
FP = False positive
HM = Historic maximum
RM.3n = Recent maximum (within 3 n)
PM = Population mean
n = Generation length
B_{ref} = Reference biomass
TH = Threshold
t = tonne

Abundance
Threshold
Abrupt decline
Fixed B_{ref}
HM, B_{ref}
RM.3n, B_{ref}
Collapsed

Benchmark: SSB < Blim, F1 = 1.00

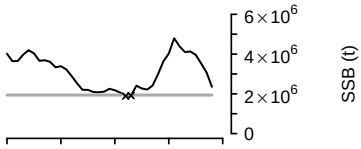

Literature and proposed definitions

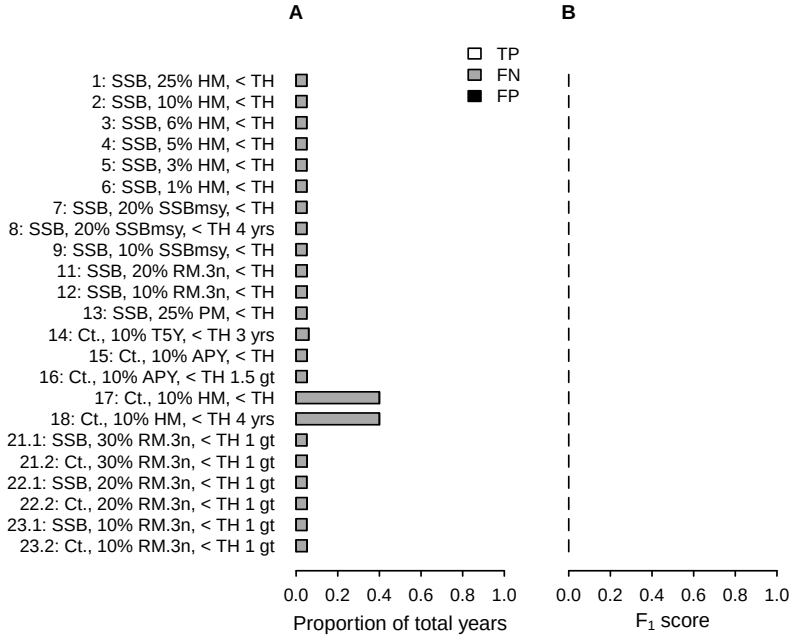

Simulated definitions

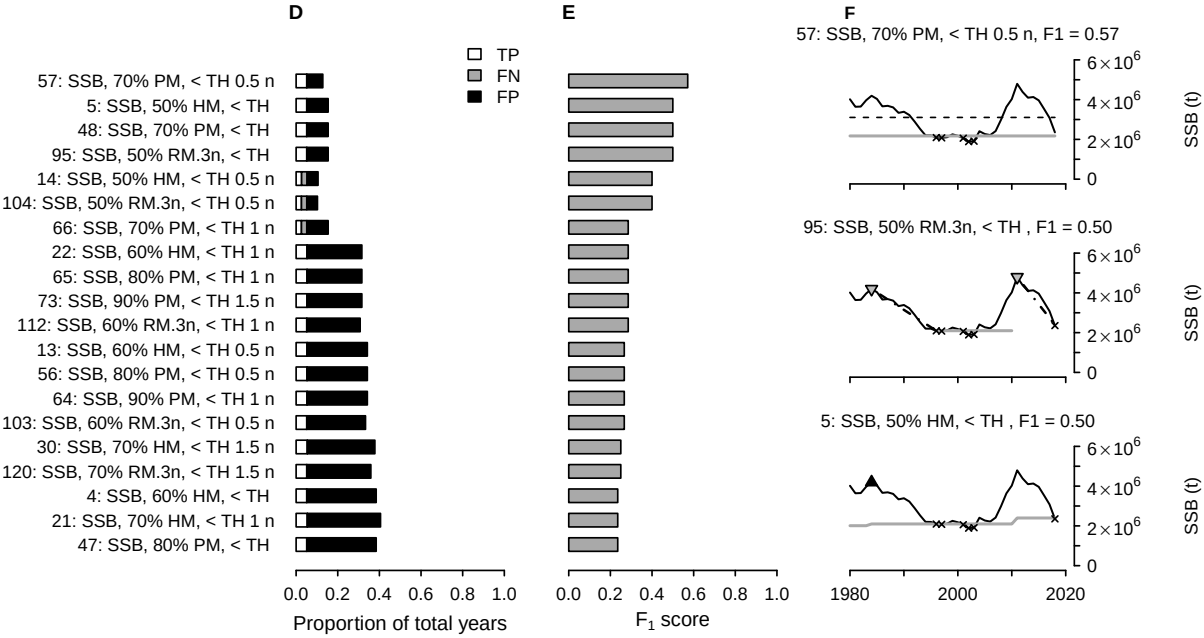

Megrim (CtS.AIW) − meg.27.8c9a

Abbreviations

TP = True positive
FN = False negative
FP = False positive
HM = Historic maximum
RM.3n = Recent maximum (within 3 n)
PM = Population mean
n = Generation length
B_{ref} = Reference biomass
TH = Threshold
t = tonne

Abundance
Threshold
Abrupt decline
Fixed B_{ref}
HM, B_{ref}
RM.3n, B_{ref}
Collapsed

Benchmark: SSB < Blim, F1 = 1.00

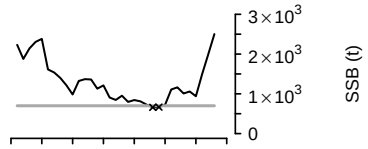

Literature and proposed definitions

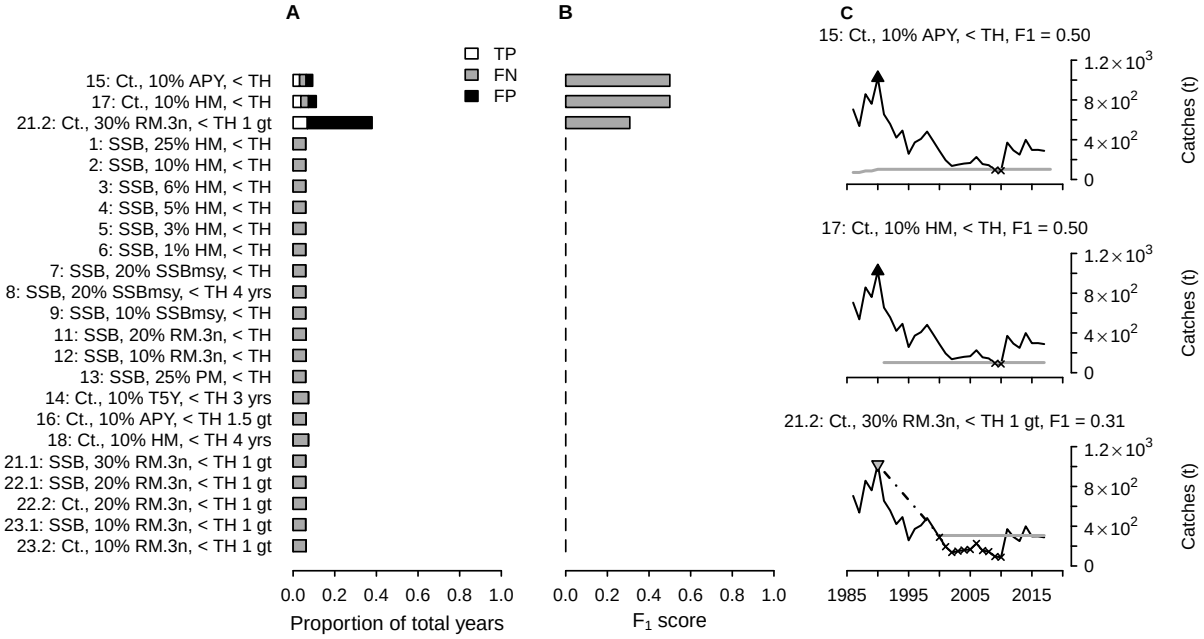

Simulated definitions

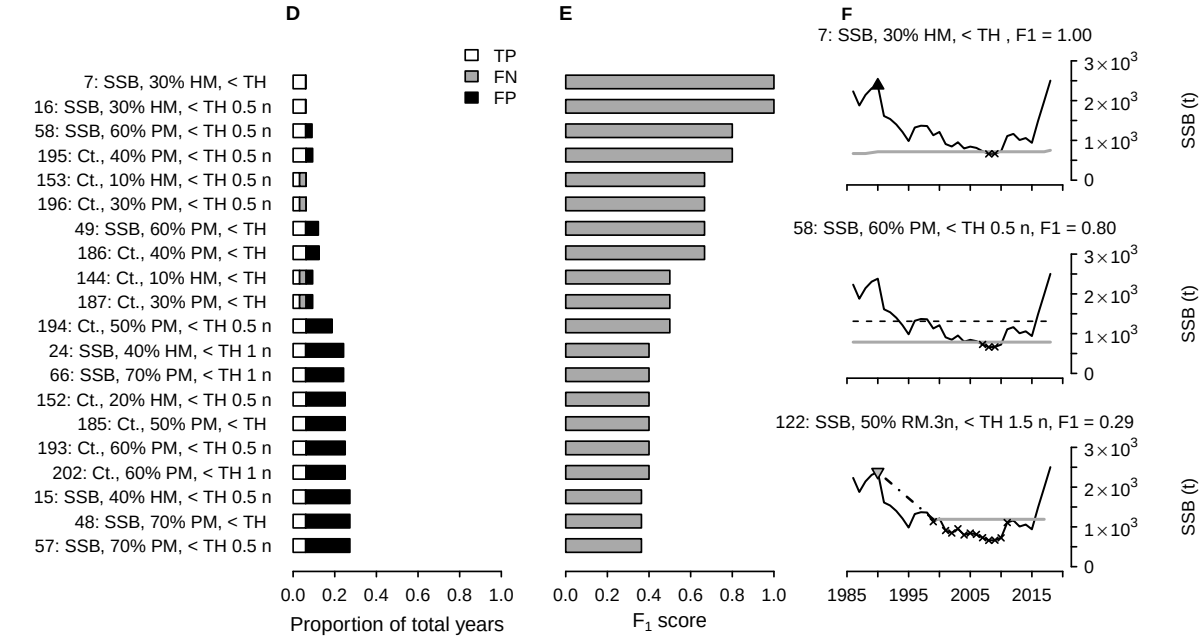

White anglerfish (CtS.AIW) − mon.27.8c9a

Abbreviations

TP = True positive
FN = False negative
FP = False positive
HM = Historic maximum
RM.3n = Recent maximum (within 3 n)
PM = Population mean
n = Generation length
B_{ref} = Reference biomass
TH = Threshold
t = tonne

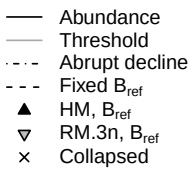

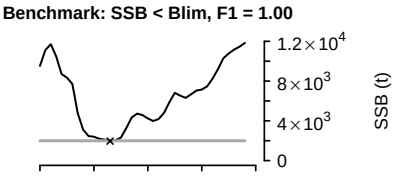

Literature and proposed definitions

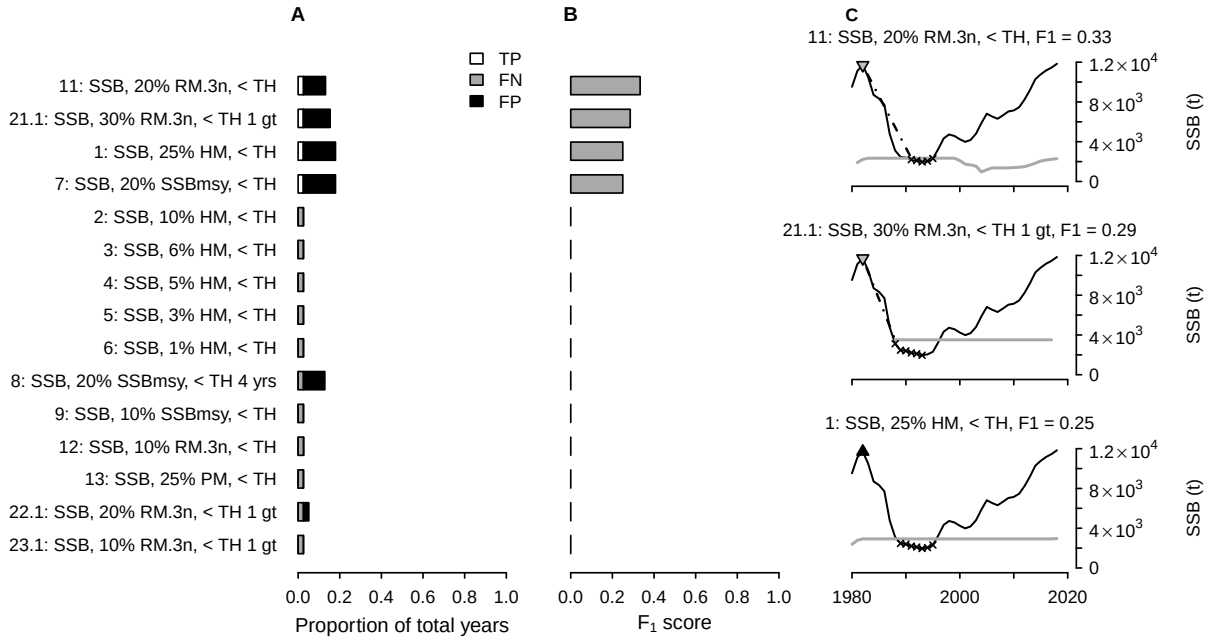

Simulated definitions

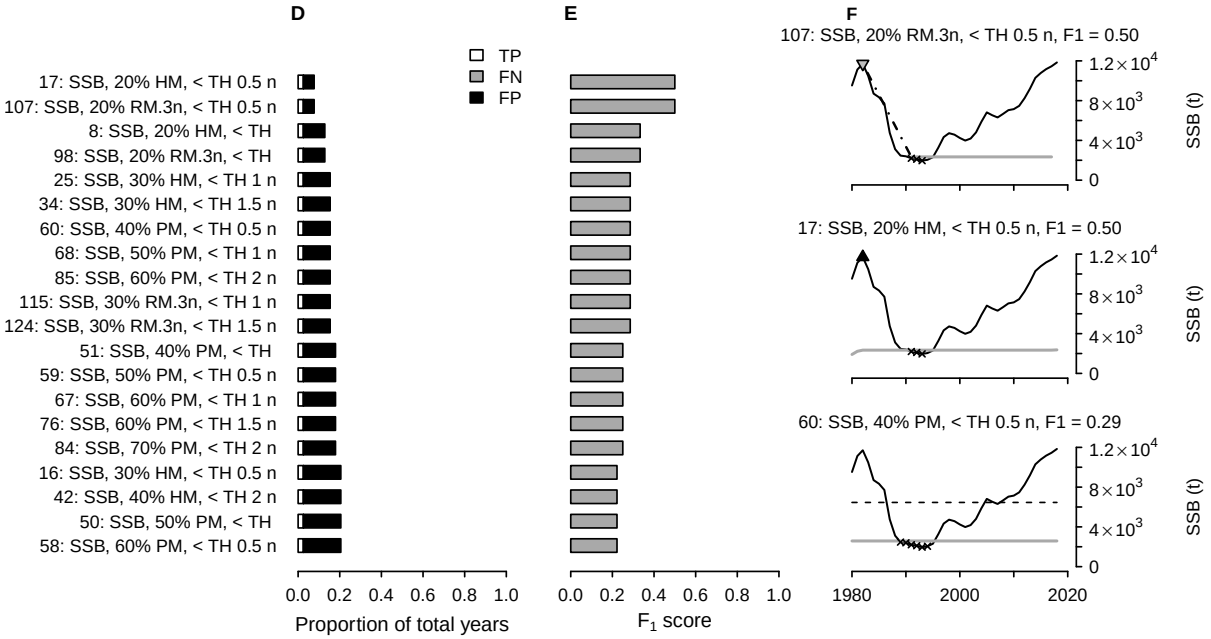

Norway pout (NS.Sk.Kt) − nop.27.3a4

Abbreviations

TP = True positive
FN = False negative
FP = False positive
HM = Historic maximum
RM.3n = Recent maximum (within 3 n)
PM = Population mean
n = Generation length
B_{ref} = Reference biomass
TH = Threshold
t = tonne

Abundance
Threshold
Abrupt decline
Fixed B_{ref}
HM, B_{ref}
RM.3n, B_{ref}
Collapsed

Benchmark: SSB < Blim, F1 = 1.00

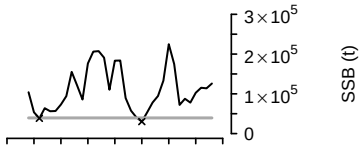

Literature and proposed definitions

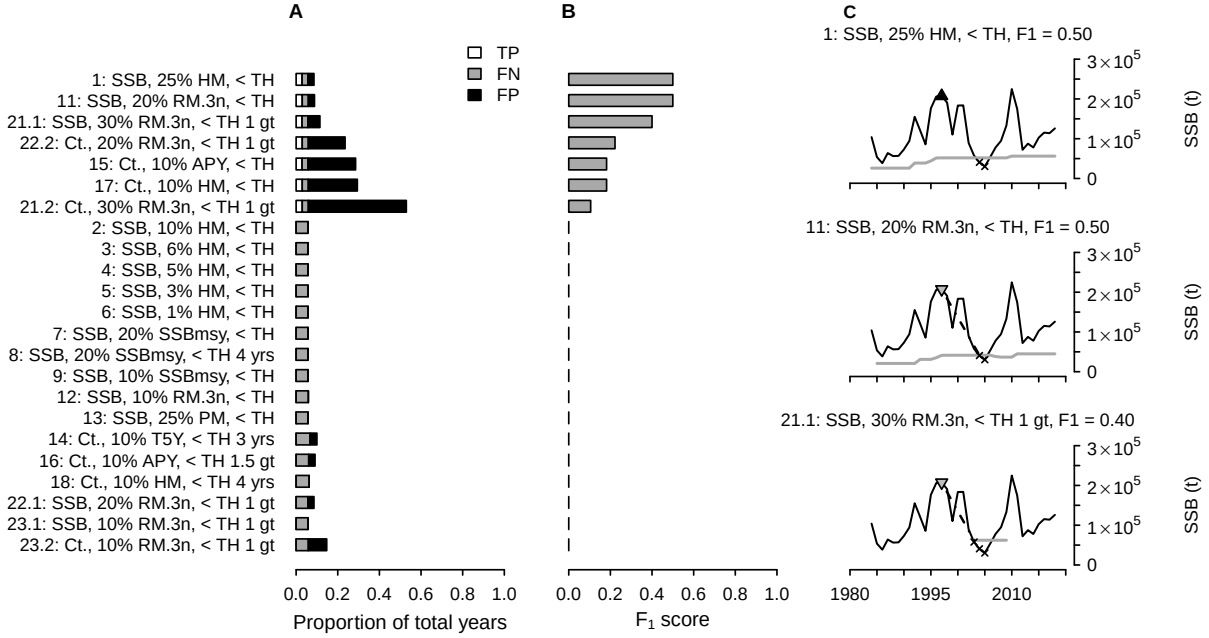

Simulated definitions

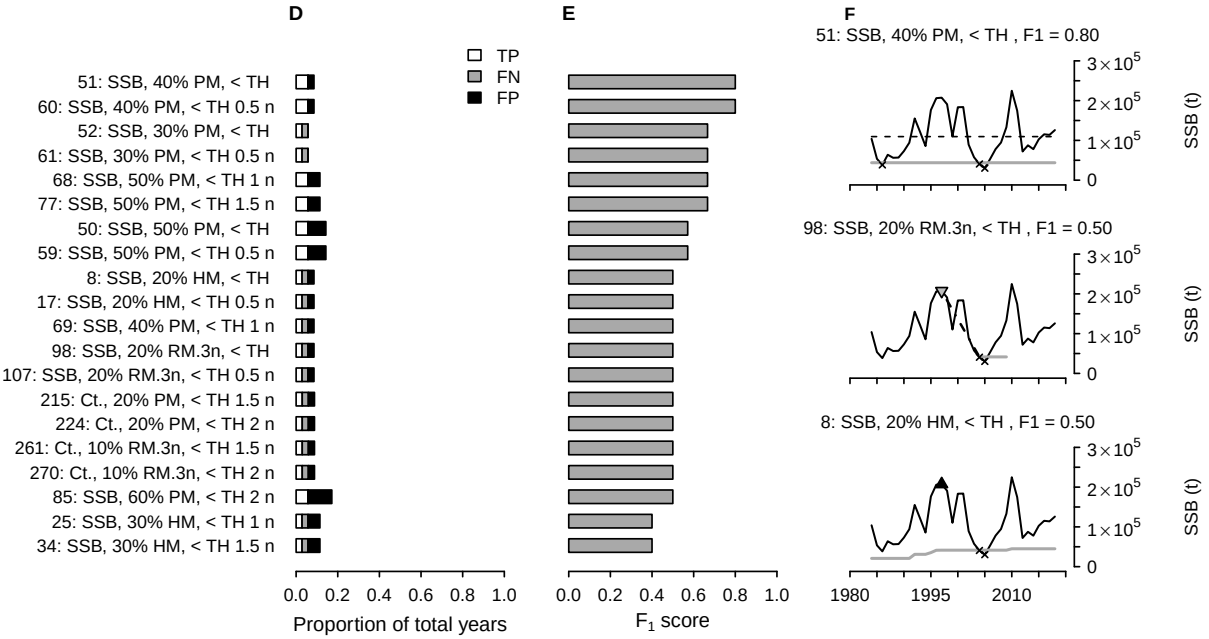

Sardine (CtS.AIW) − pil.27.8c9a

Abbreviations

TP = True positive
FN = False negative
FP = False positive
HM = Historic maximum
RM.3n = Recent maximum (within 3 n)
PM = Population mean
n = Generation length
B_{ref} = Reference biomass
TH = Threshold
t = tonne

Abundance
Threshold
Abrupt decline
Fixed B_{ref}
HM, B_{ref}
RM.3n, B_{ref}
Collapsed

Benchmark: SSB < Blim, F1 = 1.00

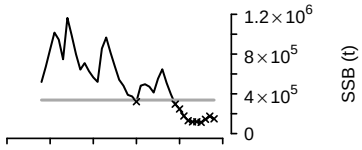

Literature and proposed definitions

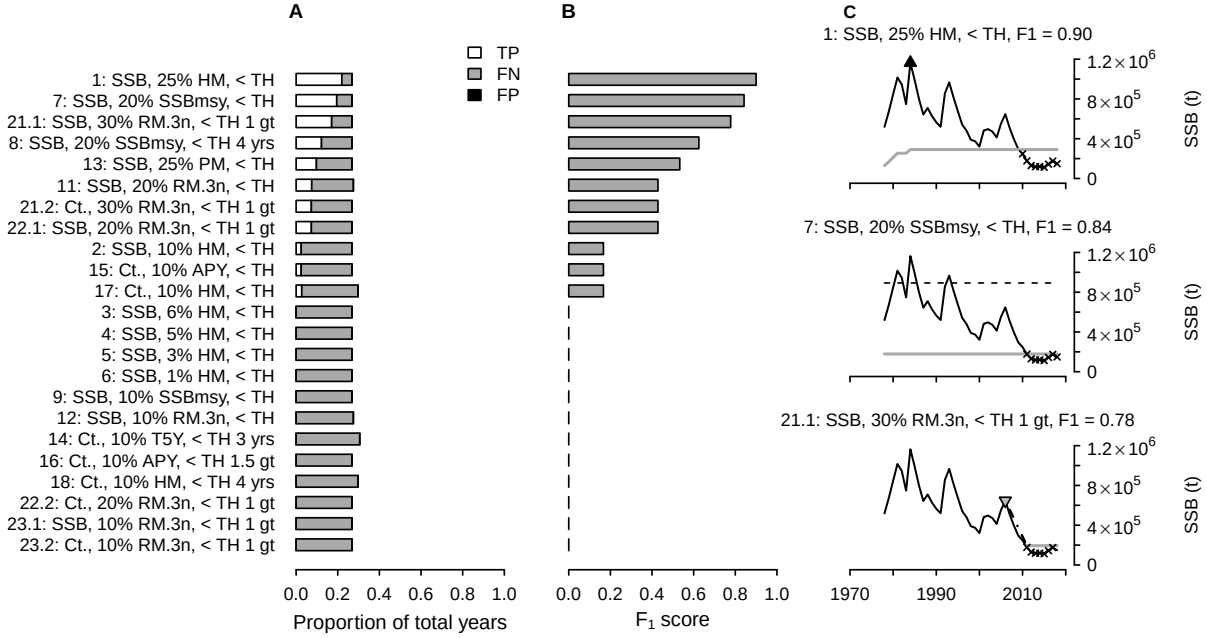

Simulated definitions

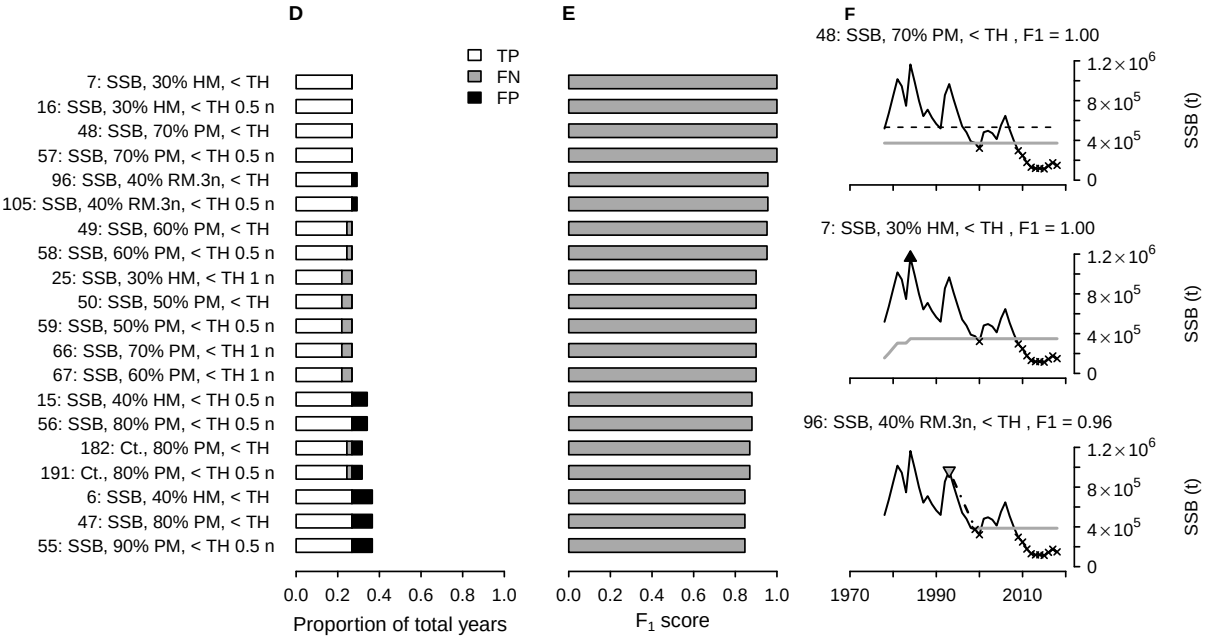

Plaice (NS.Sk) − ple.27.420

Abbreviations

TP = True positive
FN = False negative
FP = False positive
HM = Historic maximum
RM.3n = Recent maximum (within 3 n)
PM = Population mean
n = Generation length
B_{ref} = Reference biomass
TH = Threshold
t = tonne

Abundance
Threshold
Abrupt decline
Fixed B_{ref}
HM, B_{ref}
RM.3n, B_{ref}
Collapsed

Benchmark: SSB < Blim, F1 = 1.00

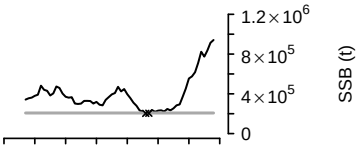

Literature and proposed definitions

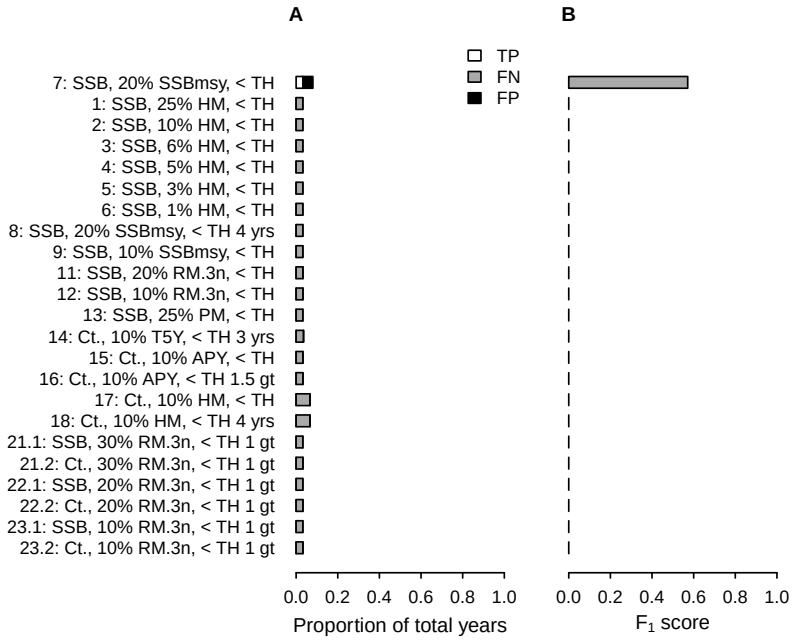

C

7: SSB, 20% SSBmsy, < TH, F1 = 0.57

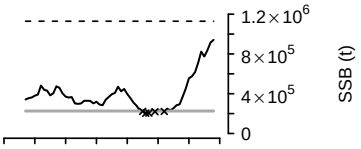

Simulated definitions

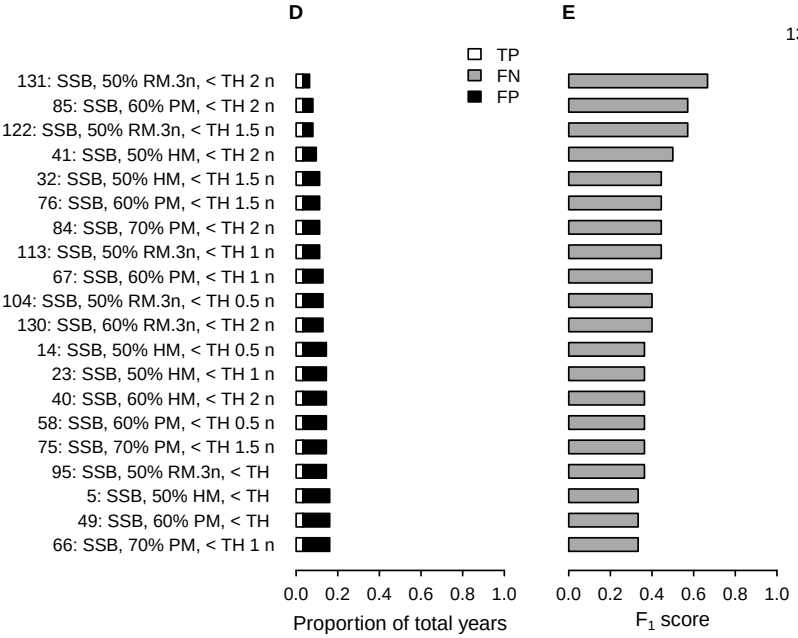

F

131: SSB, 50% RM.3n, < TH 2 n, F1 = 0.67

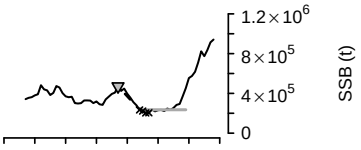

85: SSB, 60% PM, < TH 2 n, F1 = 0.57

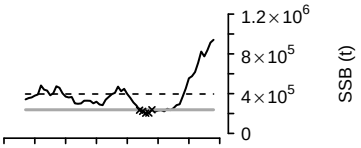

41: SSB, 50% HM, < TH 2 n, F1 = 0.50

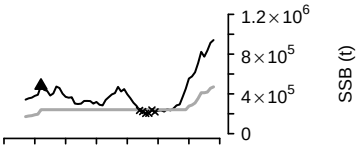

Plaice (IS) − ple.27.7a

Abbreviations

TP = True positive
FN = False negative
FP = False positive
HM = Historic maximum
RM.3n = Recent maximum (within 3 n)
PM = Population mean
n = Generation length
B_{ref} = Reference biomass
TH = Threshold
t = tonne

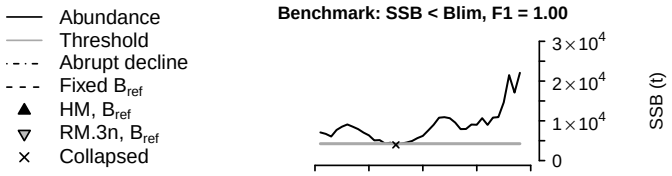

Literature and proposed definitions

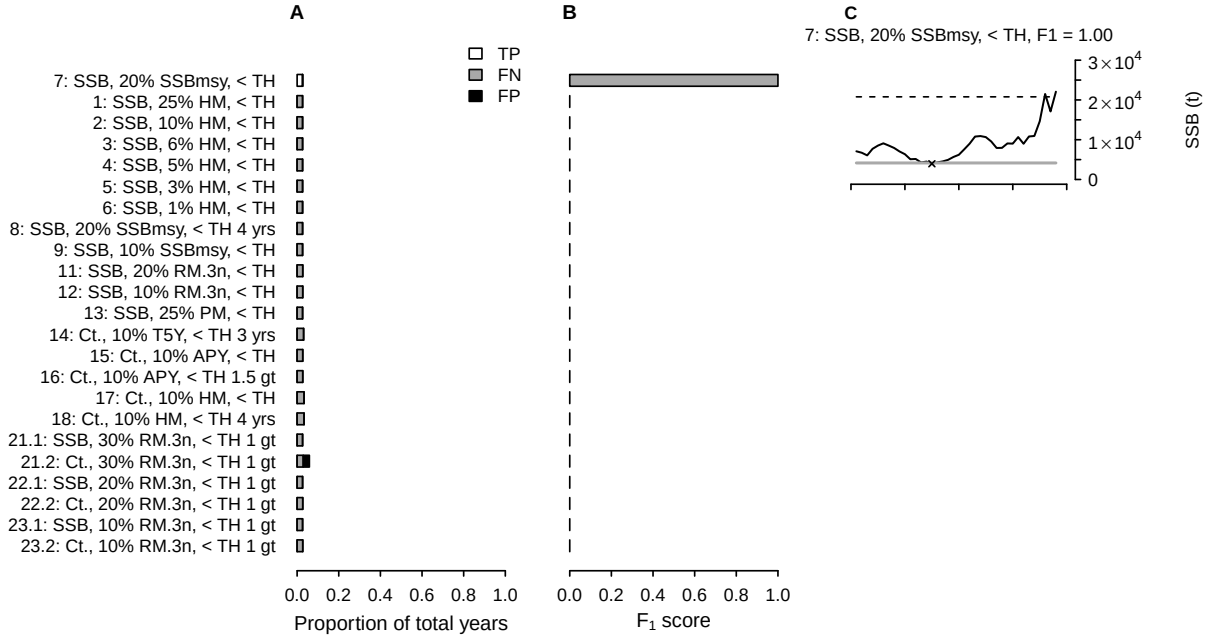

Simulated definitions

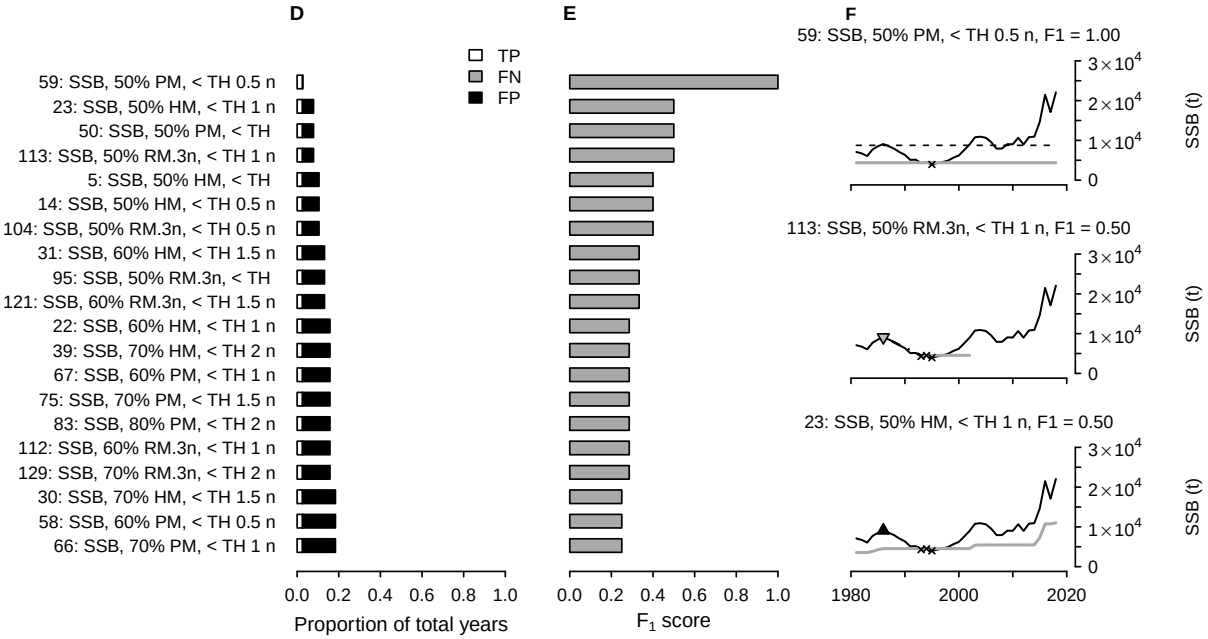

Saithe (NEA) − pok.27.1−2

Abbreviations

TP = True positive
FN = False negative
FP = False positive
HM = Historic maximum
RM.3n = Recent maximum (within 3 n)
PM = Population mean
n = Generation length
B_{ref} = Reference biomass
TH = Threshold
t = tonne

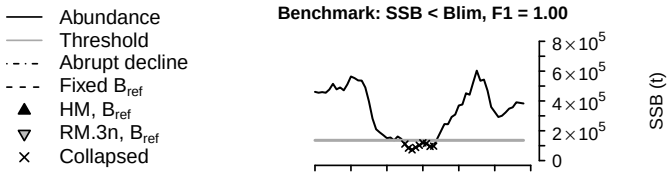

Literature and proposed definitions

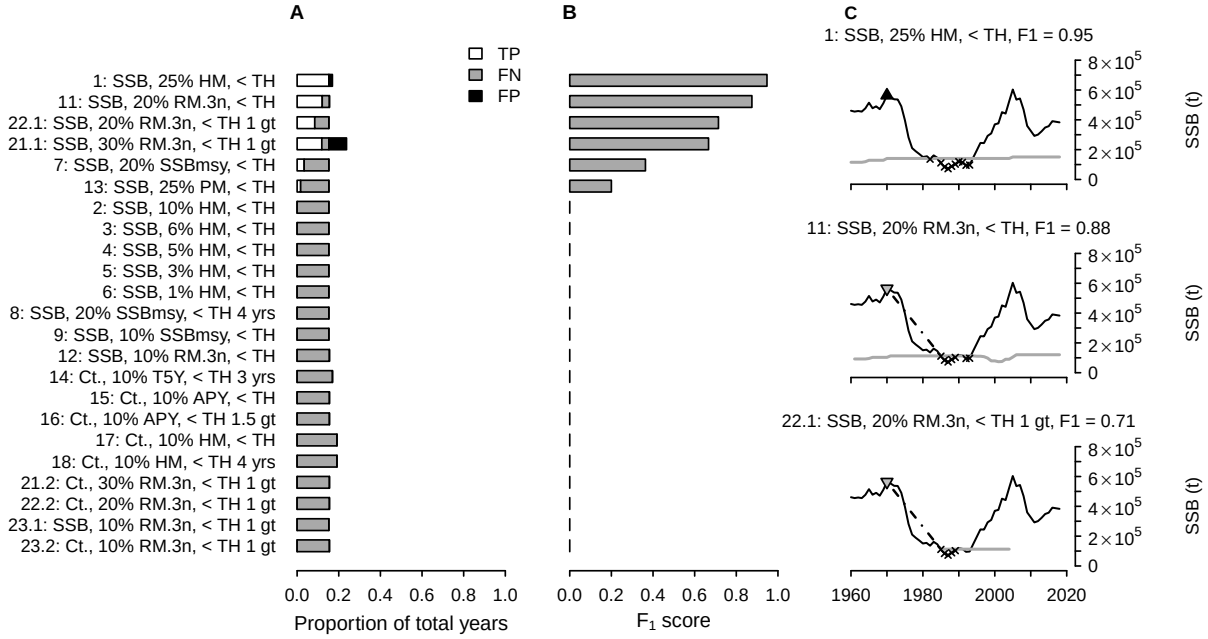

Simulated definitions

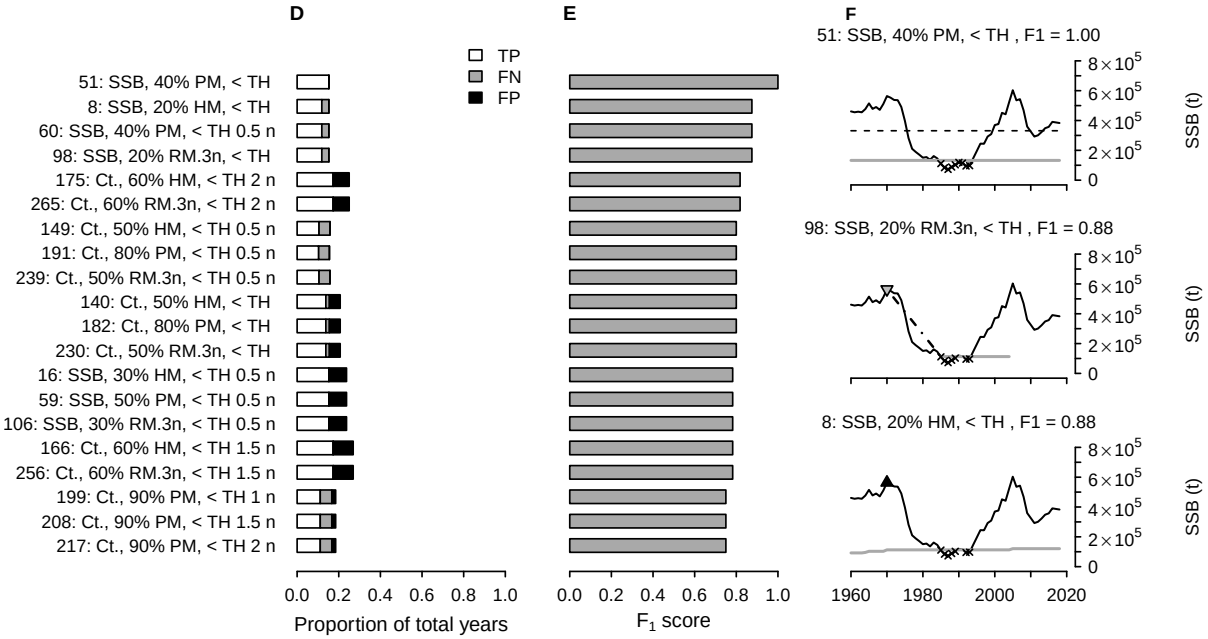

Golden redfish (NEA) − reg.27.1−2

Abbreviations

TP = True positive
FN = False negative
FP = False positive
HM = Historic maximum
RM.3n = Recent maximum (within 3 n)
PM = Population mean
n = Generation length
B_{ref} = Reference biomass
TH = Threshold
t = tonne

Abundance
Threshold
Abrupt decline
Fixed B_{ref}
HM, B_{ref}
RM.3n, B_{ref}
Collapsed

Benchmark: SSB < Blim, F1 = 1.00

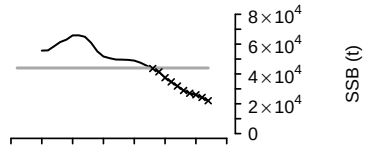

Literature and proposed definitions

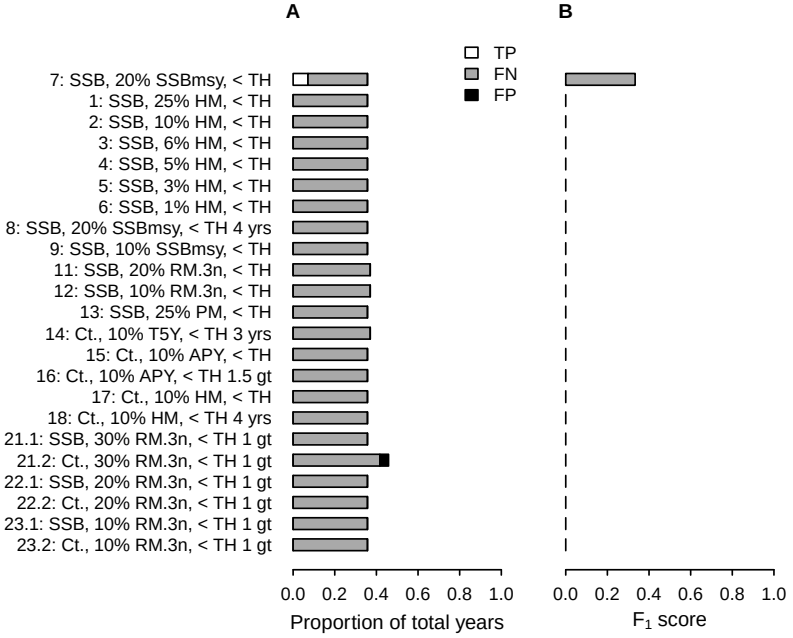

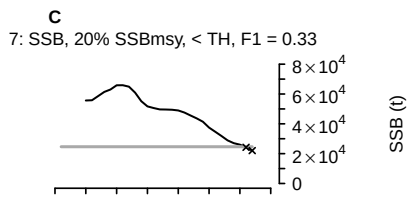

Simulated definitions

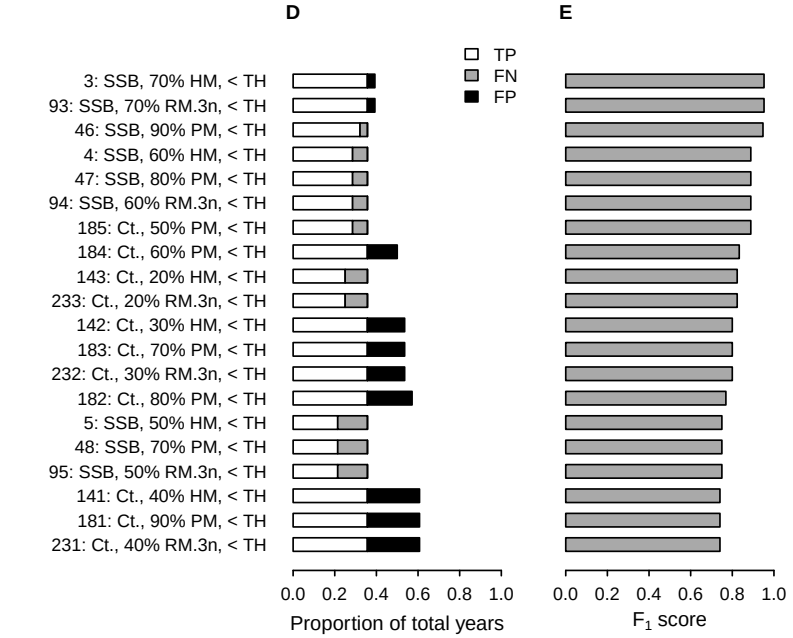

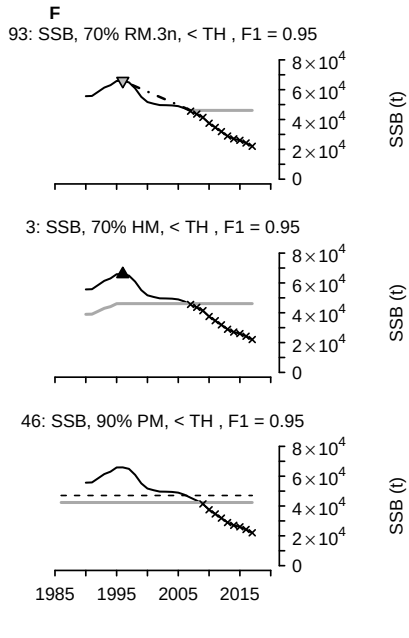

Golden redfish (IG.FG.WS.NA.EG) − reg.27.561214

Abbreviations

TP = True positive
FN = False negative
FP = False positive
HM = Historic maximum
RM.3n = Recent maximum (within 3 n)
PM = Population mean
n = Generation length
B_{ref} = Reference biomass
TH = Threshold
t = tonne

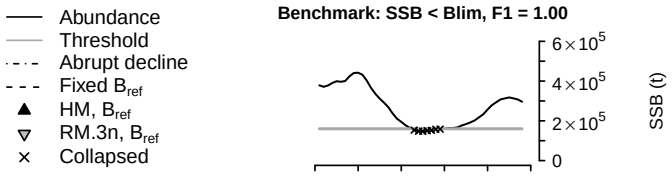

Literature and proposed definitions

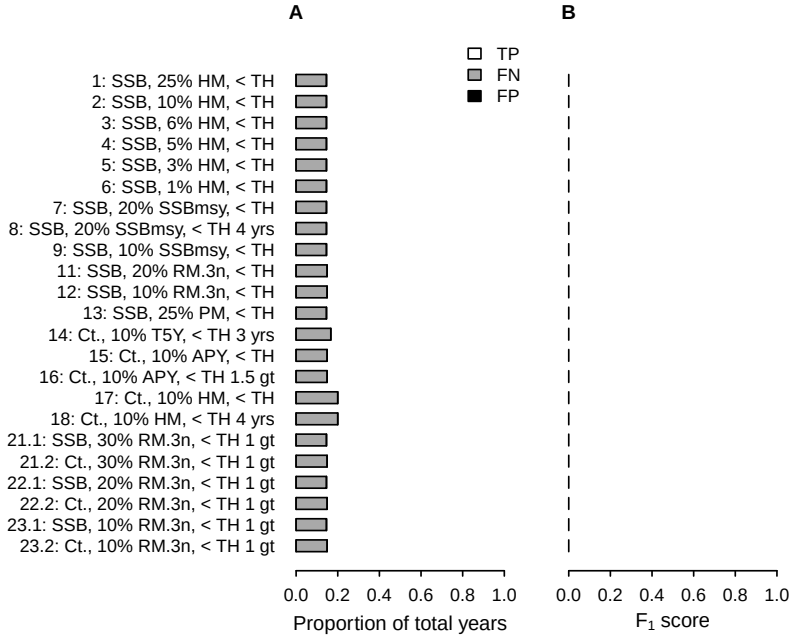

Simulated definitions

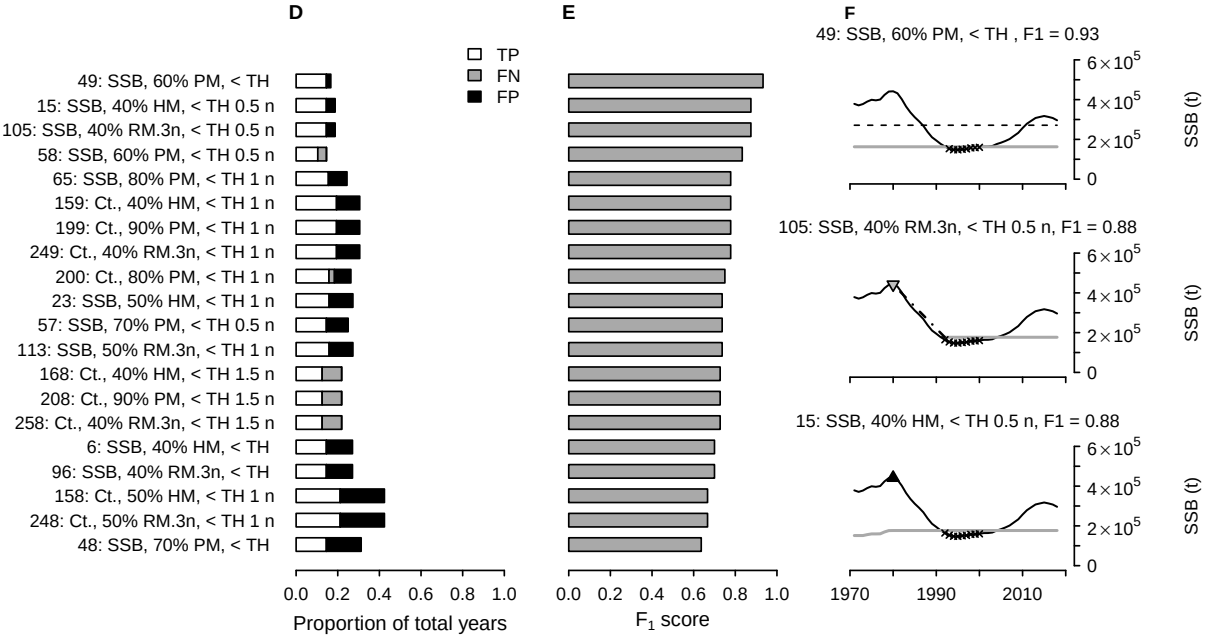

Sandeel (csNS.DB) − san.sa.1r

Abbreviations

TP = True positive
FN = False negative
FP = False positive
HM = Historic maximum
RM.3n = Recent maximum (within 3 n)
PM = Population mean
n = Generation length
B_{ref} = Reference biomass
TH = Threshold
t = tonne

Abundance
Threshold
Abrupt decline
Fixed B_{ref}
HM, B_{ref}
RM.3n, B_{ref}
Collapsed

Benchmark: SSB < Blim, F1 = 1.00

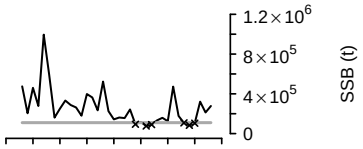

Literature and proposed definitions

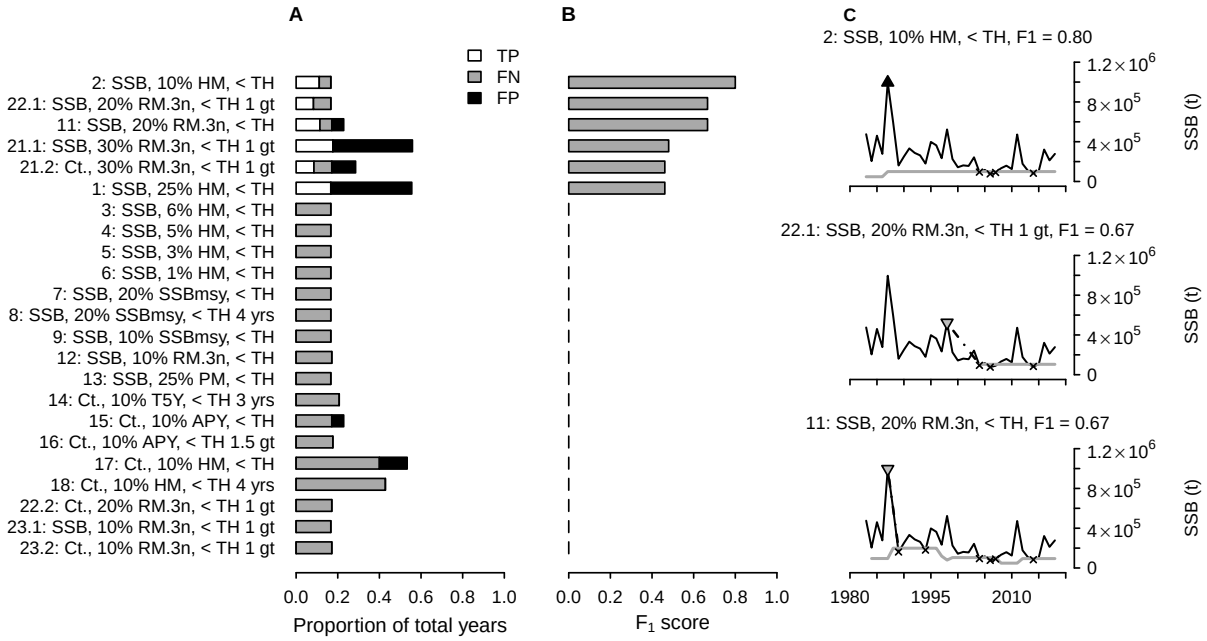

Simulated definitions

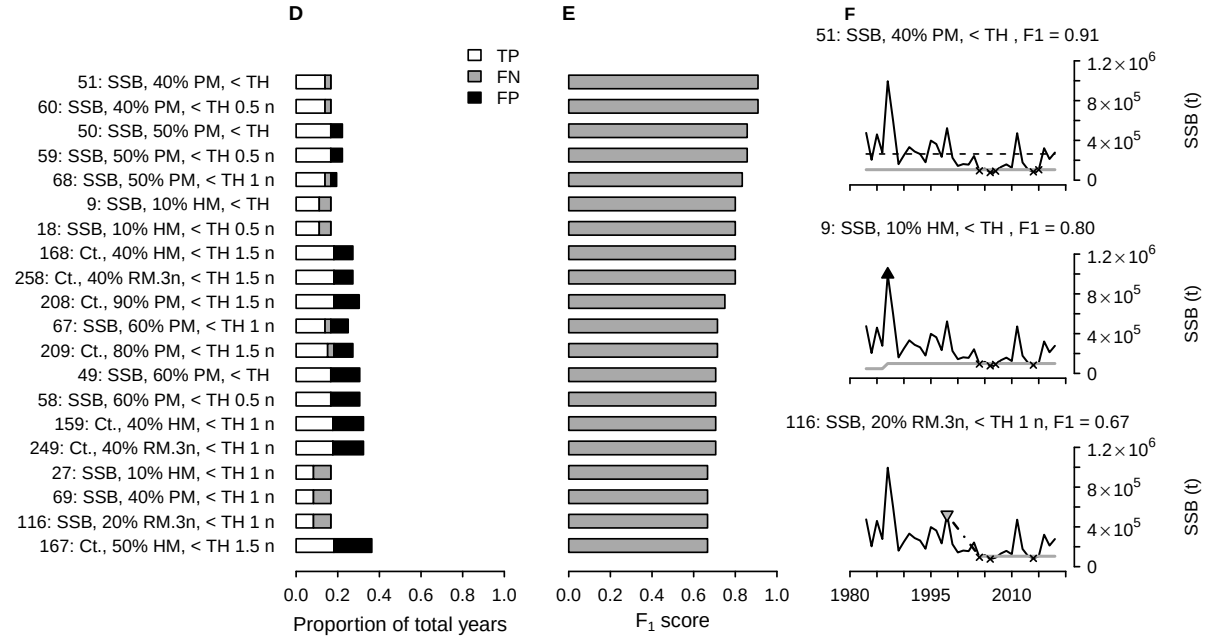

Sandeel (Sk.csNS) − san.sa.2r

Abbreviations

TP = True positive
FN = False negative
FP = False positive
HM = Historic maximum
RM.3n = Recent maximum (within 3 n)
PM = Population mean
n = Generation length
B_{ref} = Reference biomass
TH = Threshold
t = tonne

Abundance
Threshold
Abrupt decline
Fixed B_{ref}
HM, B_{ref}
RM.3n, B_{ref}
Collapsed

Benchmark: SSB < Blim, F1 = 1.00

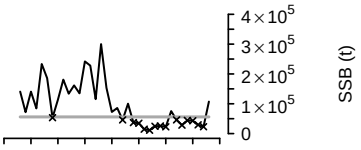

Literature and proposed definitions

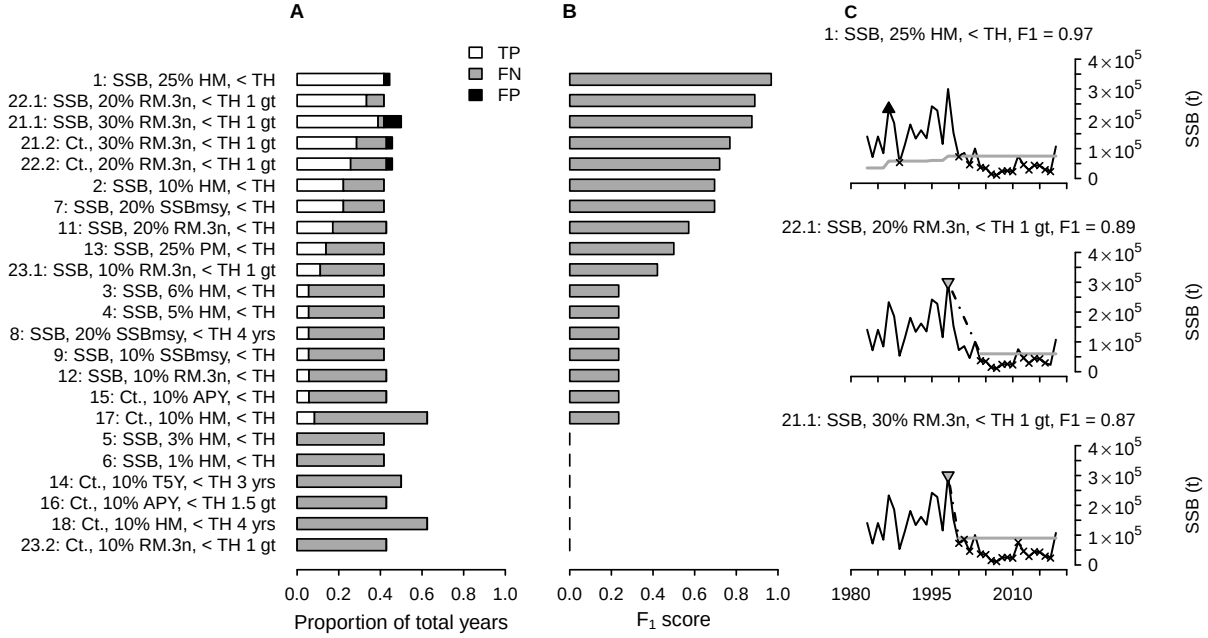

Simulated definitions

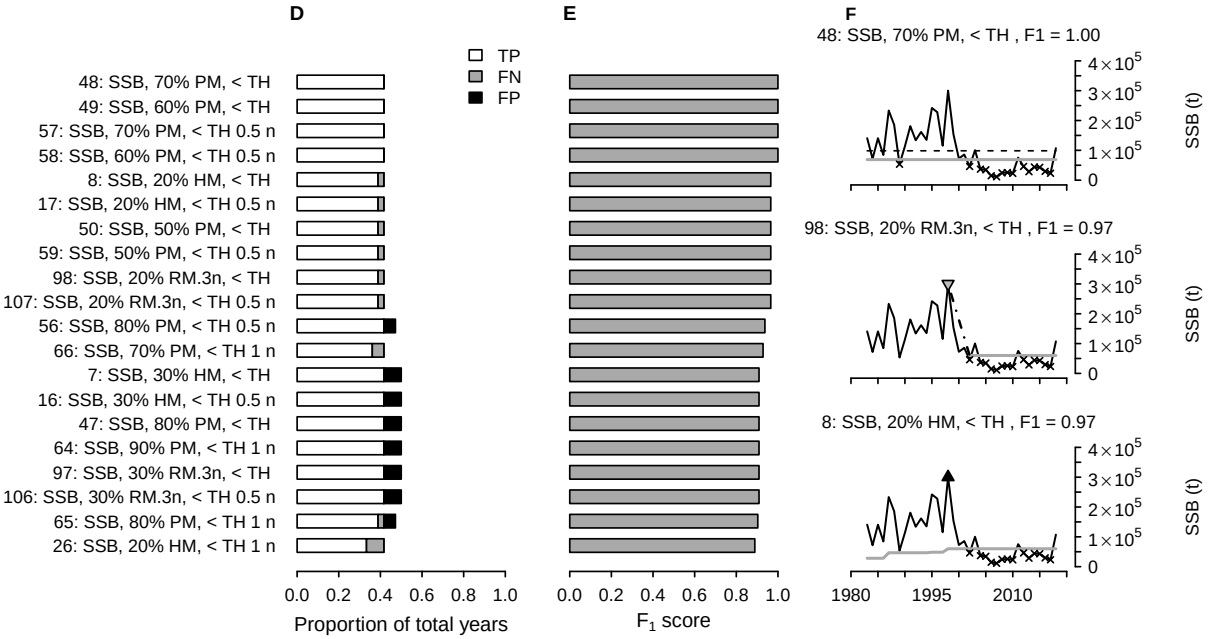

Sandeel (Sk.ncNS) − san.sa.3r

Abbreviations

TP = True positive
FN = False negative
FP = False positive
HM = Historic maximum
RM.3n = Recent maximum (within 3 n)
PM = Population mean
n = Generation length
B_{ref} = Reference biomass
TH = Threshold
t = tonne

Abundance
Threshold
Abrupt decline
Fixed B_{ref}
HM, B_{ref}
RM.3n, B_{ref}
Collapsed

Benchmark: SSB < Blim, F1 = 1.00

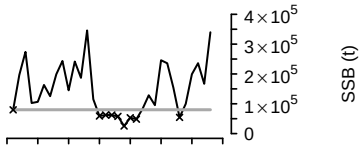

Literature and proposed definitions

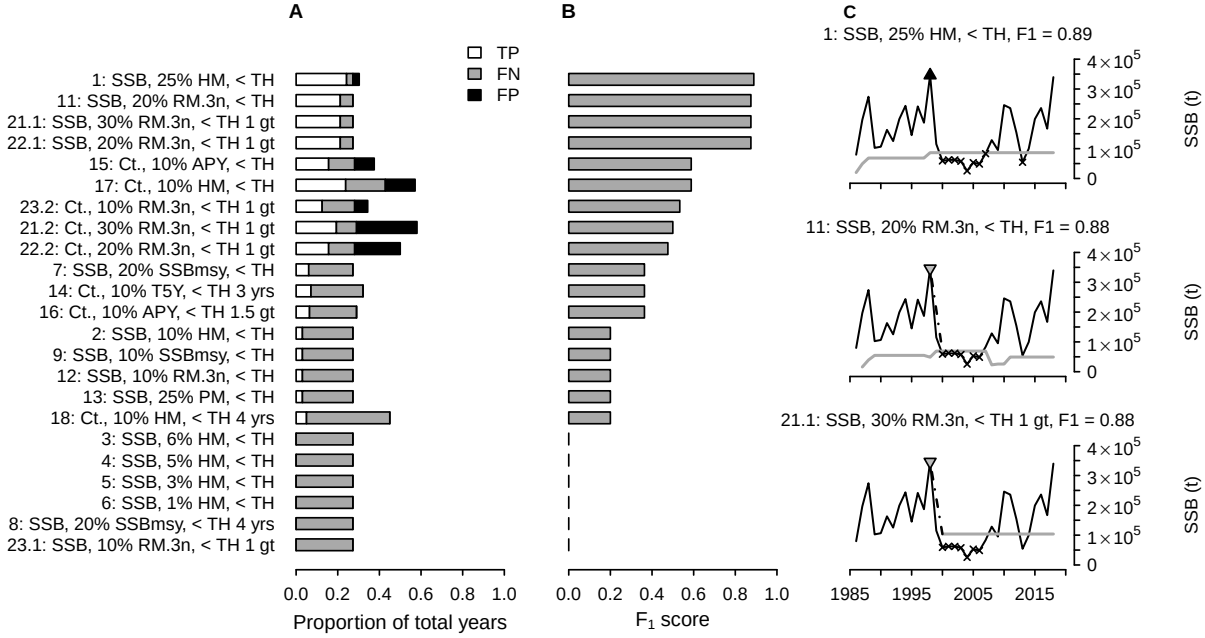

Simulated definitions

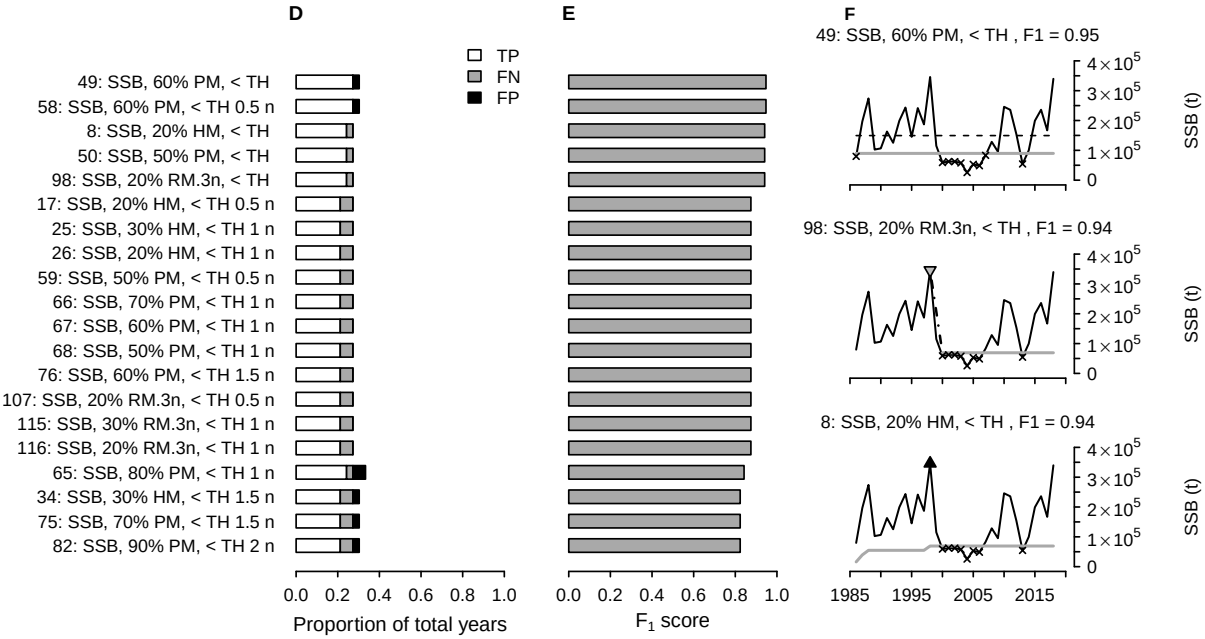

Sandeel (ncNS) − san.sa.4

Abbreviations

TP = True positive
FN = False negative
FP = False positive
HM = Historic maximum
RM.3n = Recent maximum (within 3 n)
PM = Population mean
n = Generation length
B_{ref} = Reference biomass
TH = Threshold
t = tonne

Abundance
Threshold
Abrupt decline
Fixed B_{ref}
HM, B_{ref}
RM.3n, B_{ref}
Collapsed

Benchmark: SSB < Blim, F1 = 1.00

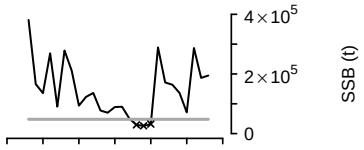

Literature and proposed definitions

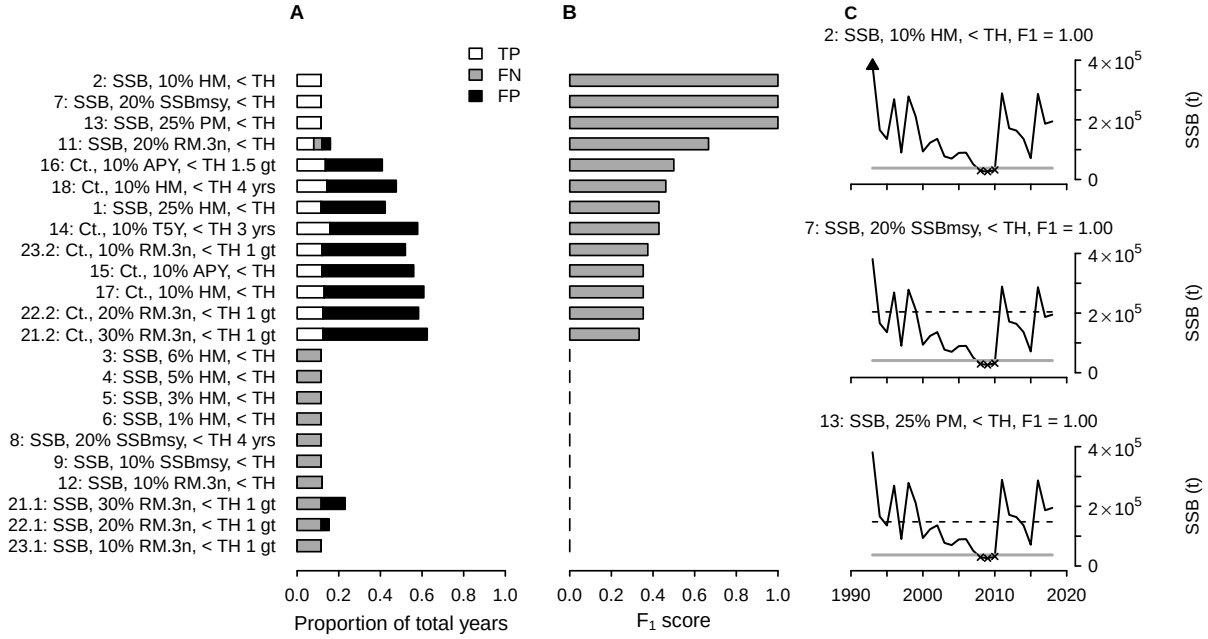

Simulated definitions

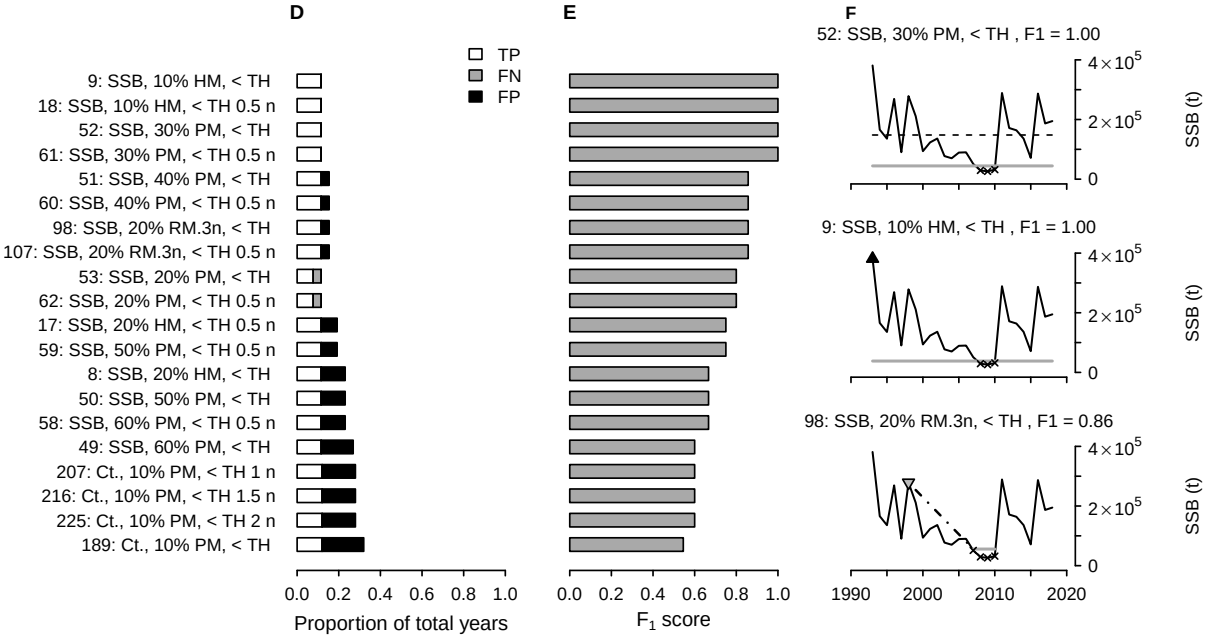

Sole (NS) − sol.27.4

Abbreviations

TP = True positive
FN = False negative
FP = False positive
HM = Historic maximum
RM.3n = Recent maximum (within 3 n)
PM = Population mean
n = Generation length
B_{ref} = Reference biomass
TH = Threshold
t = tonne

Abundance
Threshold
Abrupt decline
Fixed B_{ref}
HM, B_{ref}
RM.3n, B_{ref}
Collapsed

Benchmark: SSB < Blim, F1 = 1.00

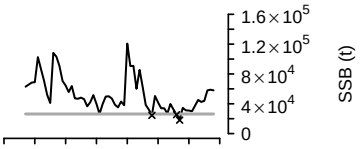

Literature and proposed definitions

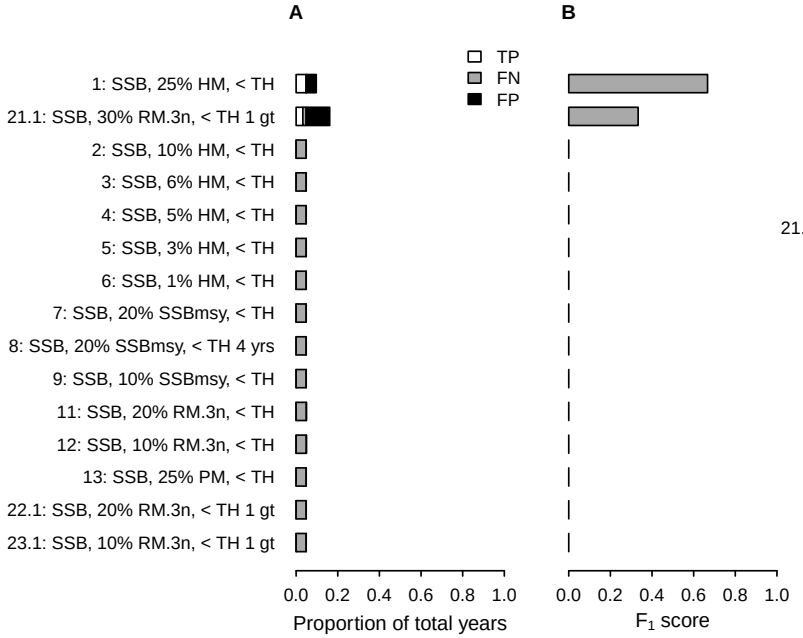

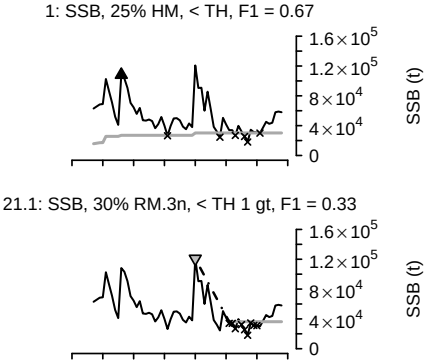

Simulated definitions

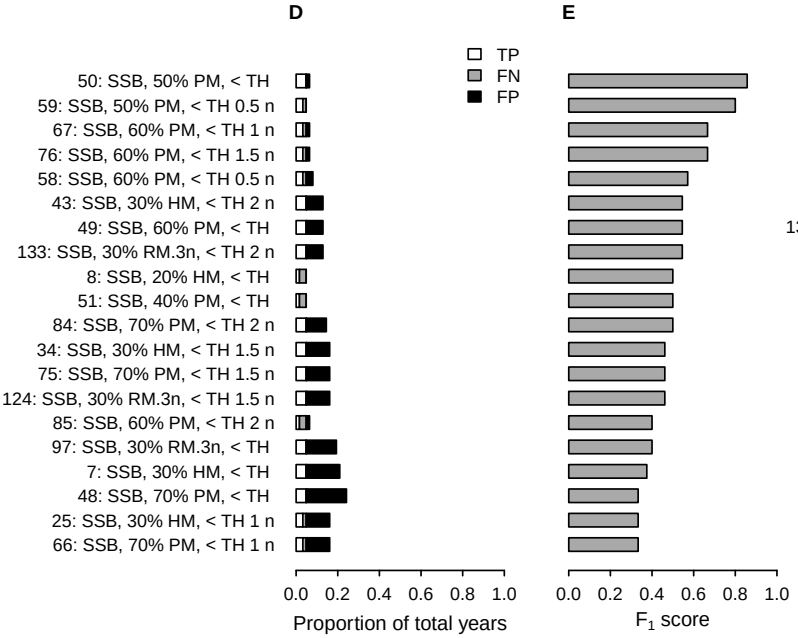

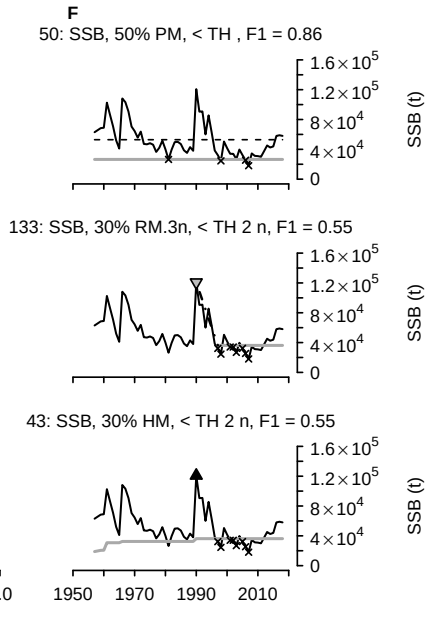

Sole (IS) − sol.27.7a

Abbreviations

TP = True positive
FN = False negative
FP = False positive
HM = Historic maximum
RM.3n = Recent maximum (within 3 n)
PM = Population mean
n = Generation length
B_{ref} = Reference biomass
TH = Threshold
t = tonne

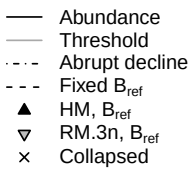

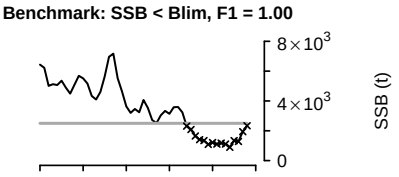

Literature and proposed definitions

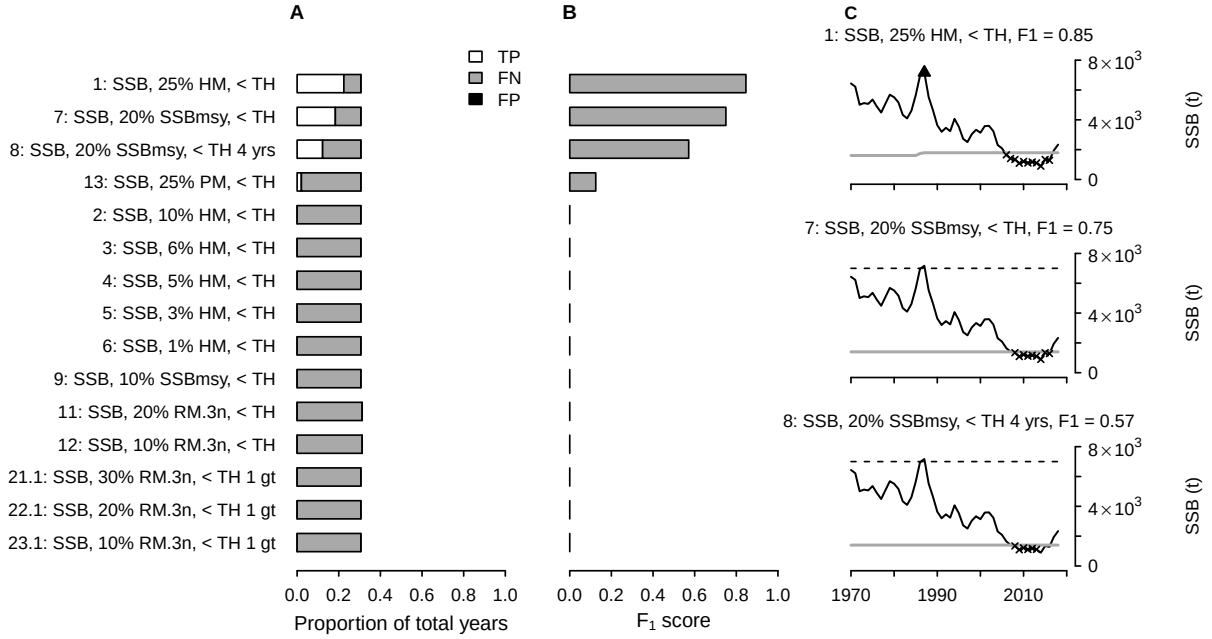

Simulated definitions

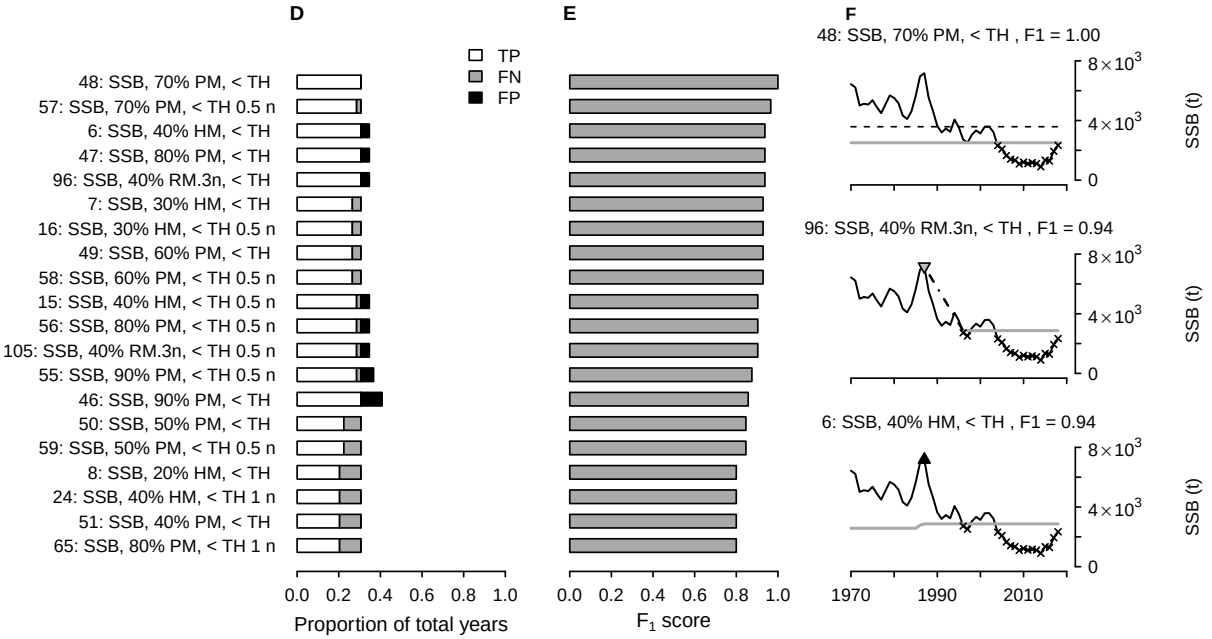

Sole (BC.CS) − sol.27.7fg

Abbreviations

TP = True positive
FN = False negative
FP = False positive
HM = Historic maximum
RM.3n = Recent maximum (within 3 n)
PM = Population mean
n = Generation length
B_{ref} = Reference biomass
TH = Threshold
t = tonne

Abundance
Threshold
Abrupt decline
Fixed B_{ref}
HM, B_{ref}
RM.3n, B_{ref}
Collapsed

Benchmark: SSB < Blim, F1 = 1.00

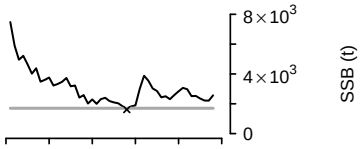

Literature and proposed definitions

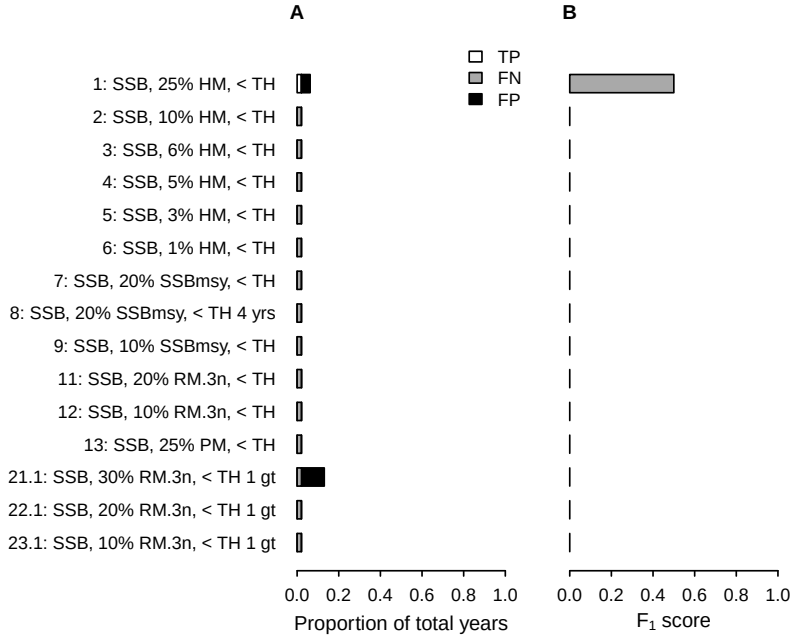

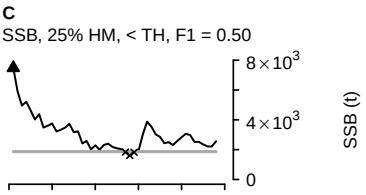

Simulated definitions

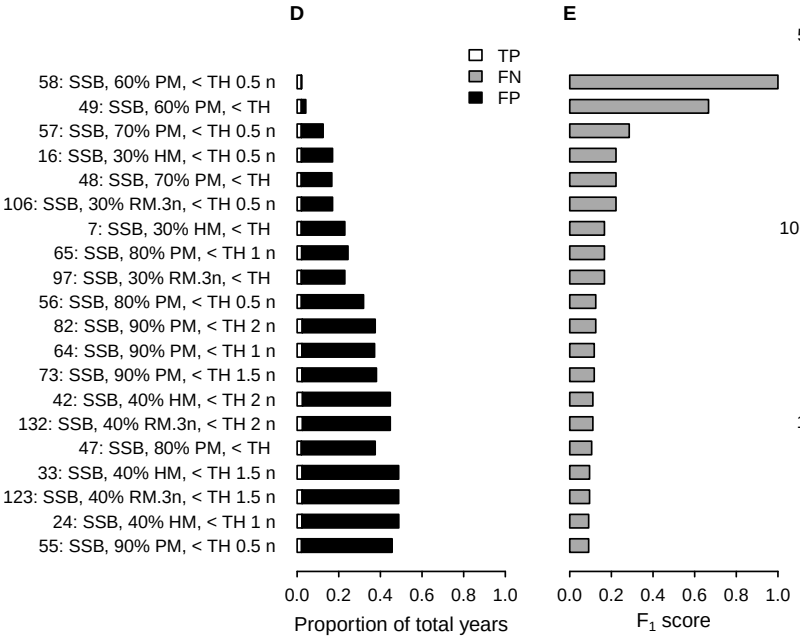

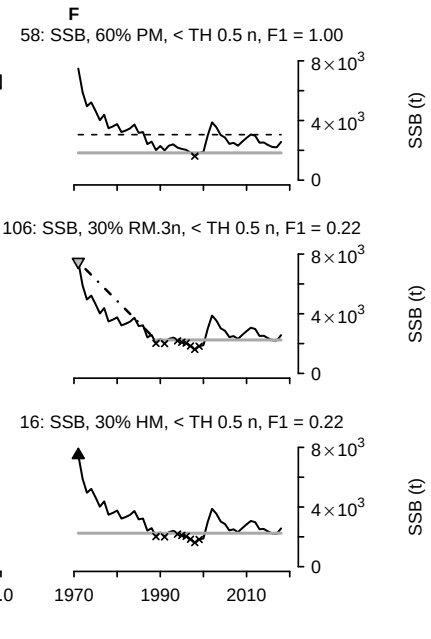

Sprat (NS) − spr.27.4

Abbreviations

TP = True positive
FN = False negative
FP = False positive
HM = Historic maximum
RM.3n = Recent maximum (within 3 n)
PM = Population mean
n = Generation length
B_{ref} = Reference biomass
TH = Threshold
t = tonne

Abundance
Threshold
Abrupt decline
Fixed B_{ref}
HM, B_{ref}
RM.3n, B_{ref}
Collapsed

Benchmark: SSB < Blim, F1 = 1.00

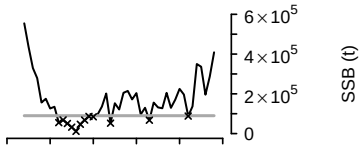

Literature and proposed definitions

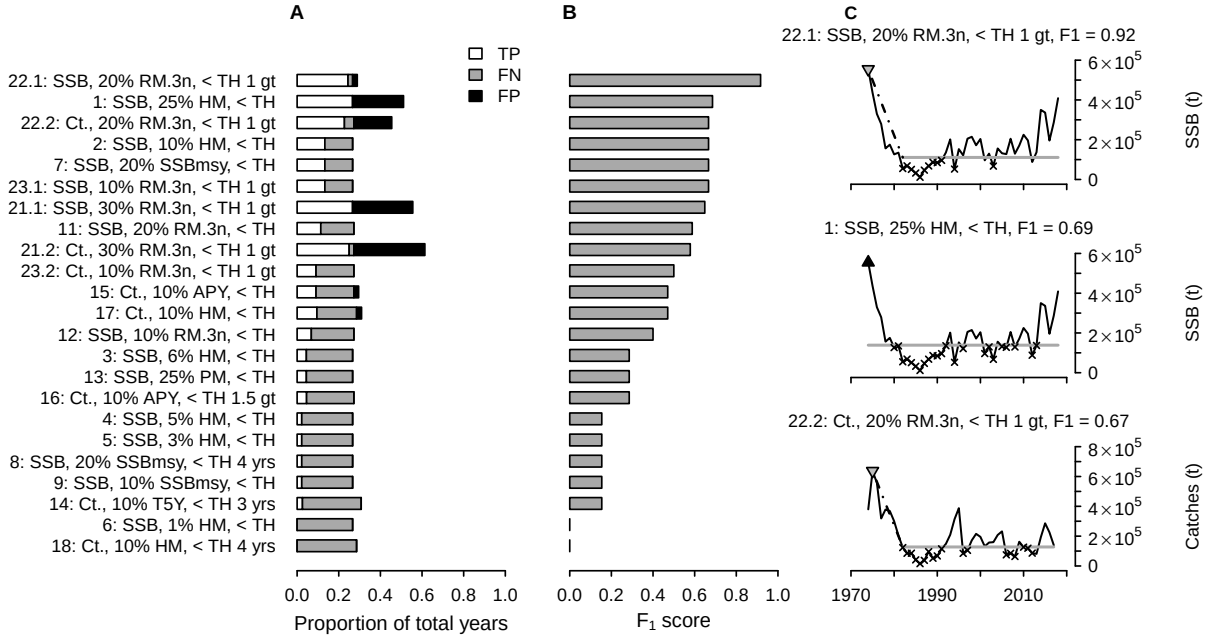

Simulated definitions

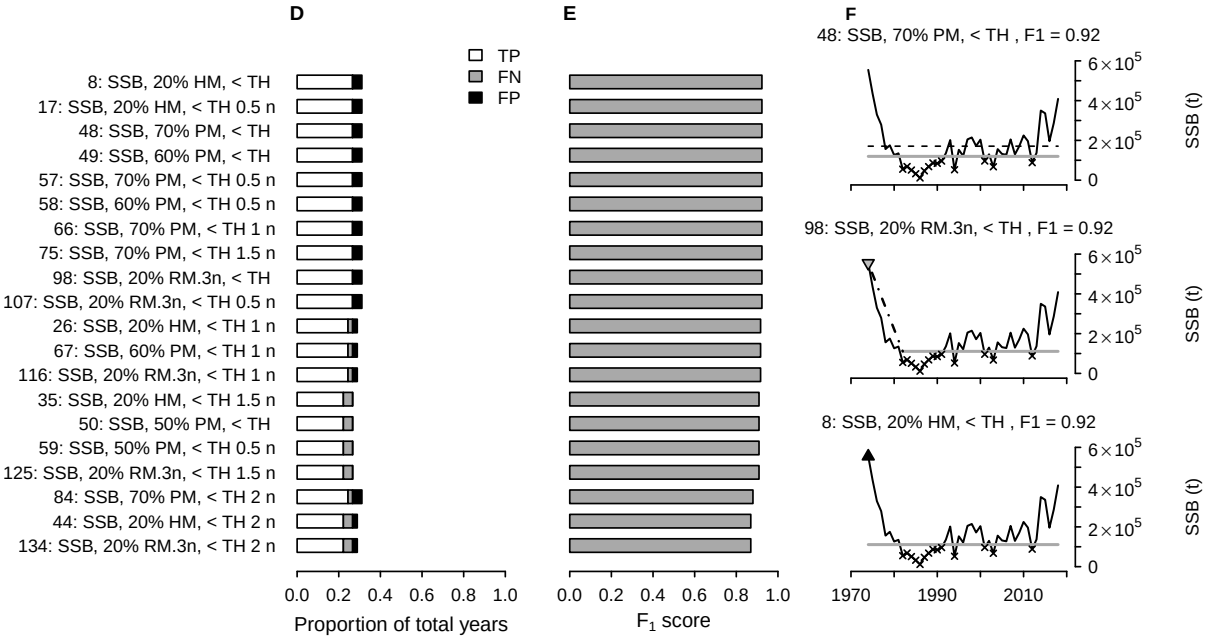

Whiting (WS) − whg.27.6a

Abbreviations

TP = True positive
FN = False negative
FP = False positive
HM = Historic maximum
RM.3n = Recent maximum (within 3 n)
PM = Population mean
n = Generation length
B_{ref} = Reference biomass
TH = Threshold
t = tonne

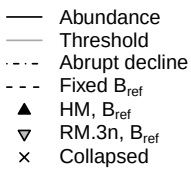

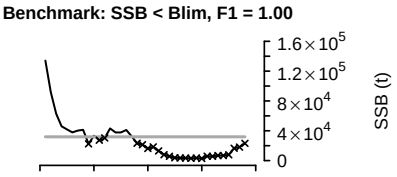

Literature and proposed definitions

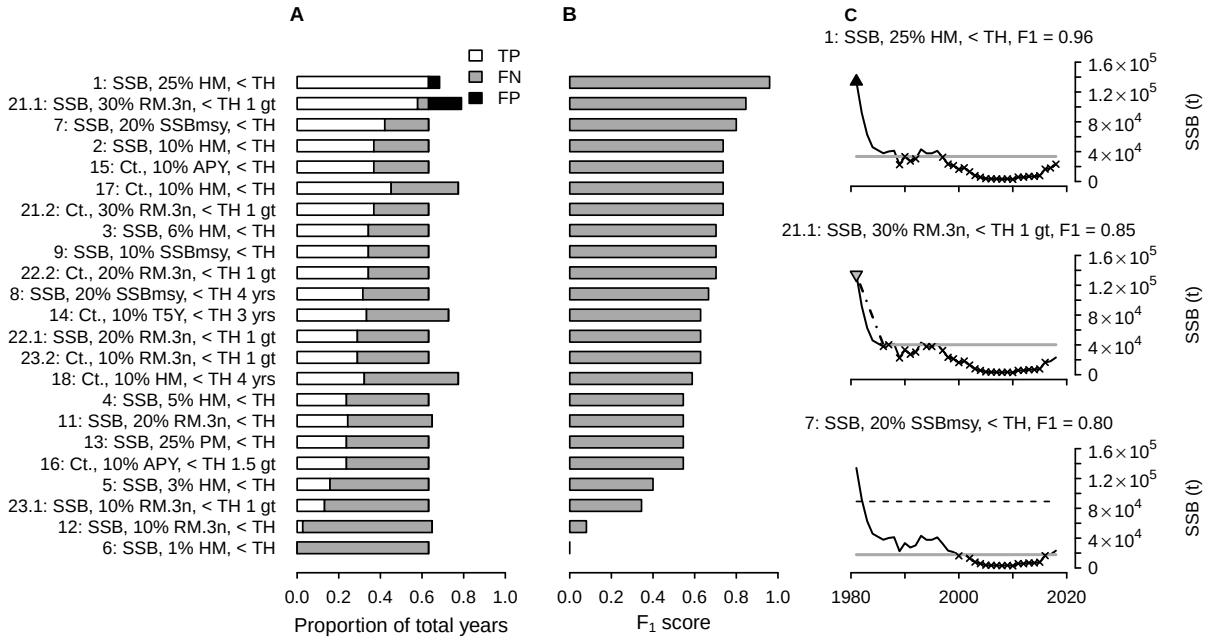

Simulated definitions

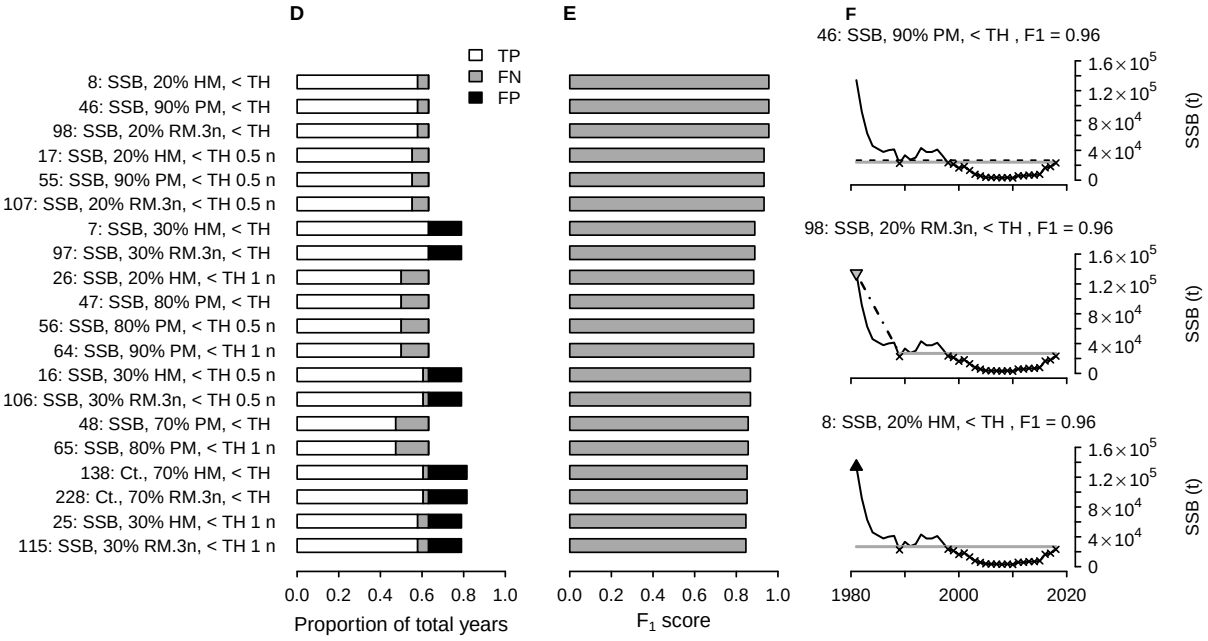

Whiting (IS) − whg.27.7a

Abbreviations

TP = True positive
FN = False negative
FP = False positive
HM = Historic maximum
RM.3n = Recent maximum (within 3 n)
PM = Population mean
n = Generation length
B_{ref} = Reference biomass
TH = Threshold
t = tonne

Abundance
Threshold
Abrupt decline
Fixed B_{ref}
HM, B_{ref}
RM.3n, B_{ref}
Collapsed

Benchmark: SSB < Blim, F1 = 1.00

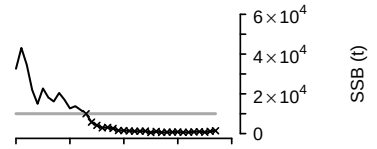

Literature and proposed definitions

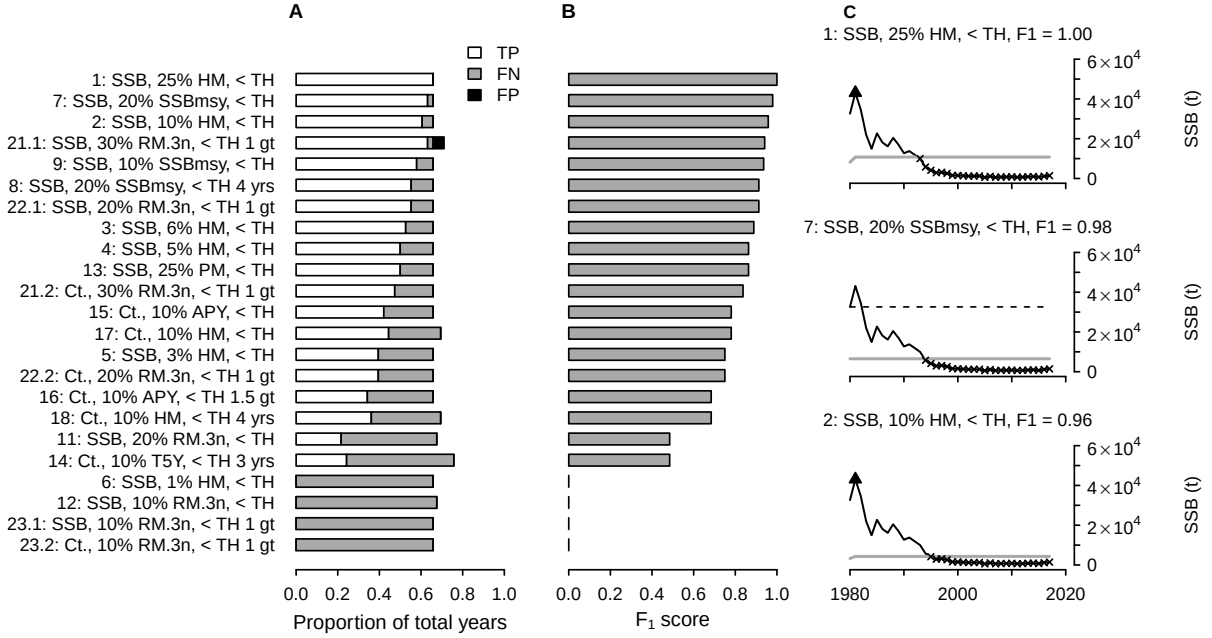

Simulated definitions